Université de Toulouse

THÈSE

En vue de l'obtention du

DOCTORAT DE L'UNIVERSITÉ DE TOULOUSE

Délivré par :
Institut National Polytechnique de Toulouse (INP Toulouse)

Discipline ou spécialité :

Génie des procédés et de l'Environnement

Présentée et soutenue par :
Jorge Raúl PEREZ GALLARDO

le : vendredi 25 octobre 2013

Titre :
Ecodesign of large-scale photovoltaic (PV) systems with multi-objective optimization and Life-Cycle Assessment (LCA)

Écoconception de systèmes photovoltaïques (PV) à grande échelle par optimisation multi-objectif et Analyse du Cycle de Vie (ACV)

Ecole doctorale :
Mécanique, Energétique, Génie civil et Procédés (MEGeP)

Unité de recherche :
Laboratoire de Génie Chimique - UMR 5503

Directeur(s) de Thèse :
Mme Catherine AZZARO-PANTEL (INP-Toulouse, France)
M. Stéphan ASTIER (INP-Toulouse, France)

Rapporteurs :

Mme Valérie LAFOREST (ENSM-Saint-Etienne, France)
M. Moises GRAELLS (UPC-Barcelone, Espagne)

Membre(s) du jury :

Mme Corinne ALONSO (LAAS CNRS-Toulouse, France)
M. Pascal ESCRIBE (EDF EN France Région Sud, France)
M. Serge DOMENECH (INP-Toulouse, France)
M. Xavier ROBOAM (INP-Toulouse, France)
M. Pascal MAUSSION (INP-Toulouse, France)

Abstract

.

Ecodesign of large-scale photovoltaic (PV) systems with multi-objective optimization and Life-Cycle Assessment (LCA)

Because of the increasing demand for the provision of energy worldwide and the numerous damages caused by a major use of fossil sources, the contribution of renewable energies has been increasing significantly in the global energy mix with the aim at moving towards a more sustainable development. In this context, this work aims at the development of a general methodology for designing PV systems based on ecodesign principles and taking into account simultaneously both techno-economic and environmental considerations. In order to evaluate the environmental performance of PV systems, an environmental assessment technique was used based on Life Cycle Assessment (LCA). The environmental model was successfully coupled with the design stage model of a PV grid-connected system (PVGCS). The PVGCS design model was then developed involving the estimation of solar radiation received in a specific geographic location, the calculation of the annual energy generated from the solar radiation received, the characteristics of the different components and the evaluation of the techno-economic criteria through Energy PayBack Time (EPBT) and PayBack Time (PBT). The performance model was then embedded in an outer multi-objective genetic algorithm optimization loop based on a variant of NSGA-II. A set of Pareto solutions was generated representing the optimal trade-off between the objectives considered in the analysis. A multi-variable statistical method (*i.e.*, Principal Componet Analysis, PCA) was then applied to detect and omit redundant objectives that could be left out of the analysis without disturbing the main features of the solution space. Finally, a decision-making tool based on M-TOPSIS was used to select the alternative that provided a better compromise among all the objective functions that have been investigated.

The results showed that while the PV modules based on c-Si have a better performance in energy generation, the environmental aspect is what makes them fall to the last positions. TF PV modules present the best trade-off in all scenarios under consideration.

A special attention was paid to recycling process of PV module even if there is not yet enough information currently available for all the technologies evaluated. The main cause of this lack of information is the lifetime of PV modules. The data relative to the recycling processes for m-Si and CdTe PV technologies were introduced in the optimization procedure for ecodesign. By considering energy production and EPBT as optimization criteria into a bi-objective optimization cases, the importance of the benefits of PV modules end-of-life management was confirmed. An economic study of the recycling strategy must be investigated in order to have a more comprehensive view for decision making.

Keywords: Ecodesign, Multi-objective Optimization, Life-Cycle Assessment (LCA), Photovoltaic (PV) system, Genetic Algorithm (GA), Principal Component Analysis (PCA), Multiple Criteria Decision Making (MCDM)

Résumé

Écoconception de systèmes photovoltaïques (PV) à grande échelle par optimisation multi-objectif et Analyse du Cycle de Vie (ACV)

En raison de la demande croissante d'énergie dans le monde et des nombreux dommages causés par l'utilisation des énergies fossiles, la contribution des énergies renouvelables a augmenté de manière significative dans le mix énergétique global dans le but de progresser vers un développement plus durable. Dans ce contexte, ce travail vise à l'élaboration d'une méthodologie générale pour la conception de systèmes photovoltaïques, basée sur les principes d'écoconception, en tenant compte simultanément des considérations technico-économiques et environnementales. Afin d'évaluer la performance environnementale des systèmes PV, une technique d'évaluation environnementale basée sur l'Analyse du Cycle de Vie (ACV) a été utilisée. Le modèle environnemental a été couplé d'une manière satisfaisante avec le modèle de conception d'un système PV connecté au réseau pour obtenir un modèle global, apte à un traitement par optimisation. Le modèle de conception du système PV résultant a été développé en faisant intervenir l'estimation du rayonnement solaire reçu dans une zone géographique concernée, le calcul de la quantité annuelle d'énergie produite à partir du rayonnement solaire reçu, les caractéristiques des différents composants et l'évaluation des critères technico-économiques à travers le temps de retour énergétique et le temps de retour sur investissement. Le modèle a ensuite été intégré dans une boucle d'optimisation multi-objectif externe basée sur une variante de l'algorithme génétique NSGA-II. Un ensemble de solutions du Pareto a été généré représentant le compromis optimal entre les différents objectifs considérés dans l'analyse. Une méthode basée sur une Analyse en Composantes Principales (ACP) est appliquée pour détecter et enlever les objectifs redondants de l'analyse sans perturber les caractéristiques principales de l'espace des solutions. Enfin, un outil d'aide à la décision basé sur M- TOPSIS a été utilisé pour sélectionner l'option qui offre un meilleur compromis entre toutes les fonctions objectifs considérées et étudiées.

Bien que les modules photovoltaïques à base de silicium cristallin (c-Si) ont une meilleure performance vis-à-vis de la production d'énergie, les résultats ont montré que leur impact environnement est le plus élevé des filières technologiques de production de panneaux. Les technologies en « couches minces » présentent quant à elles le meilleur compromis dans tous les scénarios étudiés.

Une attention particulière a été accordée aux processus de recyclage des modules PV, en dépit du peu d'informations disponibles pour toutes les technologies évaluées. La cause majeure de ce manque d'information est la durée de vie relativement élevée des modules photovoltaïques. Les données relatives aux procédés de recyclage pour les technologies basées sur CdTe et m-Si sont introduites dans la procédure d'optimisation par l'écoconception. En tenant compte de la production d'énergie et du temps de retour sur énergie comme critères d'optimisation, l'avantage de la gestion de fin de vie des modules PV a été confirmé. Une étude économique de la stratégie de recyclage doit être considérée et étudiée afin d'avoir une vision plus globale pour la prise de décision.

Mots-clés: Écoconception, Optimisation Multi-objectif, Systèmes Photovoltaïques (PV), Algorithme Génétique (AG), Analyse en Composantes Principaux (ACP), Méthode d'aide à la décision multi-critère (MADMC)

Resumen

Ecodiseño de sistemas fotovoltaicos (FV) a gran escala por optimización multi-objetivo y Análisis de Ciclo de Vida (ACV)

Debido a la creciente demanda de energía a nivel mundial y los numerosos daños causados por el uso de fuentes fósiles, la contribución de las energías renovables en el mix energético global se ha incrementado significativamente con el objetivo de avanzar hacia un desarrollo más sostenible. En ese contexto, el presente trabajo tiene como objetivo el desarrollo de una metodología general para el diseño de sistemas fotovoltaicos basados en los principios del ecodiseño considerando de manera simultánea los aspectos técnico-económicos y ambientales. Con el fin de evaluar el desempeño ambiental de los sistemas FV, una técnica de evaluación ambiental basada en el Análisis de Ciclo de Vida (ACV) fue utilizada. El modelo ambiental fue acoplado exitosamente con el modelo para el diseño de un sistema fotovoltaico conectado a la red eléctrica. El modelo para el diseño de un sistema fotovoltaico fue desarrollado a partir de la estimación de la radiación solar recibida en una ubicación geográfica específica, el cálculo de la energía anual generada a partir de la radiación solar recibida, las características de los diferentes componentes y la evaluación de los criterios tecno-económicos a través del tiempo de retorno energético (EPBT, en ingles) y el periodo de recuperacion de la inversion (PRI). En seguida, el modelo fue incrustado en un bucle externo destinado a la optimización multi-objetivo tomando como referencia una variante del algoritmo genético NSGA-II. Un conjunto de soluciones de Pareto fue generado, el cual representa el compromiso óptimo entre los objetivos considerados en el análisis. El método de Análsis de Componentes Principlaes (ACP) fue aplicado para detectar y eliminar los objetivos redundantes existentes sin alterar las principales características del espacio de soluciones. Finalmente, una herramienta de ayuda para toma de decisiones basado en M-TOPSIS fue utilizado para seleccionar la alternativa que ofrece un mejor compromiso entre todas las funciones objetivo consideradas y estudiadas.

Los resultados mostraron que los módulos fotovoltaicos basados en silicio cristalino (c-Si) tienen un mejor desempeño en la generación de energía, sin embargo el impacto ambiental que generan es el más elevado de entre todas las tecnologías de paneles solares consideradas. Los módulos fotovoltaicos fabricados a partir de TF presentan el mejor compromiso en todos los escenarios estudiados.

Una atención especial fue puesta a los procesos de reciclaje de módulos fotovoltaicos, a pesar de que actualmente no existe suficiente información disponible para todas las tecnologías evaluadas. La principal causa de esta falta de información es la vida útil de los módulos fotovoltaicos. Los datos relativos a los procesos de reciclado para las tecnologías de CdTe y m-Si fueron introducidos en el procedimiento de optimización basado en el ecodiseño. La importancia de los beneficios que tiene la gestión de los módulos fotovoltaicos al final de su vida útil fue puesta en evidencia al considerar la producción de energía y el tiempo de retorno energético como criterios de optimización. Un estudio económico de las estrategias de reciclage debe ser considerado e investigado con el fin de tener una visión más integral para la toma de decisiones futura.

Palabras claves: Ecodiseño, Optimización Multi-objetivo, Análisis de Ciclo de Vida (ACV), sistemas fotovoltaicos (FV), Algoritmos Genéticos (GA), Análisis de Componentes Principales (ACP), Métodos de Ayuda a la Toma de Decisiones Multi-critério

CONTENT

Introduction Générale 1

1. Motivation for the study and state-of-the art review 5

1.1 Introduction 7

1.2 General context 7

1.3 Solar energy 10

1.4 PV System 11

1.4.1 PV module 13

1.4.2 DC /AC Inverter 14

1.4.3 Mounting system 14

1.5 Historical PV market development 15

1.5.1 European Market 16

1.5.2 Production market of PV modules 17

1.5.3 PVGCS situation 18

1.6 PV System design 18

1.7 Organization of the manuscript 22

2. Life-Cycle Assessment (LCA) for PV systems 23

2.1 Introduction 25

2.2 Manufacturing processes for PV technologies 26

2.2.1 Crystalline silicon technology 26

2.2.2 Amorphous silicon thin-film 30

2.2.3 Cadmium Telluride thin-film 32

2.2.4 Copper Indium Selenide (CIS) thin-film 35

2.2.5 Discussion 39

2.3 Environmental assessment techniques 40

2.4 LCA Methodology 43

2.4.1 Goal and scope definition 44

2.4.2 Inventory analysis 45

2.4.3 Impact assessment 46

2.4.3.1 Selection of impact categories and characterization models 46

2.4.3.2 Impacts and damages classification 48

2.4.3.3 Characterization of impacts and damages 48

2.4.3.4 Optional elements: Normalisation, Grouping and Weighting 50

2.4.4 Interpretation of results 51

2.4.5 Limitations of LCA 52
2.4.6 LCA software tools 52
2.5 LCA study for m-Si based PV module 53
2.5.1 Goal and scope definition 53
2.5.2 Inventory analysis 54
2.5.3 Impact assessment 54
2.5.4 Interpretation of results 59
2.6 LCA study for silicon-based PV modules 62
2.6.1 Goal and scope definition 62
2.6.2 Technology assumptions, LCI and data collection 63
2.6.3 LCIA results and interpretation 63
2.7 LCA study for PVGCS 65
2.7.1 Goal and scope definition 66
2.7.2 Technology assumptions, LCI and data collection 66
2.7.3 LCIA results and interpretation 67
2.8 Conclusion 68

3. A modelling and simulation framework for sizing large-scale photovoltaic power plants 71
3.1 Introduction 73
3.2 Literature review on PV System design tools and work objective 74
3.3 Development of the simulation tool 77
3.4 Solar radiation model 78
3.4.1 Solar radiation 78
3.4.2 Model Description 79
3.4.2.1 Components of hourly irradiance on horizontal surface 81
3.4.2.2 Components of hourly irradiance on tilted surface 82
3.4.2.2.1 Beam irradiance 82
3.4.2.2.2 Reflected irradiance 82
3.4.2.2.3 Diffuse irradiance 83
3.4.2.3 Validation 83
3.5 PVGCS sizing model 85
3.5.1 Output energy estimation 85
3.5.2 Techniques for sizing PV systems 86
3.5.3 Mathematical sizing model 87
3.5.3.1 Direct shading 88
3.5.3.2 Output energy of solar field 89
3.5.3.3 Energy losses 89
3.6 Evaluation model 90
3.6.1 Techno-economic criteria 91
3.6.2 Environmental criteria 92
3.7 Validation of the model 92
3.7.1 Comparison with Weinstock and Appelbaum's model performances 92
3.7.2 Comparison with PVsyst 93
3.8 Conclusion 99

4. Methods and tools for ecodesign: combining Multi-Objective Optimization (MOO), Principal Component Analysis (PCA) and Multiple Criteria Decision Making (MCDM) 101

4.1 Introduction 103

4.2 Multi-objective optimization for sizing PV systems 103
4.2.1 Genetic algorithms 105
4.2.2 Multi-objective Genetic Algorithm 107
4.2.3 PVGCS optimization approach 107

4.3 Reduction of environmental objectives by Principal Component Analysis (PCA) method 111
4.3.1 PCA for environmental categories 114

4.4 Multiple-criteria decision making (MCDM) 115
4.4.1 M-TOPSIS method 117
4.4.2 Example of application of M-TOPSIS method 119

4.5 Conclusion 122

5. Ecodesign of large-scale photovoltaic power plants 125

5.1 Introduction 127

5.2 Optimal design of photovoltaic solar fields 128

5.3 Mono-objective optimization cases 129
5.3.1 Maximum annual output energy 129
5.3.1.1 Results 129
5.3.2 Minimum Field Area 134
5.3.2.1 Results 134

5.4 Bi-objective optimization cases 137
5.4.1 Q_{out} – PBT 138
5.4.2 Q_{out} – EPBT 142
5.4.3 PBT – EPBT 145
5.4.4 Area – PBT 146
5.4.5 Area – EPBT 150

5.5 Multi-objective optimization for the optimal design of PV power plant 153
5.5.1 Application of PCA method 153
5.5.2 Multi-objective optimization case: Qout – PBT – EPBT – RI – OLD – ME 155
5.5.3 Multi-objective optimization case: Qout – PBT – RI – OLD 157

5.6 Conclusion 158

6. Recycling of PV modules 161

6.1 Introduction 163

6.2 Recycling in LCA methodology 165
6.2.1 Allocation methods 166

6.3 Recycling process of spent PV modules 167
6.3.1 Crystalline silicon modules 167
6.3.2 CdTe and CIS 169
6.3.3 a-Si 171

6.4 LCA of PV modules recycling process 171
6.4.1 Crystalline silicon 171
6.4.2 CdTe 174
6.5 Conclusion 177

7. General conclusion and perspectives 179
7.1 General conclusions 181
7.2 Perspectives 183

Bibliography 185

liste of figures 195

liste of tables 199

Appendix

A. Comparative Life Cycle Assessment of Autonomous and Classical Heliostats for Heliothermodynamic Power Plants for Concentrated Solar Power **201**

B. Angle relationship for global irradiance estimation **209**

C. Validation of irradiance simulation tool **215**

D. Shadow estimation onto a tilted PV shed **221**

E. Balance of System (BOS) sizing **227**

INTRODUCTION GÉNÉRALE

L'énergie du rayonnement solaire reçue sur la Terre constitue le seul véritable apport renouvelable extérieur au « système Terre ». Elle représente 8 000 fois la consommation de l'humanité pour une année et se décline en de nombreuses formes d'énergies renouvelables exploitables (rayonnement, vent, hydraulique, biomasse, …). Cet énorme potentiel est donc invoqué pour répondre aux défis posés à l'humanité en matière d'énergie et de développement durable. Notamment, la génération directe d'électricité à partir du rayonnement solaire apparaît des plus prometteuses. Elle s'opère par deux voies principales: les centrales thermosolaires à concentration et tous les systèmes à conversion photovoltaïque exploitables dans une très large gamme de puissances. Les installations photovoltaïques ont ainsi connu une croissance récente vertigineuse, la puissance installée dans le Monde passant de 1,4 à 102 GW crête en 10 ans, notamment de 13 à 25,5 GW crête au cours de la seule année 2012 en Europe, leader dans cette avancée vers un Monde de l'énergie renouvelé et différent. Mais apparaissent dans le même temps plusieurs inconvénients dénoncés, tels que par exemple les besoins en eau des centrales thermosolaires installées en milieux ensoleillés arides, les impacts nocifs de la fabrication des matériaux photovoltaïques ou encore l'emprise au sol et sur les paysages de toutes ces installations artificielles nouvelles. Emblématique d'un développement durablela filière solaire se doit donc de veiller particulièrement à limiter son impact écologique et de maîtriser son développement de façon exemplaire.

C'est dans ce contexte que les travaux de doctorat présentés dans ce mémoire ont été menés: ils concernent particulièrement la conception et l'implantation de grands systèmes de panneaux solaires installés au sol. La bourse de thèse associée a été octroyée par CONACYT (Consejo Nacional de Ciencia y Tecnología, Mexico). Les travaux effectués ont fait l'objet d'une collaboration entre, d'une part, l'équipe COOP du Département Procédés et Systèmes Industriels (PSI) au sein du Laboratoire de Génie Chimique, LGC UMR CNRS INPT UPS 5503 et d'autre part l'équipe Genesys du LAPLACE (Laboratoire Plasma et Conversion d'Energie), UMR CNRS INPT UPS 5213. Les deux équipes ont des compétences complémentaires:

- L'équipe **COOP (C**onception **O**ptimisation **et O**rdonnancement des **P**rocédés du département PSI**)** a pour thème général de recherche l'optimisation et la conception de procédés. La démarche s'inscrit de façon prépondérante dans le développement de stratégies d'optimisation en variables mixtes (variables continues liées aux conditions

d'exploitation, variables entières relatives à la structure du procédé ou à des choix décisionnels) via des méthodes stochastiques ou déterministes, avec une forte orientation vers les méthodes d'optimisation multicritère.

- Le Groupe **GENESYS** (**EN**ergie **E**lectrique et **SYS**témique) a pour objectifs de concevoir des dispositifs hétérogènes, en considérant le système dans sa globalité et sa finalité. Ses compétences se trouvent dans les méthodes de conception intégrée (synthèse, analyse, optimisation) notamment dans les nouvelles technologies de l'énergie.

L'étude présentée a bénéficié du support financier d'un BQR PRES Université de Toulouse baptisé **OSSOLEMIO O**ptimisation **S**ystèmes **SO**laires **L**arge **E**chelle **M**ult**I O**bjectifs (2010-2012) qui a plus largement été dédié à l'étude des deux grandes voies complémentaires de production d'électricité solaire citées ci-dessus et actuellement en d'une part les centrales thermosolaires à concentration par héliostats offrent la possibilité de stocker l'énergie solaire sous forme thermique avant conversion en électricité, ce qui permet de pallier l'intermittence de la production. On peut ainsi obtenir des températures élevées nécessaires à la production de chaleur, d'électricité ou d'hydrogène [cf thèse d'Alaric Montenon (Montenon, 2013)]. D'autre part les générateurs photovoltaïques implantés en toitures ou en en plein champ, fixes ou montés sur des suiveurs solaires, débitant au fil du soleil leur production dans le réseau électrique.

L'étude présentée ici ne s'intéresse qu'à l'implantation de panneaux fixes d'un parc photovoltaïque de production d'électricité connecté au réseau.

La conception de ces systèmes photovoltaïques à grande échelle est encore actuellement surtout basée sur une approche technico-économique qui a comme objectif de maximiser la production d'énergie. Mais certains éléments, tels que le niveau d'émissions globales, notamment en gaz à effet de serre doivent être pris en compte pour renforcer l'intérêt de la filière et lui assurer un caractère effectivement durable. En fonction des technologies et de l'implantation des modules, il s'agit ici de concevoir des champs de panneaux solaires de façon optimale en combinant des critères de production et d'impact environnemental, afin de développer une méthodologie d'écoconception. Il est donc important également de considérer le recyclage des panneaux afin de régénérer les matériaux qui les constituent. Une analyse du cycle de vie complet a donc constitué une étape préliminaire afin d'évaluer le coût écologique des panneaux et du câblage associé à intégrer dès la conception du système photovoltaïque. Compte tenu du nombre de paramètres et de critères à traiter, le cœur de l'étude vise à proposer une méthode de conception par optimisation qui sélectionne les solutions les plus durables parmi un très grand nombre de choix possibles.

Le mémoire de thèse est organisé en sept chapitres dont nous ne donnons ci-dessous que les titres, la présentation de leur contenu étant donnée à la fin du premier chapitre qui permet de poser les éléments motivant cette étude et d'introduire de façon plus détaillée les chapitres de ce document :

Chapitre 1 Motivation de l'étude et présentation de l'état de l'art

Chapitre 2 Analyse du Cycle de Vie pour les systèmes photovoltaïques

Chapitre 3 Cadre de modélisation et de simulation pour les centrales photovoltaïques à grande échelle

Chapitre 4 Méthodes et outils pour l'écoconception : combiner optimisation multi-objectif, analyse en composantes principales et aide à la décision multicritère

Chapitre 5 Ecoconception de centrales photovoltaïques à grande échelle

Chapitre 6 Recyclage de modules de panneaux solaires

Chapitre 7 Conclusions et perspectives

Chapter 1

MOTIVATION FOR THE STUDY AND STATE-OF-THE ART REVIEW

Ce chapitre d'introduction vise à définir le cadre de cette étude et justifie les objectifs généraux qui ont guidé ces travaux. La partie 1 présente brièvement le contexte énergétique général. Le cas de l'énergie solaire, sur laquelle est centrée l'étude est analysé en détail dans la partie 2. Les caractéristiques techniques des systèmes photovoltaïques sont présentées dans la partie 3 et le développement du marché photovoltaïque est positionné dans la partie 4. Les méthodes traditionnelles de conception et de dimensionnement du système photovoltaïque décrites dans la littérature spécialisée sont ensuite proposées, ce qui justifie l'intérêt de développer une méthode d'éco-conception combinant analyse de cycle de vie, optimisation multiobjectif et procédures multicritères d'aide à la décision pour les systèmes photovoltaïques à grande échelle, ce qui est la base de cette étude. L'organisation du manuscrit est présentée à la fin de ce chapitre.

Nomenclature

Acronyms

APAC	Asia-Pacific region
DC/AC	Direct Current / Alternative Current
CdTe	Cadmium telluride
CIS	Copper indium diselenide
CPV	Concentrating PV
DSSC	Dry-Sensitized Solar Cell
EPIA	European Photovoltaic Industry Association
GHG	Greenhouse Gas
LCA	Life-Cycle Assessment
LCI	Life-Cycle Inventory
LCIA	Life-Cycle Impact Assessment
MEA	Middle East and Africa
PV	Photovoltaic
PVGCS	Photovoltaic Grid-Connected System
ROW	Rest of the World
a-Si	Amorphous silicon
c-Si	Crystalline silicon
m-Si	Monocrystalline silicon
p-Si	Polycrystalline silicon
ribbon-Si	Silicon sheet-defined film growth
STE	Solar Thermal Energy
TF	Thin Film

1.1 Introduction

This introduction chapter aims at defining the context of this study and justifies the general objectives that have guided this work. It is divided into 7 sections. Section 1 presents briefly the general energy context. The case of solar energy, that constitutes the centre of this study is thoroughly analysed in section 2. The technical features of PV systems are presented in section 3 and the PV market development is positioned in section 4. The traditional PV System design and sizing methods reported in the dedicated literature are then proposed, which justifies the interest to develop an ecodesign method combining Life Cycle Assessment, Multi-Objective Optimization and Multiple Criteria Decision-Making procedures for large-scale PV systems which is the core of this study and which has received little attention till now to our knowledge. The organization of the manuscript ends this chapter.

1.2 General context

During the last decades, the new technological advances have drastically changed our lifestyle. These changes try to satisfy our primary needs as human beings but equally they intended to provide comfort by eliminating repetitive tasks and facilitating our daily life. To achieve these objectives, the generation and supply of energy has become a crucial element for the sustainability of modern society. The demand for the provision of energy is increasing rapidly worldwide and the trend is likely to continue in future. Increase in its production translates into better quality of life and creation of wealth. Electricity producing systems presently in use across the world can be classified into three main categories: fossil fuels, nuclear power and renewables (Prakash & Bhat, 2009). Fossil fuels in their crude form, i.e. wood, coal and oil is traditionally the most extensive energy resource used. Nuclear power has been only accessible within developed countries. Renewable energy resources are abundant in nature and easily accessible around the world. Renewable energy sector is now growing faster than the growth in overall energy market. Solar, wind, geothermal, modern biomass, as well as hydro are some of the sources used in this category.

In 2011, the worldwide electricity generation was 21,964 TWh which 67.9% was originated from fossil fuels, 11.7% from nuclear, and 20.2% from renewable sources (Observ'ER, 2012). The graphic in Figure 1-1 represents the allocation of each of the three systems in global electricity production by 2011. Likewise, the emphasis is on the distribution of power generation of the six main sources of renewable energy. Hydroelectricity is the main source for renewable energy with a share of 80.5%.

Nowadays it is clearer that fossil fuel-based energy sources are damaging the environment and human life. Environmental pollution (of air, water, etc.) is largely linked to the increasing use of energy. Climate change due to use of fossil fuel with emissions of sulphur dioxide (SO_2), nitrogen oxide (NO_X) and carbon dioxide (CO_2) is a worldwide problem that has a big impact in the future of all the species living in the Earth. The Kyoto Protocol (United Nations, 2013), an international environmental treaty, sets the obligations for industrialised countries to reduce overall emissions from six greenhouse

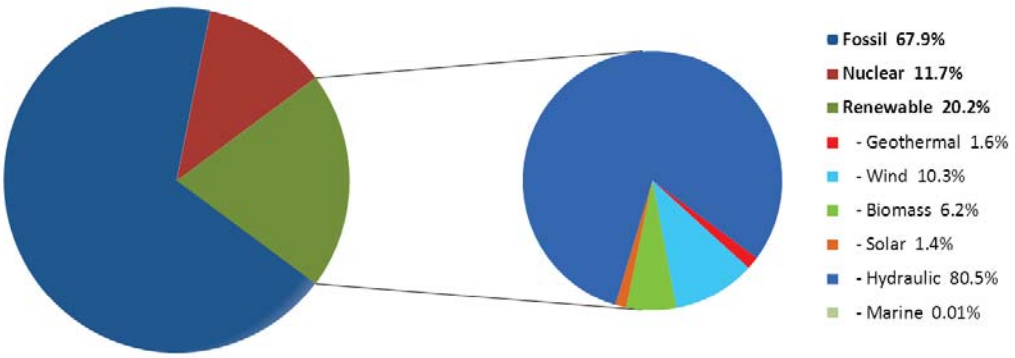

Figure 1-1 Structure of electricity production in 2011 (Observ'ER, 2012)

gases (GHG): carbon dioxide (CO_2), methane (CH_4), nitrous oxide (N_2O), sulphur hexafluoride (SF_6),hydrofluorocarbons (HFCs) and perfluorocarbons (PFCs). Because of this situation, the development of renewable energy systems is a current international priority for response to global warming. Some long-term scenarios postulate a rapidly increasing share of renewable technologies. Under these scenarios, in the second half of the 21st century, renewable source could satisfy between 20% to 50% of world's total energy demand with the right policies in place and new technology developments (Akella, Saini, & Sharma, 2009). Table 1-1 shows the evolution from 2001 to 2011 of world electricity production by source. From this information wind (28.3%) and solar (45.8%) sources have considerably increased their contribution among renewable sources.

Several problems and disadvantages of the use of renewable energy can be yet highlighted:

- A first apparent drawback, often cited is related to the low efficiency of the transformation of the initial energy provided by the source into electricity. But, it is important to underline that an usual 33% efficiency of conversion of traditional fossil or nuclear plants implies the dramatic waste of the two third of a precious natural reserve of energy, definitely lost for the future generations, while the typical 14% efficiency of a photovoltaic conversion simply means that only this proportion is extracted out of a permanently renewable source otherwise 100% available for the local environment for natural biosynthesis or local heating. Thence and moreover, such low conversion efficiency can augur a low local environmental impact. However and on another hand, as renewable sources are generally available with low space densities, a true difficulty is to harvest enough final energy required by supplied applications while not using a very large land space. This latter one is of course especially larger with lower efficiency conversion devices. Furthermore, improved devices with higher conversion efficiency are often much more expensive with these very new technologies still in early development. So, the main consequence of this situation is on one hand a larger spreading on land space which may modify the natural landscapes in a non-friendly way and on the other hand a high cost of the generated electricity (see following point). This may lead to search an optimum compromise between cost and occupied land space. So, in our opinion, a low conversion efficiency of a renewable energy should not be directly considered and cited as an obvious drawback by itself.

Table 1-1 World electricity production by source in TWh (2001-2011) (Observ'ER, 2012)

Source	2001	2008	2009	2010	2011	Variation 2001-2011
Renewable	*2,862.4*	*3,812.5*	*3,951.1*	*4,225.2*	*4,447.5*	*4.50 %*
- Geothermal	51.7	65.3	67.3	68.5	69.9	3.10 %
- Wind	37.9	219.6	276.4	351.5	459.9	28.30 %
- Biomass	134.1	232.0	250.8	270.1	276.0	7.50 %
- Solar	1.4	12.8	21.0	33.5	61.6	45.80 %
- Hydraulic	2,636.8	3,282.3	3,335.2	3,501.1	3,579.5	3.10 %
- Marine	0.575	0.546	0.527	0.558	0.555	-0.40 %
Fossil	*10,010.6*	*13,637.5*	*13,409.6*	*14,340.4*	*14,908.1*	*4.10 %*
Non-renewable waste	*39.3*	*38.7*	*40.0*	*43.1*	*40.3*	*0.30 %*
Nuclear	*2,637.7*	*2,730.8*	*2,696.4*	*2,755.1*	*2,568.2*	*-0.30 %*
Total Production	***15,55.,075***	***20,219.546***	***20,097.227***	***21,363.858***	***21,964.055***	

- The current cost of renewable energy technology is an impediment for its development. The establishment of government policies that subsidize the implementation of these facilities as well as investment in research of materials and mechanisms to increase processing efficiency and reduce manufacturing cost are necessary to achieve its growth and consolidate its position as the main source of replacing traditional methods of energy generation. Particularly, these technologies require expensive installation investments with long payback times.
- It must be also said that an enormous amount of fossil energy is required to manufacture, install and operate all forms of renewable energy systems. Without the input of fossil fuel the existing renewable energy projects probably could never have been built and could not be maintained in operation actually. The raw materials and components used require energy intensive extraction and fabrication techniques to be produced, and along with the finished products, also have to be transported across substantial distances. But, in most cases with the present improved technologies, the assessment on energy on the total life cycle is now positive which augurs of a sustainable development.
- A main drawback which becomes a very strong impediment for a large development of renewable sources of electricity is the dependency to geographic and meteorological conditions, making them sometimes very variable along different time scales (night and day, different seasons) and even sometimes and somewhere unpredictable and inconsistent. As the usual electric grid reliable work requires the very good knowledge of consumptions and productions and very good regulations often based on well controlled sources of electricity these properties set a new crucial problem to be solved by means of the so-called new "smart-grids" with new architectures and technologies, for example larger grid connected storage unities. Besides the necessary breakthroughs, this situation generates an increasing of the costs.

In that context, it is an imperative that the use of renewable energy must be efficiently integrated with the natural environment during its whole lifecycle following ecological design. **Ecodesign** is the use of the ecological design principles and strategies to design products, processes and systems that take

into account their impact on the environment at all stages of their life cycle, so that they integrate benignly and seamlessly with the natural environment that includes the biosphere, which contains all the forms of life that exist on earth. This goal must be the fundamental basis for the design of all our human-made environments. The PhD thesis focuses exclusively **on solar energy** with ecodesign guidelines in mind.

1.3 Solar energy

Solar energy is the renewable source that has the most important growth rate (see Table 1-1). Solar irradiation available is more than enough to satisfy the world's energy demands. The total solar energy that reaches the Earth's surface could meet global energy needs 10,000 times over (EPIA, 2011).

Where there is more Sun, more power can be generated that is why the sub-tropical areas of the world offer some of the best locations for solar power generation. Figure 1-2 compares the potential solar irradiation with existing energy sources. As it can be seen in this representation, maximizing the use of solar energy can meet the annual energy consumption across the planet.

The main advantages for solar energy are on the one hand:

- the power source, the Sun, is totally free.
- does not emit any GHG during the energy generation phase.
- can be used in any area on Earth, especially remote areas where it is too expensive to extend the electricity power grid. It can be on or off the grid.
- a very high reliability and a very low maintenance during their 20 - 30 years lifespan despite it is very new and sophisticated technologies.

On the other hand, the main disadvantages for solar energy are:

- the biggest disadvantage is the fact that it is not constant. Solar energy is harnessed when it is daytime. But also, beyond normal daily fluctuations, solar production largely varies with seasons outside the tropical latitudes and everywhere with meteorological conditions.
- large areas of land can be required to harness enough energy for aplications.
- solar systems, made with recent and sophisticated technologies are relatively expensive although prices are falling very rapidly and strongly with the market development.

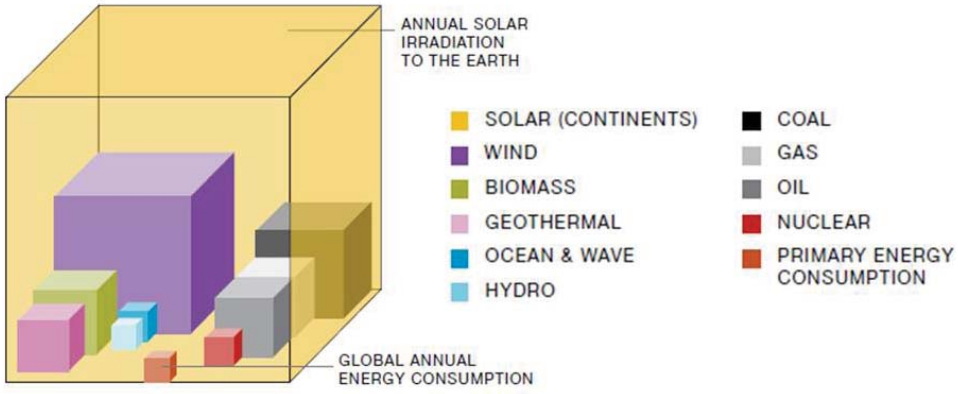

Figure 1-2 Solar irradiation versus global energy resources (EPIA, 2011)

- low conversion efficiency is often cited as a drawback but refer to 1.1 above.

Solar energy can be converted directly into other forms of energy, such as heat and electricity. Heat can be directly used for industrial or domestic use (hot washing water). Electricity can be generated by means of different ways as:

- **Solar thermal energy (STE)** is a technology for harnessing solar energy for thermal energy (heat). In STE, the light from the sun is concentrated to create heat, and that heat is used to run a heat engine, which turns a generator to make electricity. Water, oil, salts, air, nitrogen, helium are used as the fluid heated by the concentrated sunlight. Currently, there are three types of solar thermal power systems in use: the solar dish, solar power tower and parabolic trough (Solar Thermal, 2008).
- **Photovoltaic energy conversion (PV)** directly converts the light of Sun into electricity. Some materials that are sensitive to the solar radiation react in such a way that they can produce electricity. The conversion is generqlly accomplished through a thin plate of light sensitive material called solar cell or PV cell.

This work will address **PV energy conversion**.

1.4 PV System

PV technology has shown the potential to become a major source of power generation for the world. Proof of this is the fact that at the end of 2009 the PV cumulative installed capacity in the world was approaching 24 GW and in 2012, more than 100 GW are installed globally and they can produce at least 110 TWh of electricity every year (EPIA, 2013). This represents a growth of capacity of three times.

PV power generation employs PV modules composed of a number of solar cells containing a photovoltaic material that converts sunlight into electricity (see Figure 1-3 for a diagram of the photovoltaic effect). A typical PV system is basically made up of one or more photovoltaic PV modules, a mounting system that holds the PV modules and electrical interconnections, a DC/AC power converter (also known as inverter) which can deliver standard alternating voltage and current. A battery system for electricity storage may be included.

PV systems are classified in either off-grid systems or grid-connected systems (see Figure 1-4) (EPIA, 2011; Luque & Hegedus, 2003; Markvart & Castañer, 2003). Off-grid systems, also known as stand-alone systems, have no connection to an electricity grid. That is why a battery is required to deliver the electricity needed at anytime especially during night or after several days of low irradiation. Stand-alone systems fall into one of three main groups:

- Off-grid industrial applications. To power repeater station for mobile telephones, traffic signals, remote lighting, highways signs, marine navigation aids among others.
- Off-grid systems for electrification. To bring electricity to remote areas or developing countries

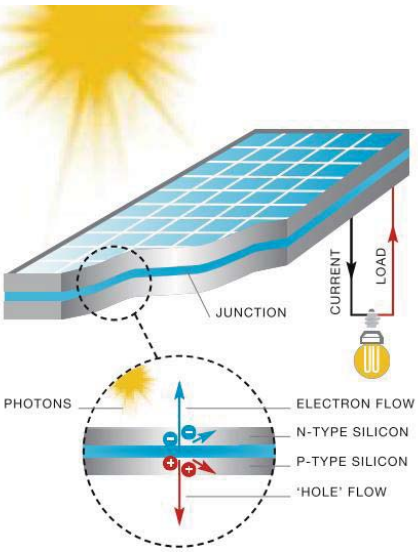

Figure 1-3 Photovoltaic effect (EPIA, 2011)

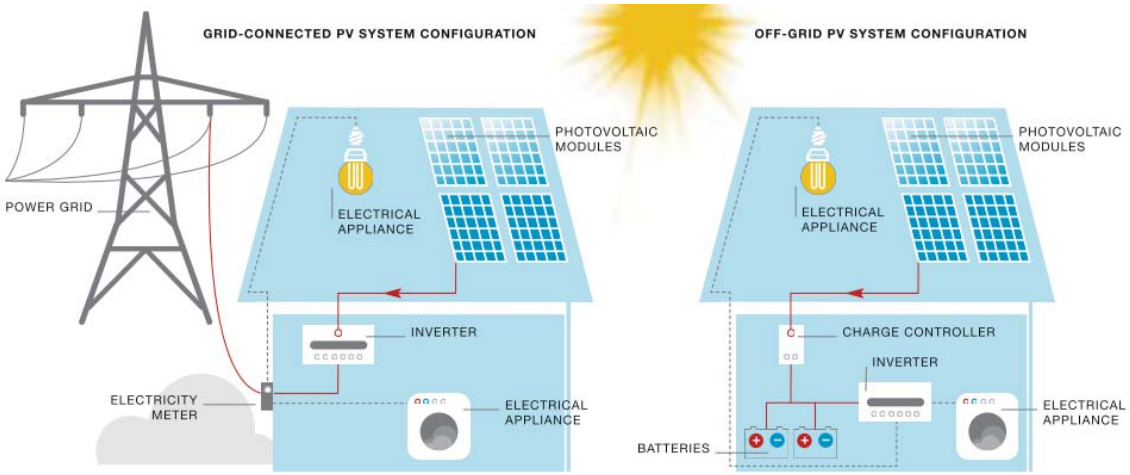

Figure 1-4 Different configurations of PV solar systems from (EPIA, 2011)

- Consumer goods. Like those found in several electrical applications such as calculators, toys, watches, etc.

Grid-connected systems (PVGCS) are the most popular type of solar PV system and will be the core of this study. Connection to the local electricity network allows any excess power produced to be sold. PVGCSs are classified in two main groups: residential and commercial systems and, industrial and utility-scale power plants. Residential and commercial systems are the most extensible used PVGCS because they can be installed on homes and businesses. By connecting to the local electricity network, owners can sell their excess power, but, when solar energy is not available, electricity can be drawn from the grid. This type of PVGCS generates up to 100 kWp (kilo Watt-peak). It must be said at this level of the presentation that kilo Watt-peak stands for peak power. This value specifies the output power delivered by a photovoltaic device (cell, module or system) working at its maximum power under set Standard Test Conditions i.e. a solar radiation of 1,000 watts per square meter, a cell temperature of 25°C and an Air Mass of 1.5.

Industrial and utility-scale power plants produce enormous quantities of electricity (>1 MWp). They need a large space to be installed. The solar panels are usually mounted on frames on the ground. However, they can also be installed on large industrial buildings such as warehouses, airport terminals or railway stations.

A PVGCS is integrated through the following key elements: PV modules, DC/AC inverter and mounting system.

1.4.1 *PV module*

PV modules are made of PV cells incorporated into a unit, usually by soldering them together under a sheet of glass. Module producers usually guarantee a power output of 80% of the nominal power even after 20-25 years. Modules can be connected to each other in series (known as an array) to increase the total voltage produced by the system. The arrays are connected in parallel to increase the system current.

PV modules are grouped as first, second or third generation according the technology uses for manufacturing the solar cell (Lund, Nilsen, Salomatova, Skåre, & Riisem, 2008; Petter Jelle, Breivik, & Drolsum Røkenes, 2012). The first generation includes modules made by silicon cells. Silicon cells have a quite high efficiency, but very pure silicon is needed so the manufacturing process requires a big amount of energy. Efficiencies of more than 20% have been obtained with silicon cells already produced in mass production (EPIA, 2011). Mono-crystalline (m-Si), poly-crystalline (p-Si) and silicon sheet-defined film growth (ribbon-Si) are considered in this generation. These technologies are named crystalline-Silicon technology (c-Si). Silicon-based modules dominate the current market (EPIA, 2013).

The so-called thin film (TF) PV modules are considered as second-generation PV technologies. It includes three main families: amorphous silicon (a-Si), Cadmium-Telluride (CdTe) and Copper-Indium-Selenide (CIS). TF solar cells are comprised of successive thin layers, just 1 to 4 μm thick (Luque & Hegedus, 2003). The combination of using less material and lower cost manufacturing processes allow the manufacturers to produce and sell PV modules at a much lower cost. In addition, TFs can be packaged into flexible and lightweight structures. The main disadvantage is the lower efficiency (7-12%) (EPIA, 2011).

Third-generation PV modules include technologies that are still under demonstration or have not yet been widely commercialised. There are four types of third-generation PV technologies: concentrating PV (CPV), dry-sensitized solar cells (DSSC), organic solar cells and, novel and emerging solar cell concepts. The goal of these technologies is to improve on the solar cells already commercially by growing the conversion efficiency, make them less expensive, and to develop more and different uses. In laboratory tests, they had reached an efficiency of 30% (EPIA, 2011).

According to EPIA (EPIA, 2013), c-Si technology has currently the highest market share (more than 80%) and is expected to maintain it in the future. TF technologies represented about 15% of the

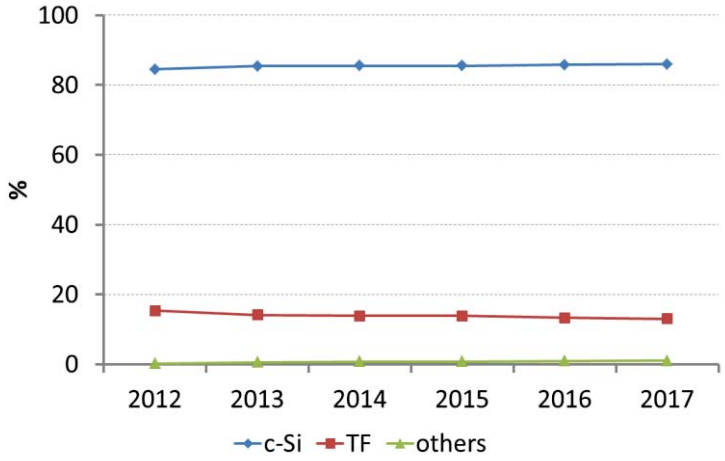

Figure 1-5 PV module technology market share, based on (EPIA, 2013)

market share in 2012, while third-generation technology represented less than 1% of market share but it is attended to get 1% of market for 2017. Figure 1-5 shows the PV technology market share in 2012 and the projection of PV market until 2017.

1.4.2 *DC /AC Inverter*

The DC/AC inverter is the second most important component. PV modules produce direct current (DC). However, most appliances run on alternating current (AC). Consequently, an inverter must be used to convert the DC into AC. Inverters are widely used for many industrial applications. The PV inverter has another very important role in PV systems achieving a Maximum Power Point Function (MPPT). This MPPT function consists in varying the electrical operating point of the PV array in order to maintain its output power at the maximum value possible which mainly depends on the environmental conditions: solar irradiation and temperature, that is, the variable bias point at which the PV array produces highest power extraction. Changes of temperature and insolation change the voltage where maximum power extraction occurs. Today, intelligent inverter control includes very effective maximum power point tracking systems (MPPT).

Inverters have often been the source of poor reliability in early systems. Feedback to manufacturers and more robust components has greatly reduced these problems, taking benefit of the tremendous development of power electronics and of the PV systems market.

Today most inverter models are additionally equipped with data loggers and measurement computers, which allow the power, voltage, current and other operating parameters to be recorded continuously and often available by an internet link.

1.4.3 *Mounting system*

The structures of mounting system are typically pre-engineered systems of aluminium or steel racks. Mounting structures vary depending on where the PV systems are sited, with different solutions of ground-mounted systems. PV modules must be mounted such that they face the best angle. Because of their low value and substantial weight, mounting and racking structures are generally assembled locally.

Simple fixed platforms are commonly the most used, due their very high reliability. It is possible to install tracking platforms that can tilt the PV sensors surface along one or two axis by means of electric motors and a control device that determines the actual position of the sun. Not surprisingly, tracking can provide a significant energy boost so long that it is reliable. However, this comes at a cost and reduced reliability, as the tracking mechanics are more complicated and expensive.

1.5 Historical PV market development

Figure 1-6 exhibits the evolution of PV cumulative installed capacity in the world from 2000 to 2012. Figure 1-6 also displays the cumulative capacity by region. Europe leads with more than 70 GW installed about 70% of total, particularly thanks to a very strong policy of Germany, the far leader. Next in the ranking are Asia-Pacific region (APAC) with 12.4 GW installed, America with almost 8.7 GW and not far away China with 8.3 GW. Middle East and Africa (MEA) and the Rest of the World (ROW) represent about 3 GW of world's total PV capacity in 2012.

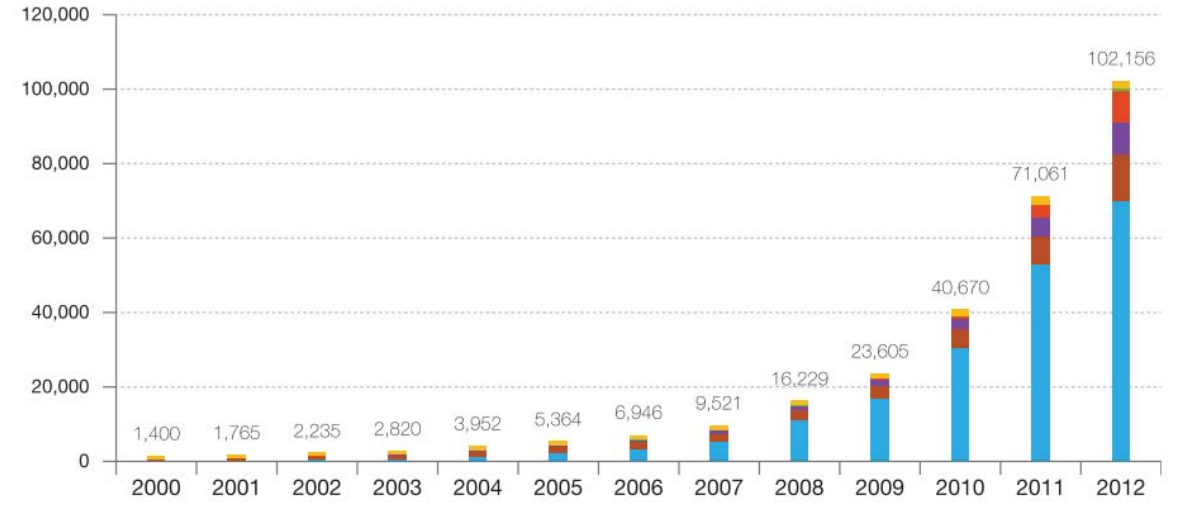

	2000	2001	2002	2003	2004	2005	2006	2007	2008	2009	2010	2011	2012
ROW	751	807	887	964	993	1,003	1,108	1,150	1,226	1,306	1,590	2,098	2,098
MEA	n/a	n/a	n/a	n/a	1	1	1	2	3	25	71	192	601
China	19	24	42	52	62	70	80	100	140	300	800	3,300	8,300
Americas	146	178	225	290	394	501	650	863	1,209	1,752	2,780	4,959	8,717
APAC	355	495	686	916	1,198	1,500	1,825	2,096	2,631	3,373	4,956	7,628	12,397
Europe	129	262	396	598	1,305	2,289	3,281	5,310	11,020	16,850	30,472	52,884	70,043
Total	1,400	1,765	2,235	2,820	3,952	5,364	6,946	9,521	16,229	23,605	40,670	71,061	102,156

Figure 1-6 Evolution of global cumulative installed capacity 2000-2012 (MW) (EPIA, 2013)

Table 1-2 Top 10 countries with the highest PV cumulative installed capacity in 2012 (EPIA, 2013)

	Country	Cumulative in GW		Country	Cumulative in GW
1	Germany	32.4	6	Spain	5.2
2	Italy	16.3	7	France	4.0
3	China	8.3	8	Belgium	2.7
4	United States	7.8	9	Australia	2.4
5	Japan	6.9	10	Czech Republic	2.1

Table 1-2 shows the top 10 countries with the highest PV cumulative installed capacity in 2012. Not surprisingly, Germany continues to be, and with a large difference, the world leader (32.4 GW).

According to the predictions made by the European Photovoltaic Industry Association (EPIA) (EPIA, 2013), a fastest PV growth is expected to continue in China and India, followed by Southeast Asia, Latin America and the MEA countries. The projections for the growth of PV cumulative installed capacity in the world until the year 2017 by region are presented in Figure 1-7 with two possible scenarios. The first called *Business-as-Usual scenario* assumes a pessimistic market with no major reinforcement or replacement of existing support mechanisms. This scenario also assumes that if the country is close to energy transition, markets are significantly slowing down because the policy mechanisms designed to accelerate investment in renewable energy technologies are phased out. The second scenario called *Policy-Driven scenario* assumes the continuation, adjustment or introduction of adequate support mechanisms with strong policies to allow considering PV as a major power source in the coming years.

1.5.1 *European Market*

During 2012 in Europe around 17 GW of new PV installations were mounted. That is why PV became the number-one electricity source among the countries of European Union (EU) in terms of added installed capacity. Figure 1-8 shows the number of new power generation capacities by source added in 2012. It can be seen that for traditional sources (fossil fuel and nuclear) the installed capacity balance turned negative last year. A significant number of facilities were dismantled.

Germany contributed to 44.31% of new PV installations that allow the European market to keep a reasonable level in relation to the other regions. Figure 1-9 indicates the percentage of new grid-connected PV capacities by country in Europe during 2012.

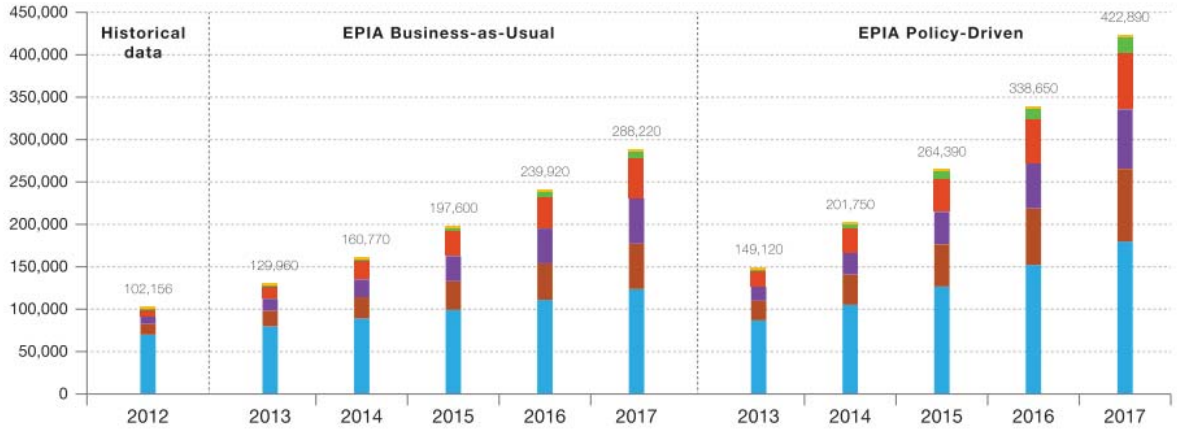

	2012	2013	2014	2015	2016	2017	2013	2014	2015	2016	2017
ROW*	2,098	2,098	2,098	2,098	2,098	2,098	2,098	2,098	2,098	2,098	2,098
MEA	601	1,260	2,180	3,480	5,380	7,780	2,100	4,800	8,200	12,700	18,750
China	8,300	14,300	21,300	29,300	37,300	47,300	18,300	28,300	39,300	51,300	66,300
Americas	8,717	14,430	21,090	29,880	41,090	53,820	16,810	25,900	38,400	53,790	70,380
APAC	12,397	18,130	25,060	33,720	43,230	53,590	22,990	35,470	49,760	66,760	85,810
Europe	70,043	79,750	89,040	99,120	110,830	123,640	86,820	105,180	126,630	152,010	179,560
Total	102,156	129,960	160,770	197,600	239,920	288,220	149,120	201,750	264,390	338,650	422,890

Figure 1-7 Evolution of global PV cumulative installed capacity per region until 2017 in MW (EPIA, 2013)

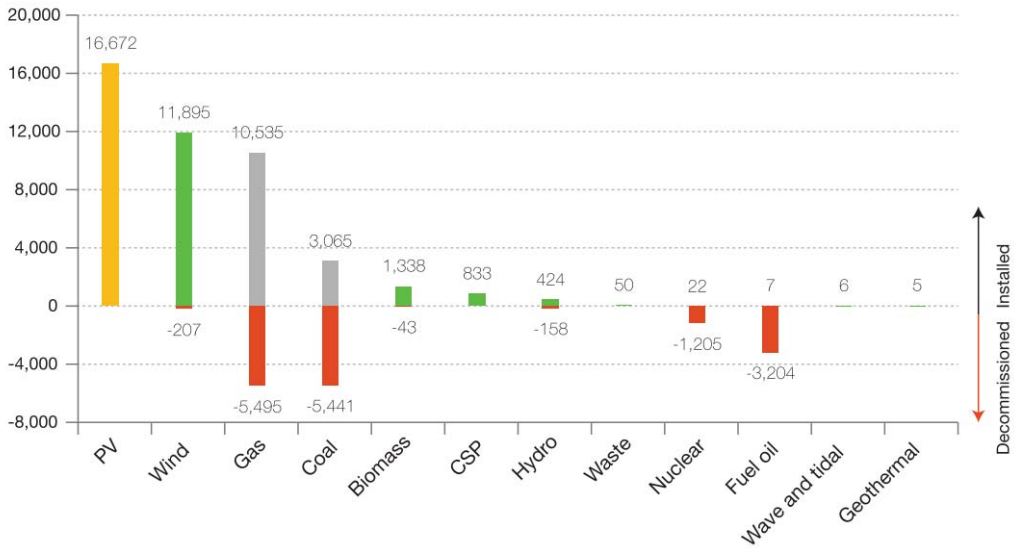

Figure 1-8 Power generation capacities added in the EU 27 in 2012 (MW) (EPIA, 2013)

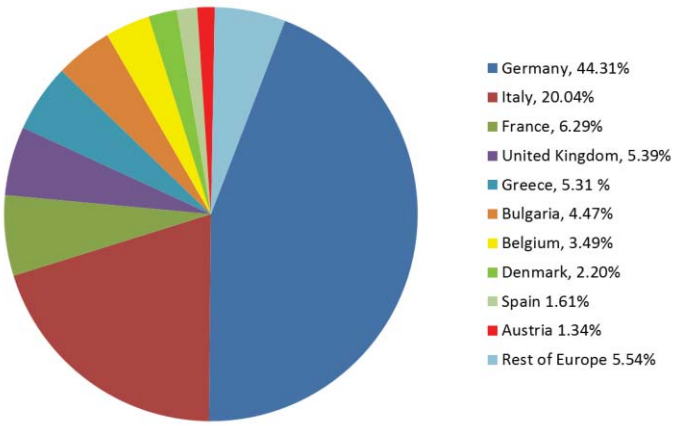

Figure 1-9 European new grid-connected PV capacities in 2012 (EPIA, 2013)

1.5.2 *Production market of PV modules*

The regional share of actual production of different PV module technologies in 2012 is presented in Figure 1-10. PV industry remained strong in Asia with China playing a leading role. China leads the production market of crystalline modules (c-Si) while the APAC region, with Japan and Malaysia as top producers, leads the TF production market with more than 60% of production share.

EPIA 2012 (EPIA, 2013) report indicates that no major changes should be expected in the main PV technologies, crystalline silicon (c-Si) and TF in the next five years. A slightly higher growth rate is expected for c-Si (6.34%) mainly due to the uncertainty of amorphous silicon (a-Si) technologies, for which the growth rate might be reduced by around 3% until 2017. The reason is the lower module efficiency of a-Si in comparison with the rapid evolution of CdTe and Copper Indium Gallium Selenide (CIGS) with efficiencies below 10% on module level. It is expected that by 2017 CdTe has a 5.95% growth while for CIGS growth will be 8.70%.

Moreover, the permanent decreasing of PV crystalline silicon (c-Si) due to a fast growing of production unities and market, particularly in China, slows down the diffusion of theoretically less

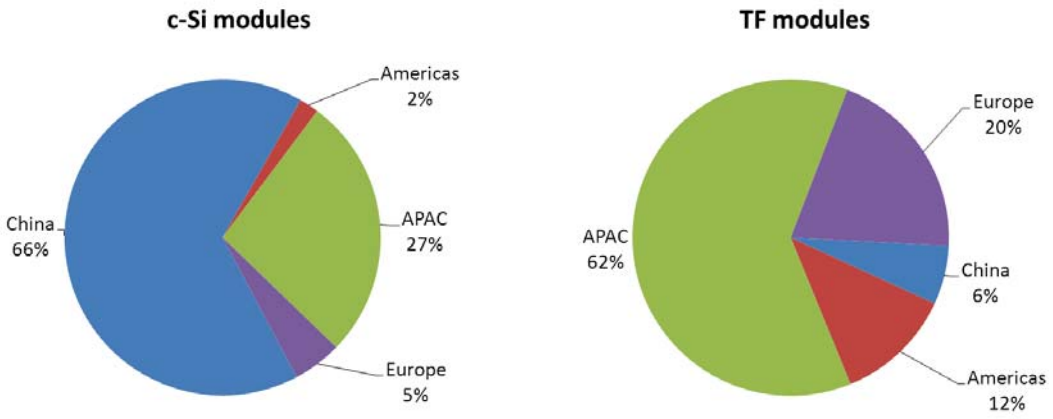

Figure 1-10 Global PV production in 2012 by region (EPIA, 2013)

expensive other technologies.

1.5.3 *PVGCS situation*

In 2012 utility-scale applications reached more than 9 GW. EPIA expects utility-scale plants to grow much faster than rooftop applications. In the Policy-Driven scenario, utility-scale market could quadruple from 9 to 37 GW. This can be explained by the nature of the investors in the most promising markets and the reduced opposition to ground-mounted PV systems (Figure 1-11).

At the regional level, the utility-scale segment is expected to at best stagnate in Europe even as it booms in the Americas and Asia including China. In both scenarios, the APAC region including China should see the largest share of new utility-scale applications, ahead of the Americas.

The design and sizing of large-scale PV plants with more efficient energy production are then needed.

1.6 PV System design

Several works have been devoted to the optimized design of PV systems, mainly from a techno-economic viewpoint. The majority of the reported works in the dedicated literature is related either to the minimization of an economic criterion or to the maximization of annual energy produced.

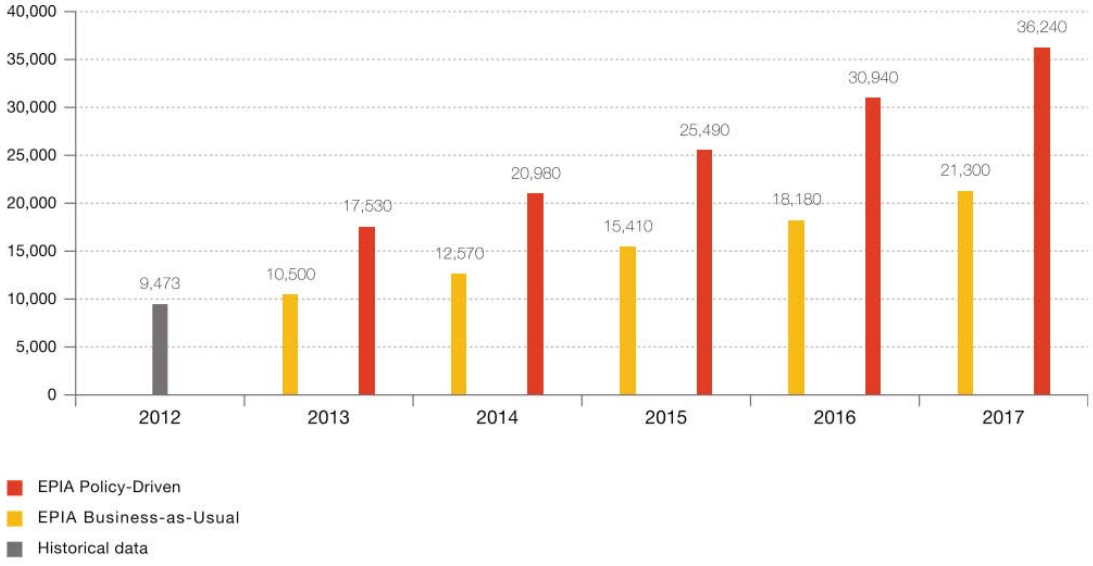

Figure 1-11 Global utility-scale PV development scenarios until 2017 (MW) (EPIA, 2013)

However, these studies have adopted mainly simulation approaches to evaluate the system performance and are exclusively devoted to the electrical performance. An optimal unit sizing method has not been established to rationally determine device capacities in consideration of device operational strategies for seasonal and hourly variations of solar insolation and electricity demand.

Generally, two approaches have been adopted. The former one is a deterministic approach where the system performance is evaluated on the basis of original data on solar isolation and electricity demand obtained through measurement. The latter is a probabilistic approach which is based on probability distributions of solar insolation and electricity demand assumed from their original data.

The performance of the PV system depends upon several factors, especially the meteorological conditions such as solar radiation, ambient temperature and wind speed. Normally, the information provided about the PV module and other components from the manufacturers is used for sizing the PV system by a rough estimation of the system output based on average values of daily meteorological data inputs. The parameters that are most used for sizing a PVGCS are field surface, tilt angle and array size. A summary of some works in this field is proposed in Table 1-3.

From the abovementioned works, it is possible to establish a general scheme for the configuration of a PVGCS, as shown in Figure 1-12.

It must be yet emphasized that even if power generation from PV systems is free from fossil fue1 use and greenhouse gas (GHG) emissions, a considerable amount of energy is consumed in the manufacturing and transport of the elements of the system. Besides, the amount of energy and emissions from a decommissioning phase of the system must not be neglected. Moreover, any artificial installation implies an ecological impact on the local or even the global environment. For any energy source versus the aim of sustainable development, if to be “renewable” is an obvious “necessary condition”, it is not a “sufficient condition”! Indeed, many other impact factors than energy resource exhaustion can be considered to be taken into account.

Ecodesign methods are thus necessary to check whether renewable energy systems as PV systems are truly environment-friendly (green). Generally the environmental assessment is performed as a post-design stage of the PV systems. The objective of this work is to integrate the environmental assessment from the design stage. Table 1-4 displays some of the works that have evaluated environmental impacts generated by PV systems.

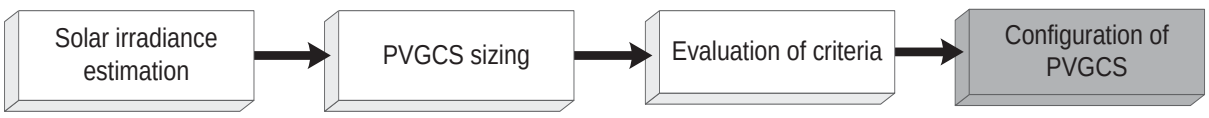

Figure 1-12 General scheme for the configuration of a PVGCS

Table 1-3 Summary of literature works for sizing PV systems

Authors	Year	Subject
(Pehnt, 2006)	2006	Dynamic life cycle assessment (LCA) of renewable energy technologies
(Prakash & Bhat, 2009)	2009	Energy, economics and environmental impacts of renewable energy systems
(Ménard et al., 2011)	2011	Environmental impact assessment of electricity production by photovoltaic system using GEOSS recommendations on interoperability
(Beylot et al., 2012)	2012	Environmental impacts of large-scale grid-connected ground-mounted PV installations
(Alsema & Wild-scholten, 2006)	2006	Environmental Impacts of Crystalline Silicon Photovoltaic Module Production System boundary LCA study New LCI data set
(Raugei, Bargigli, & Ulgiati, 2007)	2007	Life cycle assessment and energy pay-back time of advanced photovoltaic modules: CdTe and CIS compared to poly-Si
(Nishimura et al., 2010)	2010	Life cycle assessment and evaluation of energy payback time on high-concentration photovoltaic power generation system
(Desideri, Proietti, Zepparelli, Sdringola, & Bini, 2012)	2012	Life Cycle Assessment of a ground-mounted 1778kWp photovoltaic plant and comparison with traditional energy production systems
(Sherwani & Usmani, 2010)	2010	Life cycle assessment of solar PV based electricity generation systems: A review
(Kannan, Leong, Osman, Ho, & Tso, 2006)	2006	Life cycle assessment study of solar PV systems: An example of a 2.7kWp distributed solar PV system in Singapore
(Hondo, 2005)	2005	Life cycle GHG emission analysis of power generation systems: Japanese case
(Raugei & Frankl, 2009)	2009	Life cycle impacts and costs of photovoltaic systems: Current state of the art and future outlooks
(Sumper, Robledo-García, Villafáfila-Robles, Bergas-Jané, & Andrés-Peiró, 2011)	2011	Life-cycle assessment of a photovoltaic system in Catalonia (Spain)
(Dones & Frischknecht, 1998)	2000	Life-cycle Assessment of Photovoltaic Systems: Results of Swiss Studies on Energy Chains
(Ito, Komoto, & Kurokawa, 2010)	2010	Life-cycle analyses of very-large scale PV systems using six types of PV modules
(Fthenakis & Kim, 2011)	2011	Photovoltaics: Life-cycle analyses
(Akella, Saini, & Sharma, 2009)	2009	Social, economic and environmental impacts of renewable energy systems

Table 1-4 Summary of literature works for environmental assessment of PV systems

Authors	Year	Subject
(Mirhosseini, Agelidis, & Ravishankar, 2012)	2012	Modeling of large-scale grid-connected photovoltaic systems: Static grid support by reactive power control
(Li et al., 2010)	2010	Modeling and simulation of large-scale grid-connected photovoltaic system
(Kornelakis & Koutroulis, 2009)	2010	Contribution for optimal sizing of grid-connected PV-systems using PSO
(Notton, Lazarov, & Stoyanov, 2010)	2010	Optimal sizing of a grid-connected PV system for various PV module technologies and inclinations, inverter efficiency characteristics and locations
(Wissem, Gueorgui, & Hédi, 2012)	2012	Modeling and techno–economic optimization of an autonomous photovoltaic system
(Mondol, Yohanis, & Norton, 2009)	2009	Optimizing the economic viability of grid-connected photovoltaic systems
(Gautam & Kaushika, 2002)	2002	Development of an efficient algorithm to the electrical performance simulation of solar photovoltaic arrays
(Weinstock & Appelbaum, 2004)	2004	Optimal Solar Field Design of Stationary Collectors
(Weinstock & Appelbaum, 2009)	2009	Optimization of Solar Photovoltaic Fields
(Weinstock & Appelbaum, 2007)	2007	Optimization of Economic Solar Field Design of Stationary Thermal Collectors
(Fernández-Infantes, Contreras, & Bernal-Agustín, 2006)	2006	Design of grid connected PV systems considering electrical, economical and environmental aspects: A practical case
(Gong & Kulkarni, 2005)	2005	Design optimization of a large scale rooftop photovoltaic system
(Mellit, Kalogirou, Hontoria, & Shaari, 2009)	2009	Artificial intelligence techniques for sizing photovoltaic systems: A review
(Smiley, Jones, & Stamenic, 2000)	2000	Optimizing photovoltaic array size in a hybrid power system
(Kumar Sharma, Colangeki, & Spagna, 1995)	1995	Photovoltaic technology: basic concepts, sizing of a standalone photovoltaic system for domestic applications and preliminary economic analysis
(Posadillo & López Luque, 2008)	2008	Approaches for developing a sizing method for stand-alone PV systems with variable demand

1.7 Organization of the manuscript

This PhD work aims at determining a general methodology for designing PVGCS, taking into account simultaneously both techno-economic and environmental considerations.

The manuscript consists of six chapters that are organized as follows:

Chapter 1 is focused on the presentation of the general context of PV systems as well as on the literature review for designing and sizing PV systems and justifies the scientific objectives of this work.

In **Chapter 2**, the methodology chosen for the assessment of environmental impacts asscoiated with PVGCS based on Life Cycle Assessment methodoloy is presented.

Chapter 3 is dedicated to the presentation of the model that has been developed for sizing a large-scale PV system.

Chapter 4 discusses the methods and tools that are the support of the methodological study for ecodesign. They combine multi-objective optimization, principal component analysis and multiple criteria decision-making

The integration of the environmental and sizing PVGCS models in the multi-objective optimization framework is presented in **Chapter 5**. Different examples serve as an illutrsation of the performances of the proposed methodology for sizing a PV system taking into account simultaneously techno-economic and environmental criteria. Particular emphasis is devoted to the reduction of the objectives in the multi-objective approach to make the analysis more consistent and facilitate result interpretation.

Chapter 6 presents a review of current recycling processes of PV modules. In addition, two examples of integration of the recycling process in the environmental assessment model developed in Chapter 2 will show the importance of recycling in the ecodesign procedures. Finally, the manuscript ends with conclusions and perspectives in **Chapter 7**. A vision of the report structure is presented in Figure 1-13:

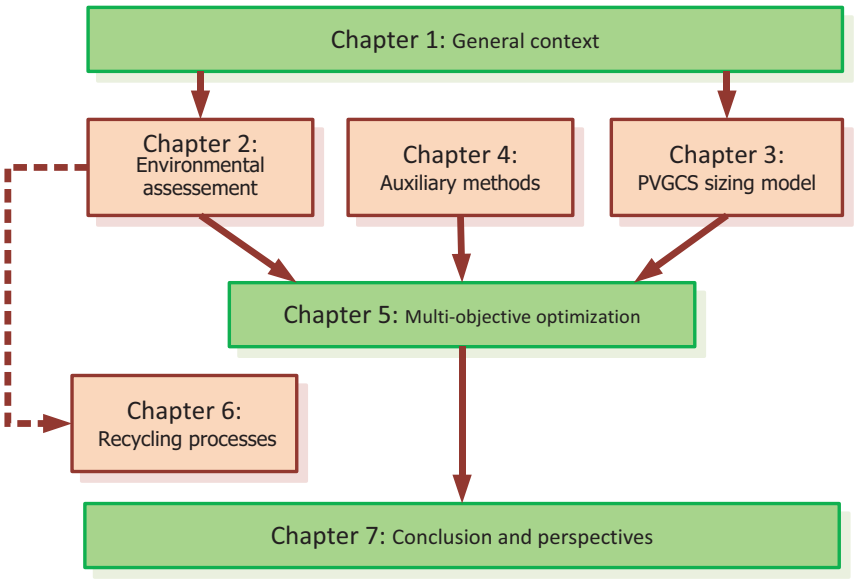

Figure 1-13 Organization of manuscript

Chapter 2

LIFE-CYCLE ASSESSMENT (LCA) FOR PV SYSTEMS

L'objectif de ce chapitre est de présenter le modèle environnemental retenu dans le cadre de cette étude. L'approche par Analyse du Cycle de Vie (ACV) largement appliquée dans plusieurs domaines, notamment pour la production d'énergie, est utilisée pour mesurer la performance environnementale des systèmes photovoltaïques.

Ce chapitre présente tout d'abord les procédés de fabrication utilisés pour cinq technologies de modules PV (m-Si, p-Si, a-Si, CdTe et CIS). La connaissance du procédé est perçue comme un point fondamental pour comprendre les limitations liées à une technologie d'un point de vue environnemental. Une analyse de la littérature dédiée des approches d'évaluation environnementale est ensuite menée. Les principes fondamentaux de l'ACV finalement retenue sont ainsi décrits. Trois exemples d'études de l'ACV sont proposées. Le premier exemple traite le cas du module PV basé sur la technologie m-Si, de la production du silicium de qualité solaire à l'assemblage du module PV. L'influence du « mix » énergétique est pris en compte. La deuxième illustration est consacrée à la comparaison des impacts environnementaux de 3 technologies (m-Si, p-Si, Si en ruban). En final, l'évaluation et la comparaison de 5 configurations de systèmes photovoltaïques connectés au réseau sont présentées. Le modèle environnemental proposé ici sert de brique de base pour l'intégration de l'analyse environnementale dans le cadre d'une optimisation multiobjectif pour le dimensionnement de champs de panneaux solaires. Le cas du recyclage des panneaux fera l'objet d'un chapitre dédié en fin de manuscrit. Le manque de données lors du démarrage de ces travaux et qui perdure pour certaines technologiques n'a pas permis une vision holistique sur laquelle reposer certes une démarche ACV.

Nomenclature

Acronyms

AA	Aquatic Acidification midpoint category
AE	Aquatic Ecotoxicity midpoint category
AEU	Aquatic Eutrophication midpoint category
C	Carcinogen midpoint category
CBA	Cost-Benefit Analysis
CBD	Chemical Bath Deposition
CdTe	Cadmium Telluride
CIS	Copper indium diselenide
CSS	Closed Space Sublimation
CSVT	Closed Space Vapour Transport
CVD	Chemical Vapor Deposition
CZ	Czochralski process
DC/AC	Direct Current / Alternative Current
EIA	Environmental Impact Assessment
ERA	Environmental Risk Assessment
EVA	Ethylene Vinyl Acetate
FU	Functional Unit
GW	Global Warming midpoint category
IO	Ionizing Radiation midpoint category
LCA	Life-Cycle Assessment
LCI	Life-Cycle Inventory
LCIA	Life-Cycle Impact Assessment
LO	Land Occupation midpoint category
ME	Mineral Extraction midpoint category
MFA	Material Flow Analysis
MILP	Material Intensity Per unit Service
NC	Non-Carcinogen midpoint category
NR	Non-Renewable energy midpoint category
OLD	Ozone Layer Depletion midpoint category
PV	Photovoltaic
PVGCS	Photovoltaic Grid-Connected System
RE-PECVD	Radio Frequency Plasma Enhanced Chemical Vapor Deposition
RI	Respiratory Inorganic midpoint category
RO	Respiratory Organic midpoint category
m-Si	Monocrystalline silicon
p-Si	Polycrystalline silicon
a-Si	Amorphous silicon
TAN	Terrestrial Acidification/Nitrification midpoint category
TCO	Transparent Conducting Oxide
TE	Terrestrial Ecotoxicity midpoint category
TF	Thin Film PV technology

Symbols

η	PV module efficiency, %
EI	Overall environmental impact indicator
$FD_{i,d}$	Damage characterization factor for the impact category i in the damage category d
$FI_{s,i}$	Characterization factor for the substance s in the impact category i
M_s	Mass of substance s
N_k	Normalised score of the impact or damage categories k
PF_k	Weighting factor for impact category k
SD_d	Damage score for the damage category d
SI_i	Characterization score for the impact category i
VR_k	Reference value for the impact or damage categories k

2.1 Introduction

During the last years, climate change and other environmental threats have come more into focus by government and enterprises. Nowadays, environmental considerations are integrated as an important element in the evaluation of projects and other decision made by business, individuals, and public administrations. For this purpose, the development and use of environmental assessment and management techniques to better understand the environmental impacts are thus required. These techniques aim at identifying opportunities for reducing the environmental impacts and risks of projects, processes, products, and services.

Among the environmental assessment techniques, the methodological development in Life Cycle Assessment (LCA) technique has been strong, and LCA is now broadly applied in practice in several fields such as energy production.

LCA provides a well-established and comprehensive framework to compare renewable energy technologies with fossil-based and nuclear energy technologies (Akella et al., 2009; Bhat & Prakash, 2009; World Energy Council, 2004). The improvement among renewable energy technologies can also be compared by LCA (Akella et al., 2009; Bhat & Prakash, 2009). Even if renewable energy technologies are free of fossil fuel use and greenhouse gas (GHG) emissions during the energy generation phase, a considerable amount of energy and resources are generally consumed for the manufacturing of the different elements required to achieve the energy generation but also in the disposal of these elements at their end-of-life.

This chapter first discusses the environmental assessment of manufacturing processes used for PV modules by use of the LCA technique that will be further used to perform the environmental assessment of a PVGCS. Then, the manufacturing processes of the currently five most sold PV technologies (m-Si, p-Si, a-Si, CdTe and CIS) are described. Process knowledge is indeed considered as a cornerstone to properly apply the LCA methodology, since silicon production is highly energy intensive. To streamline the presentation of some processes which be exhaustive, some explanations

are as an additional focus. It is necessary to understand the bottlenecks of the manufacturing processes that are involved in the various technologies.

Subsequently, a literature review of some of the most common techniques for environmental assessment will be presented in order to better position the LCA technique. The fundamentals and principles of LCA will be thus described.

This chapter concludes with three examples of LCA studies. The first example assesses the manufacturing process of m-Si PV module from solar grade silicon production to the PV module assembly. In this example, the influence of the energy mix will be analyzed. A comparison of environmental impacts between the three crystalline silicon-based technologies (m-Si, p-Si and ribbon-Si) is proposed as a second example of application. Finally, the evaluation and comparison of five configurations of PVGCS are presented. The environmental model resulting will be then considered as the basis for the integration of environmental analysis in multi-objective optimization for sizing a large-scale PV system.

2.2 Manufacturing processes for PV technologies

The manufacturing process of the product or system under study is a key element of the environmental study in order to determine to the system boundaries and to identify the material and energy requirements and the associated emissions. In this section, the manufacturing processes of the main commercial PV modules technologies are described.

As mentioned in Chapter 1, PV technologies are classified according to first, second or third generation. Only, the first and second PV module generation will be taken into consideration because they correspond to more than 80% of the current PV global market. It must be highlighted that there is a lack of information on the manufacturing process of the third generation of PV modules for a reliable study. Several of the modules of the latest generation are still in development phase.

2.2.1 *Crystalline silicon technology*

Crystalline silicon (c-Si) PV modules are made from thin slice cells, called wafers, cut from a single crystal or a block of silicon. There are three main types of crystalline cells mono-crystalline (m-Si), polycrystalline or multi-crystalline (p-Si) and ribbon and sheet-defined film growth (ribbon-Si). The main difference between them is how the wafers are made.

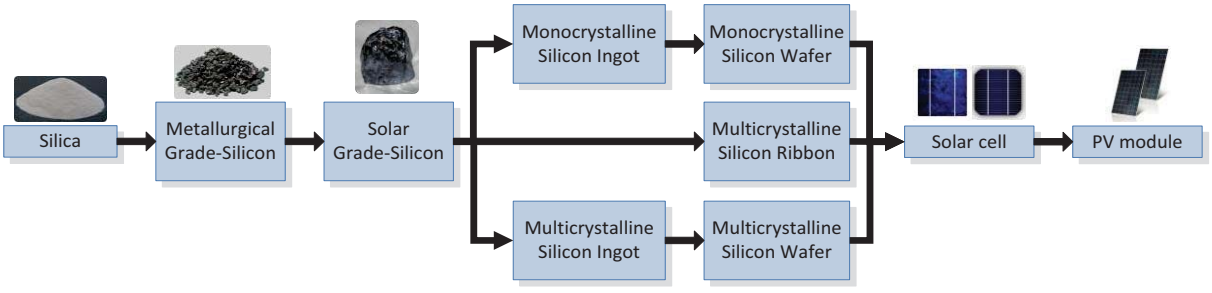

Figure 2-1 Production flow of crystalline silicon PV modules based on (de Wild-Scholten & Alsema, 2005)

Figure 2-1 contains the main stages of the manufacturing process for the three types of crystalline modules. The three technologies share the same process both at the beginning and end. The difference, as mentioned above, corresponds to wafer manufacturing process. Each step is described in detail (Luque & Hegedus, 2003; Singh Solanki, 2011):

Mining and refining of silica

Silicon is the second most abundant element in the Earth's crust. Quartz and sand are the raw materials for the production of silica (SiO_2). The mining of quartz or sand is a widely established technology. In this study, the process characteristics for this step are assumed identical for all three cases. After mining, the sand is transported, classified, scrubbed, conditioned, floated and deslimed.

Reduction of silica to Metallurgical Grade silicon

Silica is reduced to silicon with carbon by a thermal reaction according to:

$$SiO_2 + 2C \rightarrow Si + 2CO \quad (2.1)$$

The carbon used in the reduction is supplied by cokes, low ash coal and wood scrap. The reaction is made in an arc furnace at temperature of more than 1,600°C. The resulting silicon is primarily used in the metallurgical industry and is thus called metallurgical grade silicon (MG-Si). The MG-Si is 98% pure.

Production of Solar Grade silicon

MG-Si still contains too many impurities to be used in solar cell manufacturing. The polysilicon required for solar cells can be up to 99.999999% pure. This polysilicon is named Solar Grade silicon (SoG-Si). SoG-Si is usually produced by ether the Siemens process or fluidized-bed process. It important to highlight that less than 5% of worldwide MG-Si produced is used in making SoG-Si. Figure 2-2 summarizes the SoG-Si operations.

Production of wafers

The arrangement of Si atoms in SoG-Si and the size are yet not adequate. An atomic arrangement is needed to give a defined shape (circular or square) but also the final characteristics of PV module. The manufacturing process for each of the three crystalline silicon-based PV technologies is presented in Figure 2-3.

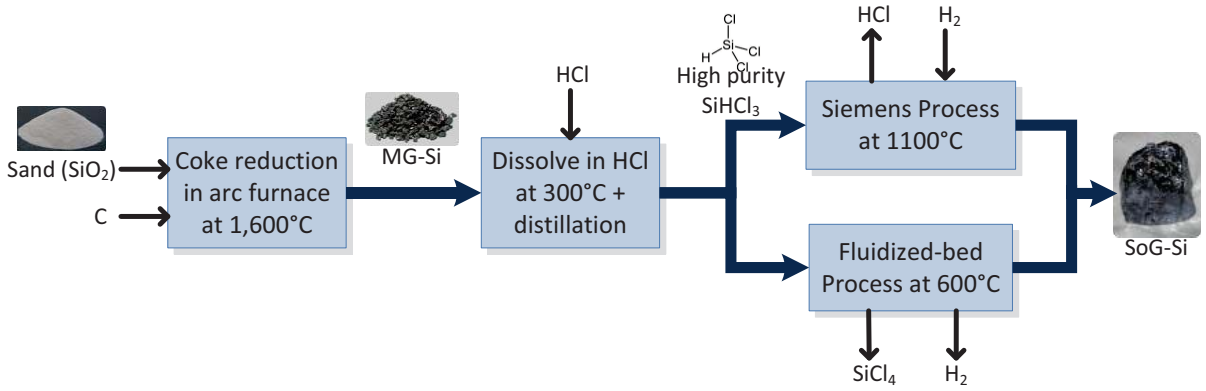

Figure 2-2 Main manufacturing processes of SoG-Si

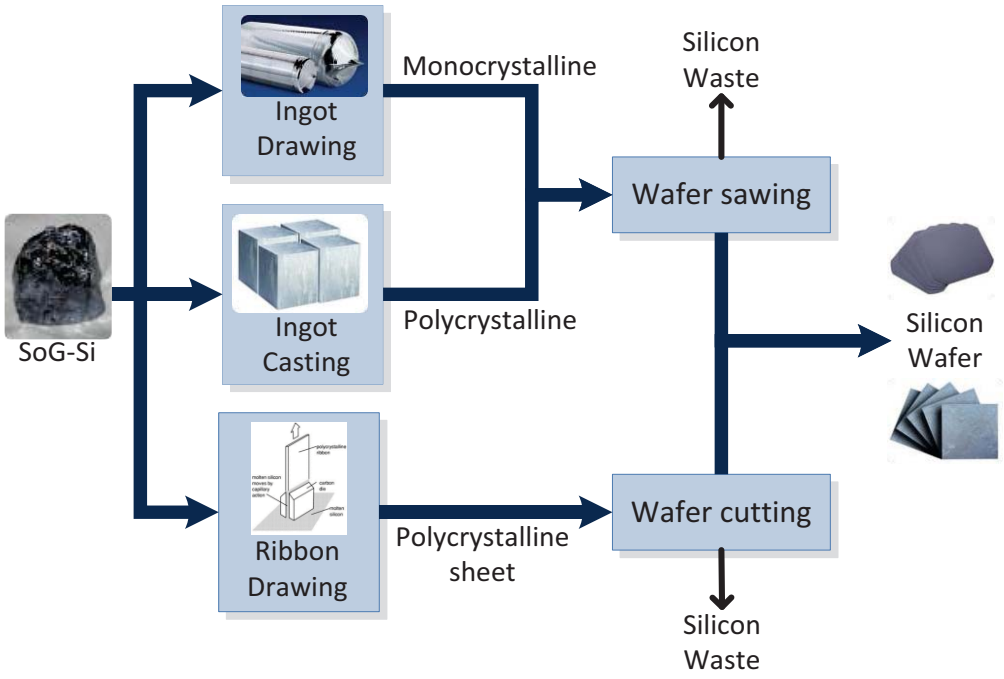

Figure 2-3 Manufacturing processes of silicon wafer

Focus on SoG-Si solidification processes

First, a High Purity Si Containing Gases is needed for both processes. MG-Si is pulverized in fine power and reacted with anhydrous hydrogen chloride in a fluidized-bed reactor at 300°C in the presence of catalyst. During the process, trichlorosilane ($SiHCl_3$) and several other unwanted chlorides are formed, following an exothermic reaction:

$$Si + 3HCl \rightarrow SiHCl_3 + H_2 + Heat \quad (2.2)$$

In the next step, using a fractional distillation, $SiHCl_3$ is easily separated from the other impurities.

a/ Siemens process

The high purity trichlorosilane is converted in solid SoG-Si by chemical vapor deposition (CVD) process. Solidification of Si is done using a Siemens type reactor. In a Siemens reactor, a thin Si rod is heated at more than 1,100°C. A mixture of $SiHCl_3$ and H_2 is introduced in the chamber and the $SiHCl_3$ is reduced following the equation:

$$2SiHCl_3 + 2H_2 \rightarrow 2Si + 6HCl \quad (2.3)$$

As the process continues, the Si rod becomes thicker and thicker. The rod rises to 30 cm in diameter and 2 m in length. The deposited Si is of polycrystalline type.

b/ Fluidized-bed process

In fluidized-bed process, the $SiHCl_3$ is decomposed in silane according to:

$$4SiHCl_3 \rightarrow SiH_4 + 3SiCl_4 \quad (2.4)$$

Using a CVD in a fluidized-bed reactor silane is converted into solid SoG-Si. In this process, silane is solidified using Si seed particles. At 600°C, the gas phase

decomposition of silane takes place by reaction (see Equation (2.5)) and the Si atoms get deposited on the floating seed particles.

$$SiH_4 \rightarrow Si + 2H_2 \quad (2.5)$$

The particles grow up to 2 mm in size. When the weight of the Si particles is high enough, they fall on the bottom of the reactor, where they are collected for further use.

Focus on CZ/FZ processes

In CZ process, the SoG-Si is placed in a quartz crucible. Si is melted by induction heating and then cooled to form a long solid block called an ingot. A seed crystal gives the arrangement of Si atoms. Melts attain a temperature or more than 1,400°C. The ingot's diameter can reach be up to 300 mm. The length of ingot is 1 or 2 m. CZ process is the most commonly used process for ingot pulling.

In FZ process, the contact of melt with any crucible is avoided. The melt zone is a float zone. A seed crystal is melted with polysilicon rod using induction heating. As the process proceeds, the heated zone is moved upwards. The left behind melted zone solidifies in the form of m-Si ingot.

The m-Si wafers have a regular, perfectly-ordered crystal structure. To achieve this configuration, two processes are generally used: Czochralski process (CZ process) and float zone process (FZ process).

The p-Si wafers have square shape. This allows higher packing density of cells in the module. In p-Si ingots manufacturing process, SoG-Si is melted and poured into a square-shaped SiO-SiN-coated graphite crucible. The controlled directional solidification of the crucible results in p-Si block consisting of several smaller crystallites of varying sizes and orientation.

The m-Si and p-Si ingots need to be diced in order to obtain Si wafer. A wire saw is used to slice the wafer from the ingot. The saw is about the same thickness as the wafer. This method of slicing produces significant wastage up to 40% of the silicon (known as kerf loss).

Ribbon/sheet-Si produce wafer equivalent sheets directly from high purity polysilicon (without growing ingots and then sawing). The main problems found in this process are as follows: the required purity level could not be achieved and many defects are created in the crystal during the crystallization process.

The *edge defined film-fed growth (EFG)* technique is the most advanced for producing thin sheets of Si. Here a thin sheet is pulled from molten Si. The sheet is formed by the capillarity action of molten Si, and capillarity is defined by a graphite die. The material quality obtained is similar to p-Si. The Si sheet thickness is about 250 μm. The Si wafers are cut using laser scribing. The use of a laser cutter reduces kerf loss.

Focus on Transforming the wafer into a solar cell

The solar cell is the unit that produces electricity. It is created using four main steps:

a. Surface treatment: The wafer's top layer is removed to make it perfectly flat.

b. Creation of the potential difference (p-n) junction.

c. Deposition of an anti-reflective coating.

d. Add metal grid (metallization)

Focus on Module manufacturing

The solar cells are placed between layers of coating material to protect them from the environment and breakage. Transparent glass is used for the front, while a weatherproof backing (typically a thin polymer) is applied to the back of the module. The cover is attached using thin sheets of ethylene vinyl acetate (EVA). Frames can be placed around the modules to increase their strength.

2.2.2 *Amorphous silicon thin-film*

The amorphous silicon or a-Si material has become an interesting material when it was discovered that its conductivity can be changed. The term "amorphous" is given to non-crystalline materials prepared by deposition from gases. The a-Si alloyed with hydrogen (a-Si:H) shows a very high absorption coefficient in the visible range and requires only about a micron thick layer. The manufacturing process of a-Si-based PV modules has a similar beginning to PV modules based crystalline silicon (Section 2.2.1). Figure 2-4 represents the manufacturing process flow for a-Si:H-based PV.

Mining and refining of silica and MG-Si process are the same as used for obtaining PV modules of c-Si. Silane (SiH_4) is produced in a fluidized-bed process according to the reaction (2.4). The remaining steps are detailed in the boxes (Luque & Hegedus, 2003; Markvart & Castañer, 2003; Singh Solanki, 2011).

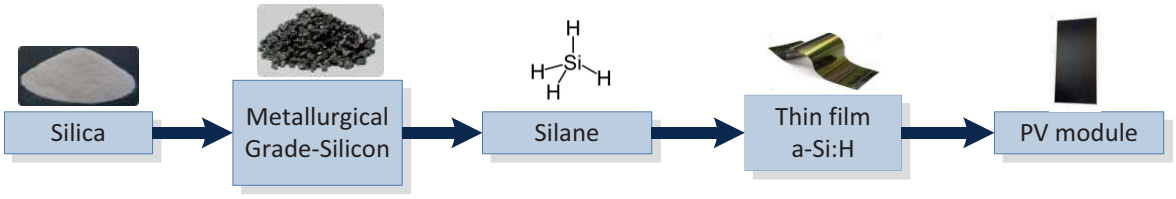

Figure 2-4 Production flow of a-Si PV modules

Focus on thin film single junction a-Si:H

The key component is deposition of a-Si:H layer with desired composition and thickness. Radio frequency plasma enhanced chemical vapor deposition (RE-PECVD) technique is the most commonly used to deposit the a-Si:H film. Figure 2-5 shows a typical RE-PECVD chamber. In this process, a mixture of SiH_4 and H_2 flows into a vacuum chamber that is evacuated by a pump. Two electrode plates are installed inside, and a radio frequency power is applied between them in which plasma will occur. The plasma excites and decomposes the gas and generates radicals and ions in the chamber. Various substrates may be mounted on one or both of the electrodes, and thin hydrogenated silicon films grow on the substrates as these radicals diffuse into them. The substrates are heated to achieve optimum film quality.

The typical parameters for obtaining high quality a-Si:H using RE-PECVD are the following one: silane flow of 20 sccm to 50 sccm (standard cubic centimeters per minute), chamber pressure of 0.5 to 1 Torr, substrate temperature of 150 – 350°C, RF power should be 20 – 50 $\mu W/cm^2$, electrode to substrate distance between 1-3 cm. A typical deposition rate is 0.1-0.2 nm per second. About 300 nm thickness of absorbed layer is required.

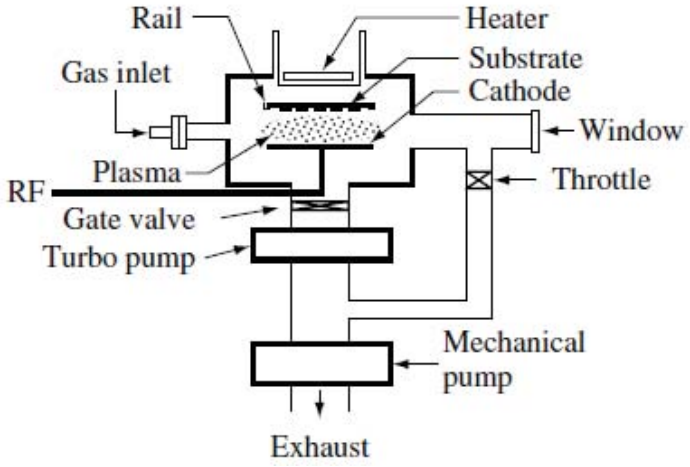

Figure 2-5 Principle of a RF-PECVD deposition tool (Luque & Hegedus, 2003)

Focus on module manufacturing

The process consists of four steps: substrate washing, sputter deposition of the back reflector, a-Si semiconductor deposition, and the transparent conducting oxide (TCO) deposition. At the end of TCO deposition process, the a-Si solar cell is cut by a slab cutter. It is then covered with EVA and Tefzel (a modified ethylene-tetrafluoroethylene fluoroplastic), and vulcanized in a furnace for lamination. This is then followed by selected module framing. The typical structure of a.Si:H solar cell is given in Figure 2-6.

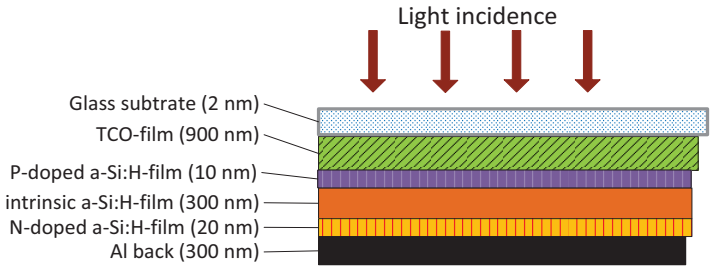

Figure 2-6 Structure of a-Si:H-based solar cell (Singh Solanki, 2011)

2.2.3 *Cadmium Telluride thin-film*

The CdTe (cadmium telluride) is a binary compound semiconductor of Cd (cadmium) and Te (tellurium). It is typically deposited in polycrystalline form. Due to a high absorption coefficient, a maximum thickness of about 1μm of material is required. CdTe layers are chemically and thermally stable and are less prone to efficiency degradation.

CdTe is manufactured from pure Cd and Te, both of which are by-products of smelting prime metals (e.g. Cu, Zn, Pb, and Au). Figure 2-7 shows a flow diagram from raw material acquisition to manufacturing stage of CdTe-based PV module. First cadmium production process will be described from Zn production. The different steps are detailed below (V. M. Fthenakis, 2004; V. Fthenakis, Wang, & Kim, 2009; Luque & Hegedus, 2003; Markvart & Castañer, 2003; Singh Solanki, 2011).

Mining zinc ores

Cadmium minerals are not found alone. They are mainly generated as a by-product of smelting zinc ores. Zinc is found in the earth's crust as zinc sulfide (ZnS). Zinc ore contains, beside Zn, Cd, Cu, Pb, Ag and Fe. The ore is excavated by drilling machines, processed through a primary crusher, and then conveyed to surface where is screening and milling to reduce the ore to powder. The particles are separated from the gangue and concentrated in a liquid medium by gravitation and/or selective flotation, followed by cleaning, thickening, and filtering.

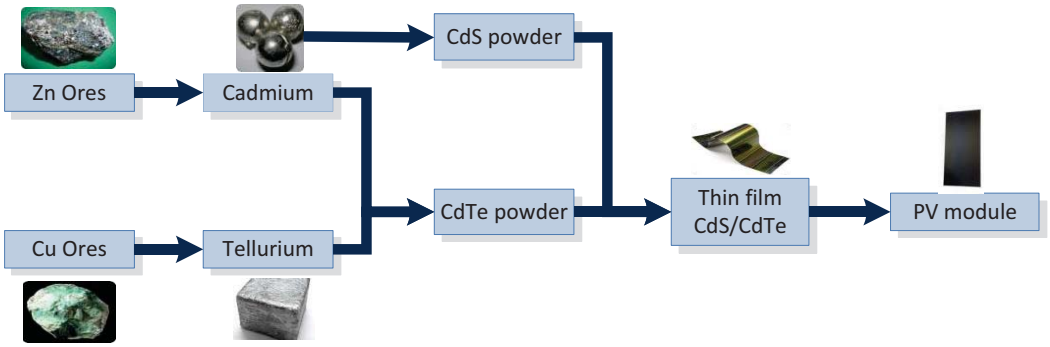

Figure 2-7 Production flow of CdTe PV modules (V. Fthenakis et al., 2009)

Cadmium production

Zinc concentrate is transferred to smelters/refiners to produce the primary metals. Sulfuric acid and other metals, e.g. Cd, are frequent by-products from most smelters. Zn can be refined by either pyrometallurgical or hydrometallurgical treatment. The process consists of five steps but only the first three are important for Cd production (see Figure 2-8).

Tellurium minerals, as Cd, are not found alone. It is a rare metal than can be extracted as by-product of processing copper ores. The production process for Cu is described to explain Te production.

Mining copper ores

Primary Cu is obtained mainly from sulfide ores. Cu ores contain, beside Cu, Fe, Te, Se, Mo, Ag and other metals. The ore is mined then it is crushed, ground and concentrated. In concentrated process, ground ore is slurred with water. The process continues as described in Figure 2-9.

Purification of Cd and Te

Metallurgical grade Cd and Te (i.e. 99.99% pure) metal is used in current applications except for semiconductor materials that require higher purity. To elaborate semiconductor CdTe, a high purity (i.e. 99.9999%) of Cd and Te powders are needed. Purification can be made by electrolysis and subsequent melting and atomization or by vacuum-distillation followed by zone refining.

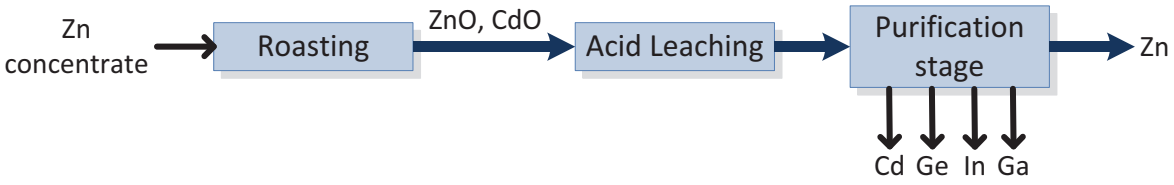

Figure 2-8 Flows in Zn refining (V. Fthenakis et al., 2009)

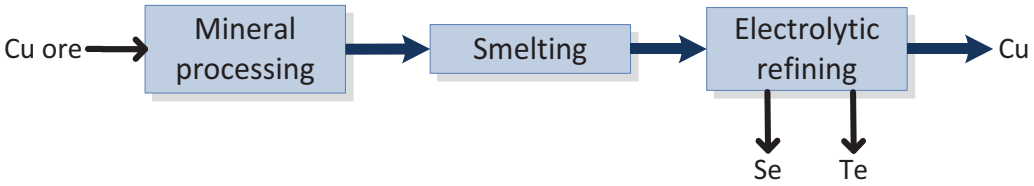

Figure 2-9 Extractive metallurgy of Cu (V. Fthenakis et al., 2009)

Focus on cadmium production steps

a/ Roasting. Oxidizing roast at high temperature removes sulfur and converts the zinc, iron, cadmium, and other metals to oxides. The concentrates are fed to fluidized-bed furnaces where they are burnt with air and direct oxygen. Zinc calcine, mainly composed by Zn oxide with small amount of Fe, Cd, and others metal is cooled, passed through a mill and collected in cyclones and electrostatic precipitators.

b/ Leaching. Leaching of the metals from the calcine is accomplished by sulfuric acid. This process dissolves the zinc to make a solution of zinc sulfate and other acid-soluble

metals. The leachate, that contains Cd, is sent to the purification section.

c/ Purification. Cd, Ge, In and Ga are removed. The Cd extracted at this step is formed into briquettes that then are melted. This refining Cd has metallurgical grade (99.95% pure) and is cast and cut into sticks.

Focus on tellurium production

After separation, Cu is transferred to smelters where it is processed in furnaces. Impurities in Cu typically include Se and Te. Cu production follows with either pyrometallurgical or hydrometallurgical refined process. The pyrometallurgy of Cu is a multistage process, beginning with the mining and concentrating of low-grade ores, and followed by smelting and electrolytic refining to produce a pure copper cathode (see Figure 2-9). In electrolytic refining, the impurities are separated by electrolysis in a solution containing copper sulfate and sulfuric acid. The metallic impurities precipitate forming sludge. The sludge contains Cu, Te, Se and other metals. Oxidative pressure-leaching with dilute sulfuric acid at 80–160°C is used to remove Cu and 50-80% of Te. Tellurium is recovered from solution by cementation with copper. Copper telluride is leached with caustic soda and air to produce a sodium telluride solution. The latter is used as the feed for producing commercial grade Te metal or TeO_2.

Focus on thin-film CdTe/CdS

CdTe is commonly deposed using Closed Space Sublimation (CSS) process, also known as Closed Space Vapour Transport (CSVT). A schematic CSS process is shown in Figure 2-10. It contains a CdTe plate (source plate) which is transported to the substrate in vapour form. The driving force for transfer is the temperature difference between the source (650-750°C) and the substrate (600°C). The pressure is about 10 Torr. The space between both plates lies between 1-15 µm and the growth rate is 1-5 µm/min. An inert gas such as N_2, Ar, or He is used for CCS. CdS film can be deposited by the same process as CdTe.

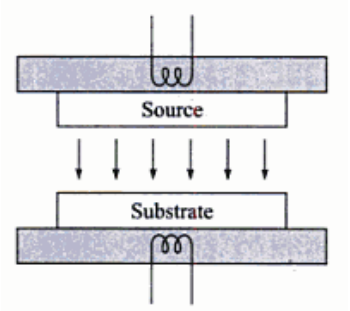

Figure 2-10 Schematic CSS deposition tool (Singh Solanki, 2011)

Focus on module manufacturing

The cells are deposited in superstrate arrangement (see Figure 2-11). The process starts with transparent conducting oxide (TCO) coated glass layer, such as SnO_2 at around 250°C. After cleaning the TCO layer, the area of the cell is defined by laser scribing. Then, an n-CdS film is deposited, followed by the p-conducting CdTe film at about 500°C. The absorbed layer is laser scribed according to cell area defined by first laser cut. The junction is activated with a $CdCl_2$ treatment. The treatment consists of doping of solution of $CdCl_2$ in methanol onto CdTe coated substrate, letting the methanol solvent evaporate and heat treating the substrate at 450°C for 15 min. Then, back metal layer is deposited. Another laser cut is made in which the series connection of solar cell get completed. The last step is encapsulation with EVA and finally covering of the module with top glass cover.

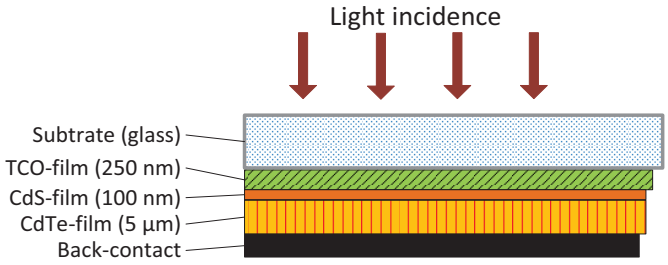

Figure 2-11 Structure of CdTe-based solar cell (Singh Solanki, 2011)

2.2.4 *Copper Indium Selenide (CIS) thin-film*

$CuInSe_2$-based solar cells is a promising solar cell technologies due to its low-cost, high-rate semiconductor deposition over large areas using layers only a few microns thick and for fabrication of monolithically interconnected modules. Perhaps more importantly, very high efficiencies have been demonstrated with CIS at both the cell and the module levels in laboratory. The performance is increased by adding gallium (Ga) to the compound, thus making it $Cu(In,Ga)Se_2$ or CIGS.

The CIS manufacturing process is summarized in Figure 2-12. Indium (In) and Ga can be acquired as by-products of the production of Zn. About 5% of the global production of gallium is obtained from residues in zinc processing but 95% of the global supply is obtained as a by-product of alumina production from bauxite. Selenium (Se) is obtained as by-product from Cu ores. Processes for Zn and Cu were described in the previous section. In Figure 2-8, In and Ga production starts during the purification process of Zn. As indicated in Figure 2-9, Se is obtained during the electrolytic refining process for Cu. The next steps for the manufacture of CIS-based PV module are described in respective boxes (V. M. Fthenakis, 2004; V. Fthenakis et al., 2009; Luque & Hegedus, 2003; Markvart & Castañer, 2003; Singh Solanki, 2011). The copper production process was described in the previous section and the process flow is given in Figure 2-9.

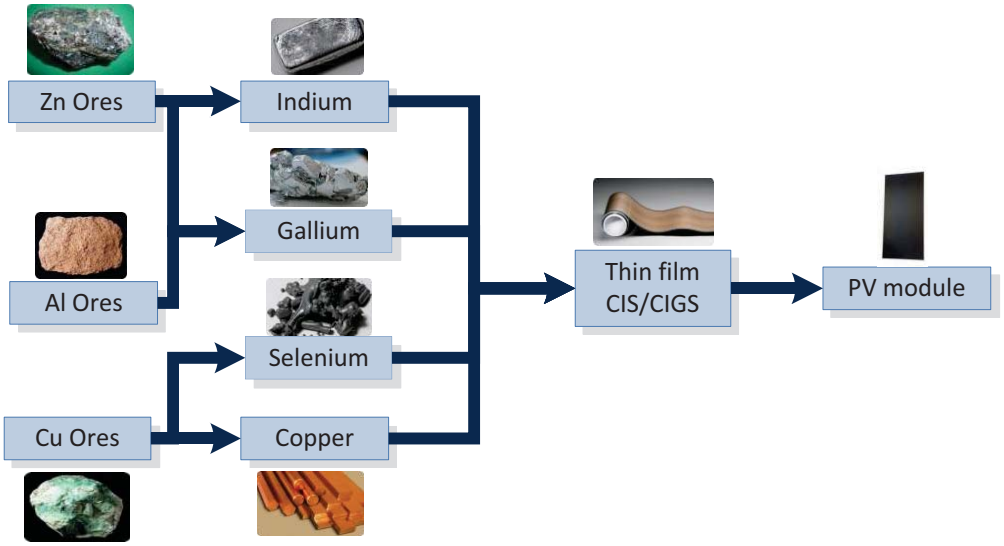

Figure 2-12 Production flow of CIS PV module

Focus on indium production

Soda is added to the residue resulted in the purification process of Zn that contains particles of In in order to precipitate it. About 10% of In remains in the residue, which is leached with sodium hydroxide to create crude indium hydroxide. The crude indium hydroxide is leached with dilute hydrochloric acid. The solution is purified by cementation of copper and arsenic with iron, followed by cementation of tin and lead with indium. Finally, In is removed by adding aluminium to create indium cement. Further purification is done by electrolysis to produce high purity grade (99.9999%). Figure 2-13 represents the production process of In.

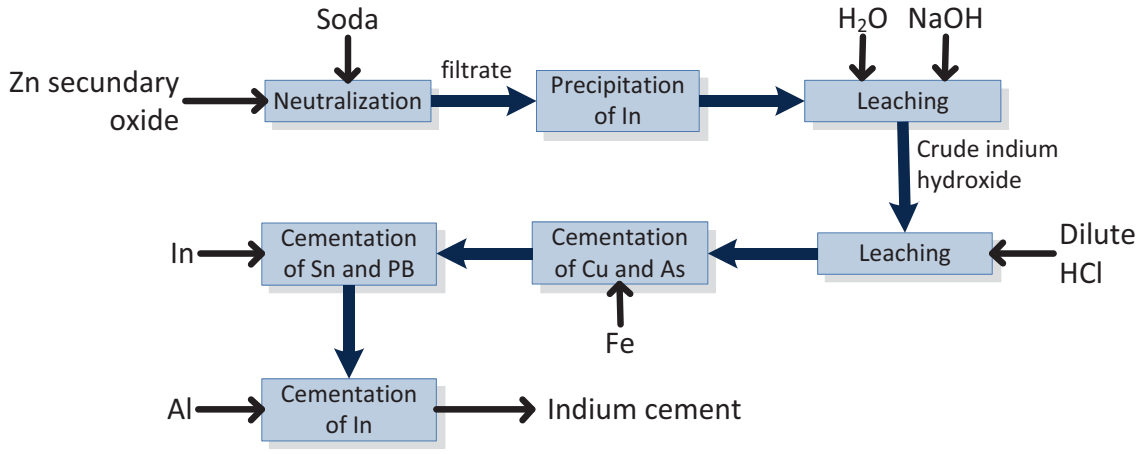

Figure 2-13 Process flows for In production (V. Fthenakis et al., 2009)

Focus on gallium production

Most gallium is extracted from the crude aluminum hydroxide solution of the Bayer

process for producing alumina (see Figure 2-14). In the Bayer process, bauxite is digested by washing with a hot solution of sodium hydroxide (NaOH) at 175°C under pressure. This converts the aluminium oxide in the ore to soluble sodium aluminate. The solution is clarified by filtering off the solid impurities, commonly with a rotary sand trap, and a flocculent such as starch, to get rid of the fine particles. The alkaline solution is cooled and treated by bubbling carbon dioxide into it, through which aluminium hydroxide precipitates. Gallium is separated by selective precipitation. Hydrochloric acid is used to dissolve gallium from the metal hydroxides. Then the gallium is separated by solvent extraction with ether. Finally, the crude gallium is recovered by electrolysis. The metal produced can be purified by melting in temperature controlled vessels.

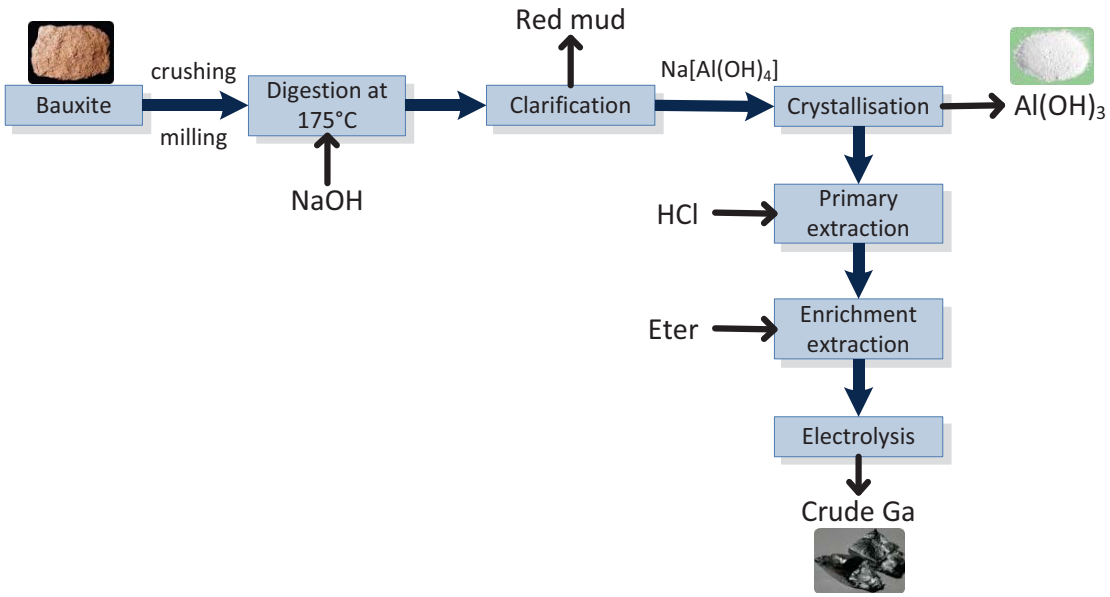

Figure 2-14 Process flows for Ga production (V. Fthenakis et al., 2009)

Focus on selenium production

It is recovered as a by-product, mostly from the anode slimes in the electrolytic refining of copper. Two major processes of extracting selenium from copper refinery slime include roasting with soda ash and roasting with sulphuric acid. Soda ash roasting is a traditional method to recover selenium. This method is described in Figure 2-15.

Electrolytic copper refinery slimes are intensely mixed with soda ash binder and water to form a paste which is roasted at 530-650°C. Then the paste is leached in water to dissolve sodium selenate. Residues are separated from the selenate with filtration. Sulphuric acid is used to remove the impurities in hydrolysis. Hydrochloric acid or ferrous iron salt is used for the reduction of hexavalent selenium. Iron chloride is discarded, which contain small amounts of selenium but is also extremely corrosive and creates problems for disposal. The remaining solution is precipitated with sulphur

dioxide and then filtrated. The final steps are melting and shooting to produce selenium metal.

After Se is extracted from copper refinery slimes, the average purity is approximately 99%. For photovoltaic, the simplest and the most common method of achieving 99.99% pure selenium is vacuum distillation.

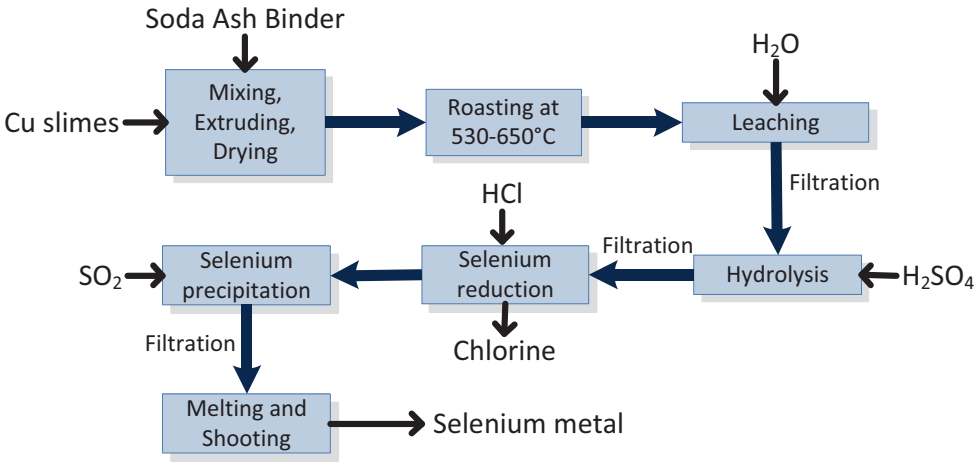

Figure 2-15 Process flows for Se production (V. Fthenakis et al., 2009)

Focus on thin-film CIS/CIGS

The CIGS absorbed layer is commonly deposited with co-evaporation techniques (see Figure 2-16). The substrate in the co-evaporation process reaches a temperature range between 400 and 600°C. In this process, all the elements are evaporated together on the substrate. The deposition of the material and formation of the compound happens together. This is achieved by thermal evaporation from elemental sources at temperatures greater than 1,000°C for Cu, In and Ga. A mass controller is used. The CIGS absorbed layer thickness is about 2 μm.

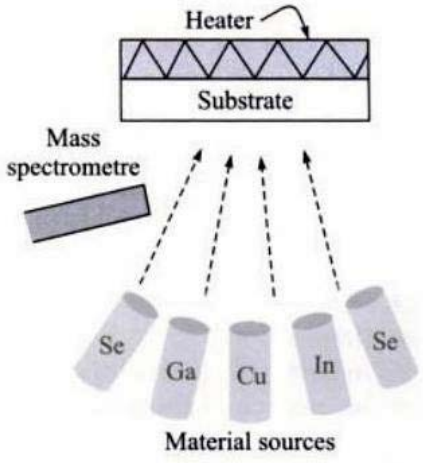

Figure 2-16 Deposition of CIGS layer using co-evaporation (Singh Solanki, 2011)

Focus on module manufacturing

The process starts with the deposition of the absorber layer on the molybdenum coated glass substrate. A soda-lime substrate composed of about 70% silica, 15% sodium oxide, 9% calcium oxide, and 6% of others compounds is chosen due to the importance of Na. The CIGS layer is deposited. After the absorbed layer, the buffer layer of CdS is deposited using chemical bath deposition (CBD) method. On the top of CdS buffer layer, a TCO layer is added. The ZnO is typically used as TCO.

Finally, the electrical wire and buss bars are attached. These are metal stripes that can be soldered, welded, or glued to contact areas near the edges of the substrate plates. Lamination with a front cover glass, which is usually EVA is next. Edge sealing and framing finished the product. The arrangement of CIS-based solar cell is found in Figure 2-17.

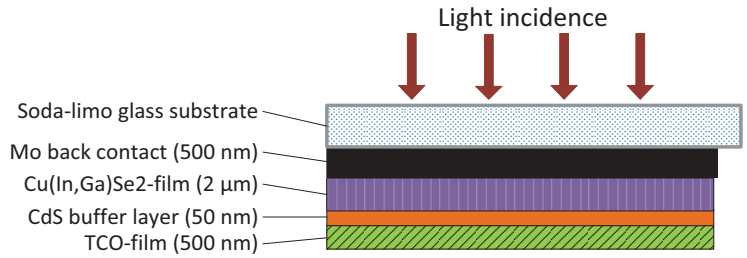

Figure 2-17 Structure of CIS-based solar cell (Singh Solanki, 2011)

2.2.5 *Discussion*

A valid question raised in scrutinizing technologies regarded as environmentally friendly is whether they are truly "sustainable" or not. For alternative energy systems in particular, this query translates in one key sense to whether they represent a net gain – do they generate more energy than was used to create them in the first place and if so to what extent?

From the description of the manufacturing processes for the top five PV modules technologies describe above is possible to note the large amount of energy that is required for both the production and purification of the raw material to obtain the degree of purity that allows them an efficient conversion energy, and the high temperatures required for each one of the processes for the manufacture of the module.

When comparing the embodied primary energy of the five production processes from the information above, it is emphasized that technologies based on c-Si (m-Si and p-Si mainly) are those that require the highest amount of material and energy on the one hand by the dimensions and thickness of the module and on the other hand by the purification process and growth of Si to form the ingot that subsequently will be transformed into the wafer.

The main advantage presented by the TF PV modules is related, because of their thickness, to the smaller amount of material and energy needed for manufacturing them. As mentioned in the previous

chapter, the combination of less materials and energy needed to manufacture a PV module results in a much lower cost on manufacturing and therefore a lower price compared to c-Si PV modules.

Some works try to answer if indeed the energy produced by a PV module during its lifetime is enough to offset the amount of energy they consume during the manufacturing process (Ayompe, Duffy, McCormack, & Conlon, 2010; Dale, 2012; Knapp & Jester, 2000; Lloyd & Forest, 2010; Nawaz & Tiwari, 2006). They conclude that not all financial cost reductions lead to reductions in embodied energy, an economic analysis should be supplemented with energy analysis. Also PV systems with lower energy costs provide more net energy.

The net gain concept must be extended as well to pollutants (e.g. SOx, NOx, particulates) or global greenhouse gas emissions (e.g. CO_2). A truly sustainable technology should represent a net gain to the humanity that wish to continue its standard of living, historically correlated with energy use. The presentation of environmental assessment techniques is then proposed in what follows to identify the method that will be selected.

2.3 Environmental assessment techniques

According to Sadler (Sadler & Verheem, 1996), environmental assessment is defined as "a systematic process for evaluating and documenting information on the potentials, capacities and functions of natural systems and resources in order to facilitate sustainable development planning and decision making in general, and to anticipate and manage the adverse effects and consequences of proposed undertakings in particular". There are many different procedures and methods to assess the environmental issues or impacts of plans, projects and programmes. Table 2-1 summarizes some of these techniques.

Among the techniques mentioned in Table 2-1, LCA is the most well-known and powerful tool (Finnveden et al., 2009; Heijungs, Huppes, Zamagni, & Masoni, 2011; Manuilova, Suebsiri, & Wilson, 2009). Studies have shown that LCA can complement and add value to the other techniques (Finnveden et al., 2009; Manuilova et al., 2009). There is no single tool or approach to address all the problems of environmental management. The Society of Environmental Toxicology and Chemistry (SETAC) conducted a discussion within a working group in order to define the relationship of LCA with the others techniques (Heijungs et al., 2011).

In addition to the advantages described, LCA employs many of the principles of the other techniques, e.g. LCA always requires to establish the inventory of flow of materials and substances as MFA, some of the LCA methods to assess the human health impacts use ERA principles, LCA shares with the EIA and MILP the use of characterization indices and impact factors.

Furthermore, LCA allows the comparison between different environmental impacts through design of alternative scenarios or making the comparison of different product's processes that perform the same function. These reasons explain why LCA has been selected as an environmental assessment technique in this work. A more detailed description of the LCA technique will be discussed in the following section of this chapter.

Table 2-1 Environmental assessment techniques

Method	Description and key points	Strengths	Weaknesses
Cost-benefit analysis (CBA) (Burgess & Brennan, 2001; Hanley & Spash, 1993; Pearce, Giles, & Mourato, 2006)	Constitutes an "environmental economics" approach. This approach tries to estimate the economic value of any loss (cost) or gain (benefit) of environmental quality to use these values in the traditional costs and benefits evaluation of a project. Determines whether and how much a project can contribute to national economic welfare, which of several options should be selected for action, and when the investment is to be executed. The essential steps are: defining the project, identifying economically relevant impacts, physically quantifying impacts, calculation monetary valuation, discounting, weighting, and sensitivity analysis.	- The effect of time is considered. - Decision makers are already familiar with monetary units.	- Many environmental cost and benefits cannot easily be quantified. - Some of the traditional elements of the CBA are questionable as for environmental analysis ,e.g. discount rate - Some valuation techniques are unlikely to be practicable in the framework of most current engineering design decisions.
Environmental Impact Assessment (EIA) (Burgess & Brennan, 2001; Kessler, 200AD; Manuilova, Suebsiri, & Wilson, 2009)	Analyses and evaluates the positive and negative impacts that human activities can have on the environment. Considers all possible environmental and socio-economic issues associated with the proposed project in a qualitative and quantitative way. Provide decision makers with the resulting information. Uses environmental indices. EIA has three major phases: screening and scoping of the project, environmental impact assessment, and decision-making and review.	- Environmental damage of the project can then be minimised and any environmental benefits identified. - Considers local impacts. - EIA is a systematic process.	- A specific site and time must be defined to estimate environmental impacts. - Only direct impacts that fall within the boundaries of the system under study are analysed. - Rigorous and quantitative analysis of the data is often required to make sense of the large amounts of uncollected data. - It is more a legal procedure than a detailed environmental assessment tool.
Exergy analysis (Brunner & Rechberger, 2011; Szargut, 2005)	Measures the maximum amount of work that can be obtained by bringing a resource into equilibrium with its surroundings through a reversible process	- Provides information to identify the location, resources and causes of problems form deviations of the ideal system in balance.	- Only focuses a thermodynamic viewpoint. - Complexity in defining the reference state (ideal system in balance).

Table 2-1 Continuation…

Method	Description and key points	Strengths	Weaknesses
Life Cycle Asseessment (LCA) (Ayres & Ayres, 2002; Finnveden et al., 2009; Manuilova et al., 2009)	Identifies and quantifies the process flows and systems which are major contributors to environmental degradation. Encompasses extraction and processing of raw materials, manufacturing and assembly processes, product distribution, use, re-use, maintenance, recycling and final disposal Regulated and guided by the ISO norm. Four main steps are comprised: goal and scope definition, inventory analysis, impact assessment, and interpretation.	- Considers a range of environmental impact categories. - Total economic and environmental burdens of a process can be quantified by performing an LCA in conjunction with a techno-economic feasibility study. - A non-site-specific approach to environmental impacts is required - Long term strategic planning - Identifies the areas for improvement which will have the greatest influence on total life cycle impacts	- Lack of data can restrict the conclusions that can be drawn from a specific study. - The intrinsic risks of the processes are not addressed. - LCI data must be used cautiously since production processes differ from country from country.
Material Flow Analysis (MFA) (Ayres & Ayres, 2002; Brunner & Rechberger, 2011)	Delivers a complete and consistent set of information about all flows and stocks of a particular material within a system. Is based on two fundamental principles: system approach and mass balance. This permit to create a list of the amounts of the different flows. Usually comprises four steps: goal and systems definition, process chain analysis, accounting and balancing, modelling and evaluation.	- The analysis can be applied at industrial, national or worldwide scale. - Requires the history of pollution and consumption of resources in an area or region. - Mass balance are required to evaluate the stock of material ignored or underestimated.	- Focus on a single material. - To determine the environmental impacts a LCA or exergy analysis is needed.
Material Intensity Per unit Service (MILP) (Brunner & Rechberger, 2011; Ritthof, Liedtke, & Merten, 2002; Schmidt-Bleek, 1993)	Measures the total mass flow of material caused by production, consumption and waste disposal of defined service unit (fabrication of a kitchen, washing cycle of a dishwasher,…) or product. Only uses the input flows (consider input flows equal to output flows). The material input is calculated in five categories: abiotic raw materials, biotic raw materials, water, erosion, and air. All material consumption during manufacture, use and recycling or disposal is calculated back to resource consumption by using simple calculation factors expressed in kg or ton. The aim is to reduce the total amount of the addition of all the material and energy flows expressed in kg or tons.	- Allow comparisons of resource consumption of different solutions to produce the same service. - Reveals the magnitude of resource use along the life-cycle and help to focus efforts on the most significant phases to reduce environmental burden of the product. - Measures material and energy in the same unit constitutes an excellent communication tool to identify the main problems.	- Does not take into account ecotoxicity of materials or biodiversity.

2.4 LCA Methodology

As abovementioned, Life cycle assessment (LCA) evaluates the environmental impacts of products, processes and services. The results of LCA can identify major emissions, thereby enabling consideration of measures for their reduction.

LCA evaluates the material and energy flows involved in the whole life cycle of the product as it is represented in Figure 2-18. It is possible to classify them in:

- Elementary flows: consist of flows that each process exchanged with the ecosphere: *primary resources* as water, fuels, minerals..., and *waste emissions* as solid waste, effluents and gaseous emissions.
- Intermediate flows: material or energy flows between the different stages of the life cycle.

For an adequate interpretation of the results that will be generated by an LCA, the goal must be appropriately defined and will guide the LCA operator to manage and focus the efforts to collect the information that best suit the purpose and interpret the outcomes appropriately.

For Jolliet et al. (Jolliet, Saadé, & Crettaz, 2010), LCA evaluates the environmental impact of a product, service or system related to a particular function, considering all stages of its life cycle. It identifies all the points on which a product can be improved and it contributes to the development of new products.

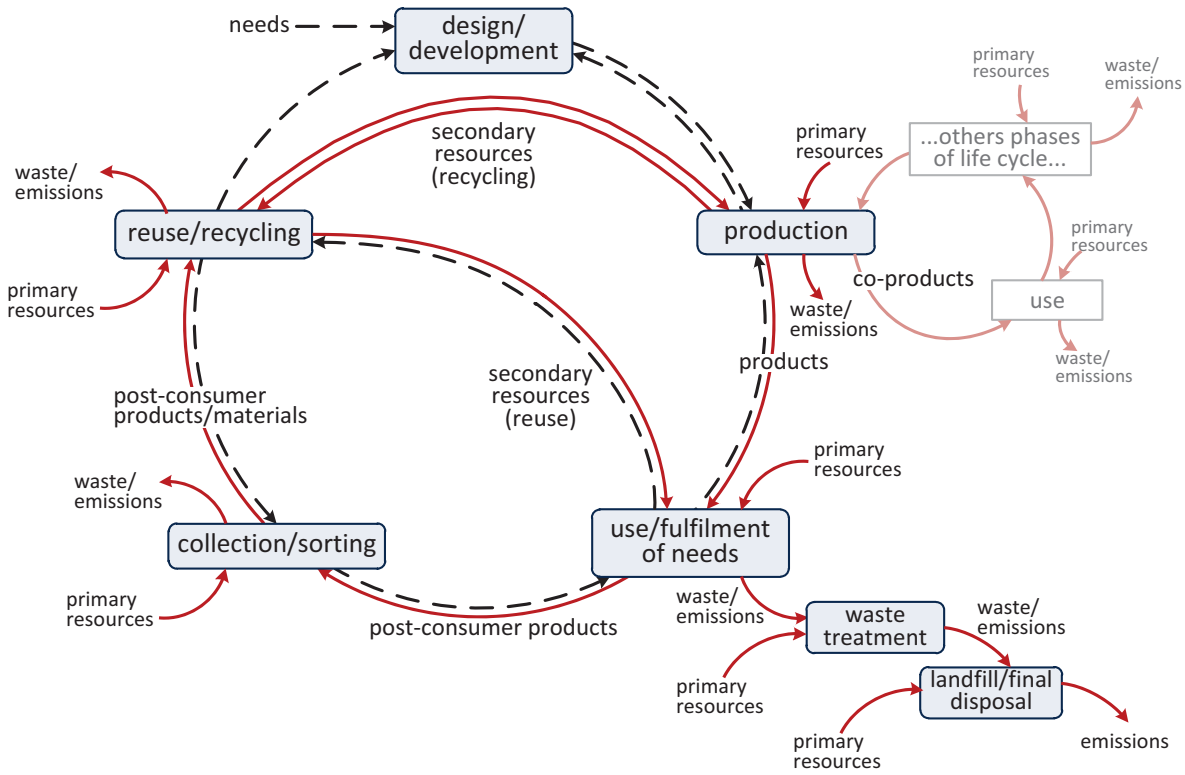

Figure 2-18 Schematic representation of the life cycle of a generic product (based on (Rebitzer et al., 2004))
(the full arrows represent material and energy flows, while the dashed arrows represent information flows, the presence of a secondary life cycle (in watermark) shows that several life cycles can be nested into each other).

From the LCA investigations that were already implemented and mentioned in numerous studies, (Jolliet et al., 2010) for instance, several strengths of the LCA methodology can be highlighted.

- In eco-design, LCA can help to take into account environmental criteria during the design phase of a new product or product improvement already created. This is typically one of the first motivations of this work.
- In the evaluation and improvement of product, LCA can identify critical areas on which it is possible to focus to optimize the environmental performance and to compare different manufacturing processes.
- LCA can also be useful to obtain elements of decision support for the implementation of industrial policy (choice of design, product improvement, selection of procedures, etc..) or public policies (choice of recovery processes, eco-labelling criteria, etc..).

The objective of this study is to develop an environmental module for PV modules based on LCA that reflects the different options in PV manufacturing, based on existing data.

Two main advantages can be found by using LCA for PV systems:

1. When using LCA, the system can be optimized from an environmental viewpoint taking into account CO_2 emissions, human health impacts and effects on the local fauna and flora ….
2. The second advantage is comparability. When comparing energy generation technologies (e.g., when searching for the installation of a PV system as a supply of alternative energy as opposed to other generation systems, or when installing energy supply systems based on multiple generation technologies), LCA can provide quantitative results, thereby enabling comparison of each technology on an equal footing.

The application of LCA requires a protocol defined by the International Organization for Standardization (ISO) that has developed and formalized a series of standards for the Environmental Management. These standards include the ISO-14040 (International Standard Organization, 1997), which describes the principles and framework for LCA and ISO-14044 (International Standard Organization, 2000), which explains the requirements and guidelines of LCA. The research and analysis scheme for LCA consists in four stages as shown in Figure 1-8. Only the key points are briefly recalled in what follows.

2.4.1 *Goal and scope definition*

Defining the objectives and scope of the study is the first and essential step to guarantee the quality of the study. The definition of the problem establishes a rigorous framework for the study. It involves an accurate description of the study to be performed and the identification of the purpose, to whom it may concern and the possible applications.

The scope determines which product system or process will be analysed, the unit processes evaluated, functional unit, system boundaries, impact categories, data requirements, and limitations. Some important concepts in the LCA are:

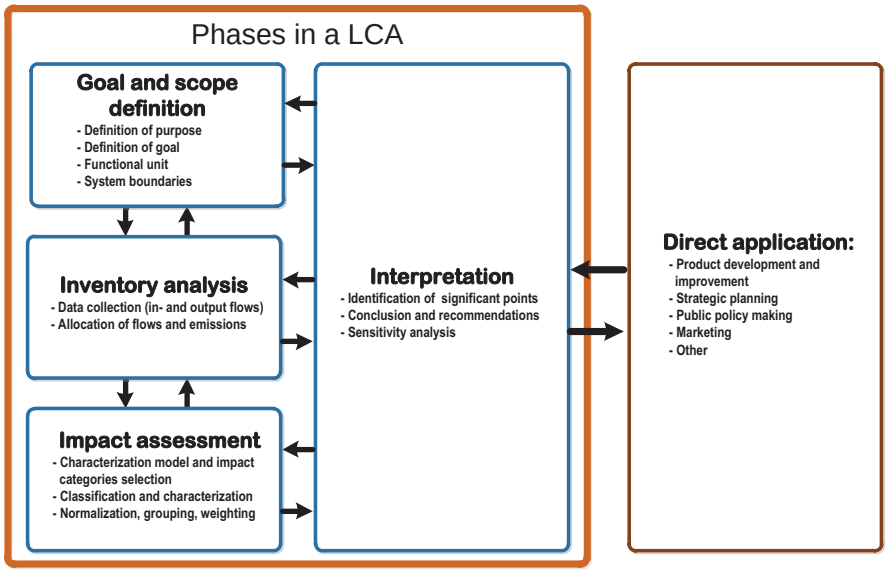

Figure 2-19 LCA framework (ISO 14040:1997)

A *unit process* describes a stage within the life cycle of a product and serves as the basic element of analysis in the LCA. The identification of unit processes facilitates the quantification of the inputs and outputs flows at each phase of the life cycle. The set of unit processes gives the *product system.* It involves the production, use, and disposal of a product or service throughout its life cycle.

System boundaries specify the unit processes, defined at the scope of the analysis, to be included in the LCA. The accurate description of the system and of its boundaries has strong implications for the results of the assessment.

It necessary to define a reference unit to quantify the inputs and outputs flows. This unit is called the *functional unit* (FU). The FU must be fully specified and measurable. It also serves as the basis for comparison when considering the environmental impacts of multiple product systems.

2.4.2 *Inventory analysis*

Life-cycle inventory (LCI) analysis involves data collection and calculation procedures to quantify relevant input and output flows of the product system(s). The LCI phase requires the highest efforts and resources of an LCA. Data collection consists in the identification and quantification of relevant inputs and outputs for each unit process of a specific product system taking into account the FU. Data for each unit process within the system boundary include energy and raw material flows, products and co–products, waste and emissions to air, water, and soil (Figure 1-10).

Data for each unit process are either provided directly from industry or using an LCI database, such as Ecoinvent, European Life Cycle Database (ELCD) or US life cycle inventory database. Databases provide industrial data on energy supply, resource extraction, material supply, chemicals, metals, agriculture, waste management services, and transport services for a variety of generic unit processes that allow for the development of more complex product systems (Ecoinvent Center, 2010).

The LCI must be done from the process tree in which the reference flows were defined and related to

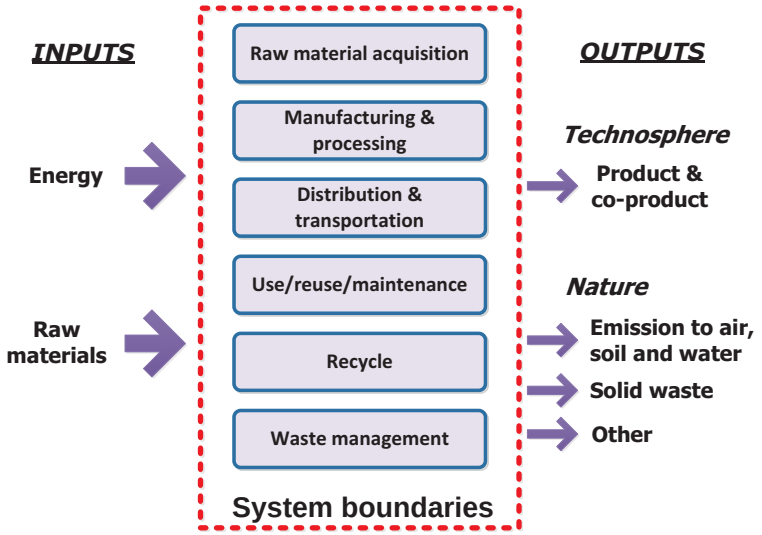

Figure 2-20 LCI schema

the FU. The process tree represents the set of unit processes that constitute the system under analysis. For each unit process, its inputs (intermediate flows of the system) and direct emissions (elementary flows) are determined. The next step is to search for the values of the indirect emissions and extractions related to each of the inputs flows. Indirect emissions and extractions are calculated by multiplying the quantity of input flows per FU and the emission factors per unit of input flow. Total emissions and extraction will be the sum of the direct elementary flows and the indirect emissions and extractions related to the inputs.

2.4.3 *Impact assessment*

The Life-cycle impact assessment (LCIA) stage uses the LCI results to evaluate the significance of potential environmental impacts. The impacts are the effects of the flows measured in LCI, such as the health effects caused by the inhalation of given emissions. The structure of this phase distinguishes between mandatory and optional elements (Figure 2-21).

2.4.3.1 Selection of impact categories and characterization models

The selection of impact categories must be comprehensive in the sense that they cover all relevant environmental issues related to the analysed system. Two main schools of methods have been developed depending on the level of analysis along the cause-effect chain (Finnveden et al., 2009; Jolliet et al., 2003). The primary effects represent the direct result of activities studied e.g. the greenhouse gas emissions. They can be distinguished from side effects, which are the consequences of primary effects. For example, the ozone layer depletion generates the growth of UV radiation that reaches the ground, this situation increasing the human health problems.

Problem-oriented methods will model the relatively early stages in the cause-effect chain to limit uncertainties. These methods are known as *midpoint* method. Damage-oriented methods, the so-called *endpoint* methods, try to consolidate the impact on the final results, as far as possible in the cause-effect chain. They provide more concrete information, but they remain more uncertain.

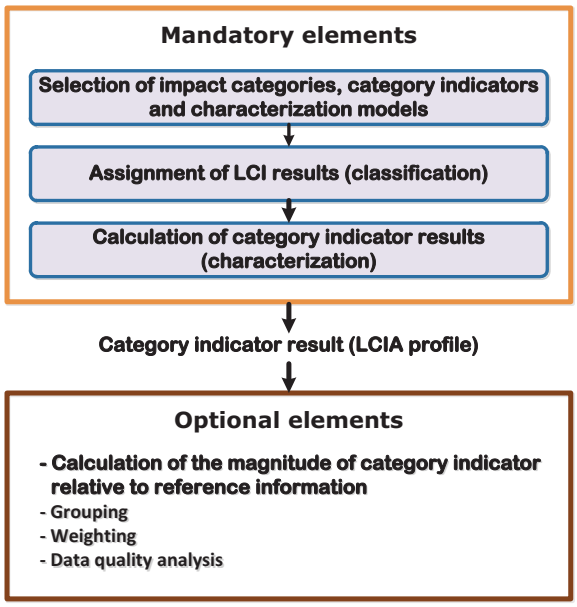

Figure 2-21 Elements of LCIA (ISO 14042:2000)

The methods for analysis of the impacts have been widely described in the literature. These methods are the result of several years of work and each has their specificities. In 2010, the European Commission (European Commission, Joint Research Centre, & Institute for Environment and Sustainability, 2010) published a guide with the description of some of these methods. In this publication, an analysis of the strengths, particularities, methodology used and impact categories pre-selected of each method was made. Table 2-2 presents some of the most used LCIA methodologies described by the European Commission.

In this work, the IMPACT 2002+ approach was selected as LCIA method. IMPACT 2002+ (IMPact Assessment of Chemical Toxics) proposes a feasible implementation of a combined midpoint/damage approach, linking all types of life cycle inventory results via 14 midpoint categories to four damage categories (Jolliet et al., 2003). IMPACT 2002 + combines the advantages that different existing LCIA methods have as well as internal developments in various impacts categories. In IMPACT 2002 +, the characterization factors for Human Toxicity and Aquatic & Terrestrial Ecotoxicity from the methodology IMPACT 2002, the other characterization factors are adapted from existing

Table 2-2 Methods for LCIA (European Commission et al., 2010)

		Impact modelling depth			
Methodology	**Developed by**	Midpoint	Endpoint	Normalisation	**Source**
CML 2002	CML (Netherlands)	X		X	(Guinée et al., 2002)
Eco-indicator 99	PRé (Netherlands)		X	X	(M. Goedkoop & Spriensma, 2001)
IMPACT 2002+	Ecole Polytechnique Fédérale de Lausanne (Switzerland)	X	X	X	(Jolliet et al., 2003)
ReCiPe	Radboud University Nijmegen + PRé + CML + RIVM (Netherlands)	X	X	X	(Mark Goedkoop et al., 2009)

characterizing methods, i.e. Eco-indicator 99, CML 2001, IPCC and the Cumulative Energy Demand. New concepts and methods were developed, especially for the comparative assessment of human toxicity and ecotoxicity (Frischknecht et al., 2007).

2.4.3.2 Impacts and damages classification

In classification phase, emissions and extractions flows obtained in the LCI are assigned to the impact categories selected, some emissions or extractions can contribute to several categories. According to the characterization method selected, the classification of impacts is different because of the impact categories pre-selected. Impact categories include climate change, stratospheric ozone depletion, photooxidant formation (smog), eutrophication, acidification, water use, noise, etc. (Pennington et al., 2004)

It is possible to elaborate a damage classification (endpoint). Three major groups, commonly referred to as areas of protection (European Commission et al., 2010; Pennington et al., 2004), are considered for the classification of damages: resource use, human health consequences and ecological consequences.

2.4.3.3 Characterization of impacts and damages

This step consists of modelling, by using factors, the classified LCI flow data for each of the impact categories. To all classified flows a quantitative characterization factor shall be assigned for each category to which the flow relevantly contributes. This factor expresses how much that flow contributes to the impact category indicator (at midpoint level) or damage category indicator (at endpoint level).

For midpoint level indicators, this relative factor typically relates to a reference flow, e.g. *kg CO_2-equivalents* per kg elementary flow in case of Global Warming Potential. For endpoint level indicators, it typically relates to a specific damage that relates to the broader area of protection, e.g. for species loss measured the *potentially displaced fraction of species for an affected area and duration* (PDF*m²*a) is used (European Commission et al., 2010).

The characterization of each impact categories is the sum of the product of the mass of the substances listed at the LCI classified by impact category and their own characterization factor. (Equation (2.6))

$$\mathrm{SI_i} = \sum_{S} FI_{s,i} \times M_S \qquad (2.6)$$

where SI_i represents the characterization score for the impact category i, $FI_{s,i}$ is the characterization factor for the substance S in the impact category i, and M_s is the mass of substance s from the LCI.

The impact categories can be grouped into the damage categories. Each impact category has a higher or lower contribution for the selected damage category. Therefore, a damage characterization factor is needed.

To pass from the impact characterization through the damage evaluation and calculate the damage score, the characterization score should be multiplied by its damage characterization factor. (Equation (2.7))

$$SD_d = \sum_i FD_{i,d} \times SI_i \quad (2.7)$$

SD_d represents the damage score for the damage category *d*, $FD_{i,d}$ is the damage characterization factor for the impact category *i* in the damage category *d*.

The characterization factors differ from one characterization method to another. They are available in the literature, in the form of databases, as well as in LCA support software tools. Table 2-3 and Figure 2-22 contain the midpoint and damage categories which IMPACT 2002+ works and the reference flow for each category.

Where:

- Kg_{eq} *Substance x* (kg equivalent of a reference substance x) expresses the amount of a reference flow x that equals the impact of the considered pollutant.
- *DALY* (Disability Adjusted Life Years) characterizes the disease severity, accounting for both mortality and morbidity.

Table 2-3 Characterisation reference substances and reference flow used in IMPACT 2002+ (Based on (Margni, Jolliet, & Humbert, 2005))

Midpoint category	Midpoint reference flow (Kg_{eq} Substance x)	Damage category	Reference flow
Human Toxicity (carcinogens + non-carcinogens)	Kg_{eq} chloroethylene into air	Human health	DALY
Respiratory effects (inorganic)	Kg_{eq} PM2.5 into air		
Ionizing radiation	Bq_{eq} carbon-14 into air		
Ozone layer depletion	Kg_{eq} CFC-11 into air		
Photochemical oxidation (Respiratory organics)	Kg_{eq} ethylene into air		
Aquatic ecotoxicity	Kg_{eq} triethylene glycol into water	Ecosystem quality	PDF*m²*a
Terrestrial ecotoxicity	Kg_{eq} triethylene glycol into soil		
Terrestrial acid/nutri	Kg_{eq} SO_2 into air		
Land occupation	M^2_{eq} organic arable land-year		
Aquatic acidification	Kg_{eq} SO_2 into air		*Under development*
Aquatic eutrophication	Kg_{eq} PO_4^3 into water		*Under development*
Global warming	Kg_{eq} CO_2 into air	Climate change	Kg_{eq} CO_2 into air
Non-renewable energy	MJ Total primary non-renewable or kg_{eq} crude oil (860kg/m^3)	Resources	MJ
Mineral extraction	MJ additional energy or kg_{eq} iron		

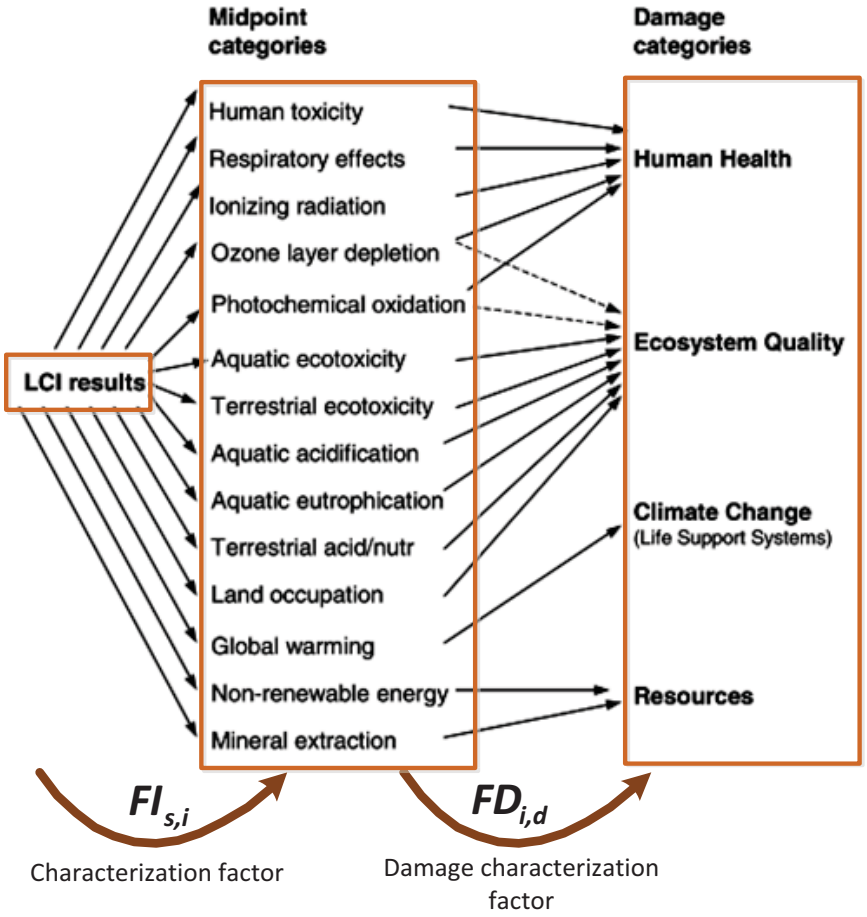

Figure 2-22 General approach of LCIA of emissions on the major categories of environmental damage

- *PDF*m²*yr* (Potentially Disappeared Fraction of species per m^2 per year) is the unit to "measure" the impacts on ecosystems. PDF*m^2*yr represents the fraction of species disappeared on 1 m^2 of earth surface during one year.

2.4.3.4 Optional elements: Normalisation, Grouping and Weighting

The purpose of the *normalisation* is to facilitate interpretation of the LCIA results by analyzing the importance of the respective contribution to the overall environmental impact. As impact or damage categories have different units, normalisation is used to make these categories dimensionless.

Normalized LCIA results are obtained by dividing the LCIA results by the reference value, separately for each impact category (Equation (2.8)). Each characterization method proposes its own reference value. There are numerous methods of selecting a reference value, including the total emissions or resource use for a given area that may be global, regional or local in a given period of time, or the total emissions or resource use for a given area in a per capita basis in a given period of time. Normalisation results can provide input to grouping or weighting.

$$N_k = \frac{S_k}{VR_k} \tag{2.8}$$

N_k represents the normalised score of the impact or damage categories k, S_k is the characterization or damage score of the impact or damage categories k, and VR_k is the reference value for the impact or damage categories k.

Grouping is a qualitative or semi-qualitative process that involves sorting and / or ranking among normalised scores. Grouping may result in a broad ranking, or hierarchy, of impact categories with respect to their importance. Such a ranking can provide structure to help draw conclusions on the relative importance of different impact or damage categories (Pennington et al., 2004). For example, categories could be grouped in terms of high importance, moderate importance and low priority issues. *Weighting* involves assigning distinct quantitative weights to all impact categories expressing their relative importance. A weighting of the normalised indicator results may be performed. This can include aggregation to a single indicator. It is often applied in the form of linear weighting factors:

$$EI = \sum_k PF_k S_k \quad or \quad EI = \sum_k PF_k N_k \tag{2.9}$$

where *EI* is the overall environmental impact indicator, PF_k is the weighting factor for impact category k.

Methods for weighting can be based on (Pennington et al., 2004):

- A distinction between impact indicators defined early (midpoints) or late (endpoints) in the impact chain.
- The expressed preference. People are asked the relative importance of damages or impact categories.
- Distance to target, where characterization results are related to target levels.
- Monetization. These monetized weighting factors are derived from reactions to different situations, such as insurance payouts, health care expenditures, fines, costs incurred.

2.4.4 *Interpretation of results*

The interpretation of LCIA results is the last phase. It analyzes the results provides in the phase above based on the objectives and scope of the study previously defined. Conclusions are thus made, and areas for improvement can be detected in order to start looking for possible alternatives of solutions to finally take a decision.

The interpretation proceeds through three main activities:

- Identify the significant issues. An analysis and organization of the results must be done to identify the main contributors to the LCIA results (processes and elementary flows) and the most relevant impact categories. Significant choices as assumptions, foreground and background data used for deriving the process inventories, LCIA methods used, as well as the normalisation and weighting factors must also be identified because of the potential influence in the precision of the final results of the LCA.
- Determine the influence of significant issues on the overall results of the LCA. The evaluation is performed in close interaction with the identification of significant issues in order to determine the reliability and robustness of the results. The evaluation involves completeness

check, sensitivity check in combination with scenario analysis and potentially uncertainty analysis and consistency check.

- Formulate the conclusions and recommendations of the LCA study. Recommendations based on the final conclusions of the LCA study must be logical and be reasonable and plausible founded in the conclusions and strictly relate to the intended applications as defined in the goal of the study.

2.4.5 *Limitations of LCA*

LCA studies present various limitations like:

- A LCA study, because of its "holistic" nature, requires a lot of time and economical resources. The more detailed a LCA is the more time-consuming and expensive it will be. High costs are partly caused by the need for professional consultation and expert knowledge in the stages of impact and improvement analyses.
- LCA is a tool based on linear modelling so it regards all processes as linear. Some progress is being made in reducing this limitation.
- There is not a unique LCA methodology even if the main steps are regulated and guided by the ISO norm. Each impact assessment method has its own impact and/or damage categories, characterization factors and references values for the normalisation. This situation makes difficult the comparison of LCA studies between products or processes if they were not made under the same impact assessment method.
- The assumptions made in such studies (for example the boundary determination, the source of data and the impact assessment choice) might be subjective.
- The accuracy of a LCA study depends on the quality and the availability of the relevant data, and if these data are not accurate enough, the accuracy of the study is limited. These facts affect the precision of the final results.
- Because LCA studies are focused on national and regional level, they might not be suitable for local applications.
- The availability, customization and updating of the database is another problem. Even if the databases are being developed for several countries, considering its particularities, and the format for databases is being standardised, data are frequently obsolete, incomparable, or of unknown quality. Some of the data are available in aggregated format.
- LCA approach cannot replace the decision making process. It only provides information for decision support.

2.4.6 *LCA software tools*

Nowadays, many LCA software tools have been developed based on the methodology of LCA. Most of them include a certain number of databases and impact assessment methods.

These tools facilitate the estimation of total emissions and extraction for the LCI as well as the calculation of characterization, damage and normalised score. Some of them generate a report with the

Table 2-4 Main LCA software tools

Software name	Supplier	Website
TEAM	ECOBILAN-PricewaterhouseCoopers	http://ecobilan.pwc.fr/fr/boite-a-outils/team.jhtml
GaBi Software	PE INTERNATIONAL	http://www.gabi-software.com/france/software/
Umberto	ifu Hamburg GmbH	http://www.umberto.de/en/
SimaPro	PRé Consultants	http://www.pre-sustainability.com/simapro-lca-software
openLCA	GreenDelta GmbH	http://www.openlca.org/openlca

results obtained through graphs. Evaluation of scenarios and sensitivity analysis are other optional features of these software tools. Table 2-4 shows some of the LCA software tools currently available on the market.

To perform the LCA study for PVGCS, the SimaPro software tool with the EcoInvent database was selected. It is widely mentioned in the dedicated literature for this kind of study.

The environmental impact results are available through graphs or tables that can be exported. Several processes or scenarios can be compared.

2.5 LCA study for m-Si based PV module

The LCA methodology is first applied to a simple case, the production of a PV module, in order to fully understand each of the abovementioned steps. In this first example, a description of each step of the LCA applied to the manufacturing process of the m-Si based PV module is made. The data were collected from the literature, particularly from the work developed by Alsema et al (Alsema & Wild-scholten, 2006; de Wild-Scholten & Alsema, 2005).

2.5.1 *Goal and scope definition*

As shown in Figure 2-19, the first step in the methodology is to define the objective and scope of the study.

The objective of this study is to identify and evaluate the overall environmental impacts associated of a PV module made by m-Si solar cells. The assessment was mainly focused on energy and material flows during the production of the PV modules.

System boundaries are set as shown in Figure 2-23. The evaluation begins with the purification of Si to obtain SoG-Si using the Siemens process to the final assembly of PV module. The description of each of the processes taken into account is given in Section 2.2.1.

The functional unit for this LCA is a finished piece of m-Si based PV module. The characteristics of the PV module are the same as Alsema et al. consider in their work (de Wild-Scholten & Alsema, 2005). The PV module is composed by 72 m-Si solar cells of 125 mm x 125 mm (1.25 m^2 module area), with glass/EVA/Tedlar lamination. Glass thickness was set at 3.6 mm and the aluminium frame is 3.8 kg. The m-Si wafers are made following CZ process.

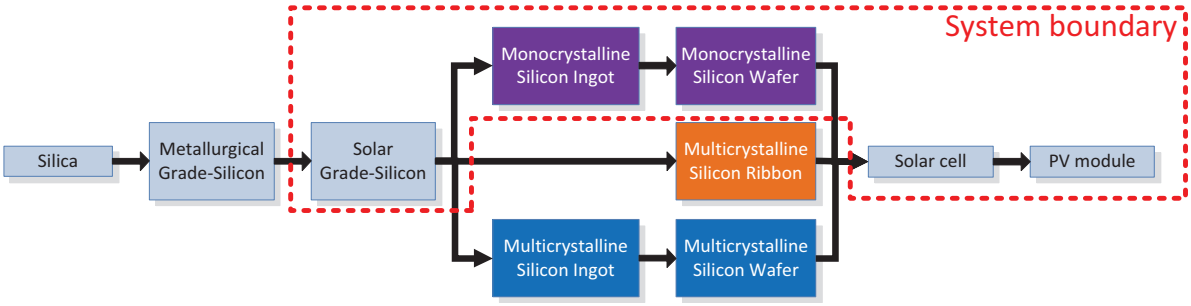

Figure 2-23 System boundaries for m-Si PV module LCA

The PV module is assumed to be manufactured in Germany. The energy mix of Germany is then used in the computations.

2.5.2 *Inventory analysis*

From the data given by Alsema et al. for each unit process involved in the system boundary considering the interconnexion of the units constituting the whole manufacturing process, the material requirements and the emissions per PV module of m-Si (LCI) are calculated. Table 2-5 shows input and output flows for each unit process.

As it can be seen, each unit process has its own reference flow (per kg feedstock, m² of wafer or per solar cell). Yet it must be kept in mind that finally all material must be estimated per functional unit (per piece of PV module). Table 2-6 shows the amount of total inputs (intermediate flows) and direct emission for each process unit considering the FU.

The next step is to calculate the total emissions and extraction flows. SimaPro and more precisely Ecoinvent database are particularly useful. The different unit processes considered within the boundaries of the system is created in SimaPro. Inputs and outputs as indicated in Figure 2-23 are introduced by using the processes that are then included into the Ecoinvent database. The program calculates both direct and indirect emissions and displays the total emissions. For the manufacture of the PV module, the program identifies 890 different types of substances that are released either into water, land and air. Table 2-7 shows only some of the 890 emissions that are produced during the manufacture of m-Si based PV module.

2.5.3 *Impact assessment*

The third step in the LCA methodology involves the assessment of environmental allocation caused by the emissions that were listed in the previous step. One of the characterization methods listed in Table 2-2 is required. As mentioned in Section 2.4.3.1, IMPACT 2002+ was chosen because it allows the classification and characterization of environmental impacts (midpoint) and damage consequences (endpoint).

The selected LCIA method is found within Ecoinvent database, taking into account the classification and characterization of each of the 890 substances into the categories considered by IMPACT 2002+ (see Table 2-3). For the sake of illustration, Table 2-8 and Table 2-9 indicate the total characterization score for two midpoint categories, i.e. Global Warming and Respiratory Inorganic respectively.

Table 2-5 LCI data for manufacturing process of m-Si PV module from (de Wild-Scholten & Alsema, 2005)

1 kg of polycrystalline SoG-Si by Siemens process	Amount	Unit
Materials		
MG-silicon	1.13	kg
Chemicals inorganic	2.00	kg
Heat, natural gas	185.00	MJ
Electricity/heat		
Natural gas	45.00	kWh
Electricity, hydropower	65.00	kWh

1 m² of m-Si wafer by CZ process	Amount	Unit
Materials		
Polycrystalline SoG-Si	1.5800	kg
Sand	0.3600	kg
Flat glass, uncoated	0.0100	kg
Steel	1.4900	kg
Silicon carbide	2.6100	kg
Argon	6.2000	kg
Dipropylene glycol	0.3000	kg
Adhesive for metals	0.0020	kg
Surfactant	0.2400	kg
Sodium hydroxide, 50% in H_2O	0.0150	kg
Hydrochloric acid, 30% in H_2O	0.0027	kg
Acetic acid, 98% in H_2O	0.0390	kg
Tap water	0.0060	kg
Water, deionised	65.0000	kg
Electricity/heat		
Electricity, medium voltage	45.000	kWh
Natural gas	65.000	kWh
Final waste flows		
Silicon waste	0.400	kg
Waste to treatment		
Waste, silicon wafer production	6.000	kg

1 piece of m-Si solar cell	Amount	Unit
Resource		
Water, cooling	1.56×10^{-2}	m^3
Materials		
m-Si wafer	1.060	p
Phosphorus	2.27×10^{-5}	kg
Metallization paste	1.17×10^{-3}	kg
Polystyrene, expandable	6.36×10^{-6}	kg
Nitrogen	2.89×10^{-2}	kg
Oxygen	1.59×10^{-3}	kg
Argon	4.01×10^{-4}	kg
Ammonia	1.05×10^{-4}	kg
Silicon tetrahydride	1.89×10^{-5}	kg
Sodium hydroxide, 50% in H2O	2.45×10^{-3}	kg
Acetic acid, 98% in H2O	4.42×10^{-5}	kg
Hydrochloric acid, 30% in H2O	7.12×10^{-4}	kg
Hydrogen fluoride	5.89×10^{-4}	kg
Nitric acid, 50% in H2O	4.17×10^{-4}	kg
Phosphoryl chloride	3.39×10^{-6}	kg
Phosphoric acid, industrial grade, 85% in H2O	1.19×10^{-4}	kg
Sodium sulphate	1.17×10^{-3}	kg
Calcium chloride	3.37×10^{-4}	kg
Isopropanol	1.23×10^{-3}	kg
Ethanol	9.98×10^{-6}	kg
Solvents, organic	2.24×10^{-5}	kg
Water, deionised	2.15	kg
Electricity/heat		
Electricity, medium voltage	5.90×10^{-1}	kWh
Natural gas	7.42×10^{-2}	MJ
Fuel oil	5.11×10^{-4}	kg
Emissions to air		
Aluminium	1.21×10^{-5}	kg
Hydrogen chloride	4.16×10^{-6}	kg
Hydrogen fluoride	7.56×10^{-8}	kg
Lead	1.21×10^{-5}	kg
Particulates, unspecified	4.15×10^{-5}	kg
Silicon	1.13×10^{-6}	kg
Silver	1.21×10^{-5}	kg
Sodium hydroxide	7.56×10^{-7}	kg
Tin	1.21×10^{-5}	kg
VOC, volatile organic compounds	3.02×10^{-3}	kg
Final waste flows		
Photovoltaic cell waste	4.13×10^{-3}	kg

1 piece of m-Si PV module	Amount	Unit
Materials		
m-Si cell	73.4000	p
Aluminium	3.8000	kg
Solar glass	11.4000	kg
Ethylene vinyl acetate copolymer	1.3000	kg
Polyvinylfluoride	0.1600	kg
Polyethylene terephthalate (PET)	0.1600	kg
Copper	0.1400	kg
Tin	0.0070	kg
Lead	0.0040	kg
Nickel	0.0002	kg
Flux, wave soldering	0.0100	kg
Methanol	0.0162	kg
Silicone product	0.0029	kg
Cardboard carbon storage	1.3700	kg
Tap water	27.0000	kg
Electricity/heat		
Electricity, medium voltage	8.3300	kWh
Final waste flows		
Photovoltaic cell waste	0.0150	kg
Waste to treatment		
Recycling glass	0.1100	kg
Ethylvinylacetate treatment	0.0100	kg
Recycling PET	0.0100	kg

Table 2-6 LCI of total flows for production of 1 piece of m-Si PV module

SoG-Si	Amount	Unit
Materials		
MG-silicon	131.05	kg
Chemicals inorganic	231.94	kg
Heat, natural gas	21,454.82	MJ
Electricity/heat		
Natural gas	5,218.74	kWh
Electricity, hydropower	7,538.18	kWh

Wafer	Amount	Unit
Materials		
Polycrystalline SoG-Si	115.97	kg
Sand	26.42	kg
Flat glass, uncoated	0.73	kg
Steel	109.37	kg
Silicon carbide	191.57	kg
Argon	455.08	kg
Dipropylene glycol	22.02	kg
Adhesive for metals	0.147	kg
Surfactant	17.62	kg
Sodium hydroxide, 50% in H_2O	1.10	kg
Hydrochloric acid, 30% in H_2O	0.20	kg
Acetic acid, 98% in H_2O	2.86	kg
Tap water	0.44	kg
Water, deionised	4,771.00	kg
Electricity/heat		
Electricity, medium voltage	10,643.00	kWh
Natural gas	5,651.80	kWh
Final waste flows		
Silicon waste	29.36	kg
Waste to treatment		
Waste, silicon wafer production	440.40	kg

Solar cell	Amount	Unit
Resource		
Water, cooling	1.150	m^3
Materials		
m-Si wafer	77.804	p
Phosphorus	0.002	kg
Metallization paste	0.086	kg
Polystyrene, expandable	0.0005	kg
Nitrogen	2.121	kg
Oxygen	0.117	kg
Argon	0.029	kg
Ammonia	0.008	kg
Silicon tetrahydride	0.001	kg
Sodium hydroxide, 50% in H2O	0.180	kg
Acetic acid, 98% in H2O	0.003	kg
Hydrochloric acid, 30% in H2O	0.052	kg
Hydrogen fluoride	0.043	kg
Nitric acid, 50% in H2O	0.031	kg
Phosphoryl chloride	0.0002	kg
Phosphoric acid, industrial grade, 85% in H2O	0.009	kg
Sodium sulphate	0.086	kg
Calcium chloride	0.025	kg
Isopropanol	0.090	kg
Ethanol	0.0007	kg
Solvents, organic	0.002	kg
Water, deionised	157.810	kg
Electricity/heat		
Electricity, medium voltage	43.306	kWh
Natural gas	5.446	MJ
Fuel oil	0.038	kg
Emissions to air		
Aluminium	0.0009	kg
Hydrogen chloride	0.0003	kg
Hydrogen fluoride	5.549×10^{-6}	kg
Lead	0.0009	kg
Particulates, unspecified	0.003	kg
Silicon	8.29×10^{-5}	kg
Silver	0.0009	kg
Sodium hydroxide	5.55×10^{-5}	kg
Tin	0.0009	kg
VOC, volatile organic compounds	0.223	kg
Final waste flows		
Photovoltaic cell waste	0.303	kg

m-Si PV module	Amount	Unit
Materials		
m-Si cell	73.4000	p
Aluminium	3.8000	kg
Solar glass	11.4000	kg
Ethylene vinyl acetate copolymer	1.3000	kg
Polyvinylfluoride	0.1600	kg
Polyethylene terephthalate (PET)	0.1600	kg
Copper	0.1400	kg
Tin	0.0070	kg
Lead	0.0040	kg
Nickel	0.0002	kg
Flux, wave soldering	0.0100	kg
Methanol	0.0162	kg
Silicone product	0.0029	kg
Cardboard carbon storage	1.3700	kg
Tap water	27.0000	kg
Electricity/heat		
Electricity, medium voltage	8.3300	kWh
Final waste flows		
Photovoltaic cell waste	0.0150	kg
Waste to treatment		
Recycling glass	0.1100	kg
Ethylvinylacetate treatment	0.0100	kg
Recycling PET	0.0100	kg

Table 2-7 LCI of total emission for manufacturing a m-Si based PV module (extracted from SimaPro)

Substance	Emission to	Amount	Unit
1-Butanol	Air	5.47×10^{-10}	kg
1-Butanol	Eau	2.57×10^{-06}	kg
1-Pentanol	Air	3.31×10^{-10}	kg
1-Pentanol	Eau	7.94×10^{-10}	kg
1-Pentene	Air	2.50×10^{-10}	kg
1-Pentene	Eau	6.00×10^{-10}	kg
1-Propanol	Air	4.54×10^{-08}	kg
1-Propanol	Eau	1.94×10^{-09}	kg
1,4-Butanediol	Air	1.14×10^{-08}	kg
1,4-Butanediol	Eau	4.56×10^{-09}	kg
2-Aminopropanol	Air	7.65×10^{-11}	kg
2-Aminopropanol	Eau	1.92×10^{-10}	kg
2-Butene, 2-methyl-	Air	5.55×10^{-14}	kg
2-Methyl-1-propanol	Air	1.01×10^{-09}	kg
2-Methyl-1-propanol	Eau	2.44×10^{-09}	kg
2-Methyl-2-butene	Eau	1.33×10^{-13}	kg
2-Nitrobenzoic acid	Air	1.36×10^{-10}	kg
2-Propanol	Air	1.52×10^{-4}	kg
2-Propanol	Eau	7.83×10^{-10}	kg
Carbon dioxide	Air	0.019	kg
Carbon dioxide, biogenic	Air	439.29	kg
Carbon dioxide, fossil	Air	8196.96	kg
Carbon dioxide, land transformation	Air	0.965	kg
Carbon disulphide	Air	0.009	kg
Carbon disulphide	Eau	3.35×10^{-08}	kg
Carbon monoxide	Air	3.25×10^{-05}	kg
Carbon	Sol	0.086	kg

Substance	Emission to	Amount	Unit
Heat, waste	Air	1.93×10^{5}	MJ
Heat, waste	Eau	3,426.05	MJ
Heat, waste	Sol	297.17	MJ
Helium	Air	0.001	kg
Heptane	Air	0.007	kg
Hexane	Air	0.062	kg
Hydrocarbons, aliphatic, alkanes, cyclic	Air	9.41×10^{-06}	kg
Hydrocarbons, alkanes, unspecified	Air	0.041	kg
Hydrocarbons, alkanes, unspecified	Eau	0.004	kg
Hydrocarbons, alkenes, unspecified	Air	4.38×10^{-09}	kg
Hydrocarbons, alkenes, unspecified	Eau	2.47×10^{-08}	kg
Hydrocarbons, aliphatic, unsaturated	Air	0.007	kg
Hydrocarbons, aliphatic, unsaturated	Eau	0.0004	kg
Hydrocarbons, aromatic	Air	0.014	kg
Hydrocarbons, aromatic	Eau	0.018	kg
Hydrocarbons, chlorinated	Air	3.27×10^{-05}	kg
Hydrocarbons, unspecified	Eau	0.015	kg
Methane, bromo-, Halon 1001	Air	5.42×10^{-14}	kg
Methane, bromochlorodifluoro-, Halon 1211	Air	0.0001	kg
Methane, bromotrifluoro-, Halon 1301	Air	1.76×10^{-05}	kg
Methane, chlorodifluoro-, HCFC-22	Air	0.0004	kg
Methane, chlorotrifluoro-, CFC-13	Air	5.20×10^{-10}	kg
Methane, dichloro-, HCC-30	Air	4.92×10^{-07}	kg
Methane, dichloro-, HCC-30	Eau	0.0007	kg
Methane, dichlorodifluoro-, CFC-12	Air	5.81×10^{-07}	kg
Methane, dichlorofluoro-, HCFC-21	Air	7.82×10^{-09}	kg
Methane, fossil	Air	17.66	kg

Table 2-8 Characterization of LCI emission into GW impact category

	Emission to	Amount	Unit	$FI_{s,i}$	Score kg CO_2 eq
TOTAL					15,789.18
Carbon dioxide	Air	1.89×10^{-2}	kg	1.00	1.89×10^{-2}
Carbon dioxide. fossil	Air	1.52×10^{4}	kg	1.00	1.52×10^{4}
Carbon dioxide. land transformation	Air	1.80	kg	1.00	1.80
Carbon monoxide	Air	3.25×10^{-5}	kg	1.57	5.11×10^{-5}
Carbon monoxide. fossil	Air	7.77	kg	1.57	1.22×10^{1}
Chloroform	Air	1.44×10^{-5}	kg	9.00	1.30×10^{-4}
Dinitrogen monoxide	Air	7.21×10^{1}	kg	156.00	1.13×10^{2}
Ethane. 1.1.1.2-tetrafluoro-. HFC-134a	Air	6.42×10^{-4}	kg	400.00	2.57×10^{-1}
Ethane. 1.1.1-trichloro-. HCFC-140	Air	4.55×10^{-8}	kg	42.00	1.91×10^{-6}
Ethane. 1.1.2-trichloro-1.2.2-trifluoro-. CFC-113	Air	1.00×10^{-5}	kg	2,700.00	2.71×10^{-2}
Ethane. 1.1-difluoro-. HFC-152a	Air	1.38×10^{-6}	kg	37.00	5.09×10^{-5}
Ethane. 1.2-dichloro-1.1.2.2-tetrafluoro-. CFC-114	Air	1.94×10^{-4}	kg	8,700.00	1.68
Ethane. hexafluoro-. HFC-116	Air	4.95×10^{-5}	kg	18,000.00	8.90×10^{-1}
Methane	Air	3.41×10^{-3}	kg	7.60	2.59×10^{-2}
Methane. biogenic	Air	1.86	kg	7.60	1.42×10^{1}
Methane. bromo-. Halon 1001	Air	5.61×10^{-14}	kg	1.00	5.61×10^{-14}
Methane. bromochlorodifluoro-. Halon 1211	Air	1.72×10^{-4}	kg	390.00	6.69×10^{-2}
Methane. bromotrifluoro-. Halon 1301	Air	1.92×10^{-5}	kg	2,700.00	5.18×10^{-2}
Methane. chlorodifluoro-. HCFC-22	Air	6.69×10^{-4}	kg	540.00	3.61×10^{-1}
Methane. chlorotrifluoro-. CFC-13	Air	5.20×10^{-10}	kg	16,300.00	8.48×10^{-6}
Methane. dichloro-. HCC-30	Air	1.10×10^{-6}	kg	3.00	3.30×10^{-6}
Methane. dichlorodifluoro-. CFC-12	Air	8.01×10^{-7}	kg	5,200.00	4.16×10^{-3}
Methane. dichlorofluoro-. HCFC-21	Air	8.07×10^{-9}	kg	65.00	5.24×10^{-7}
Methane. fossil	Air	3.43×10^{1}	kg	10.35	3.55×10^{2}
Methane. monochloro-. R-40	Air	1.29×10^{-6}	kg	5.00	6.44×10^{-6}
Methane. tetrachloro-. CFC-10	Air	1.10×10^{-4}	kg	580.00	6.38×10^{-2}
Methane. tetrafluoro-. CFC-14	Air	4.30×10^{-4}	kg	8,900.00	3.83
Methane. trichlorofluoro-. CFC-11	Air	4.46×10^{-9}	kg	1,600.00	7.14×10^{-6}
Methane. trifluoro-. HFC-23	Air	1.20×10^{-7}	kg	10,000.00	1.20×10^{-3}
Sulfur hexafluoride	Air	1.19×10^{-3}	kg	32,400.00	3.86×10^{1}

Table 2-9 Characterization of LCI emission into RI impact category

	Emission to	Amount	Unit	$FI_{s,i}$	Score kg PM2.5 eq
TOTAL					5.1569
Ammonia	Air	3.38×10^{-1}	kg	0.121	4.10×10^{-2}
Carbon monoxide	Air	3.25×10^{-5}	kg	0.001	3.40×10^{-8}
Nitrogen oxides	Air	1.70×10^{1}	kg	0.127	2.16
Particulates. < 10 um	Air	3.12×10^{-4}	kg	0.536	1.67×10^{-4}
Particulates. < 10 um (mobile)	Air	1.82×10^{-6}	kg	0.536	9.77×10^{-7}
Particulates. < 10 um (stationary)	Air	7.58×10^{-6}	kg	0.536	4.06×10^{-6}
Particulates. < 2.5 um	Air	1.40	kg	1	1.40
Sulfur dioxide	Air	1.99×10^{1}	kg	0.078	1.55
Sulfur oxides	Air	1.03×10^{-4}	kg	0.078	8.07×10^{-6}
Sulfur trioxide	Air	1.31×10^{-7}	kg	0.062	8.20×10^{-9}

Table 2-10 Characterization score of impact categories

Impact category	Amount	Unit
Carcinogens	77.43	kg C_2H_3Cl eq
Non-carcinogens	53.03	kg C_2H_3Cl eq
Respiratory inorganics	5.16	kg PM2.5 eq
Ionizing radiation	448,213.72	Bq C-14 eq
Ozone layer depletion	0.0016	kg CFC-11 eq
Respiratory organics	2.73	kg C_2H_4 eq
Aquatic ecotoxicity	499,953.26	kg TEG water
Terrestrial ecotoxicity	103,003.74	kg TEG soil
Terrestrial acid/nutri	118.31	kg SO_2 eq
Land occupation	50.49	m^2org.arable
Aquatic acidification	33.29	kg SO_2 eq
Aquatic eutrophication	4.16	kg PO_4 P-lim
Global warming	15,789.18	kg CO_2 eq
Non-renewable energy	289,745.99	MJ primary
Mineral extraction	60.24	MJ surplus

Table 2-11 Characterization score of damage categories

Damage category	Amount	Unit
Human health	0.004	DALY
Ecosystem quality	1,017.93	PDF*m2*yr
Climate change	15,789.18	kg CO2 eq
Resources	289,806.23	MJ primary

The characterization score of the emissions from the production of an m-Si PV module in all impact categories is shown in Table 2-10. Finally, the characterization scores obtained for the four damage categories are presented in Table 2-11.

Due to the complexity to understand the information provided in the tables above, the normalisation of results was performed. The reference values for both impact and damages categories are listed in Table 2-12. Table 2-13 shows the normalised values.

2.5.4 *Interpretation of results*

Figure 2-24 represents the normalised scores. Comparing among the impact categories, GW and NR are those with the highest values. This result indicates that on the one hand GW and NR have a major influence within the overall environmental assessment for a module of m-Si. On the other hand, half of the impact categories have a very small contribution.

GW and NR are mainly related to the energy requirements of the process. Looking at the process flow for manufacturing the m-Si PV module, a large amount of energy is consumed to achieve the temperatures required to get the degree of purity and uniformity needed by this type silicon module. Because of this, a question arises: what would happen if the module was manufactured in another country with a different energy mix?. The Ecoinvent database has different energy mix. Five scenarios will be tested. USA, China, Spain and France energy mix are chosen. The composition of the five

Table 2-12 IMPACT 2002+ reference values for normalisation (Margni et al., 2005)

Midpoint category	Reference value	Unit	Damage category	Reference value	Unit
Carcinogens	2,533.00	kg C_2H_3Cl eq/ pers/year[1]	Human health	0.0071	DALY/ pers/year
Non-carcinogens	2,533.00	kg C_2H_3Cl eq/ pers/year			
Respiratory inorganics	10.00	kg PM2.5 eq/ pers/year			
Ionizing radiation	33,772,000	Bq C-14 eq/ pers/year			
Ozone layer depletion	6.75	kg CFC-11 eq/ pers/year			
Respiratory organics	3,330.00	kg C_2H_4 eq/ pers/year			
Aquatic ecotoxicity	272,881,000	kg TEG water/ pers/year	Ecosystem quality	13,700	PDF * m^2 * yr/pers/year
Terrestrial ecotoxicity	1,732,000	kg TEG soil/ pers/year			
Terrestrial acid/nutri	13,100.00	kg SO_2 eq/ pers/year			
Land occupation	12,600.00	m^2org.arable/ pers/year			
Aquatic acidification	*Under development*				
Aquatic eutrophication	*Under development*				
Global warming	9,900.00	kg CO_2 eq/ pers/year	Climate change	9,900	Kg_{eq} CO_2/pers/yr
Non-renewable energy	151,975.00	MJ primary/ pers/year	Resources	152,000	MJ/ pers/yr
Mineral extraction	150,600.00	MJ surplus/ pers/year			

Table 2-13 Normalised scores for both impact and damage categories

Midpoint category	Reference value	Unit	Damage category	Reference value	Unit
Carcinogens	0.03057	pers/year	Human health	0.57482	pers/year
Non-carcinogens	0.02094	pers/year			
Respiratory inorganics	0.50899	pers/year			
Ionizing radiation	0.01327	pers/year			
Ozone layer depletion	0.00023	pers/year			
Respiratory organics	0.00082	pers/year			
Aquatic ecotoxicity	0.00183	pers/year	Ecosystem quality	0.07431	pers/year
Terrestrial ecotoxicity	0.05948	pers/year			
Terrestrial acid/nutri	0.00898	pers/year			
Land occupation	0.00402	pers/year			
Aquatic acidification	-----				
Aquatic eutrophication	-----				
Global warming	1.59471	pers/year	Climate change	1.59471	pers/yr
Non-renewable energy	1.90653	pers/year	Resources	1.90693	pers/yr
Mineral extraction	0.00040	pers/year			

[1] The reference value used by IMPACT 2002+ considered the European population in a year.

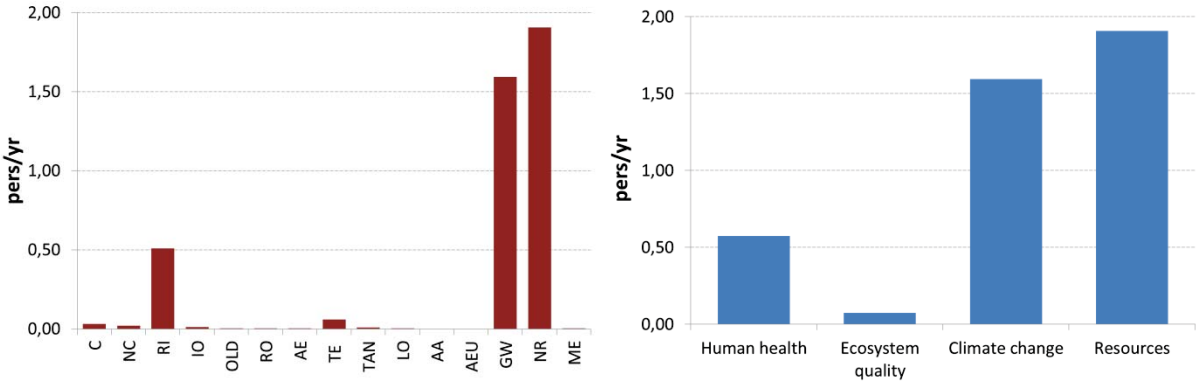

a) Midpoint categories b) Damage categories

Figure 2-24 Normalised scores for both midpoint and damages categories. IMPACT 2002+

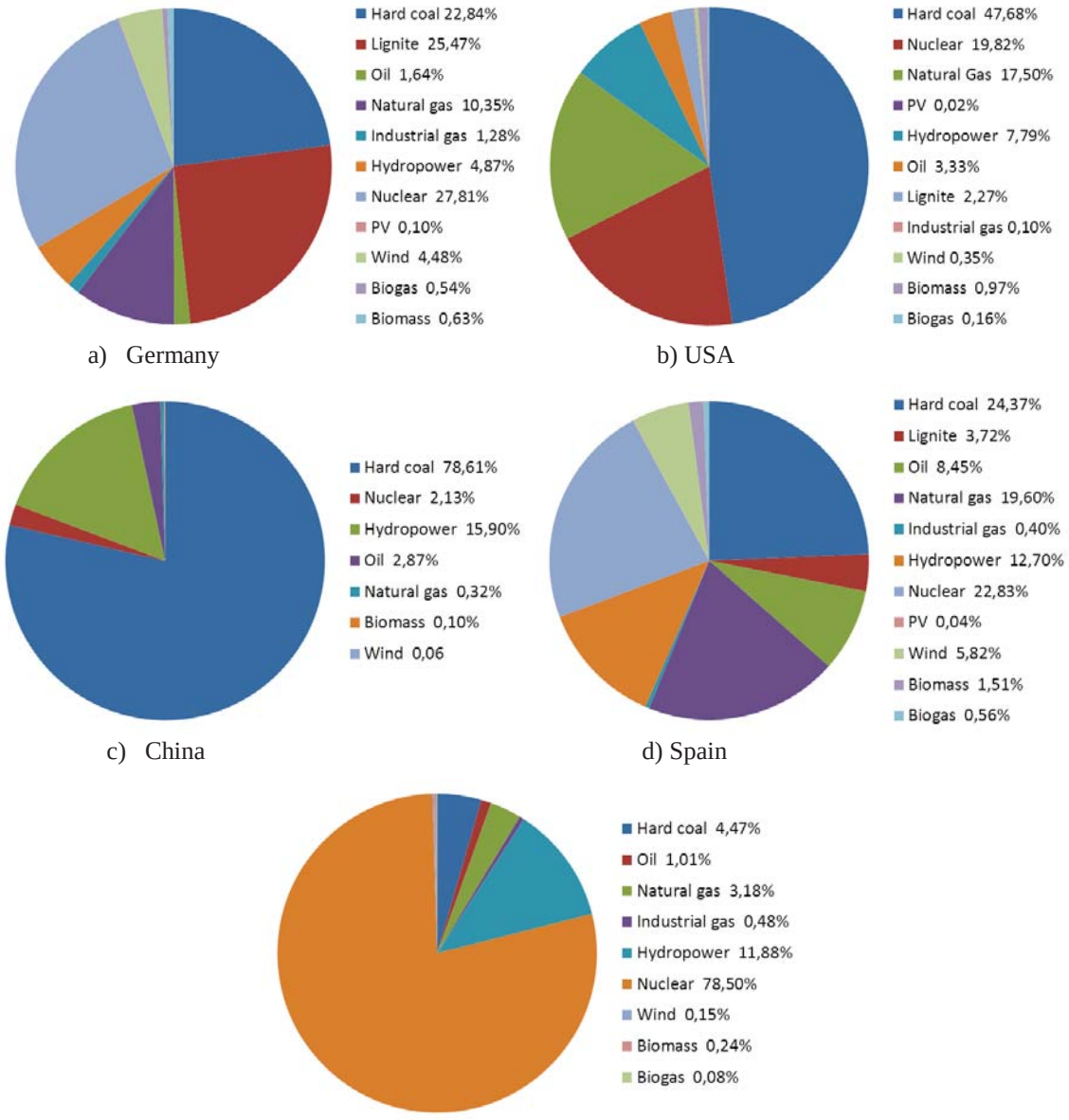

a) Germany b) USA

c) China d) Spain

f) France

Figure 2-25 Energy mix composition of Germany, USA, China, Spain and France

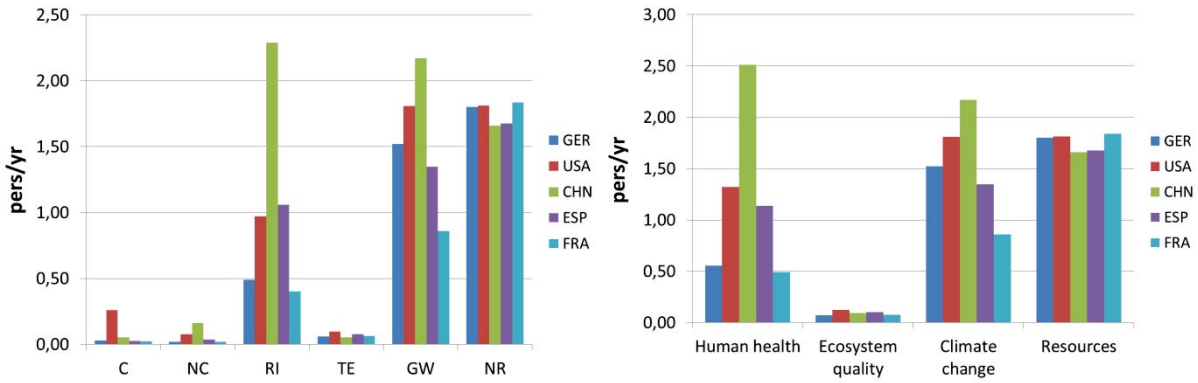

a) Main score at midpoint categories b) Damage categories

Figure 2-26 Normalized scores both midpoint and damages categories of five scenarios. IMPACT 2002+

energy mixes is displayed in Figure 2-25.

To make the comparison, it was necessary to change the energy source used for each of the unit process according to the energy mix scenario. Once again LCI was performed for each scenario as well as the classification and characterization of emissions. Normalisation of score was also performed to compare the results. In Figure 2-26, it can be seen that an m-Si PV module made in China generates the high environmental affectations among the five scenarios, especially into Human Health and Climate Change categories. The large dependence of hard coal, a fossil source, in Chinese mix causes these high values. The opposite case is found when the PV module is made entirely using the French mix. The low scores are due to the way that emissions from nuclear are classified and characterized.

2.6 LCA study for silicon-based PV modules

Another advantage of LCA technique is the possibility to carry out a comparative analysis between processes, products or services. In this second example, a comparison between three technologies of PV modules (m-Si, p-Si and ribbon-Si) is made. LCA is conducted following the data published by Alsema et al. (Alsema & Wild-scholten, 2006; de Wild-Scholten & Alsema, 2005) to manufacture PV modules based on silicon.

2.6.1 *Goal and scope definition*

More precisely, the aim of this study is to compare the environmental impact of some manufacturing processes of crystalline silicon-based PV module (m-Si. p-Si and ribbon-Si). The standard manufacturing processes for these PV modules were described Section 2.2.1. Figure 2-27 shows the system boundaries. Data on the assembly of all components were collected by choosing a functional unit 1 kW_p of installed power[2], which is more convenient as several technologies have to be compared. The manufacturing process for each of the three c-Si-based PV module technologies is divided into 4 main groups: SoG-Si, wafer, solar cell, and PV module (see Figure 2-27). In the case of m-Si and p-Si PV modules, the process of ingot growth and wafer sawing were grouped together.

[2] A kW_p specifies the output power achieved by a PV module under Standard Test Conditions (an incident sunlight of 1000 W/m², a cell temperature of 25°C and an Air Mass of 1.5)

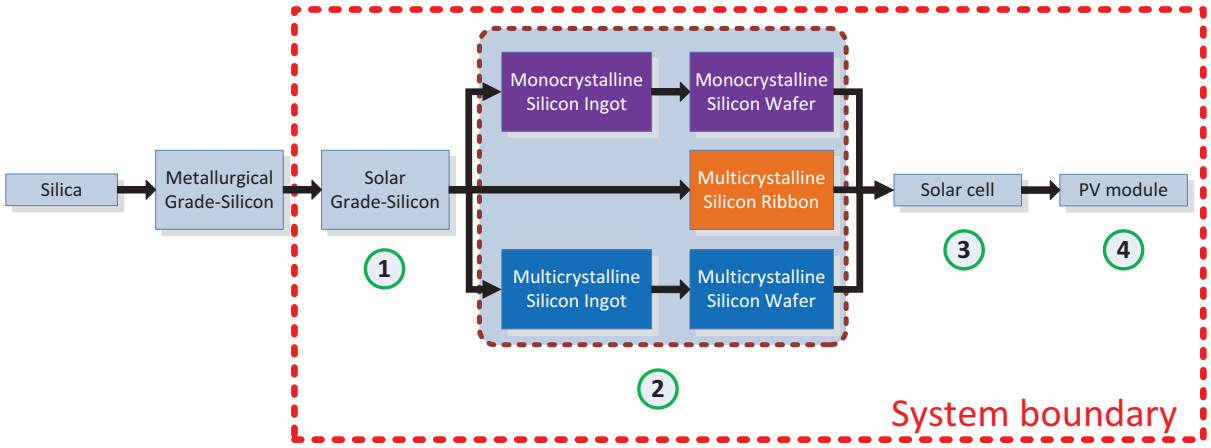

Figure 2-27 Scheme of system boundaries

2.6.2 *Technology assumptions, LCI and data collection*

The wafer dimensions that are considered are set at 125 x 125 mm as the standard size for all wafer technologies (including ribbon). Wafer thickness lies in the range of 270-300 µm for m-Si and p-Si wafers and 300-330 µm for ribbon wafers. Only one standard module type with 72 cells (1.25 m^2 module area) and with glass/EVA/Tedlar lamination is considered. Glass thickness is set at 3.6 mm.

LCI for the three technologies is established from data published by de Wild-Scholten and Alsema (de Wild-Scholten & Alsema, 2005). Complementary data were acquired from Ecoinvent database implemented in SimaPro LCA software tool for all manufacturing processes. As previously mentioned, a German electricity mix is chosen.

2.6.3 *LCIA results and interpretation*

IMPACT 2002+ (Jolliet et al., 2003) method is selected for LCIA. The same procedure used in Section 2.5.3 was followed to classify and characterize the emissions. As in the previous case, the score of both impact and damage categories are normalized using the same factors contained in Table 2-12. Figure 2-28 shows the normalised results of main midpoint categories and damages categories for the three types of PV modules in order to analyze the importance of the respective contribution of each category in the overall environmental impact. Not surprisingly, it is observed that m-Si technology has the highest score for all impact categories while the silicon ribbon modules have the lowest impact. When comparing the categories of damage (see Figure 2-28b), it can be seen that Resource depletion and Climate Change have the largest contributions in terms of global environmental impacts. Figure 2-28a indicates that the categories relating to Non-renewable energy and Global Warming lead to higher scores among the midpoint categories.

A more realistic comparison to evaluate different technologies for PV is to consider the number of panels required to meet a given amount of energy. Using the same considerations as above, the minimum number of panels required to meet a demand of 1 kWh (see Table 2-14) with an average daily irradiance of 1 kWh / m² is computed. The new FU is the demand of 1kWh. This functional unit corresponds now to the service t hat is produced corresponding to energy production which is more

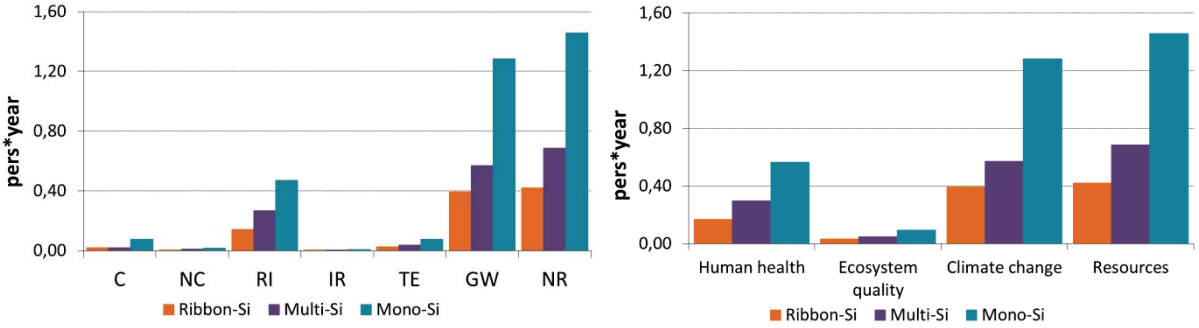

(a) Midpoint categories (b) Damage categories

Figure 2-28 Normalised results for the three PV module technologies. IMPACT 2002+

realistic. The conversion efficiency of the modules is based on the average efficiency of each technology proposed by de Wild-Scholten and Alsema (Alsema & Wild-scholten, 2006) (see Table 2-14). LCI was created from Ecoinvent database. IMPACT 2002+ was kept as the LCIA method. Figure 2-29 shows the results of the LCA. A similar trend relative to the impact of each technology assessed is observed.

A closer look can be made to identify the steps of the manufacturing process that generate the highest impact. Global warming midpoint category is selected for the analysis.

Figure 2-30 demonstrates that the largest contribution comes from the first two stages of module manufacturing (i.e. silicon wafer and solar cell) for the three technologies. It can be clearly pointed out that for the m-Si module, the wafer manufacturing process generates more than half of the total impact of the category, because of the high energy consumption involved during CZ crystal growth. The main causes are related to the emissions corresponding to the energy needs of the process as it can be highlighted through the analysis of the resources involved in the manufacturing process of m-Si wafers (see Figure 2-31).

Table 2-14 Efficiencies and number of PV modules required

	Ribbon-Si	**p-Si**	**m-Si**
Efficiency	11.5%	13.2%	14.0%
No. PV module	7	7	6

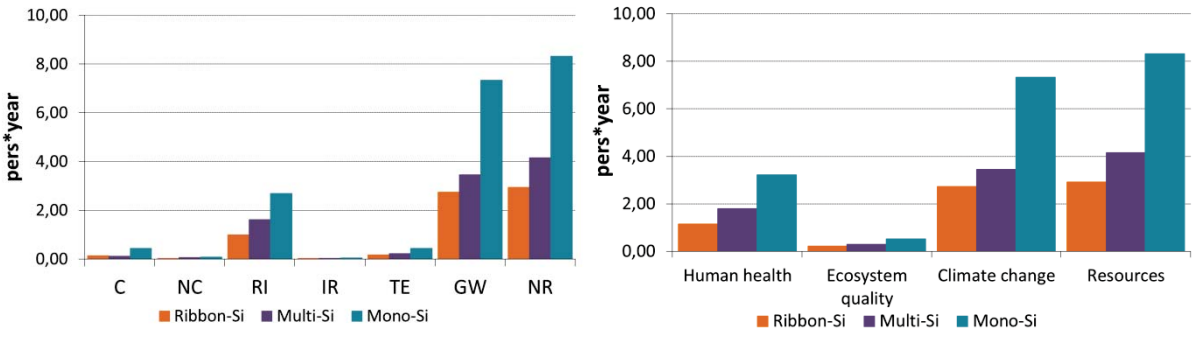

(a) Midpoint categories (b) Damage categories

Figure 2-29 Normalised results for the three PV module technologies. FU: 1 kWh demanded. IMPACT 2002+

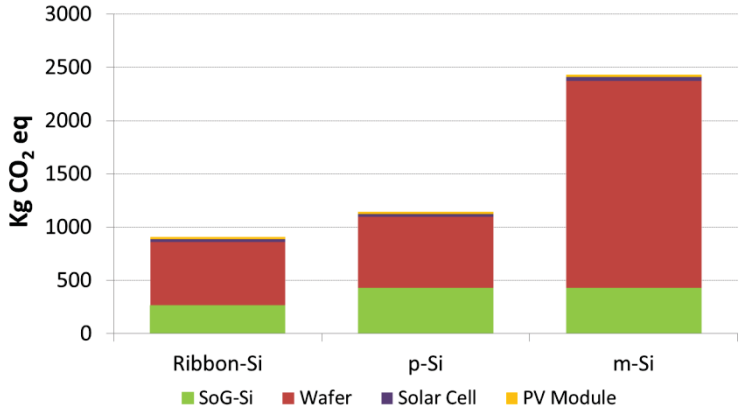

Figure 2-30 Result of main processes in Global Warming category for 3 PV module technologies

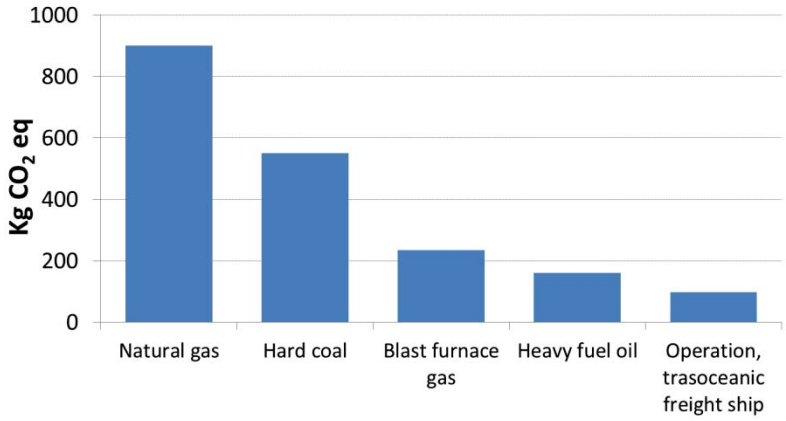

Figure 2-31 Score of the five main resources that contribute to GW characterization for m-Si PV module at wafer elaboration process.

2.7 LCA study for PVGCS

Another LCA is implemented to compare 5 different PV modules technologies in a large-scale PVGCS. The five PV module technologies are the most commercialized ones: m-Si, p-Si, a-Si, CdTe and CIS. In this example all the components of a PV system (PV modules, BOS components and the mounting system) are analysed. The procedure followed in this example as well as the resulting flow inventory will provide the basis for the integration and evaluation of the environmental aspect into the main model for the dimensioning of a large-scale PV system.

A guide published by International Energy Agency (V. Fthenakis et al., 2011) for LCA of PV system determines four main aspects that must be taken into consideration:

- **Technical characteristics related to PV systems.** The life expectancy of PV components and systems is not the same. e.g. 20-30 years for PV modules or 10 year for AC/DC inverter. Depending on the goal of the study, the irradiation collected by modules or their degradation can be important.
- **LCI/LCA modelling aspects.** The appropriate system model depends on the goal of the LCA. It can have a short-term prospective as for the choice of a PV electricity-supplier or comparisons between PV systems or electricity-generating technologies; or long-term

prospective as for comparison of future PV systems or of future electricity-generating technologies. The electricity mix must be considered carefully as well as the reference flow to enable comparisons. The reference flow can be expressed in *kWh electricity produced* (used for comparing PV technologies and modules), m² of module or *kWp rated power*.

- **Discuss and interpretation of results.** Beside the impact indicators used in LCIA it may be helpful use another indicator as energy payback time (EPBT)
- **Reporting and communication.** Some key parameters must be kept in mind : irradiance level and location; PV module efficiency; type of mounting system; components expected lifetime; system boundaries; technical and modelling assumptions; LCA tool and database used.

2.7.1 *Goal and scope definition*

This LCA study aims at comparing the environmental impact associated with electricity production with different PVGCS configurations using the 5 most commercial PV module technologies. As in previous LCA study, the functional unit is fixed as energy demand. It concerns here the demand of 5 MWh that must be supplied by the PV power plant each year during 20 years. System boundaries are represented in Figure 2-32. They include the manufacturing of core infrastructures (modules, mounting system, cabling, and AC/DC inverter), the plant installation (excavation and mounting system) and the energy generation for a 20 year period (including component replacement).

Recycling processes of the different components of PVGCS are not included in this study due to lack of reliable information for all PV modules technologies evaluated. The different recycling processes currently implemented for PV modules and their implementation in LCA will be discussed in Chapter 6.

2.7.2 *Technology assumptions, LCI and data collection*

A yearly irradiation 1200 kWh/m^2 on an inclined plane (30°) is considered. A fixed-mounting system with aluminium supports is used. A 10-years lifetime is considered for AC/DC inverter and 20-year life time is considered for the other components. The conversion efficiency of PV modules is constant over time and is based on the characteristic given by PV modules contained at Ecoinvet database.

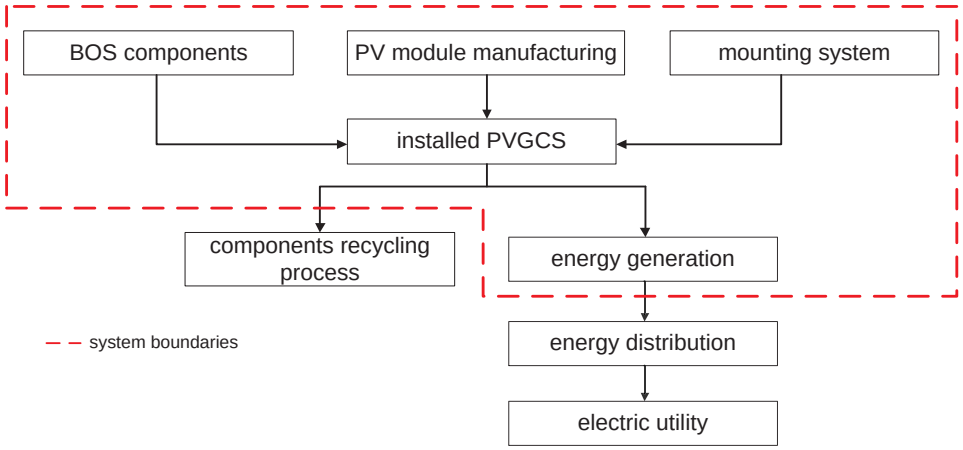

Figure 2-32 Boundaries of the system examined to compare different PV technologies

The five PV modules are found in Ecoinvent database. The datasheets contain the input and output flows in order to calculate the total emission flows. The reason why these PV modules were used was the lack of data for material and energy flow found in the literature for manufacturing process of thin-film modules. Ecoinvent database is constantly under improvement to become a more accurate tool for create the LCI of total emission for a given process or product.

The 2.5kW inverter is selected from Ecoinvent database for the five PV installations. The number of PV modules and DC / AC inverters needed to supply the energy demanded during the evaluation period as well as the main features are summarized in Table 2-15. The calculation was made taking into account the amount of irradiation received, the PV module efficiency as well as the electrical characteristics of the DC / AC inverter.

From the values shown in the Table 2-15 is noticed that the PV modules based on thin film technologies require a greater number of panels due to the low efficiency they have.

LCI of each technology under evaluation was performed from data displayed at the Table 2-15. The procedure followed was similar to the two last examples.

2.7.3 *LCIA results and interpretation*

IMPACT 2002+ method was applied for evaluating the environmental impacts. The characterization scores were obtained as in previous examples. The environmental assessment was carried out both in the main midpoint impact categories as in the four damage categories. The total score for each category was separate in order to compare the different elements that compose a PVGCS. Figure 2-33 shows the normalized results.

Looking at the total score for each of the five configurations in all categories shows that the highest environmental impacts in almost every category midpoint are obtained when a-Si PV modules are used. Only into the categories related with climate change and resources m-Si PV module configuration has the highest impacts.

A more detailed analysis, focusing into the components of a PVGCS, shows that the most influential process is PV module manufacturing for the total impact scores in all the categories. Among the five PV technologies under analysis, m-Si PV module leads in almost all the categories. CdTe PV modules had interesting results: it has the lowest total scores.

Table 2-15 Key features for LCA study

Module technology	**m-Si**	**p-Si**	**a-Si**	**CdTe**	**CIS**
Module efficiency η (%)	14.00	13.2	6.45	9.00	10.00
Module surface (m²)	1.46	1.46	1.10	0.72	0.72
Module life expectancy (years)	20	20	20	20	20
No. PV modules	22	24	58	62	69
No. AC/DC inverters	4	6	6	4	6

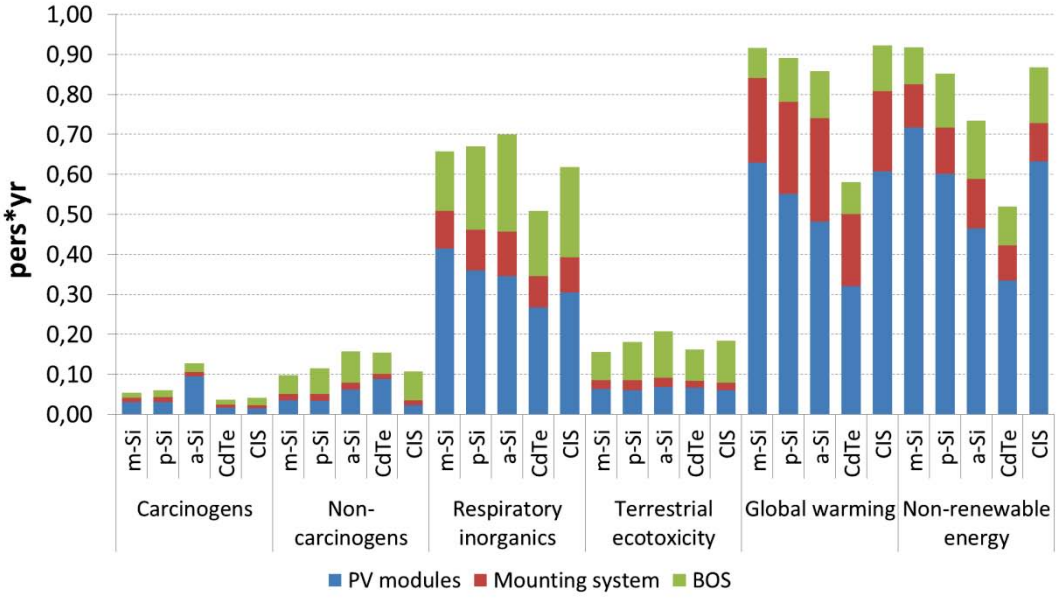

(a) Midpoint categories

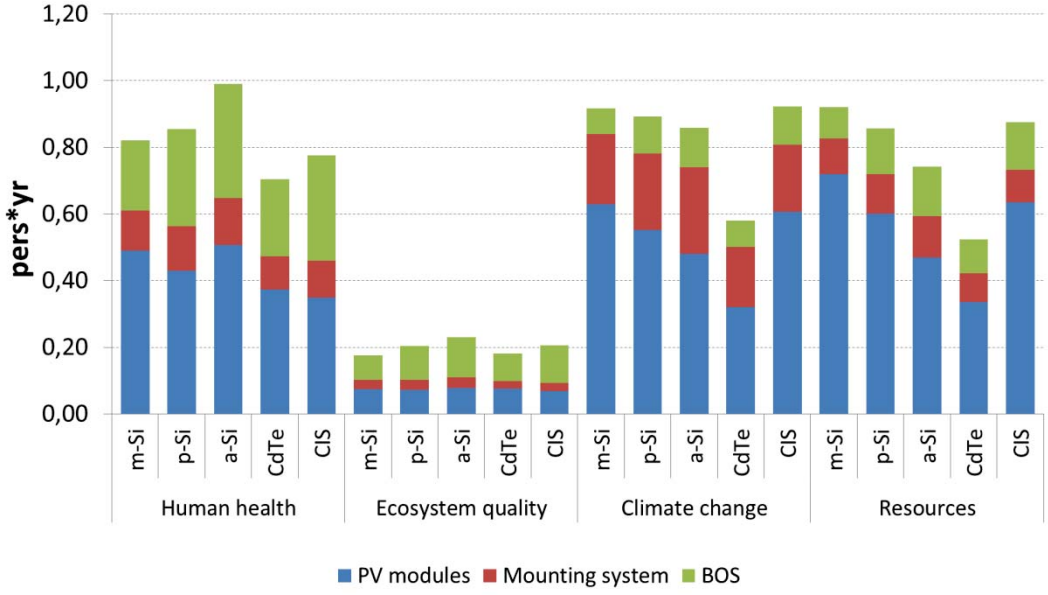

(b) Damage categories

Figure 2-33 Normalized results for the five PV installation considering 1200 kWh/m^2 yr of irradiation on an inclined plane (30°). IMPACT 2002+

The LCI as well as the procedure followed in this example will be used in the latter chapter when the evaluation of environmental impacts will be included and taken into consideration as criteria for the design of large-scale PV power plants.

2.8 Conclusion

The analysis of the manufacturing processes of the five main modules PV technology highlights that it is necessary to quantify the embodied primary energy required for their manufacture, especially with c-Si based technologies to guarantee the sustainable nature of a technology. An environmental assessment is required to confirm that, indeed, PV systems really help to reduce and / or prevent pollution. There are many techniques developed for environmental assessment and among them Life

Cycle Assessment (LCA) which is particularly interesting for energy production. Three cases have been tackled with LCA. The results show that the PV modules are the elements of a PVGCS that contribute most to the overall environmental impacts. Another aspect to mention is the influence of the composition of the electricity mix in the assessment of environmental impacts generated by a PV module.

This discussion reinforces the need for a multi-criteria study that allows establishing a methodology that conciliates both the technical-economic and environmental criteria. The procedure of LCA applied in a PVGCS will serve to integrate the environment criterion into the proposed study. To our knowledge, this kind of approach has not yet been implemented. The classical LCA tools (SimaPro and other LCA software) are generally not flexible and do not exchange with other programs. From a practical viewpoint, a specific environmental module was designed from extraction of the dedicated EcoInvent database that is used for PV systems.

It must be highlighted that this kind of study has been extended to other kinds of solar systems to compare two heliostat configurations (autonomous and classical heliostats) for heliothermodynamic power plants for concentrated solar power. This research was conducted within the OSSOLEMIO project in collaboration with the *Laboratoire Plasma et Conversion d'Energie* (LAPLACE) in the framework of Alaric Maintenon's PhD thesis (Montenon, 2013), under the supervision of Prof. Pascal Maussion.

The results indicate that even if variation between the two configurations is not so high at design stage, the electrical grid heliostat generates the most important impacts to the environment after 20 years of operation. The energy supplied for operating the grid-connected heliostat is the main element that affects the different categories analyzed in LCA. It also depends on the energy mix of the country in which the power station will be built. This work was presented at First International Conference on Renewable Energies and Vehicular Technology (REVET) (see Appendix A).

Chapter 3

A MODELLING AND SIMULATION FRAMEWORK FOR SIZING LARGE-SCALE PHOTOVOLTAIC POWER PLANTS

L'objectif de ce chapitre est de présenter l'approche de modélisation qui sera utilisée dans ce travail pour représenter les performances d'une installation photovoltaïque. Une analyse des logiciels disponibles qui peuvent être utilisés pour concevoir et évaluer la performance de PVGCS à grande échelle est tout d'abord présentée dans un but d'intégration dans une démarche d'écoconception. Les manques ou limitations des approches recensées ont conduit à développer un cadre spécifique pour la modélisation et la simulation du système PV système, basé par une méthodologie en trois étapes. La première étape consiste en l'estimation d'un rayonnement solaire reçu par le système en fonction de la localisation géographique. Un modèle mathématique pour le dimensionnement du PVGCS qui fournit l'énergie annuelle produite par les caractéristiques des composants et les limites de la conception des installation constitue la deuxième étape. La dernière étape correspond à l'évaluation des critères technico-économiques (retour économique et retour énergétique) et environnementaux (catégories intermédiaires de la méthode Impact 2002+). L'approche est ensuite validée par un exemple extrait de la littérature. Une comparaison de cinq technologies de modules photovoltaïques sert également d'illustration de la démarche. Les résultats obtenus confirment l'intérêt d'utiliser une approche d'optimisation pour rechercher la solution la plus intéressante en tenant compte simultanément des aspects technico-économiques et environnementaux.

Nomenclature

Acronyms

ADEME	Agence de l'Environnement et de la Maîtrise de l'Energie
AI	Artificial Intelligence
CdTe	Cadmium telluride
CIS	Copper indium diselenide
EPBT	Energy PayBack Time
LCA	Life Cycle Assessment
MBE	Mean Squared Error
NREL	National Renewable Energy Laboratory
PBT	PayBack Time
PV	Photovoltaic
PVGCS	Photovoltaic Grid-Connected System
RMSE	Root Mean Square Error
a-Si	Amorphous silicon
m-Si	Monocrystalline silicon
p-Si	Polycrystalline silicon
VBA	Visual Basic for Applications
WAP	Weinstock and Appelbaum approach

Symbols

α	Sun elevation angle, degree
β	PV collector inclination angle, degree
η	PV module efficiency, %
θ	Angle of incidence
θ_z	Zenith angle
ρ	Reflectivity ground index
D	Distance between PV sheds, m
D_{min}	Minimum distance between PV sheds, m
E_{max}	Maximum PV collector height above ground, m
G	Global irradiance, W/m²
G_b	Beam irradiance, W/m²
G_d	Diffuse irradiance, W/m²
G	Extraterrestrial irradiance, W/m^2
G_{sc}	Solar constant, 1367 W/m2
G_β	Global irradiance onto PV module tilted, W/m²
$G_{\beta,b}$	Beam irradiance onto PV module tilted, W/m²
$G_{\beta,d}$	Diffuse irradiance onto PV module tilted, W/m²
$G_{\beta,r}$	Reflected irradiance onto PV module tilted, W/m²
H	PV collector height, m
H_m	PV module height, m
H_{max}	Maximum PV collector height, m
K	Number of PV sheds
Kt	Clearness index
L	Solar field length, m

Symbols

L_C	PV collector length, m
L_m	PV module length, m
n	Day number; 1 to 365
N_c	Number of PV modules columns in the collector
N_r	Number of PV modules rows in the collector
Q_m	PV module's output energy, kWh
Q_{out}	Yearly output energy of the field, kWh
r_b	Beam ratio factor
t	Hour number, 1 to 24
T_m	PV module temperature, °C
W	Solar field width, m
Z^+	Positive natural number set

3.1 Introduction

System modelling forms a key part of the PV system design. It can provide answers to a number of important issues such as the overall array size, orientation and tilt, and the electrical configuration. The design criteria depend generally on the nature of the application. The applications of PVGCS vary from small building integrated systems to PV power plants. The performance of PVGCS depends upon solar resource at site, system configuration and load parameters. Modelling tools are available to provide solar radiation data, assess possible shading effects and produce the resulting electrical layout of the array.

The objective of this chapter is to present the modelling approach that will be used in this work to represent the performance of a PV power plant, taking into account its mains features.

This chapter is dived into seven sections. Section 2 first presents an overview of the available software tools that can be used to design and evaluate the performance of large-scale PVGCS. The list of software tools is not exhaustive but includes the most reported ones in the dedicated literature. The analysis of the reported contributions led to the development of a specific framework for PV modelling and simulation purpose that is proposed in section 3. The objective is then to couple it with an outer optimization module for generating optimal configuration alternatives. The system implies a three-step methodology:

(1). The estimated solar radiation received by the system according to the geographic location is the core of section 4.

(2). A mathematical model for PVGCS sizing is presented in section 5: it provides the annual energy generated from the characteristics of the system components and limitations on the design of the installation.

(3). The evaluation of techno-economic (PayBack Time and Energy PayBack) and environmental (IMPACT 2002+ midpoint categories) criteria is then presented in section 6.

The approach is then validated with a reference example from the literature (Weinstock and Appelbaum (Weinstock & Appelbaum, 2009)).

Finally, the integration of the proposed model in order to compute evaluation functions, based on techno-economic and environmental aspects, in an optimization loop is a natural extension of this work.

3.2 Literature review on PV System design tools and work objective

Following the guidelines presented in Chapter 1 (Figure 1-12) for PVGCS design, the first step is the estimation of the radiation received at the site as well as the amount of energy supplied to the utility grid.

Power generation through photovoltaic conversion is very difficult to make an accurate assessment when designing a PVGCS because it depends upon incident solar radiation and PV module performance which are affected by uncertain parameters such as daily weather conditions or ambient air temperature. These parameters change all the time and they are not the same every year. The hourly, daily, monthly or yearly mean value is considered for PVGCS design.

Numerous commercial and academic computer models using different algorithms for modeling, analyzing, simulating PV systems are available. These tools present different degrees of complexity and accuracy depending on the specific tasks that each tool has been developed for. It is usual to distinguish between sizing tools (which determine the component size and the corresponding configuration) and simulation/modelling tools, which analyse the system output and performance once its specifications are known. Examples of these sizing and simulation tools are given in Table 3-1. They involve generally the estimation of solar radiation (using meteorological databases or mathematical models) and/or the estimation of the energy generated by the system taking into account the characteristics and location on the field of PV components (e.g. modules, the balance of system), weather consideration and solar radiation.

The main problem that can be encountered when using one of the available tools as those presented in Table 3-1 is the lack of an approach that allows the optimization of the sizing of a PVGCS considering economic and environmental criteria. Sizing is made taking into account technical objectives. In addition, the coupling of all the components via an external program to optimize the PV plant taking into consideration the three main criteria is difficult due to the closed structure used in each tool.

To overcome the problem of interoperability, the design of a simulator for received solar radiation coupled with a sizing module constitutes the most suitable option. The simulator must be designed in an open manner so that it can be interfaced easily with an outer optimization loop. The estimation of solar radiation and the output energy of the system are the two most critical aspects of any PV System design and sizing tools.

Table 3-1 System sizing and simulation programs

Program	Source	Objective	Type of system	Main characteristics	Resultants	Advantages	Inconvenient
CalSol	Institut National de l'Energie Solaire (INES), France	Simulation and data analysis of PV system	Grid-connected, stand-alone and DC-grid system	- Economic analysis tool.	- CO_2 balance. - Report of yield production and monthly irradiation. - Economic report.	- Easy to handle. - Pre-sizing. - Available online.	- Only French meteorological database - No PV components database. - Insufficient energy loss calculation and economic analysis. -No interconnection with another program is allowed.
NSol	Orion Energy Corporation, USA	PV system sizing	Grid-connected and PV-generator hybrid power	- Insolation and PV components databases.	- Quick screening analyses. - System performance.	- Easy to handle. - Optimize the array size to the inverter capacity.	-No interconnection with another program is allowed. - No shading loss calculation.
PVGIS	Institute for Energy and Transport – European Commission	Estimation of solar radiation and simulation of a PV system	Grid-connected	- Meteorological database. - Interactive maps.	- Report of yield production. - Monthly or daily radiation.	- Easy to handle. - Import meteorological data. - Available online.	- Exclusive to Europe and Africa. - No PV components database. - No energy loss calculation and economic analysis. -No interconnection with another program is allowed.
PVSOL	Solar Design Company, UK	Design, simulation and data analysis of PV system	Grid-connected and stand-alone	- Extensive meteorological and PV components database. - Calculate shading losses. - 3D design tool. - Economic analysis tool.	- Report of yield production, efficiency of system and losses. - Economic report.	- Easy to handle. - 3D animation. - Import meteorological data. - Possibility of parameter settings. - Good quality results.	- No interconnection with another program is allowed.

Table 3-1 (*continued*)

Program	Source	Objective	Type of system	Main characteristics	Resultants	Advantages	Inconvenient
PVsyst	University of Geneva, Switzerland	Size, design, simulate and data analysis of PV system	Grid-connected, stand-alone and DC-grid system	- Extensive meteorological and PV components database. - Calculation of shading losses. - 3D design tool. - Economic analysis tool.	- Report of yield production, irradiation, efficiency of system and losses. - Economic report.	- Import meteorological data. - 3D animation. - Possibility of parameter settings. - Good quality results.	- Unfriendly use. - Sizing restricted to collector configuration. - No interconnection with another program is allowed.
SolarPro	Laplace System Co., Japan	Design and simulate PV system	Grid-connected	- Meteorological and PV components database. - 3D design tool. - Calculation of shading losses.	- Report of yield production.	- Easy to handle.	- No energy loss, calculation and economic analysis. - No interconnection with another program is allowed.
System Applications and Design Consideration	Sandia National Laboratories, USA	Simulate PV system	Grid-connected	- Creation of a specific PV module and inverter. - Five models for diffuse irradiance calculation	- Report of yield production and losses. - Economic report.	- Import meteorological data. - Collaborative work. - Web site with documents and general instruction.	- No meteorological and PV components database. Programming background needed. - Restrictive interconnection with another program.

3.3 Development of the simulation tool

Most of the reported studied (Gong & Kulkarni, 2005; Aris Kornelakis & Marinakis, 2010; Mondol, Yohanis, & Norton, 2006; Notton, Lazarov, & Stoyanov, 2010; Weinstock & Appelbaum, 2007, 2009) involve PVGCS optimization considering only one criterion. Other investigations (Dones & Frischknecht, 1998; Ito, Kato, Komoto, Kichimi, & Kurokawa, 2008; Kannan, Leong, Osman, Ho, & Tso, 2006; Pacca, Sivaraman, & Keoleian, 2006) address only the issue of the environmental impact assessment of the components of a PV system with emphasis on PV module technology. The main purpose consists in generating alternatives of optimal PVGCS configurations taking into account technical and economic aspects as well as their environmental impact.

The closed structure of the tools listed in Table 3-1 makes complicated to couple them with an environmental module and with an outer optimization loop to solve the resulting optimization problem. This explains why a dedicated simulation tool was developed in order to develop the proposed methodology.

Figure 3-1 illustrates the system flow diagram for modeling solar radiation and estimating the output energy of a PVGCS. The proposed modeling framework will then coupled with an optimization module for generating optimal configuration alternatives. The system is based on the following models:

(a). The estimated solar radiation received by the system according to the geographic location.

(b). The PVGCS sizing based on a mathematical model that provides the annual energy generated from the characteristics of the system components and limitations on the design of the installation.

(c). The evaluation of economic, technical and environmental criteria.

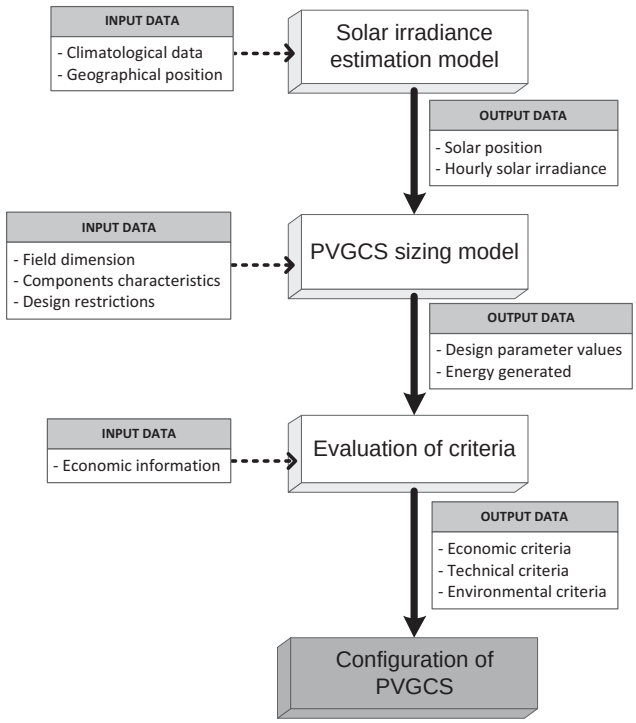

Figure 3-1 Functional flow diagram of the proposed methodology

3.4 Solar radiation model

3.4.1 *Solar radiation*

Solar radiation on tilted planes is very important to design flat plate PV collectors for power plants. When radiation passes through Earth's atmosphere, it suffers changes in its trajectory by the elements present in the atmosphere. Elements such as ozone, oxygen, carbon dioxide and water vapor absorb the radiation; some are reflected by the clouds. The dust and water droplets also cause disturbances. To eliminate the effects of local features, solar radiation is measured on horizontal surfaces free of obstacles. The result is the decomposition of the incident solar radiation into a receiver placed on the surface in different components (Lorenzo, 2003). Consequently, solar radiation data are most often given in the form of global radiation on a horizontal surface. Since PV modules are usually positioned at an angle to the horizontal plane, the radiation input to the system must be calculated from this data.

Global radiation on a tilted plane consists of three components (Figure 3-2):

- *Beam radiation.* The radiation received from the sun without having been scattered or reflected that reaches the surface. It is also known as direct radiation.
- *Diffuse radiation*. The radiation received from the sun after its direction has been changed by scattering by the atmosphere.
- *Reflected radiation*. The radiation received from the sun that is reflected by the ground. Albedo radiation is another name.

Global radiation. The total radiation falling on a surface is the sum of beam, diffuse and reflected radiation.

The calculation of irradiance arriving on a tilted surface, using as input global horizontal data, raises two main problems related on the one hand to the separation of the global horizontal radiation into its direct and diffuse components and, from them, on the other hand to the estimation of the irradiance components falling on an inclined surface.

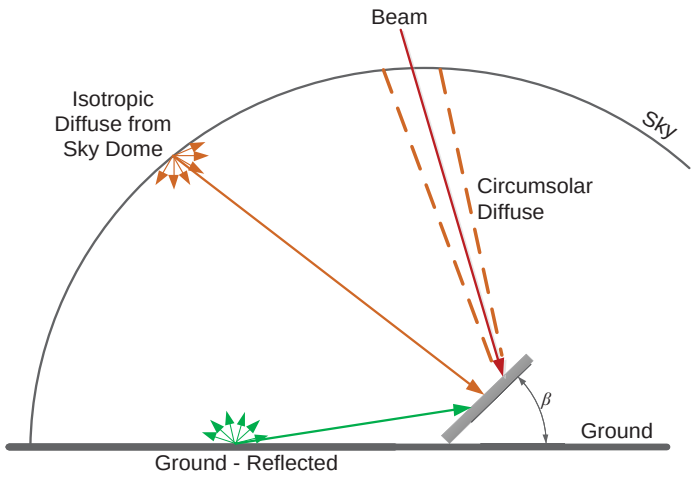

Figure 3-2 Different components of solar radiation in a tilted surface

Over the years, different models have been developed to estimate solar radiation over tilted planes (Demain, Journée, & Bertrand, 2013; Duffie & Beckman, 2006; Noorian, Moradi, & Kamali, 2008). The models can be classified as isotropic or anisotropic models. Yet, almost all models use the same method of calculating beam and ground-reflected radiation, the main difference is the treatment of diffuse radiation.

Isotropic models assume that the intensity of sky diffuse radiation is uniform over the sky dome. Hence, the diffuse radiation incident on a tilted surface depends on the fraction of the sky dome seen by it. The most widely used model belonging to this category is the one developed by Liu and Jordan (Noorian et al., 2008). Because of its simplicity, this model has achieved great popularity, despite the fact that it underestimates diffuse irradiance on surfaces tilted to the equator.

The second group of models assumes both the anisotropy of the sky diffuse radiation in the circumsolar region (sky near the solar disc) and an isotropically distributed diffuse component from the rest of the sky dome. Better results are obtained with this type of model.

3.4.2 *Model Description*

The solar radiation model computes the radiation received in the site where the future plant will be built. Figure 3-3 shows the input data necessary for the operation of the model, sub-models and the outputs.

Visual Basic for Applications (VBA) in Excel was used for simulation purpose. The main advantages include the automation of repetitive tasks and calculations, the easy creation of macros in a friendly programming language, the possibility to use existing Excel functions and formulas, ability to import and export data and the classification and management of results.

It is relevant to make a difference between power and energy when considering PV systems. The radiation term is used as a general one for referring both aspects. The following concepts are used to distinguish between:

- *Irradiance.* The density of power falling on a surface per unit area of surface at a specific time. The SI units is watt per square meter (W/m^2); others units are $MJ/m^2/day$ or $kWh/m^2/day$.

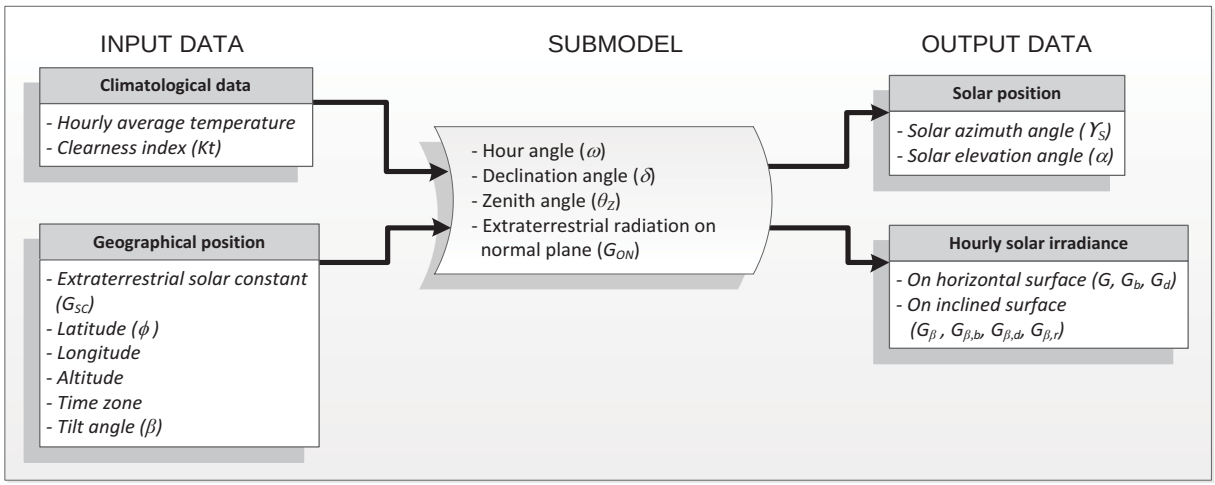

Figure 3-3 Data flow diagram of solar irradiance estimation model

- *Irradiation.* The density of energy that falls on the surface over a period of time. It is measured in Wh/m^2 or J/m^2. It is the result of the integration of the irradiance over a specific time, usually an hour or a day.

Irradiation over an hour (in Wh/m^2) is numerically equal to the mean irradiance during this hour (in W/m^2); irradiance values can be assimilated to hourly irradiation values (Duffie & Beckman, 2006). The developed model calculates the irradiance received by the PV collector surface every hour for a standard calendar year.

The inputs for this module are classified into two groups. The former group is composed of climatological data of the studied site. The average hourly temperature is obtained from collected information that is available in various databases. Another important element to establish the relationship between solar radiation on the surface of the Earth and the extraterrestrial radiation is the index of transparency of the atmosphere or clearness index (*Kt*). This index is the radio between the horizontal radiation of a particular hour and the extraterrestrial radiation for that hour, as expressed by:

$$K_t = \frac{G}{G_o} \tag{3.1}$$

Kt is imported from climatological databases.

The latter group is composed of all the data inherent to the geographic location of the site where the facility will be placed. This information allows us to estimate the position of the sun and the solar radiation that the facility will handle every hour.

Before making any estimation of the amount of energy generated by a PV system, it is necessary to understand how the energy radiated by the sun reaches the earth and the effect of the atmosphere in its way to impact the surface of the panel solar.

The Sun is a sphere composed of extremely hot gas with a diameter of 1.39×10^9 m. It acts as a perfect emitter of radiation (black body) at a temperature close to 5800° K. The sun is indeed a continuous fusion reactor, and these reactions are the cause of the energy radiated by this celestial body.

Figure 3-4 shows the relationship between the Sun and Earth. Radiation emitted by the sun and its relation to the Earth gives an almost constant solar radiation outside the Earth's atmosphere.

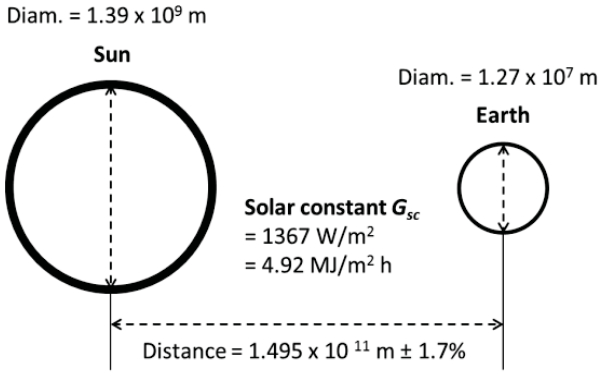

Figure 3-4 Sun-Earth relationship

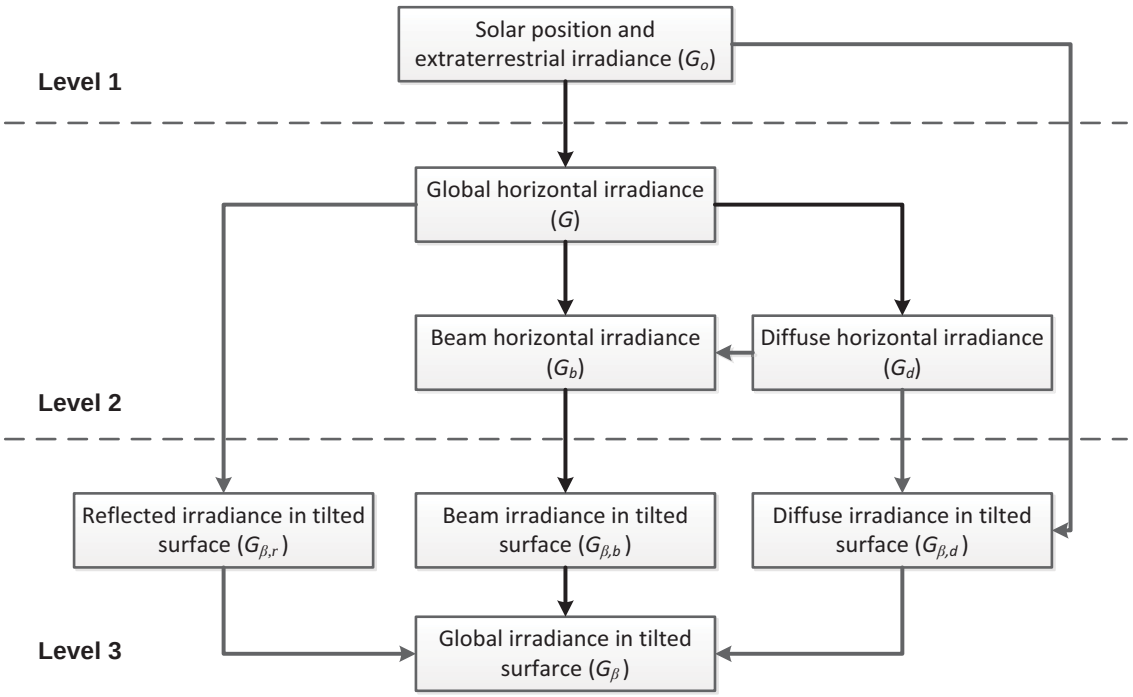

Figure 3-5 Sequence for determination of hourly global tilted irradiance

The solar constant (G_{sc}) is defined as the amount of incoming solar energy per unit area incident on a plane perpendicular to the direction of propagation of radiation, to the distance of an astronomical unit (1,495 x 10^{11} m) and before passing through the atmosphere. According to the World Radiation Center (*WRC*) (Perpiñan Lamigueiro, 2012), a value of 1,367 W/m^2 has been adopted, with an uncertainty of about 1%. The radiation falling on the ground before crossing the atmosphere known as extraterrestrial radiation (G_o) consists almost exclusively of the radiation passing through the space in a straight line from the sun.

When radiation passes through Earth's atmosphere, it suffers changes in its trajectory by the elements present in the atmosphere. The overall amount of global irradiation that reaches a receiver placed on the surface of the earth is extremely variable. On one hand extraterrestrial radiation experiences a daily variation due to the apparent motion of Sun. On the other hand, there is random variation caused by weather: clouds, rain, sandstorm, etc. Figure 3-5 shows the relations among the different levels of solar irradiance.

To estimate each of the components of the global irradiance is important to understand the relationship between a plane at any orientation at any given time and the incoming solar radiation due to the position of Sun with respect to the plane (see Appendix B). The equations employed to calculate the sun's position and their encoding were taken from the research work of Montenon (Montenon, 2013) as part of the collaboration between the two laboratories.

3.4.2.1 Components of hourly irradiance on horizontal surface

Solar irradiance received onto a horizontal surface is split into its beam and diffuse components. These components provide the basis for estimating solar radiation on tilted surfaces. Hourly irradiance received on the horizontal surfaces may be expressed by:

$$G=G_b+G_d \tag{3.2}$$

The estimation of diffuse irradiance is very complex because it depends on the composition, shape and position of the elements that cause the scattering of radiation and this may vary with time. Diffuse irradiance is essentially anisotropic. The amount of reflected radiation is affected by the nature of the ground and by a wide range of features (snow, vegetation, water, etc.).

Miguel et al. (Noorian et al., 2008) establish a correlation between the *diffuse fraction* of hourly global horizontal irradiance and the *clearness index*. This correlation is given by the following expressions:

$$\frac{G_d}{G}=\begin{cases}0.995-0.081Kt & if \quad Kt<0.21\\ 0.724+2.738Kt-8.32Kt^2+4.967Kt^3 & if \quad 0.21\le Kt\le 0.76\\ 0.180 & if \quad Kt>0.76\end{cases} \tag{3.3}$$

Then, the beam irradiance can be calculated reformulating Equation (3.2) as follows:

$$G_b=G-G_d \tag{3.4}$$

3.4.2.2 Components of hourly irradiance on tilted surface

The global irradiance on an inclined surface, G_β, is integrated by beam, diffuse and albedo irradiance (Equation (3.5)). The most adequate procedure to calculate the global irradiance on a tilted surface is to obtain separately the components.

$$G_\beta = G_{\beta,b}+G_{\beta,d}-G_{\beta,r} \tag{3.5}$$

3.4.2.2.1 Beam irradiance

The amount of beam irradiance on a tilted surface can be calculated by multiplying the beam horizontal irradiance by the *beam ratio factor* (r_b).

$$G_{\beta,b} = G_b\, r_b \tag{3.6}$$

$$r_b=\frac{cos\,\theta}{cos\,\theta_Z} \tag{3.7}$$

One consideration must be taken into account in calculating this component, when the sun shines on the back of the surface ($\cos\theta < 0$) the irradiance on the PV modules is normally not utilized, $G_{\beta,b} = 0$. A factor max (0, $\cos\theta$) is introduced in Equation (3.7).

$$r_b=\frac{\max(0,cos\,\theta)}{cos\,\theta_Z} \tag{3.8}$$

3.4.2.2.2 Reflected irradiance

The reflectivity of most types of ground is rather low (Lorenzo, 2003) except snow and ice. Consequently, the contribution of this type of irradiance falling on a receiver is low. Equation (3.9) computes ground-reflected irradiance.

$$G_{\beta,r} = \rho G\frac{1-cos\,\beta}{2} \tag{3.9}$$

where ρ is the reflectivity of the ground and depends on the composition of the ground. A value of 0.2 is commonly adopted.

3.4.2.2.3 Diffuse irradiance

The methods used to estimate the diffuse irradiance on a titled surface are classified as either *isotropic* or *anisotropic* models. The isotropic models assume that the intensity of diffuse sky radiation is uniform over the sky dome. Hence, the diffuse irradiance incident depends on the fraction of the sky dome where the surface is located. A well-known *isotropic* model was proposed by Liu and Jordan (1963).

$$G_{\beta,d} = G_d \frac{1 + \cos\beta}{2} \tag{3.10}$$

Better results are obtained with the so-called *anisotropic* models. This type of models includes a circumsolar brightening, which assumes that the highest intensity is found at the periphery of the solar disk and falls off with increasing angular distance from the periphery.

Hay and Davies (Noorian et al., 2008) propose a model based on the assumption that all of the diffuse can be represented by a circumsolar component coming directly from the sun and an isotropic component coming from the entire celestial hemisphere. The diffuse irradiance on a tilted surface is then:

$$G_{\beta,d} = G_d r_d \tag{3.11}$$

$$r_d = \frac{G_b}{G_o} r_b + \left(1 - \frac{G_b}{G_o}\right)\left(\frac{1 + \cos\beta}{2}\right) \tag{3.12}$$

Reindl et al. (Noorian et al., 2008) propose another model (Equation (3.13)).. This model extends the Hay and Davies model by adding the *horizon brightening*. The horizon brightening is assumed to be a linear source at the horizon and to be independent of azimuth. In fact, for clear skies, the horizon brightening is highest at the horizon and decreases in intensity away from the horizon. For overcast skies, the horizon brightening has a negative value.

$$r_d = \frac{G_b}{G_o} r_b + \left(1 - \frac{G_b}{G_o}\right)\left(\frac{1 + \cos\beta}{2}\right)\left[1 + \sqrt{\frac{G_b}{G_o}}\sin^3\left(\frac{\beta}{2}\right)\right] \tag{3.13}$$

3.4.2.3 Validation

The simulator was used to estimate the annual radiation received in 4 different positions: Toulouse, France (43.4° N, 1.2°E,altitude 152 m), Sydney, Australia (33.5°S, 151.1°E, altitude 42 m), Mexico City, Mexico (19.2° N, 99.1°W, altitude 2277 m) and Singapore, Singapore (1.1° N, 104.1°E, altitude 5 m). The results were compared with those estimated for the same cities by MIDC SOLPOS Calculator 2.0 (National Renewable Energy Laboratory, 2000) for extraterrestrial irradiance and PVsyst software (University of Geneva, n.d.) for horizontal and tilted irradiance. MIDC SOLPOS Calculator 2.0 was developed by the National Renewable Energy Laboratory (NREL), a research laboratory for the U.S. Department of Energy. This software tool contains a Solar Position Algorithm (SPA) (Reda & Andreas, 2008) for solar radiation applications developed by the NREL. The algorithm can calculate the sun zenith and azimuth angle with uncertainties equal to ± 0.0003°. MIDC SOLPOS Calculator calculates the position of the sun in the sky and its intensity for any given location, day and

time. It is valid from the year 1950 to 2050 and has an uncertainty of ±0.01° (National Renewable Energy Laboratory, n.d.).

As mentioned in Table 3-1, PVsyst is a PV simulation tool developed at the University of Geneva, Switzerland to be used by architects, engineers and researchers. In 2011, PVsyst got excellent results in the PHOTON Magazine evaluation (Mermoud, 2011). The evaluation considered about 20 different PV simulation software available on the market for the study of PV systems yield and tried to assess the accuracy of irradiance data in the horizontal plane and ambient temperature, as well as horizon shading.

Two statistical tests based on root mean square (RMSE) and mean bias error (MBE), were used to compare the results of the model developed in this work and the aforementioned software tools (Diez-Mediavilla, de Miguel, & Bilbao, 2005; Noorian et al., 2008).

$$RMSE = \sqrt{\frac{C_i - M_i}{n}^2} \tag{3.14}$$

$$MBE = \frac{C_i - M_i}{n} \tag{3.15}$$

where C_i is the ith calculated value, M_i is the ith measured value of the radiation, and n is the total number of observations for a specified period of time. The lower the RMSE, the more accurate the model is. A positive MBE indicates an overestimation of the calculated values while a negative MBE indicates an underestimation.

Dimensionless measures of RMSE and MBE, relative RMSE (% RMSE) and relative MBE (% MBE), were also used. They are defined as follows.

$$\%RMSE = 100\frac{RMSE}{M} \tag{3.16}$$

$$\%MBE = 100\frac{MBE}{M} \tag{3.17}$$

where M is the mean of the measured values. The results can be observed in Table 3-2 and Table 3-3. Units of RMSE and MBE are kW/m².

The difference found was minimal especially when the model uses the formulation of Hay et al. (Noorian et al., 2008) for the calculation of diffuse irradiance. Table 3-3 shows the mean of results exposed in Appendix C for estimate G_β following Lu et al., Hay et al. and, Reindl et al. equation for calculate $G_{\beta,d}$. This explains why the model of Hay et al. model was adopted in this work.

Table 3-2 Root mean square (RMSE) and mean bias errors (MBE) of proposed simulator

	Horizontal Global Irradiance				Diffusse Horizontal Irradiance				Beam Global Irradiance			
	RMSE	MBE	% RMSE	% MBE	RMSE	MBE	% RMSE	% MBE	RMSE	MBE	% RMSE	% MBE
Mexico City	39.523	-1.529	18.786	-0.727	23.401	1.706	24.345	1.774	25.065	-3.234	21.935	-2.830
Singapore	39.523	-1.529	18.786	-0.727	24.780	0.345	23.749	0.331	21.503	-2.026	26.493	-2.497
Sydney	34.634	-0.978	18.870	-0.533	23.683	4.028	28.928	4.920	25.450	-5.006	25.033	-4.924
Toulouse	27.486	-1.283	17.943	-0.837	20.181	1.909	25.464	2.409	19.480	-3.192	26.348	-4.317

Table 3-3 Comparison of G_β estimated

	Titl (°)	Lu et al.	Reindl et al.	Hay et al.
Mexico City	**RMSE**	43.688	39.231	40.704
	MBE	8.618	-1.343	0.913
	% RMSE	23.577	20.861	21.838
	% MBE	2.597	-0.636	0.898
Singapore	**RMSE**	31.051	27.197	28.190
	MBE	2.414	-0.669	1.302
	% RMSE	22.933	19.286	20.225
	% MBE	2.534	-0.391	1.576
Sydney	**RMSE**	46.319	35.474	47.361
	MBE	-5.318	-1.488	0.394
	% RMSE	26.714	19.979	27.407
	% MBE	-3.032	-0.839	0.347
Toulouse	**RMSE**	36.105	34.267	34.523
	MBE	-5.462	-1.099	0.522
	% RMSE	24.285	23.019	23.222
	% MBE	-3.636	-0.704	0.512

3.5 PVGCS sizing model

The second model of the system aims at calculating annual energy generated by the system from the radiation computed by the first model and the characteristics of the electrical components. This model considers the following aspects:

a) The field dimension where the PVGCS will be installed;
b) Technical aspects of the different elements of the PVGCS.
c) Design restrictions due to maintenance and safety purposes. These restrictions concern not only the maximum weight that the structure where the PV modules will be placed support but also the standards and best practices to ensure appropriate maintenance in case of problems during operation of PVGCS.

Figure 3-6 describes the main elements of this model. VBA in Excel was used to encode this model.

3.5.1 *Output energy estimation*

The design of PVGCS must take into account the dimensions of the field, solar radiation data and the so-called balance of system components (BOS). The BOS encompasses all the components of a photovoltaic system other than the photovoltaic panels. In addition, shading and the effect of mask (i.e. corresponding to shades on a solar panel caused by obstacles such as buildings, vegetation or relief for example) affect the collector deployment by decreasing the incident energy on collector plane of the field.

In a solar field, collectors, an array of PV modules, are deployed in different sheds with spacing allowing tilting and being useful for maintenance purpose. In this arrangement, a collector may cast a shadow on the adjacent row during the day, thus decreasing the amount of collected energy. This shading effect depends on the spacing between the collector rows, the collector height, and the tilt

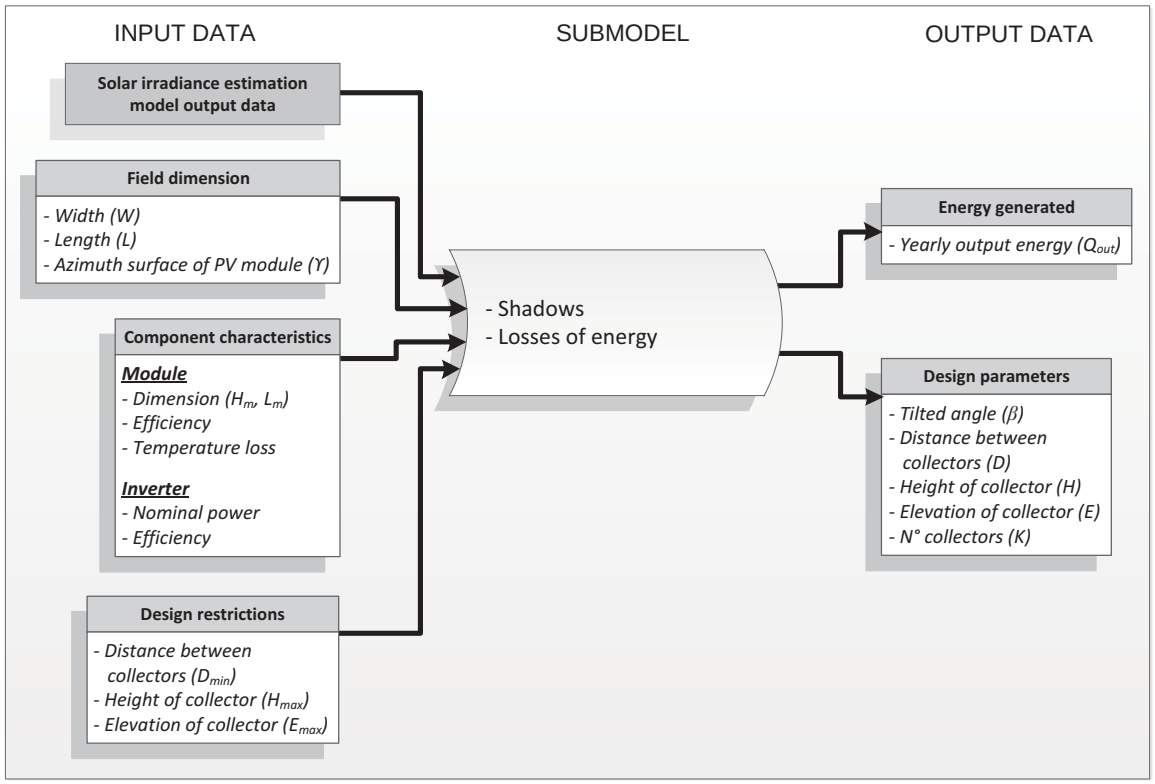

Figure 3-6 Data flow diagram of PVGCS model

angle and also on the row length and on the latitude of the solar field. The use of many rows of collectors densely deployed increases the surface that is available to transform solar irradiation but also increases the shading.

The spacing and, consequently, shading have also and influence on local environmental not allowing grass or culture to grow between and enter the PV panels. This environmental consequence was not evaluated in this work.

The balance of system (BOS) also influences the estimate of annual energy generated by the facility because of the efficiency of electrical components.

3.5.2 *Techniques for sizing PV systems*

In any PVGCS, sizing represents an important part of the design that must satisfy techno-economic requirements. Undoubtedly, at the current stage of development of PV technology, the major impediment to a wider market penetration is the high investment costs of the PV systems (EPIA, 2012).

The solar field design problem may be described by a mathematical formulation, usually multivariable and nonlinear in both the objective and constraint functions.

In the literature, the configuration of PV is made following only one objective such as the minimum field area required for producing a given amount of energy, the maximum energy generated from a given field or minimum cost of investment.

3.5.3 *Mathematical sizing model*

Weinstock and Appelbaum (Weinstock & Appelbaum, 2007) formulated the PVGCS sizing problem as a mathematical problem. The optimal design parameters of the solar field were determined to obtain the maximum annual incident energy on the collector planes from a given field size.

The improvements that were implemented relative to the model presented in (Weinstock & Appelbaum, 2007) concern the computation of the output power of the system, mainly in the following aspects:

- The equation used for calculating the diffuse irradiance received by the collector is replaced by the anisotropic model of Hay et al. (Noorian et al., 2008).
- The reflected irradiance is included in the calculation of the radiation received by the installation.
- The method used to calculate energy loss caused by the shadow generated by adjacent collectors is changed. An array indicating the number of panels covered in a collector is created following the method proposed by Ziar et al. (Ziar, Mansourpour, Salimi, & Afjei, 2011)

The model considers a horizontal field without elevations with a fixed length L and a fixed width W. It comprises K rows of solar collectors with a horizontal distance D between the rows; each collector has a length L_C, a height H, and a tilted with an angle β with respect to the horizontal Figure 3-7. Each collector is an array of PV modules arranged in N_r rows and N_c columns. The length of collector row L_C and its height H_C are given by:

$$L_c = N_c\, L_m \tag{3.18}$$

$$H = N_r\, H_m \tag{3.19}$$

The variables considered in this model are β, D, K, H where K is a discrete variable. The following constraints are also involved:

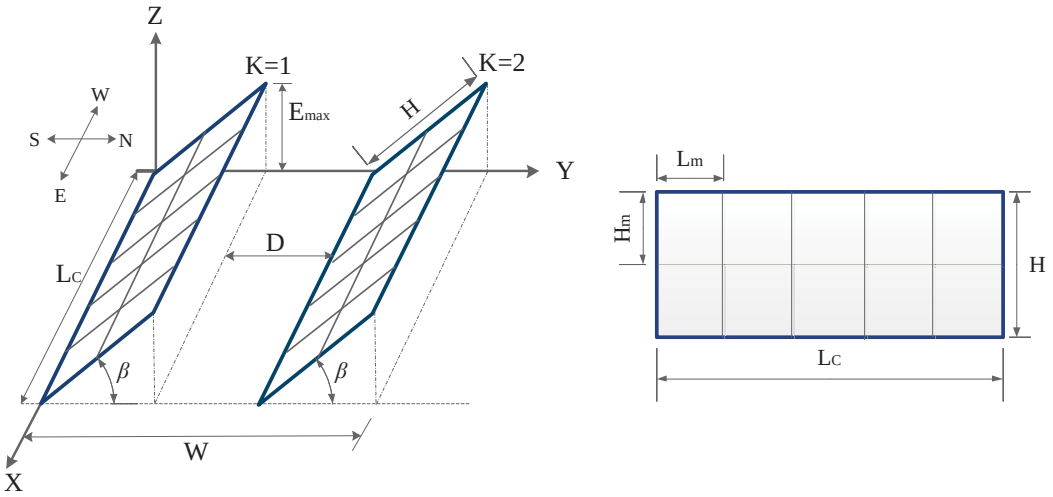

a) Position of two tilted sheds b) Solar collector configuration

Figure 3-7 Solar collector field reproduced from (Weinstock & Appelbaum, 2009)

- The variation of the collector parameter values and distances are considered by the field width, i.e.:

$$K\,H\cos\beta\ + (K-1)D \leq W \tag{3.20}$$

- The space between collector rows D is at least equal to a distance D_{min}, i.e.:

$$D \geq D_{min} \tag{3.21}$$

- Maintenance and installation constraints are required to limit the height of collector above the ground E_{max}, i.e.:

$$H\sin\beta\ \leq E_{max} \tag{3.22}$$

- The collector height H itself can be limited by the solar field construction, maintenance and by PV module manufacturer, i.e.:

$$H \leq H_{max} \tag{3.23}$$

- The collector tilt angle may vary in the range of 0° to 90°:

$$0° \leq \beta \leq 90° \tag{3.24}$$

- The number of PV shed of the final array is a least equal to 2 and takes a discrete value:

$$2 \leq K\ \in\ Z^{+} \tag{3.25}$$

3.5.3.1 Direct shading

They can be due to trees, posts, nearby buildings, etc. placed between the sun and the panels during the day, or if there are several sheds of panels arranged in the same horizontal plane. Losses can be important, because of that, the location must be carefully chosen to avoid shading as much as possible. In the case of large-scale solar plants, collectors are set in several sheds and shading by neighbors may become inevitable. The shadow that is projected from a shed to another one varies throughout the day and can be determined geometrically (Weinstock & Appelbaum, 2004a) (Appendix D).

The amount of shading depends on the distance between the collector rows D, their height H, the row length L_c, the tilt angle β and the latitude ϕ (see Figure 3-8).

A status matrix is defined, $M(j, k, t, n)$, as follows in order to determine the shaded modules of the collector in a specific hour t and in a specific day n (Weinstock & Appelbaum, 2009).

$$M(j,\,k,\,t,\,n) = \begin{cases} 1 & \text{if module in column } j \text{ and row } k \text{ is unshaded at hour } t \text{ in day } n \\ 0 & \text{if module in column } j \text{ and row } k \text{ is shaded at hour } t \text{ in day } n \end{cases} \tag{3.26}$$

This matrix makes it possible to determine if a module receives solar irradiation during the whole day or only at given hours of the day. In addition, the status matrix assumes that any partially shaded module at a given time is considered as a fully shaded module. The modelling of a partially shaded module represents a complex situation. A solution found in the literature is to consider that a module is "shaded" once a shadow is cast on it even on a smallest part of its area. This is of course the extreme case because some power may be delivered by the module when partially shaded. This hypothesis is supported by the fact that a matrix of shaded/unshaded modules simplifies the algorithmic aspect and reduces the computational time while the results are not so different to those obtained by using PVsyst.

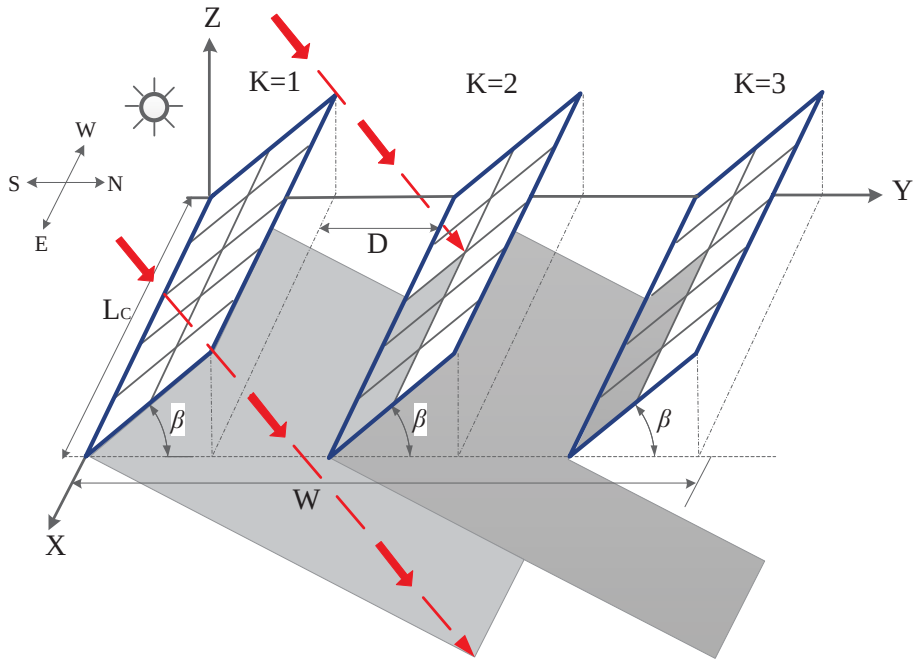

Figure 3-8 Shading by collectors in a stationary solar field reproduced from (Weinstock & Appelbaum, 2009)

3.5.3.2 Output energy of solar field

The output power of the modules in a row connected in series depends on three main factors: module efficiency (η), module temperature (T_m), and the number of shaded modules at a given time. The meteorological data at the specific site together with the geographical coordinates of the site allow calculating the power delivered by a module as a function of time.

$$Q_m(t) = \eta A G_\beta(t) \tag{3.27}$$

The module temperature was calculated according to Van Overstraeten et al. (Weinstock & Appelbaum, 2004b), Equation (3.28)), and the loss of power due to temperature rise above 25°C is taken into account in Equation (3.29)) for the power delivered by a module in time *t* at day *n*:

$$T_m(t) = 20 + 0.35 G_\beta(t) \tag{3.28}$$

$$Q_m(t,n) = \eta A G_\beta\ t,n\ [T_m(t,n) - 25] \tag{3.29}$$

The integration of Equation (3.29) over a year predicts the annual energy produced of a module. The yearly incident solar energy of the PV collectors placed in the field is given by:

$$Q_{out} = N_r N_c \sum_{n=1}^{365} \sum_{t=1}^{24} Q_m\ t,n\ + K-1 \sum_{n=1}^{365} \sum_{t=1}^{24} \sum_{k=1}^{N_r} \sum_{j=1}^{N_c} M\ j,k,t,n\ Q_m\ t,n \tag{3.30}$$

The first part of the Equation (3.30) represents the energy produced by the unshaded first shed and the second part comprises the energy produced by the *K-1* shaded sheds. This value represents the maximum amount of energy that is sent to the DC / AC inverter.

3.5.3.3 Energy losses

The losses inherent in any energy conversion process are numerous. These losses have different origins. In this chapter, we have already mentioned some of them. Table 3-4 summarizes the main

Table 3-4 Summary of the main energy losses (Brigand, 2011; Hayoun & Arrigoni, 2012)

Origin of loss	Loss (%)	Observations
Shading loss	Variable	Loss related to the geographic location of PVGCS in addition to the inclination, spacing and dimensions of the shed. (Section 3.5.3.2).
PV conversion	Variable	Loss due to the type of technology of PV module (*module* efficiency). Value indicated in the technical data sheet of the PV module.
Thermal loss	Approx. 0,5 %/°C	Loss caused by the temperature rise of the PV module. Value indicated in the technical data sheet of the PV module.
Modules array mismatch loss	≤ 3%	Loss caused by the interconnection of PV module.
Ohmic wiring loss	≤ 3%	Loss linked to the characteristics of the wiring that connects all electrical devices.
Loss due to DC/AC inverter	3-10%	Loss caused by the internal characteristics of the components of the DC / AC inverter. Value indicated in the specifications of the DC / AC inverter.

energetic losses to consider sizing a PVGCS, starting from available global horizontal irradiance until to obtain the total energy injected into the grid.

3.6 Evaluation model

The third model of the integrated system is dedicated to the evolution of the three criteria. For each criterion, a performance index was selected. These indexes will allow the evaluation and comparison of the resulting options. Figure 3-9 summarizes the different elements required by this model.

In order to determine the requirement of construction material and electric components necessary for the design of the PV power plant and, the cost incurred as well the associated environmental impacts, the scheme proposed by Kornelakis and Koutroulis (A. Kornelakis & Koutroulis, 2009) is used. A fixed mounting structure is selected because of the simplicity. A centralized inverter zone is proposed as it is indicated by the guidelines published by the Agence de l'Environnement et de la Maîtrise de

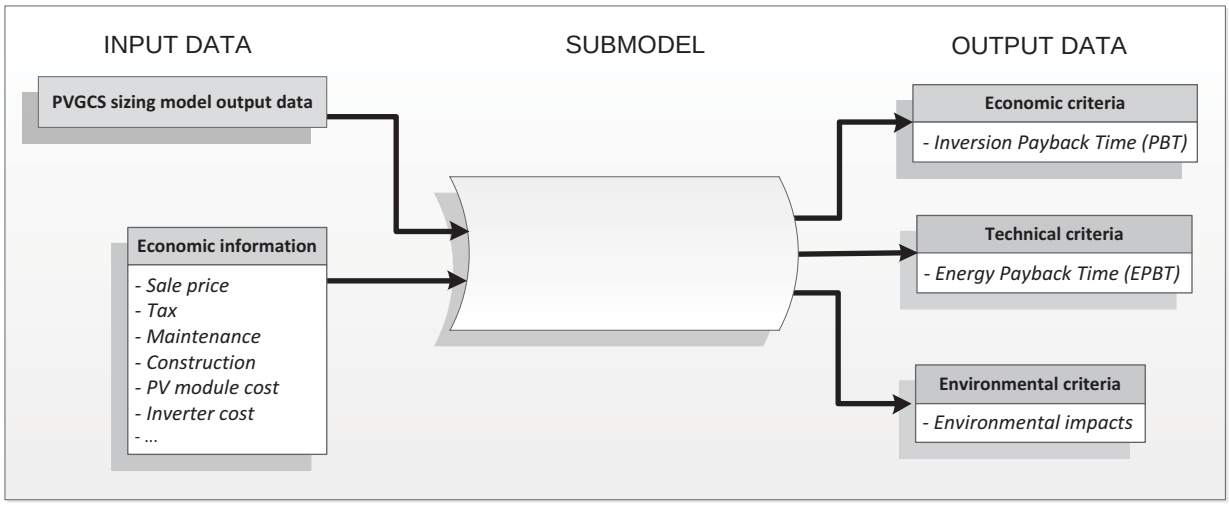

Figure 3-9 Evaluation of criteria model

l'Energie (ADEME) (Boulanger, 2003). Appendix D shows in detail the techniques used for designing the mounting structure and electrical components.

3.6.1 *Techno-economic criteria*

The techno-economic criteria chosen in this study concern the *payback time of investment* and *energy payback time,* respectively. These are classical criteria when energy production is involved. Their choice is summarized in what follows.

In project evaluation and capital budgeting, the *payback time* (PBT) is an estimation of the time that will be necessary for an investor to recover the initial investment. It is used to compare investments that might have different initial capital requirements. It is calculated by the following expression:

$$PBT = \frac{\text{Cost of project}}{\text{Annual Cash Inflows}} \tag{3.31}$$

The cost of project considers the considering all the components that make up the installation purchasing (PV modules, cables, mounting system ...), the construction and the edification cost as well as the cost of connection to grid. Annual cash flow represents the incomes by selling all energy production.

Table 3-5 summarizes the main elements of economic evaluation considered in the model. The price of electrical components (PV modules and DC / AC inverters mainly) is set by the manufacturer and the price often depends on the volume purchased. Solarbuzz (Solarbuzz, 2012a, 2012b) together with PV magazine (Schachinger, 2012) make regularly a study of PV modules technologies and DC/AC inverters market price. They proposed a price by W_p and W_{AC} respectively. The others costs were taken from (Hayoun & Arrigoni, 2012), (Di Dio, Miceli, Rando, & Zizzo, 2010) and, (A. Kornelakis & Koutroulis, 2009) works. The average sell price for the electricity generated by the PVGCS was obtained from the reports of the European Renewable Energies Federation (Fouquet, 2009, 2012).

Energy payback time (EPBT) is the time in which the input energy during the PV system life-cycle

Table 3-5 Main elements of economic evaluation

Description	**Value**
PV module	
- m-Si	0.85 €/W_p
- p-Si	0.82 €/W_p
- a-Si	0.74 €/W_p
- CdTe	0.77 €/W_p
- CIS	0.86 €/W_p
DC/AC inverter	0.40 €/W_{AC}
Fixed support structure	33.00 €/m
Cables	0.50 €/m
Concrete basements	230.00 €/m^3
Network connecting	0.05 €/W_p
Construction fee	0.39 €/W_p
Price of energy sold	0.276 €/kWh

(which includes the energy requirement for manufacturing, installation, energy use during operation, and energy needed for decommissioning) is compensated by electricity generated by the PV system.

$$EPBT = \frac{\text{Primary energy required for manufacturing}}{\text{Annual primary energy produced}} \quad (3.32)$$

Primary energy required for manufacturing is obtained as a result of the Life Cycle Assessment, identified here in the *Non-renewable energy* category. A conversion factor of 2.58 is used to transform 1 kWh electricity into primary energy (ADEME, n.d.).

3.6.2 *Environmental criteria*

As it was mentioned in Chapter 2, the environmental assessment is performed following the methodology of Life Cycle Assessment (LCA). Following the guidelines indicated in the LCA study described in Section 2.7, the system boundaries are kept without considering recycling processes (see Chapter 5). PV modules and BOS component characteristics will be modified in accordance with the data and characteristics of each situation under evaluation.

IMPACT 2002+ (Jolliet et al., 2003), included in SimaPro 7.3, was selected as a method for evaluating the environmental impacts. Only the midpoint categories are considered.

3.7 Validation of the model

3.7.1 *Comparison with Weinstock and Appelbaum's model performances*

The example given by Weinstock and Appelbaum (Weinstock & Appelbaum, 2009) (referred as WAP in the following) is used to validate the proposed model.

It must be kept in mind at this level that the objective is to verify the validity of the proposed modelling and simulation approach without considering optimization, that will be the core of the subsequent chapter. The maximization of the annual energy generation by the facility is used the reference objective. In order to check the relevance of the model, the same scenarios as those used in the WAP approach were used. WAP offers the best configuration of a PV power plant for the maximum energy generation under three different scenarios:

- in the first scenario, PV power plant is sized when maximizing the incident energy on to the total surface of PV modules without any type of energy losses;
- the second one maximizes the output energy when only considering the module efficiency and shading;
- the third one maximizes the output energy of the PVGCS with accounting of all possible energy losses (shading, temperature and interconnections losses).

The PV power plant is located in Tel Aviv, Israel (32.0°N, 34.8°E, altitude 4 m, GMT +2). The PV module has a length L_m = 1.293 m and a height H_m = 0.33 m. The technology of the PV module used by WAP is not mentioned explicitly but the computation is performed with the assumption of an efficiency of 12.42%.

The field and PV collector parameters are the following ones: W = 150 m, L = 12.93 m, and N_r = 6, N_c = 10.

The simulation of each configuration calculated by WAP for each of the three proposed scenarios was performed with the model proposed in this work. The goal is to compare the amount of energy generated between both approaches. The site data, the dimension of the field and PV module characteristics were used in the simulation runs. It must be yet emphasized that because each configuration in WAP example was obtained by optimizing a mathematical model, the value of K, β and D are not the same in each run. Table 3-6 contains the values of these parameters for each scenario.

Table 3-7 shows the comparison between the results obtained by our approach and the WAP example. The results estimated by the proposed simulator tool have a difference of about 20% with respect to the estimation of WAP. As mentioned in Section 3.5.3, this difference can be attributed to the modifications made in the model for predicting the annual amount of the energy generated.

3.7.2 *Comparison with PVsyst*

To verify this assumption, a second set of simulation runs is performed with PVsyst software (mentioned in Table 3-1) taking into account the technology type. For the simulations, the location of PV plant, the field dimensions and the parameter values for the three WAP cases (see Table 3-6) are used again.

The objective is to study the five main PV modules technologies available in the market: monocrystalline silicon (m-Si), polycrystalline silicon (p-Si), amorphous silicon (a-Si), cadmium telluride (CdTe) and copper indium diselenide (CIS). Table 3-8 shows the main characteristics for each of the 5 PV modules technologies used in the simulations.

Table 3-6 Parameter values for each scenario of WAP example

Objective function	***K***	***β (°)***	***D (m)***
Maximum incident energy on to the total surface of PV modules	58	24.62	0.80
Maximum output energy with shading losses	58	24.62	0.80
Maximum output energy of PV array (shading, temperature and interconnections losses)	57	21.23	0.80

Table 3-7 Comparison of output energy from the example of WAP and the proposed tool

Objective function	Q_{out} (kW h)		
	Weinstock et al.	This approach	Diff
Maximum incident energy on to the total surface of PV modules	2 641 034	3 187 715	+ 20,70%
Maximum output energy with shading losses	328 048	395 914	+ 20,69%
Maximum output energy of PV array (shading, temperature and interconnections losses)	268 000	326 692	+ 21,90%

Table 3-8 Typical features of various commercial PV modules technologies

Technology	H_m (m)	W_m (m)	η (%)	Nominal power (Wp)
m-Si	1.56	1.05	20.10	327.00
p-Si	1.64	0.94	15.50	240.00
a-Si	1.31	1.11	7.20	105.00
CdTe	1.20	0.60	11.50	82.50
CIS	1.26	0.98	12.20	150.00

Table 3-9 Values of *Nc* and *Nr* for simulation

Technology	N_r	N_c
m-Si	1	12
p-Si	1	13
a-Si	1	11
CdTe	1	21
CIS	1	13

The values of N_c and N_r for each of the technologies are shown in Table 3-9. In the simulations, only one technology is assumed per field which means that no mixed technologies are allowed. In order to compare the results, each of the 5 configurations is modelled with PVsyst software.

It must be highlighted that PVsyst is a software tool developed by the University of Geneva, Switzerland. This architect- and engineer-oriented tool is suitable for working in the field of renewable energy but is also for education. This program has three modules:

- *a preliminary design,* which allows making a quick evaluation of a grid-connected installation, a stand-alone installation or a pumping system;
- *a project design,* it allows sizing an installation connected to the DC network using detailed hourly simulations;
- a *tool module,* in which it possible to adjust certain parameters of the software.

PVsyst includes a database of around 330 sites in the world and it possible to import weather data from many popular meteorological sources. The component database holds over 1,750 PV modules from all common commercial technologies, 650 inverters and dozens of batteries or regulator models.

The *Preliminary design* module permits the definition of the plane orientation, PV components and location. It offers detailed parameters allowing fine effects analysis, including thermal behaviour, wiring and mismatch losses, and module quality loss. A detailed economic evaluation could be performed. A final report summarises all system parameters and the most significant result plots and tables for one given simulation.

PVsyst includes a 3-D CAD tool to draw the geometry of the system. It computes a shading factor for beam component as a function of the sun's position. Animation over a whole chosen day could be made for clarify the shading impact of a given situation.

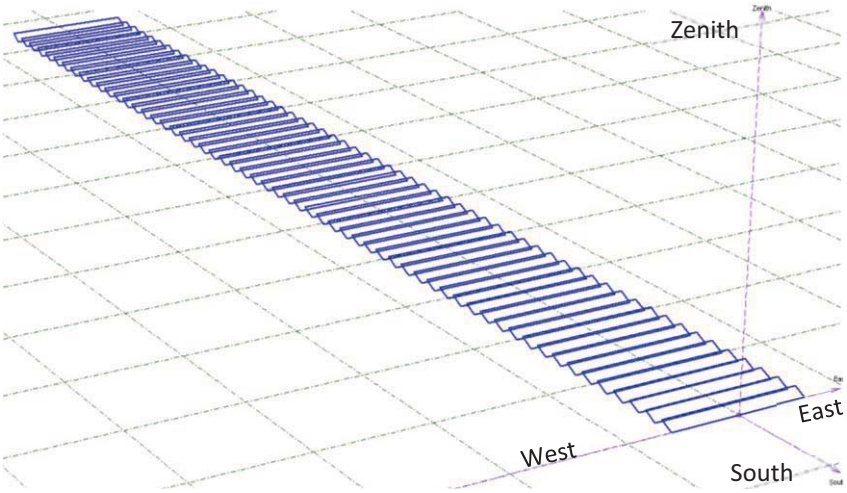

Figure 3-10 Field layout of PV power plant made in PVsyst

Figure 3-10 shows the layout generated in PVsyst showing the position of the PV sheds for calculation of the energy generated for each of the three scenarios under evaluation. The blue rectangles represent PV shed with south orientation. Each square in the floor represents 100 m². Table ***3-10*** contains the results obtained from the modelling of the three scenarios with the different types of PV modules technology both PVsyst and the simulation tool proposed in this chapter.

It must be highlighted that a good agreement is obtained between the prediction of the proposed tool and those of PVsyst. The deviation that is observed may be due to the precision adopted in PVsyst for

Table 3-10 Comparison of output energy from PVsyst and the proposed tool

		Q_{out} (kW h)		
Objective function	**Techno**	PVSyst	Simulator	Deviation
Maximum incident energy onto total surface of PV modules	m-Si	2 497 636	2 558 693	+2,44%
	p-Si	2 723 105	2 631 590	-3,36%
	a-Si	2 036 096	2 084 487	+2,38%
	CdTe	1 936 192	1 977 019	+2,11%
	CIS	2 043 586	2 084 206	+1,99%
Mean				+1,11%
Maximum output energy with shading losses	m-Si	483 935	486 919	+0,62%
	p-Si	383 003	361 782	-5,54%
	a-Si	145 525	145 813	+0,20%
	CdTe	216 193	221 715	+2,55%
	CIS	242 834	247 511	+1,93%
Mean				-0,05%
Maximum output energy of PV array (shading, temperature and interconnections losses)	m-Si	420 604	430 279	+2,30%
	p-Si	319 830	314 063	-1,80%
	a-Si	149 561	155 386	+3,89%
	CdTe	188 687	198 482	+5,19%
	CIS	210 516	218 421	+3,76%
Mean				+2,67%

some parameters required for the estimation of the output energy of the system such as PV collector inclination and position of the sun throughout the evaluation period work only: integer numbers are used in PVSyst while the proposed simulation tool uses decimal numbers. This situation concerns in particular the amount of irradiance that PV power plant can receive and the energy loss due to the shadows cast by the PV shed.

The main disadvantage of using PVsyst, as presented in Table 3-1, is its closed structure, not allowing it to be embedded in an outer optimization loop. It is then difficult to achieve the main objective of this work, which consists in the development of an ecodesign tool for PV panels.

Another disadvantage of this software tool is that, although involving a 3-D CAD tool, the use of this tool requires the configuration and arrangement of all the elements of the system to be evaluated. A change in the dimensions of the PV collector or in the number of PV sheds placed in the field cannot be performed automatically by the program. A trial and error procedure must thus be implemented.

Additional information can also be obtained with the proposed simulation tool. The result of the evaluation of PBT and EPBT for each configuration is shown in Table 3-11.

The results are presented through radar charts normalised to unity. Figure 3-11 presents the radar chart of the results of the environmental impact assessment (15 midpoint categories). To facilitate the comparison, normalisation was performed by assigning the value 1 to the maximum value of each category. The computed relative impacts represent the ratio between the environmental impact and this maximum value.

From Table 3-11, it can be seen that the choice of the PV power plant that uses PV modules of m-Si has a lower PBT as the revenue generated by the large amount of annual energy that can be injected into the grid is the highest one and compensates for the highest unit cost of all the technologies considered. Considering EPBT, the use of PV modules based on CdTe has the shortest time. This is due to the low amount of primary energy needed for manufacturing (see Chapter 2).

The graphics show that the configuration that uses technology based on m-Si has the highest impact in 13 of 15 categories, while in the other categories (Carcinogens and Mineral Extraction) the highest impacts are observed when using PV modules based on a-Si.

Another analysis is then performed taking into account the energy generated by each configuration.

This new analysis consists in assessing the environmental impact per kWh produced, as follows:

Table 3-11 PBT and EPBT for each configuration

PV module	PBT (yr)	EPBT (yr)
m-Si	6,35	1,18
p-Si	8,19	1,33
a-Si	12,28	1,37
CdTe	10,08	0,99
CIS	8,71	1,24

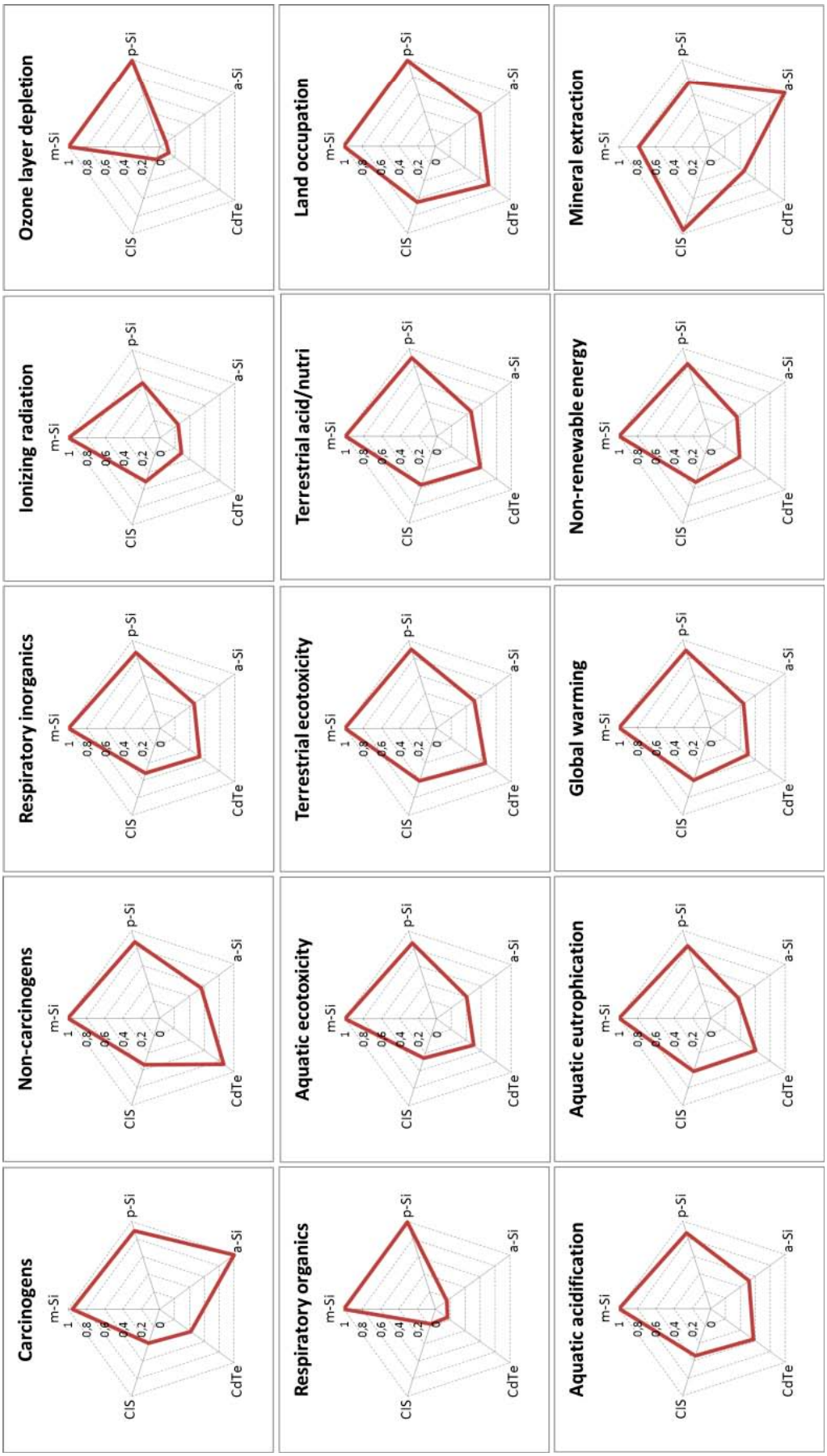

Figure 3-11 Results of the environmental impacts normalized to unity

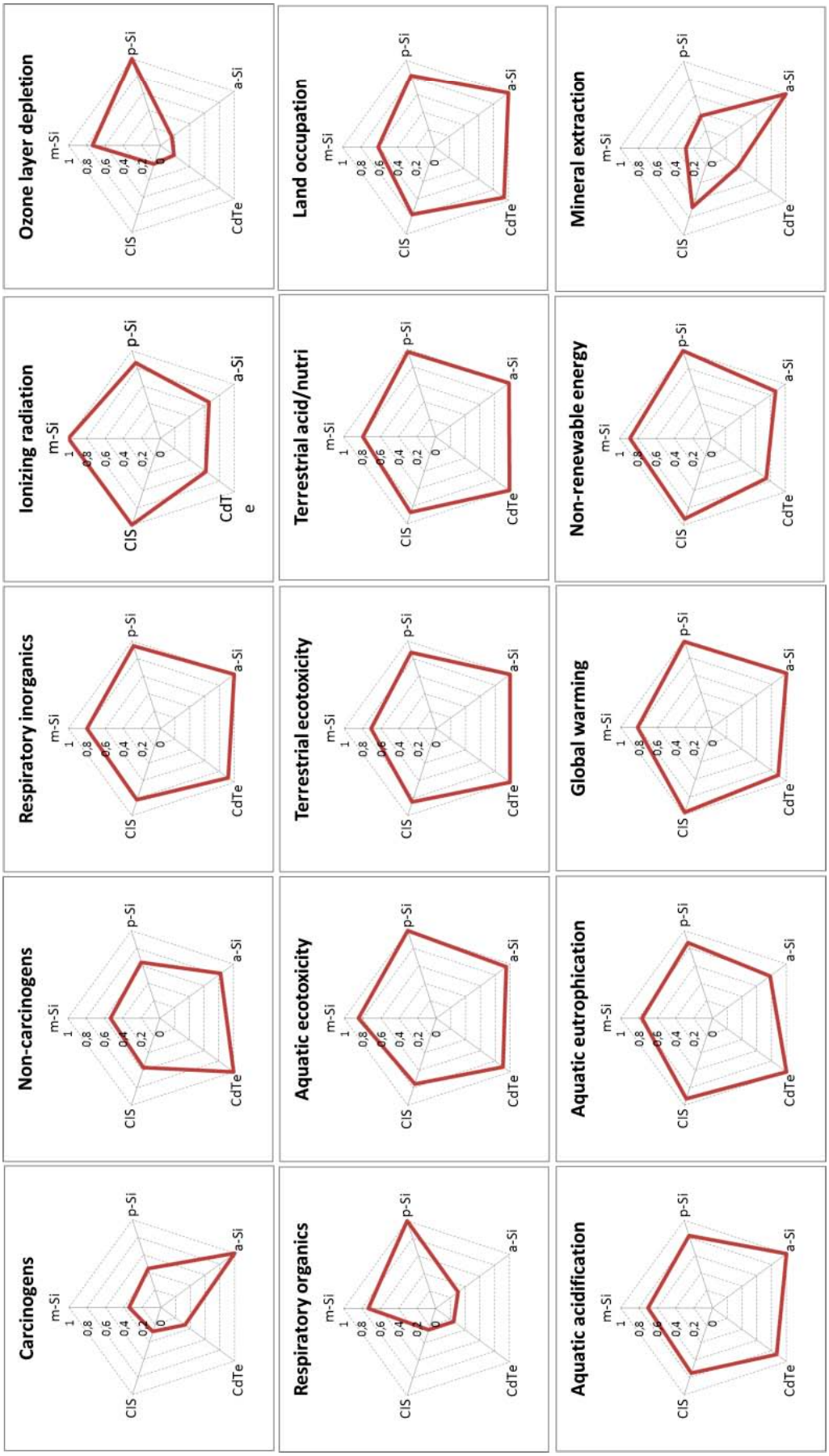

Figure 3-12 Results of the environmental impacts per annual energy generated ratio normalized to unity

$$Index = \frac{midpoint\ environmental\ impact}{yearly\ output\ energy\ of\ the\ field} \tag{3.33}$$

The results are presented through radar charts normalized to unity (Figure 3-12). It emphasizes the substantial reduction of categories led by m-Si technology from 13 to just one. The opposite case is the technology based on a-Si that increases of 2 to 6 category. These changes highlight the influence of the energy generated in a PVGCS to assess the environmental impacts generated.

Another fact to note from the graphics presented is the similarity in behaviour between some of the categories of environmental assessment. In the next chapter, a methodology will be proposed to identify the correlated impacts and the antagonist behaviour of the criteria in order to reduce their number in the optimization step.

3.8 Conclusion

The chapter was dedicated to the model developed in this work to represent the performance of a PV power plant. The model involves a three-step framework:

(1). The estimated solar radiation received by the system according to the geographic location

(2). The model provides the annual energy generated from the characteristics of the system components and limitations on the design of the installation. The design of PVGCS must take into account the dimensions of the field, solar radiation data (see first item) and the so-called balance of system components (BOS). Let us recall that BOS encompasses all the components of a photovoltaic system other than the photovoltaic panels. WAP does not consider BOS.

(3). The model is then coupled with two modules for evaluation of techno-economic (PayBack Time and Energy PayBack) and environmental (IMPACT 2002+ midpoint categories) criteria.

From the technical viewpoint, the model performance was validated for a reference example taken from the literature (Weinstock & Appelbaum, 2009) with a standard simulation tool and exhibited a good agreement.

A preliminary assessment of the economic and environmental performance of some typical technologies that can be used for PV modules shows that the proposed approach can predict with a good accuracy monocrystalline silicon (m-Si), polycrystalline silicon (p-Si), amorphous silicon (a-Si), cadmium telluride (CdTe) and copper indium diselenide (CIS).

This analysis then confirms the interest to use an optimization approach to search for the most interesting solution taking into account simultaneously techno-economic aspects and environmental concern.

The integration of the proposed model in an outer optimization loop is therefore a natural extension of this work and is the core of the following chapter.

Chapter 4

METHODS AND TOOLS FOR ECODESIGN: COMBINING MULTI-OBJECTIVE OPTIMIZATION (MOO), PRINCIPAL COMPONENT ANALYSIS (PCA) AND MULTIPLE CRITERIA DECISION MAKING (MCDM)

Les problèmes d'écoconception nécessitent en général la considération d'un grand nombre d'objectifs, induit par le jeu de catégories d'impact, de l'ordre d'une dizaine, lors de l'application de l'analyse du cycle de vie. Les méthodes d'optimisation multi-objectif, quant à elles, impliquent d'un point de vue de leur mise en œuvre pratique, des problèmes ayant un nombre plus réduit de fonctions objectifs: la résolution d'un problème bicritère ou tricritère peut se révéler complexe selon la nature des contraintes et des critères mis en jeu. Les principaux obstacles au traitement d'un grand nombre d'objectifs sont divers : stagnation possible du processus de recherche, augmentation de la dimension du front de Pareto, temps de calcul élevé, et enfin difficulté à visualiser et analyser les résultats. Par ailleurs, l'analyse des résultats de l'analyse du cycle de vie pour un produit, processus ou service montre que certains critères peuvent être redondants : les groupes de critères liés dépendent du problème à traiter. Il est donc important de bien formuler le problème pour identifier le choix de critères indépendants et mener le processus d'optimisation de façon rationnelle.

Ce chapitre, consacré aux outils et méthodes utilisés dans le cadre de ce travail, est divisé en trois parties principales. La première partie est consacrée à l'optimisation multi-objectif et le choix d'une variante de la méthode dite NSGA-II est justifié. La partie 2 présente une approche fondée sur une analyse en composantes principales (ACP) couplée avec la variante de NSGA-II sélectionnée. L'idée est d'identifier les objectifs redondants des solutions obtenues par NSGA-II et de les éliminer dans le processus d'optimisation proprement dit. La partie 3 concerne les outils d'aide à la décision multicritère mis en œuvre afin de sélectionner le meilleur compromis parmi les critères antagonistes à partir des solutions du front de Pareto.

Nomenclature

Acronyms

ACO	Ant Colonies Optimization
AI	Artificial Intelligence
CUT	CUT value for PCA
DE	Differential Evolution
EPBT	Energy Payback Time
GA	Genetic Algorithm
LCA	Life Cycle Assessment
MCDM	Multiple-Criteria Decision Making
MGA	Multi-objective Genetic Algorithms
MILP	multi-objective Mixed-Integer Linear Program
MOGA	Multi-Objective Genetic Algorithm
MOO	Multi-Objective Optimization
M-TOPSIS	Modified Technique for Order Preference by Similarity to the Ideal Solution
NSGA	Non-dominated Sorting Genetic Algorithm
NN	Neural Networks
NPGA	Niched Pareto Genetic Algorithm
PBT	Payback Time
PCA	Principal Component Analysis
PSO	Particle Swarm Optimization
PV	Photovoltaic
PVGCS	Photovoltaic Grid-Connected System
SPEA	Strength Pareto Evolutionary Algorithm
TOPSIS	Technique for Order Preference by Similarity to the Ideal Solution
VBA	Visual Basic for Applications
VEGA	Vector Evaluated Genetic Algorithm
WTG	Wind Turbine Generators

Symbols

λ_e	e^{th} eigenvalue remained in PCA method
A^+, A^-	Ideal and non-ideal solution in M-TOPSIS method
a_{ij}	Normalized result of alternative i into the criterion j
D_i^+, D_i^-	Euclidean distance for ideal and non-ideal solution for alternative i
G_j	Cumulative explained variance
R_i	M-TOPSIS ratio value for alternative i
Q_{out}	Yearly output energy of the field, kWh
v_{ij}	Weighted normalized result of alternative i into the criterion j
w_j	Weight of the individual criterion j
x^+	Most positive element of principal component
x^-	Most negative element of principal component
X_{ij}	Value of alternative i into the criterion j

4.1 Introduction

Ecodesign problems involve a large number of objectives, generally more than ten when carrying out Life Cycle Assessment. Multi-objective optimization methods are yet applied only to problems having a lower number of objectives. Among these methods, existing evolutionary multi-objective optimization methods, which turned out to be very attractive due to their ability to lead to a well-representative set of Pareto-optimal solutions in a single simulation run, are generally applied only to problems having about 5 objectives or so. The major impediments in handling a large number of objectives relate to stagnation of search process, increased dimensionality of Pareto-optimal front, large computational cost, and difficulty in visualization of the objective space. Furthermore, several objectives are redundant so that a multi-objective strategy is not, strictly speaking, necessary.

The methods and tools that are proposed in this chapter can be viewed as generic approaches for ecodesign problems. They are applied more particularly here to the PVGCS problem which is the subject of this PhD work. The PVGCS strategy and the results obtained will not be presented in this chapter. They will be deeply analysed in the following chapter.

This chapter is divided into three main sections. Section 1 is dedicated to multi-objective optimization and the choice of a variant of the so-called NSGA-II method is justified. Section 2 addresses a principal component based approach coupled with the variant of NSGA-II that is selected. The idea is to identify redundant objectives from the solutions obtained by NSGA-II and to eliminate them from further consideration. Section 3 concerns Multiple Criteria Decision Making, in order to select from the optimal Pareto front the best compromises among the antagonist criteria.

4.2 Multi-objective optimization for sizing PV systems

In any PVGCS, sizing represents an important part of the design that must satisfy techno-economic requirements. Undoubtedly, at the present stage of development of the PV technology, the major impediment to a wider market penetration is the high investment costs of the PV systems (EPIA, 2012).

The solar field design problem may be described by a mathematical formulation. The configuration of PV is based on criteria such as the minimum field area required for producing a given amount of energy, the maximum energy generated from a given field or minimum cost of investment.

Several methods for solving optimization problems have been developed. These methods can be grouped into two main groups (Figure 4-1). The former group follows a linear formulation for the constraints (either of equality or inequality type) and objective functions. In the latter group, the non-linear formulation involves a set of non-linear constraints and/or objective functions.

There are recent methods developed for sizing the parameters for PVGCS based on Artificial intelligence (AI) and Genetic algorithm (GA) techniques (Gong & Kulkarni, 2005; A. Mellit, Kalogirou, Hontoria, & Shaari, 2009; Adel Mellit & Benghanem, 2007; Mondol et al., 2006; Mondol, Yohanis, & Norton, 2009).

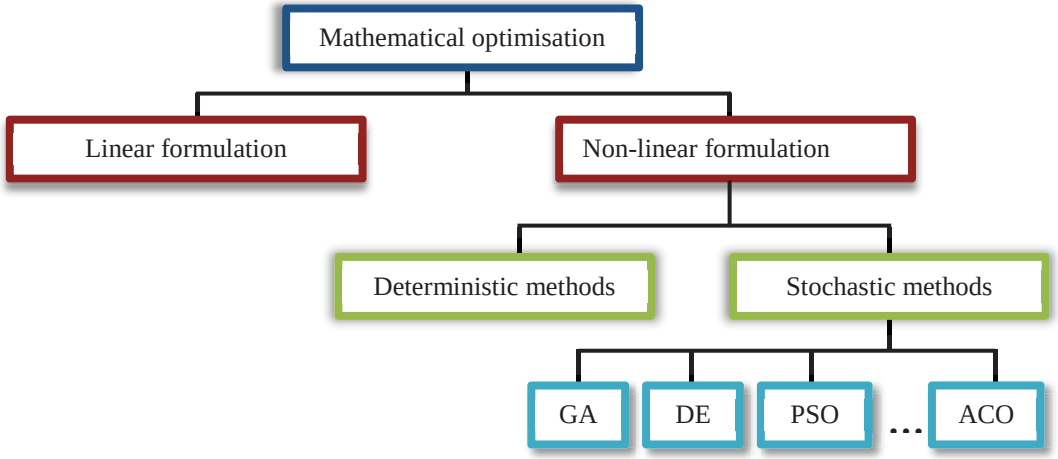

Figure 4-1 Classification of optimization methods (Garcia, Avila, Carpes, & Avila, 2005)

The literature review reveals that evolutionary or stochastic methods e.g. Genetic Algorithms (GAs), Ant Colonies Optimization (ACO), Neural Networks (NN), Particle Swarm Optimization (PSO) and Differential Evolution (DE) (Mondol et al., 2006; Notton et al., 2010) are particularly attractive for non-linear problems. These methods are suitable for "black box" problems where the mathematical properties (continuity, convexity, derivability …) of the problem are difficult to establish. The evaluation of the criteria and constraints of a set of values of independent variables is only required. These methods do evolve in one or more series of initial solutions supported by a set of probabilistic rules often imitating a process of nature.

The solar field design problem can be described by a mathematical formulation as it was explained in Chapter 3 and can be viewed as an optimization problem. Several works deal with the configuration of PVGCS based on criteria to optimize such as the field area required for producing a given amount of energy (minimization case), the energy generated from a given field (maximization case), or cost of investment (minimization case) (García-Valverde, Miguel, Martínez-Béjar, & Urbina, 2009; Kaushika & Rai, 2006; A. Kornelakis & Koutroulis, 2009; Mondol et al., 2009; Senjyu, Hayashi, Yona, Urasaki, & Funabashi, 2007; Weinstock & Appelbaum, 2004b, 2007).

From the mathematical formulation performed to describe the problem of sizing a PVGCS presented in Chapter 3, it is possible to identify that:

- the set of equations does not respect the principle of linearity;
- the relevant meteorological data, especially solar radiation, are estimated from a mathematical model.

From the abovementioned reasons, it can be deduced that the use of solution methods from linear formulation (first group) may be difficult and that an optimization method for the design of PV systems representing a comprehensive set of variables from the solar radiation estimation to PV system configuration is required.

In order to deal with this situation, several studies are reported in the dedicated literature in which PV systems are optimized based on stochastic algorithms (Gómez-Lorente, Triguero, Gil, Estrella, &

Espín Estrella, 2012; Adel Mellit & Benghanem, 2007). Stochastic algorithms have proved to be particularly efficient for solving complex problems with either linear or non-linear functions (Gómez-Lorente et al., 2012).

This study is carried out in the framework of a multi-objective problem where multiple antagonist objectives must be optimized simultaneously: an economic objective (PBT), a technical goal (EPBT) and several environmental objectives. The selected method is based on Multi-objective Genetic Algorithms (MGA). A brief overview of the main features of a GA and how it works is presented below in order to understand the operation of MGA.

4.2.1 *Genetic algorithms*

Genetic algorithms (GA) are inspired by how the organisms are adapted to the harsh realities of life in a hostile world, i.e., by evolution and inheritance. The algorithm imitates in the process the evolution of population by selecting only fit individuals for reproduction.

GAs were proposed by Holland in the 1970s as an algorithmic concept based on a Darwinian-type survival-of-the-fittest strategy with sexual reproduction, where stronger individuals in the population have a higher chance of creating an off-spring. A genetic algorithm is implemented as a computerized search and optimization procedure that uses principles of natural genetics and natural selection. The basic approach is to model the possible solutions to the search problem as binary strings. Various portions of these bit-strings represent parameters in the search problem. If a problem-solving mechanism can be represented in a reasonably compact form, then GA techniques can be applied using procedures to maintain a population of knowledge structure that represent candidate solutions, and then let that population evolve over time through competition (survival of the fittest and controlled variation). A GA will generally include the three fundamental genetic operations of selection, crossover and mutation (see Figure 4-2). These operations are used to modify the chosen solutions and select the most appropriate off-spring to pass on to succeeding generations. GAs consider many points in the search space simultaneously and have been found to provide a rapid convergence to a near optimum solution in many types of problems: in other words, they usually exhibit a reduced chance of converging to local minima.

The first step in any GA is to generate an initial population with a group of individuals randomly created. The individuals in the population are then evaluated and assigned a fitness value. The evaluation function is provided by the operator and gives the individuals a score based on how well they perform at the given task. The fitness value is always defined with respect to other members of the current population. Fitness can be assigned based on an individuals' rank in the population and forms the relation between the evaluation score and the average evaluation of all the individuals in the population. Two individuals are then selected based on their fitness, the higher the fitness, the higher the chance of being selected.

After selection has been carried out, crossover is applied to randomly paired individuals. The recombined individuals create one or more off-spring. This can be viewed as creating the new

population. The randomly mutation of the offspring is then applied. In terms of GAs, mutation means a random change of the value or a gene in the population as shown in Figure 4-2.

After the process of selection, recombination and mutation, the next population can be evaluated. The process continues until a suitable solution has been found or when a given number of generations has been reached. Figure 4-3 represents the flow chart of the process described above.

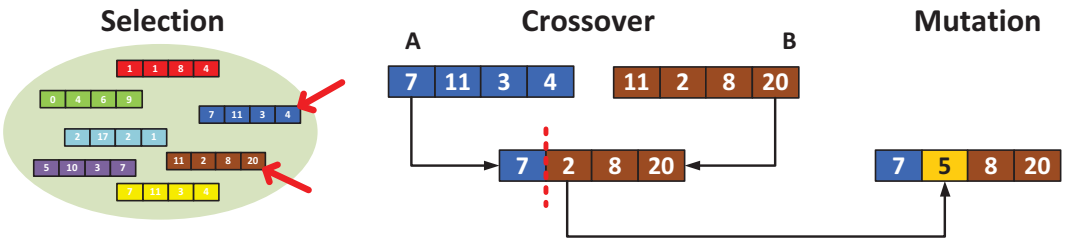

Figure 4-2 Genetic Algorithm operators

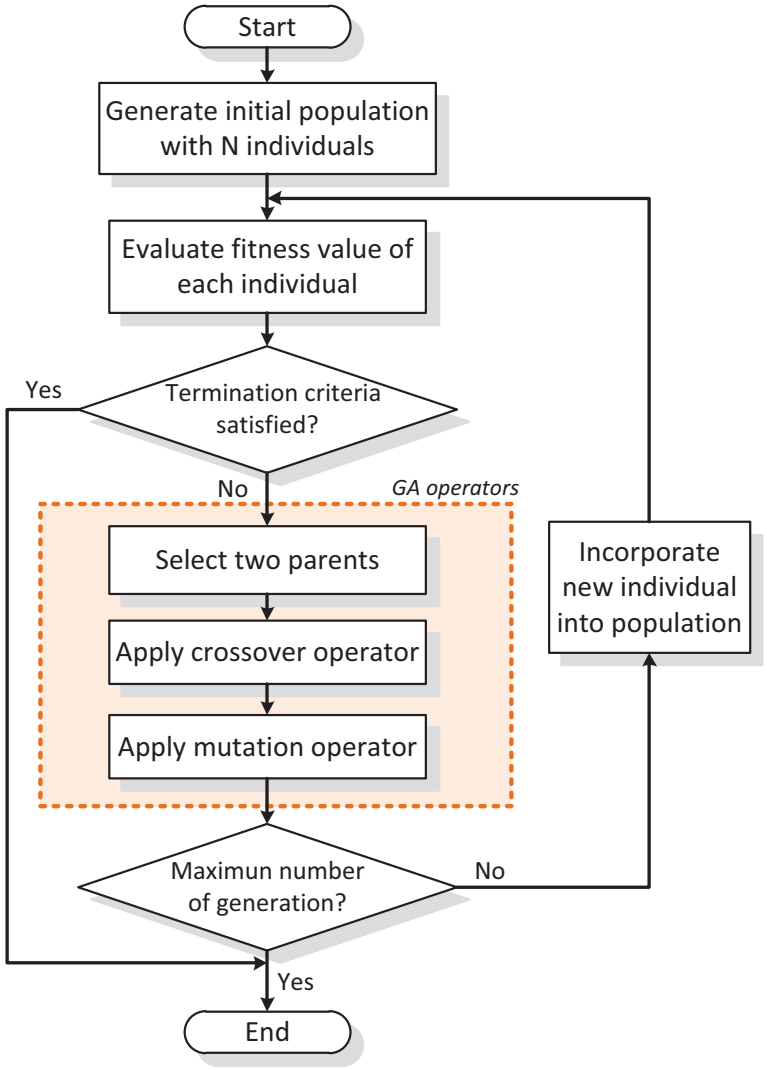

Figure 4-3 Genetic Algorithm flow chart

4.2.2 *Multi-objective Genetic Algorithm*

GAs are well suited to solve multi-objective optimization problems. The ability of GA to simultaneously search different regions of a solution space makes it possible to find a diverse set of solutions for difficult problems.

A multi-objective decision problem tries to find a vector *x** that minimizes a given set of *K* objective functions $z(x^*) = \{z_1(x^*), \dots, z_K(x^*)\}$ given a *n*-dimensional decision variable vector $x = \{x_1, \dots, x_n\}$. A set of constraints restricts the solution space (Konak, Coit, & Smith, 2006).

In many real-life problems, objectives under consideration conflict with each other. Therefore, optimizing with respect to a single objective often results in unacceptable results with respect to the other objectives. It is almost impossible to find the vector *x** that simultaneously optimizes each objective function. A reasonable solution is to investigate a set of solutions which satisfies the objectives at an acceptable level without being dominated by any other solution.

A feasible solution *x* is said to dominate another feasible solution *y*, if and only if, $z_i(x) \leq z_i(y)$ for *i* = 1,…, *K* and $z_j(x) < z_j(y)$ for least one objective function *j*. Multi-objective optimization provides a set of non-dominated solutions in the solution space called Pareto optimal set. While moving from one Pareto solution to another, there is always a certain amount of sacrifice in one objective to achieve a certain amount of gain in the other. For a given Pareto optimal set, the corresponding objective function values in the objective space are called the Pareto front. The ultimate goal of a multi-objective optimization algorithm is to identify solutions in the Pareto optimal set. The size of Pareto optimal set is related with the number of objectives.

The crossover operator of GA allows creating new non-dominated solutions in unexplored parts of the Pareto front. Another important characteristic is that most multi-objective GA do not require the user to prioritize, scale, or weigh objectives, which constitutes a major asset for MOO methods.

Several survey papers (Coello & Becerra, 2009; Coello Coello, 2005) have been published on evolutionary multi-objective optimization. A list of more than 2000 references was published by Coello Coello in his website (Coello Coello, 2010). Generally, MGAs differ according to their fitness assignment procedure, elitism, or diversification approaches. Table 4-1 highlights the advantages and disadvantages of some well-known MGA techniques found by Konak et al. (Konak et al., 2006).

4.2.3 *PVGCS optimization approach*

GA applications are appearing as alternatives to conventional deterministic approaches and in some cases are useful where other techniques have been completely unsuccessful. GAs are also used with intelligent technologies such as neural networks, expert systems, and case-based reasoning. GAs constitute a quite popular method used in engineering field.

It must be emphasized that GAs are not yet widely used for PV system sizing. A summary of applications of GAs in this field is proposed in Table 4-2. It must be highlighted that they concern mainly hybrid technologies involving either stand-alone or grid connected panels.

Table 4-1 List of well-known MGA (based on (Konak et al., 2006))

Algorithm	Fitness assignment	Elitism	Advantages	Disadvantages
MOGA (Fonseca & Fleming, 1993)	Pareto ranking	No	Simple extension of single objective GA	Usually slow convergence Problems related to niche size parameter
NSGA (Srinivas & Deb, 1994)	Ranking based on non-domination sorting	Yes	Fast convergence	Problems related to niche size parameter
NSGA-II (K. Deb, Pratap, Agarwal, & Meyarivan, 2002)	Ranking based on non-domination sorting	Yes	Single parameter (N) Well tested Efficient	Crowding distance works in objective space only
NPGA (Horn, Nafpliotis, & Goldberg, 1994)	No fitness assignment, tournament selection	No	Very simple selection process with tournament selection	Problems related to niche size parameter Extra parameter for tournament selection
SPEA (Zitzler & Thiele, 1999)	Ranking based on the external archive of non-dominated solutions	Yes	Well tested No parameter for clustering	Complex clustering algorithm
VEGA (Schaffer, 1985)	Each subpopulation is evaluated with respect to a different objective	No	Straightforward implementation	Tend to converge at the extreme of each objective

Table 4-2 Summary of applications of GAs for sizing PV systems

Authors	Year	Subject
(Dufo-López, Bernal-Agustín, & Contreras, 2007)	2007	Optimization of control strategies for stand-alone renewable energy systems with hydrogen storage
(Senjyu et al., 2007)	2007	Optimal configuration of power generating systems in isolated island with renewable energy
(Koutroulis, Kolokotsa, Potirakis, & Kalaitzakis, 2006)	2006	Methodology for optimal sizing of stand-alone photovoltaic/wind-generator systems
(El-Hefnawi, 1998)	1998	Photovoltaic diesel-generator hybrid power system sizing
(Yokoyama, Yuasa, & Ito, 1994)	1992	Multiobjective Optimal Unit Sizing of Hybrid Power Generation Systems Utilizing Photovoltaic and Wind Energy
(Seeling-hochmuth, 1998)	1998	Optimisation of hybrid energy systems sizing and operation control
(Xu, Kang, & Cao, 2006)	2006	Graph-Based Ant System for Optimal Sizing of stand-alone Hybrid Wind/PV Power Systems
(Xu, Kang, Chang, & Cao, 2005)	2005	Optimal sizing of stand-alone hybrid wind/PV power systems using genetic algorithms

For instance, proper design of standalone renewable energy power systems (Xu et al., 2005) is a challenging task, as the coordination among renewable energy resources, generators, energy storages and loads is very complicated. The types and sizes of wind turbine generators (WTGs), the tilt angles and sizes of photovoltaic (PV) panels and the capacity of batteries must be optimized when sizing a standalone hybrid wind/PV power system, which may be defined as a mixed multiple-criteria integer programming problem. A GA with elitist strategy is investigated for optimally sizing a standalone hybrid wind/PV power system. The objective is selected as minimizing the total capital cost, subject to the constraint of the loss of power supply probability. The literature review reveals that PV planners are not quite familiar with GA optimization techniques for PV design.

As explained in the previous chapter, several programs and mathematical models have been developed to calculate solar irradiance received at a given point of the planet and size a PVGCS separately. Most of the studies reviewed (Gong & Kulkarni, 2005; Aris Kornelakis & Marinakis, 2010; Mondol et al., 2006; Notton et al., 2010; Weinstock & Appelbaum, 2007, 2009) consider exclusively PVGCS optimization with only one criterion. Other authors (Dones & Frischknecht, 1998; Ito et al., 2008; Kannan et al., 2006; Pacca et al., 2006) address only the issue of the environmental impact assessment of the elements of a PV system with emphasis on PV module technology. Our main purpose consists in generating alternatives of optimal PVGCS configurations taking into account technical and economic aspects as well as their environmental impact.

The main problem found in the programs described in Table 3-1 is the lack of an integrated approach that allows the optimization of the sizing of a PVGCS. The coupling of all elements via an external program to optimize the model using a genetic algorithm is difficult due to the closed structure used.

To overcome the problem of interoperability, the design of a simulator for received solar radiation coupled with a sizing module constitutes the most suitable option. The simulator must be designed in an open manner so that it can be interfaced easily with an outer optimization loop.

The MULTIGEN environment previously developed in our research group (Gomez et al., 2010) was selected as the genetic algorithm platform. A variant of NSGA-II developed for mixed problems and implemented in the MULTIGEN environment is selected. The stopping criterion proposed in MULTIGEN (in addition to the maximum number of generations) consists in comparing the Pareto fronts associated with non-dominated solutions for populations n and $n + p$, where the period $p \in [10, 20, 30, 40, 50]$ for example. If the union of the two fronts provides a single non dominated front, the procedure stops; else the iterations continue.

It can treat either mono- and multi-objective problems. The potential of GAs to solve multi-objective problems serves as an incentive to use such an optimization strategy. This constitutes a natural way to extend this work. As it was initially developed in Visual Basic for Applications (VBA) in Excel, the same language is used for simulation purpose. The main advantages of VBA include the automation of repetitive tasks and calculations, the easy creation of macros in a friendly programming language.

NSGA-II was selected, as it is explained in (Gomez, 2008), because of the way to manage the diversity of populations. Algorithms based on the concept of niche as NPGA and MOGA do not ensure a proper convergence of the Pareto front. Algorithms such as SPEA or NSGA-II are based on the principle that single non-dominated individuals are better than individuals in dense areas. In SPEA, the probability of selection is based on the isolation of the individual, which implies a quantification of that probability, and therefore the implementation of more complex algorithms. NSGA-II opts for a simple elimination of individuals at dense areas after a sorting according to their density. In addition, NSGA-II needs low computational requirements.

The step-by-step procedure is illustrated in Figure 4-4 to Figure 4-6. Initially, a random parent population P_0 of size N is created. The population is sorted based on the non-domination principle.

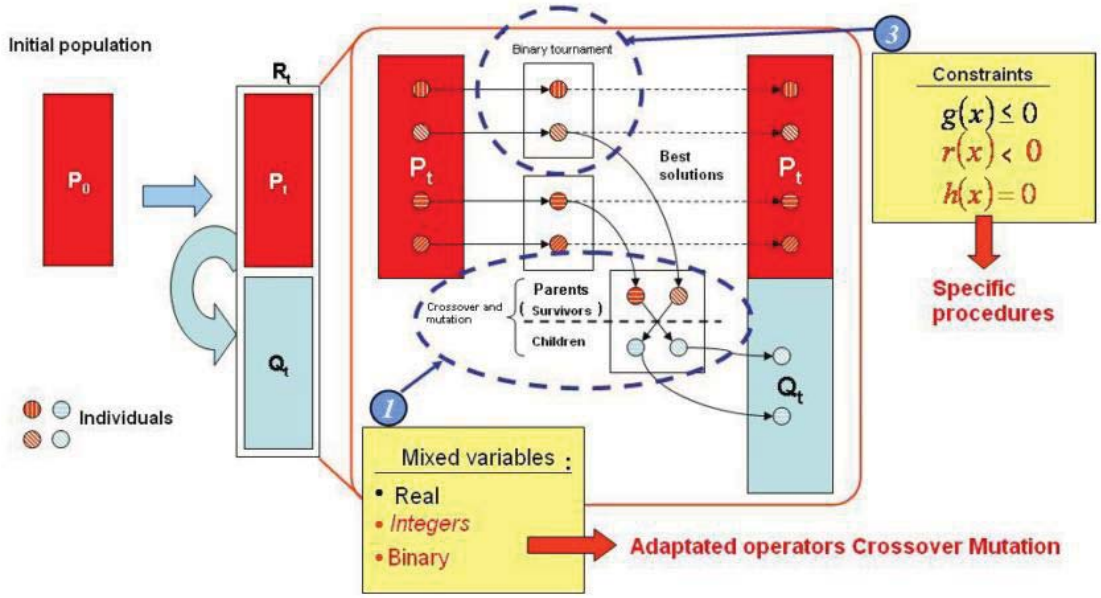

Figure 4-4 Operating principle of NSGA-II (Part 1) (Gomez, 2008)

Each individual is assigned a fitness (or rank) equal to its non-domination level (1 is the best level, 2 is the next-best level, and so on). Thus, the maximization of fitness can be performed. At first, the usual binary tournament selection, recombination and mutation operators are used to create an off-spring population Q_t of size N (Figure 4-4). Since elitism is introduced by comparing the current population with the previously best found non-dominated solutions, the procedure is different after the initial generation.

First, a combined population $R_t = P_t \cup Q_t$ is formed (Figure 4-5). The population R_t is of size $2N$. Then, the population is sorted according to non-domination. If the size of F_1 (set of individuals of rank 1) is lower then N, all the members of the set F_1 for the new population $P_t +1$ are definitely chosen. The remaining members of the population $P_t +1$ are chosen from subsequent non dominated fronts in the order of their ranking. Thus, solutions from the set F_2 are chosen next, followed by solutions from the set F_3, and so on. This procedure continues until no more set can be accommodated. Let us consider that the set F_1 is the last non-dominated set beyond which no other set can be accommodated. In general, the number of solutions in all sets from F_1 to F_l is higher than the population size.

In order to choose exactly the population members, the solutions of the last front using the crowded-comparison operator are sorted in descending order and the best solutions needed to fill all population slots are selected. The new population $P_t +1$ of size N is now used for selection, crossover and mutation to create a new population $Q_t +1$ of size N. It must be highlighted that a binary tournament selection operator is used but the selection criterion is now based on the crowded-comparison operator. Since this operator requires both the rank and crowded distance of each solution in the population, these quantities are calculated while forming the population $P_t +1$, as shown in Figure 4-6. The MULTIGEN library and NSGA-II are described in detail in (Gomez, 2008).

4.3 Reduction of environmental objectives by Principal Component Analysis (PCA) method.

LCA requires a large amount of data in its different phases and when the comparative analysis of products or processes is performed, the amount of data obtained as a result of the environmental impact assessment may be large and hard to interpret thus complicating the subsequent decision-making processes. One of the limitations of MGA when it is applied to environmental problems is that its computational burden grows rapidly in size with the number of environmental objectives.

The dimensionality of a data set can often be reduced easily without disturbing the main features of the whole data set by using multivariate reduction techniques such as Principal Component Analysis (PCA).

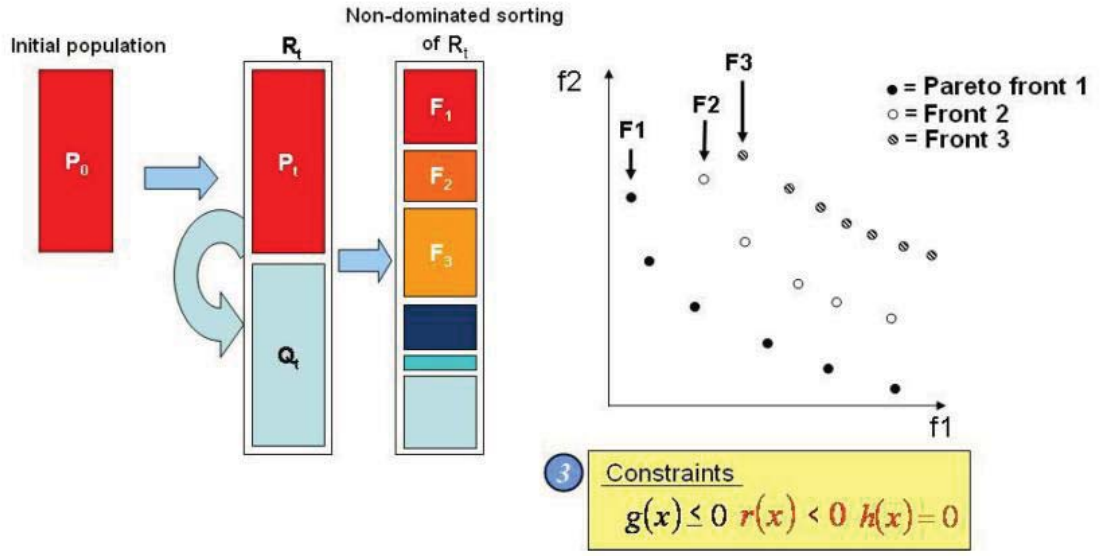

Figure 4-5 Operating principle of NSGA-II (Part 2) (Gomez, 2008)

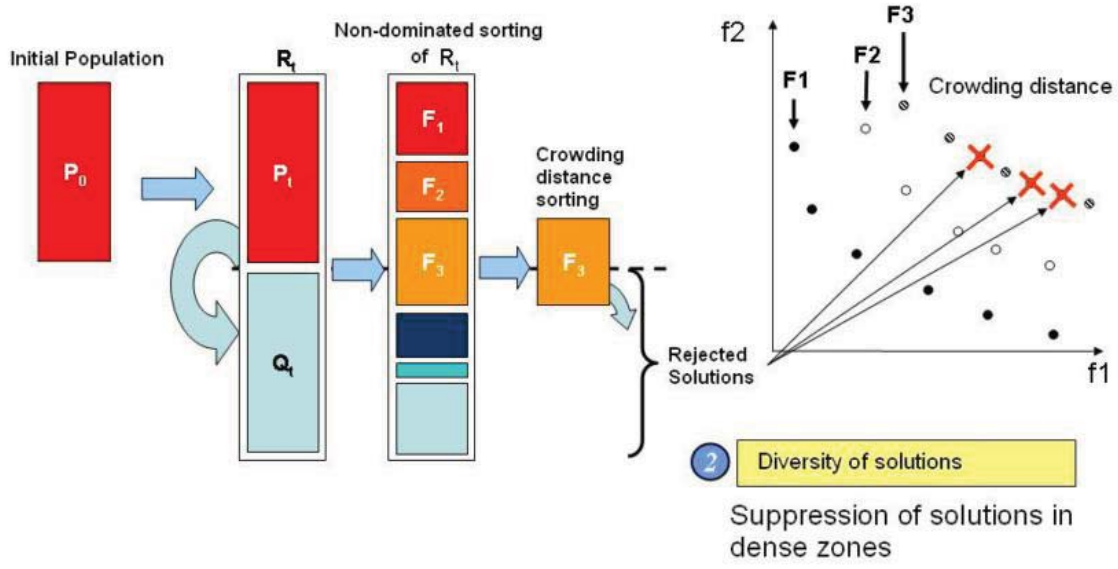

Figure 4-6 Operating principle of NSGA-II (Part 3) (Gomez, 2008)

PCA is a statistical tool for multivariate analysis. Its objective is to reduce the dimensionality of a data set with a large number of interrelated variables, retaining as much variation of the data set, as possible. This reduction in dimension is achieved by transformation of the original variables to a new smallest set of variables, called *principal components*. Each principal component is a linear combination of a subset of the original variables that have some similar characteristics. These components are uncorrelated and ordered: all principal components are ranked according to their ability in explaining the variance in the original data set. It is indeed useful to reduce the number of variables, thus avoiding extra variables, which complicate the data but do not give any extra information. The computational time will be reduced and the results analysis will be then more consistent.

PCA is computed using either the correlation matrix or the covariance matrix. The use of the correlation matrix is advantageous when measurements are in different units. The computation of principal components is usually posed as an eigenvalue-eigenvector problem. This eigenvalue used to indicate the proportion of the total variance explained from the original data by the corresponding principal component.

This technique has been applied successfully in several researches (Guillén-Gosálbez, 2011; Gutiérrez, Lozano, Moreira, & Feijoo, 2010; Sabio, Kostin, Guillén-Gosálbez, & Jiménez, 2012) for the reduction of environmental impact categories. The methodology proposed by Sabio et al. for reducing environmental impact categories in the configuration of the supply chain of hydrogen distribution in Spain was applied to the case presented in this work. This methodology follows the guidelines edited by Deb and Saxena (Kalyanmoy Deb & Saxena, 2005).

The purpose is to apply PCA once the Pareto optimal set of the optimization for sizing the PVGCS considering both technical and economic criteria as well as environmental criterion is found in order to reduce the environmental categories.

The steps to apply PCA method are:

Step 1: **Get the data**. First, it is necessary to generate a Pareto optimal set of the original problem by using the selected multi-objective algorithm (NSGA-II in this work).

Step 2: **Subtract the mean.** The data set is standardized to make its centroid equal to zero. This is done by subtracting the mean of each column from each data point in the matrix for PCA to work properly.

Step 3: Calculate the correlation matrix. For reducing the environmental categories, the correlation matrix is the best option because of the different units which each category uses.

Step 4: Calculate the eigenvectors and eigenvalues of the correlation matrix. The eigenvector corresponding to the largest eigenvalue is referred as the first principal component; one corresponding to the second largest eigenvalue is called the second principal component and so on.

Step 5: Choosing components. Applying the Kaiser-Guttman rule (Sabio et al., 2012), the eigenvalues that are less or equal to 1 are excluded from the analysis. The cumulative explained variance (G_j) of remaining eigenvalues in descendant order is determined by the equation:

$$G_j = \sum_{e=1}^{j} \frac{\lambda_e}{\sum_{e=1}^{|\lambda|} \lambda_e} \tag{4.1}$$

where λ_e represents e^{th} eigenvalue remained. A second reduction is made from G_j values. A threshold cut value (CUT) must be established in order to keep for the PCA the eigenvalues with cumulative explained variance below this value ($G_j \leq CUT$). Deb and Saxena (Kalyanmoy Deb & Saxena, 2005) suggest a CUT value of 0.95 (95%).

Step 6: Selecting environmental impact categories. This is done by analyzing the eigenvectors to identify conflicts among the categories. The heuristic procedure suggested by Deb and Saxena is followed to identify conflicts and redundancies among all the environmental categories. Technical details about this strategy are summarized in Figure 4-7. In this figure, x^+ denotes the most positive element of principal component and x^- represent the most negative element of principal component.

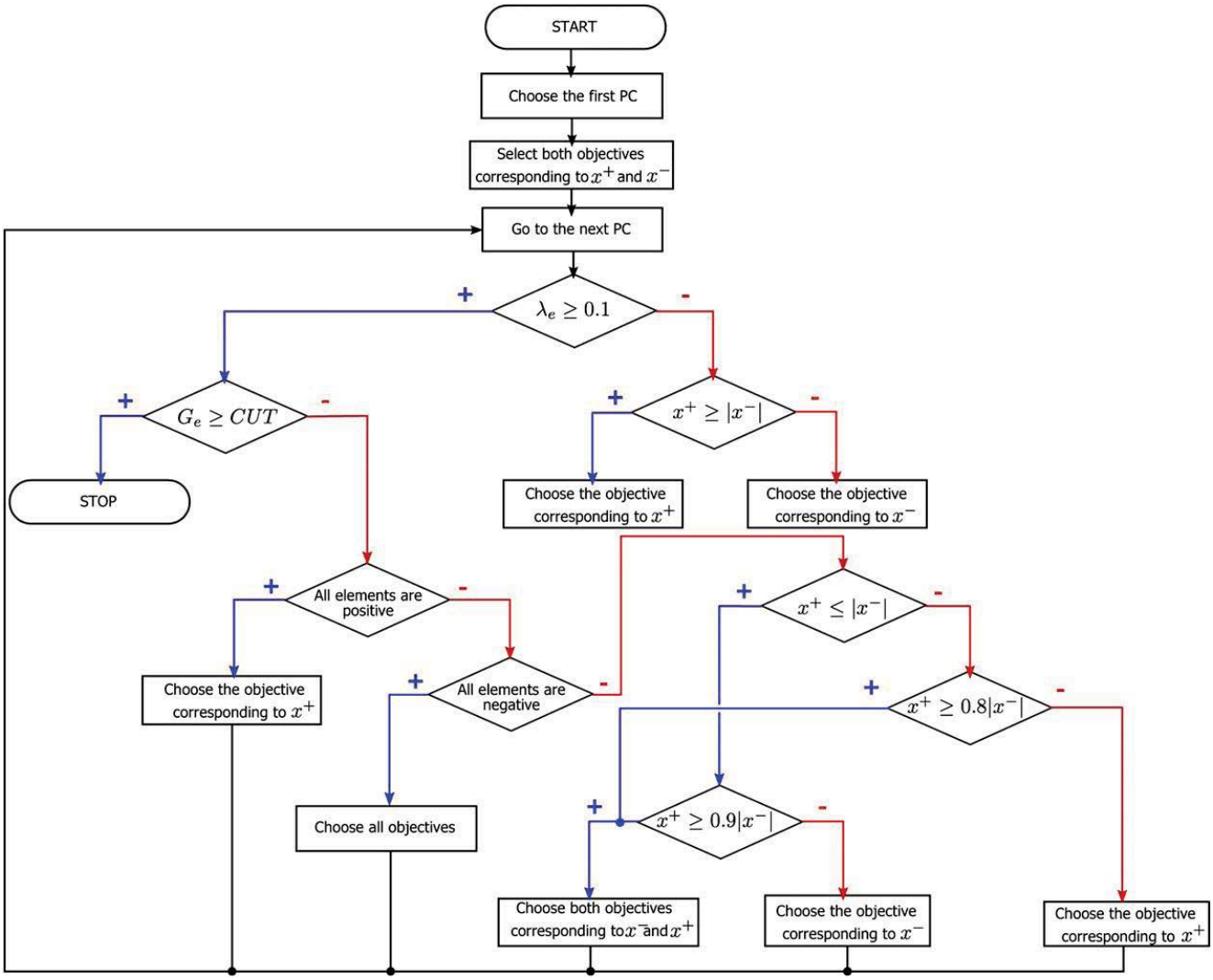

Figure 4-7 Scheme of the PCA procedure for selecting environmental impact categories (Sabio et al., 2012)

The main advantage of applying PCA for environmental objectives is the elimination of redundant environmental categories, which reduces the objectives to consider in the multi-objective optimization, decreases the resolution time of the AG and makes easier the interpretation of results.

4.3.1 *PCA for environmental categories*

An example will illustrate the usefulness of PCA method for the reduction of environmental categories. The case reported by Sabio et al. (Sabio et al., 2012) will be used to explain the method.

The goal of the problem addressed by Sabio et al. is to determine the optimal configuration of a three-echelon hydrogen supply chain for vehicle use (production-storage-market) in terms of cost and damage to the environment. A multi-objective mixed-integer linear program (MILP) formulation is employed to solve the problem. The environmental performance of the hydrogen supply chain is assessed by following 8 environmental LCA indicators: damage to human health caused by carcinogenic substances (CS), damage to human health caused by respiratory effects (RE), damage to human health caused by climate change (CC), damage to human health caused by ozone layer depletion (OLD), damage to ecosystem quality caused by ecotoxic substances (ES), damage to ecosystem quality caused by acidification and eutrophication (AE), damage to minerals (DM), and damage to fossil fuels (DFF).

The methodology described above was applied for reducing the environmental categories. After obtaining the Pareto set of solutions for the configuration of the hydrogen supply chain and standardizing the results (Steps 1 and 2), the correlation matrix is generated (See Table 4-3). It can be seen that CS, OLD and ES are highly correlated with DM, whereas AE is highly correlated with CC.

From the correlation matrix given above, the eigenvectors and eigenvalues matrix are calculated. The eigenvectors and eigenvalues of the correlation matrix are presented in Table 4-4, where the principal components are arranged in a descending order.

A graphical screen test was performed to decide the number of principal component to be kept for further analysis applying the Kaiser-Guttman rule. As observed in Figure 4-8, the fourth and subsequent components do not satisfy the Kaiser-Guttman rule. The three remain principal components represent almost the 100% of cumulative variability.

Table 4-3 Correlation matrix for Sabio et al. case

	CS	**RE**	**CC**	**OLD**	**ES**	**AE**	**DM**	**DFF**
CS	1	0.4400	0.4007	0.9995	1.0000	0.6729	0.9988	-0.0375
RE		1	0.0735	0.4517	0.4435	0.3886	0.4792	-0.8966
CC			1	0.4235	0.4027	0.9237	0.377	0.2743
OLD				1	0.9996	0.6938	0.9984	-0.0453
ES					1	0.6753	0.9989	-0.0408
AE						1	0.6621	0.0165
DM							1	-0.0847
DFF								1

Table 4-4 PCA results for Sabio et al. case. Eigenvalues and eigenvectors

	PC_1	PC_2	PC_3	PC_4	PC_5	PC_6	PC_7	PC_8
Eigenvalue (λ_e)	5.073	1.889	1.039	0.000	0.000	0.000	0.000	0.000
Variability (%)	63.407	23.609	12.983	0.002	0.000	0.000	0.000	0.000
Cumulative % (G_j)	63.407	87.016	99.998	100.000	100.000	100.000	100.000	100.000
CS	-0.4290	0.0188	0.2517	0.3581	-0.3265	0.5347	-0.0827	-0.4739
RE	-0.2436	**-0.5752**	-0.2668	0.3797	0.4647	-0.1424	-0.3915	-0.0696
CC	-0.2529	0.3791	**-0.6238**	0.1948	-0.2479	-0.4454	0.1347	-0.2955
OLD	**-0.4322**	0.0189	0.2230	-0.6102	-0.1216	-0.3151	-0.5086	-0.1337
ES	-0.4295	0.0171	0.2478	0.3595	-0.2663	-0.2309	0.0645	0.7044
AE	-0.3659	0.1852	-0.4966	-0.2990	0.1950	0.5695	-0.0363	0.3634
DM	-0.4293	-0.0165	0.2498	-0.1412	0.4973	-0.1322	0.6567	-0.1925
DFF	**0.0571**	**0.6999**	0.2370	0.2805	0.4949	-0.0298	-0.3553	0.0012

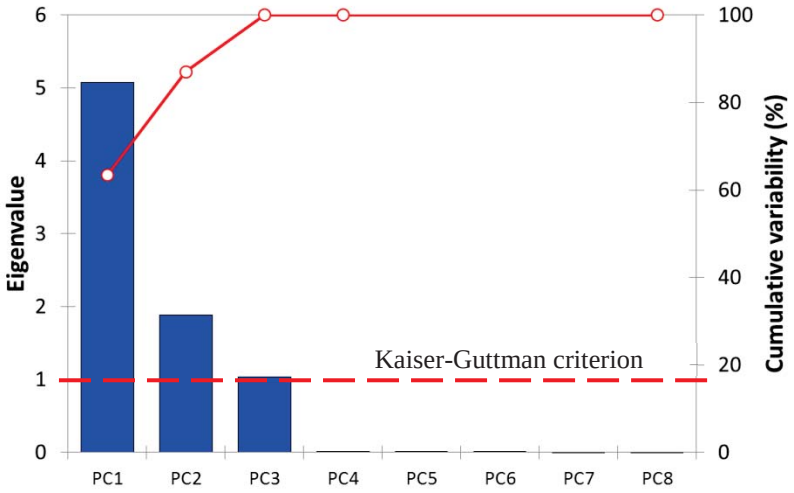

Figure 4-8 Screen plot for Sabio et al. case

The next steps consists in select the environmental impact categories. Based on the heuristic procedure of Figure 4-7 and with a CUT of 100% selected by Sabio et al., the environmental impact categories retained are highlighted in bold font in Table 4-4. Four categories were eliminated (CS, ES, AE, DM). Figure 4-9 shows the bi-dimensional and tri-dimensional plots representing the loads of the environmental objectives projected onto the sub-spaces of the first three principal components. The redundant categories are grouped based on the correlation matrix. Only RE, CC, OLD and DFF must be used in further analysis.

4.4 Multiple-criteria decision making (MCDM)

MCDM approaches are major parts of decision theory and analysis. MCDM are analytic methods to evaluate the advantages and disadvantages of multicriteria alternatives.

The objective is to help decision-makers to learn about the problems they face, and to identify a preferred course of action for a given problem. Huang et al. (Huang, Poh, & B.W., 1995) mentioned that decision analysis (DA) was first applied to study problems in oil and gas exploration in the 1960s

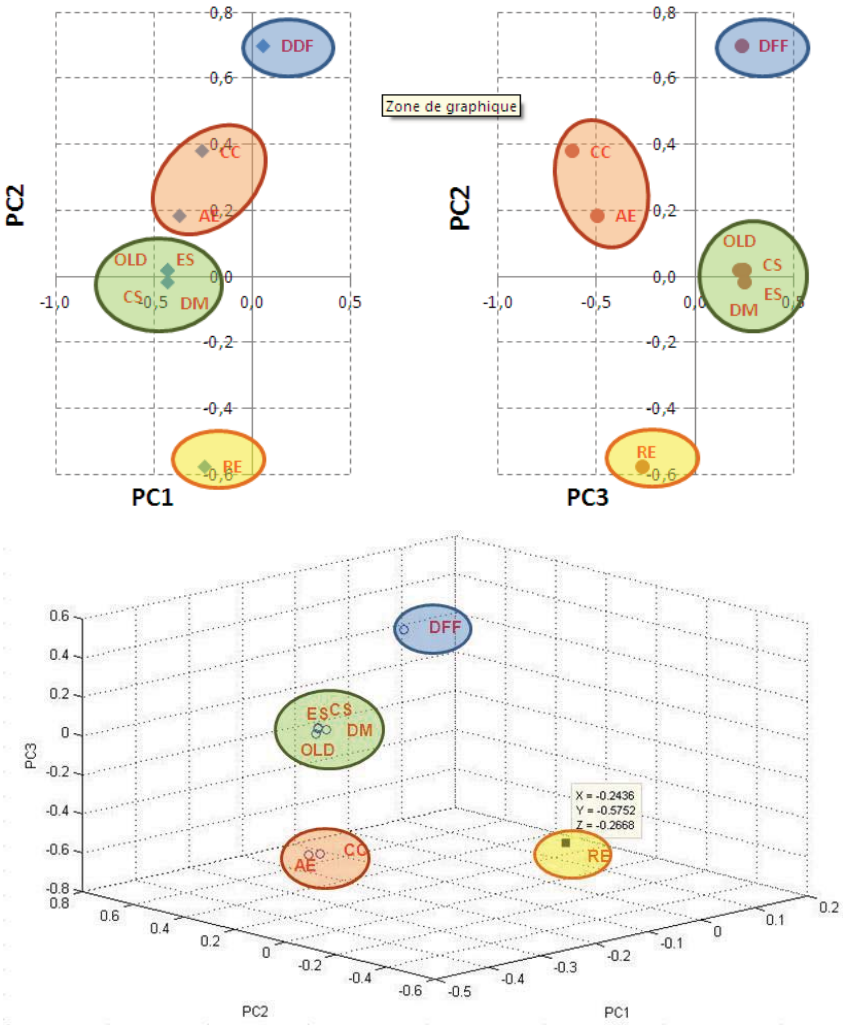

Figure 4-9 PCA results in the bi- and tri-dimensional spaces for Sabio et al. case

and its application was subsequently extended from industry to the public sector. Till now, MCDM methods have been widely used in many research fields. Different approaches have been proposed by many researchers, including single objective decision-making (SODM) methods, MCDM methods, and decision support systems (DSS). Literature shows that among MCDM methods, DA strategies are the most commonly used (Zhou, Ang, & Poh, 2006).

One of the most popular MCDM methods is TOPSIS for identifying solutions from a finite set of alternatives based upon simultaneous minimization of distance from an ideal point and maximization of distance from the nadir point. The acronym TOPSIS stands for Technique for Order Preference by Similarity to the Ideal Solution. The first developments of TOPSIS were carried out by Hwang and Yoon (Hwang & Yoon, 1981) and later by Lai et al. (Lai, Lui, & Hwang, 1994). Among the MCDM methods, TOPSIS is attractive since it requires limited subjective inputs from decision makers. The only subjective inputs needed are weights assigned to objectives. This may explain why TOPSIS (Lifeng Ren, Zhang, Wang, & Sun, 2007) is very popular in chemical engineering applications.

MCDM methods, especially TOPSIS, have often been used in multi-criteria optimization problem. Boix (Boix, 2011) used the TOPSIS method for selecting the best water network configuration

involving three criteria: amount of fresh and treated water entering the network and the number of connections.

Ouattara (Ouattara, 2011) shows how the results obtained by a MGA (NSGA-II) can be connected to a MCDM method (TOPSIS) to solve an ecodesign process problem. The objective is to take into account simultaneously the ecological and economic considerations at the preliminary design phase of chemical processes.

A variant of TOPSIS (M-TOPSIS) has been adopted in this work, integrating the guidelines proposed in (Ouattara, 2011)

4.4.1 *M-TOPSIS method*

M-TOPSIS method (Lifeng Ren et al., 2007) is an evaluation method that is often used to solve MCDM problems (Pinter & Pšunder, 2013). It is based on the concept of original TOPSIS (Hwang & Yoon, 1981). The basic idea of TOPSIS method is to choose a solution that is closest to the ideal solution (better on all criteria) and away the worst (which degrades all criteria) (Markovic, 2010; Opricovic & Tzeng, 2004; L. Ren, Zhang, Wang, & Sun, 2007) The modification introduced by Ren et al. in M-TOPSIS method could avoid rank reversals and solve the problem on evaluation failure when alternatives are symmetrical that often occurs in original TOPSIS.

A specific module with M-TOPSIS has been implemented as a tool for multi-criteria decision, thus facilitating its use after obtaining Pareto fronts. Particular attention was paid to the simultaneous treatment of problems involving minimization and maximization criteria. The stages of the M-TOPSIS procedure are listed below. The normalisation of the matrix is performed according to the original work of Hwang and Yoon (Hwang & Yoon, 1981).

Step 1: Build the decision matrix. Establish a matrix which shows *m* alternatives evaluated by *n* criteria (see Figure 4-10).

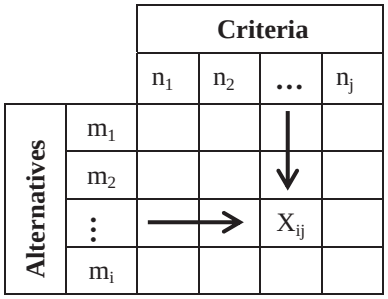

Figure 4-10 Decision matrix

All the original criteria receive tendency treatment. Usually the cost criteria are transformed into benefit criteria by the reciprocal ratio method as it shown in Equation (4.2). (García-cascales & Lamata, 2012; L. Ren et al., 2007)

$$X'_{ij} = \frac{1}{X_{ij}} \tag{4.2}$$

Step 2: Calculate the normalized decision matrix *A*. Since different criteria have different dimensions, the values in the decision matrix *X* are first transformed into normalized, non-dimensional values in order to convert the original attribute values within the interval [0, 1] under the following Equation:

$$A = [a_{ij}]_{m\,x\,n}, a_{ij} = \frac{X'_{ij}}{\sqrt{\sum_{i=1}^{n}(X'_{ij})^2}} \tag{4.3}$$

where a_{ij} stands for the normalized value; $i = 1, 2, \ldots, m$; $j = 1, 2, \ldots, n$

Step 3: Coefficient vector of importance of the criteria. This step allows decision makers to assign weights of importance to a criterion relative to others. The weighted normalized matrix *V* is calculated by multiplying each value within the individual criterion in the normalized matrix *A* by the weight of this criterion:

$$v_{ij} = w_j \cdot a_{ij} \tag{4.4}$$

where w_j stands for the weight of the individual criterion *j*; $i = 1, 2, \ldots, m$; $j = 1, 2, \ldots, n$.

Step 4: Determine the positive ideal and negative ideal solution from the matrix A. The ideal solution (A^+) is the group of weighted normalized criteria values, which indicates the ideal criteria values (maximum value for benefit criteria and minimum value for cost criteria), and the non-ideal solution (A^-) is a group of weighted normalized criteria values, which indicates the negative ideal criteria values (minimum value for benefit criteria and maximum value for cost criteria):

$$A^+ = \{v_1^+, v_2^+, \ldots, v_n^+\}, v_j^+ = \{max_i(v_{ij}), j \in J^+; min_i(v_{ij}), j \in J^-\} \tag{4.5}$$

$$A^- = \{v_1^-, v_2^-, \ldots, v_n^-\}, v_j^- = \{min_i(v_{ij}), j \in J^+; max_i(v_{ij}), j \in J^-\} \tag{4.6}$$

Where $J^+ = \{i = 1, 2, \ldots, m\}$ when *i* is associated with benefit criteria ; $J^- = \{i = 1, 2, \ldots, m\}$ when *i* is associated with cost criteria. $j = 1, 2, \ldots, n$.

Step 5: Calculate Euclidean distance. Calculate the separation measures, using the *n*-dimensional Euclidean distance. (García-cascales & Lamata, 2012; Pinter & Pšunder, 2013)

$$D_i^+ = \sqrt{\sum_{j=1}^{n}(v_j^+ - v_{ij})^2} \tag{4.7}$$

$$D_i^- = \sqrt{\sum_{j=1}^{n}(v_j^- - v_{ij})^2} \tag{4.8}$$

For $i = 1, 2, \ldots, m$.

Step 6: Calculate the relative closeness to the ideal solution. In M-TOPSIS, unlike TOPSIS, the positive ideal solution (D_i^+) and negative ideal solution (D_i^-) in finite planes are found at first; and then, the D^+ D^--plane is constructed and set the *optimized ideal reference point*. Finally, the relative distance from each evaluated alternative to the ideal reference point is calculated with (Lifeng Ren et al., 2007). Set the point A in Figure 4-11 [min (D_i^+), max (D_i^-)] as the *optimized ideal reference point* because the aim is to have the lowest distance

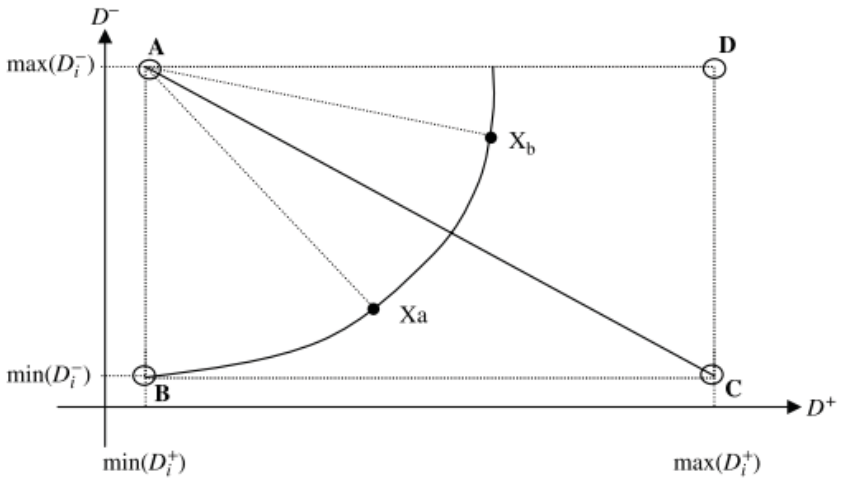

Figure 4-11 Example D^+ D^- – plane of M-TOPSIS method (Lifeng Ren et al., 2007)

between the ideal criteria set values (A^+) and get away as much as possible of non-ideal criteria set values (A^-). The ratio value of R_i is calculated as follows:

$$R_i = \sqrt{\left(D_i^+ - min\left(D_i^+\right)\right)^2 + \left(D_i^- - max\left(D_i^-\right)\right)^2} \tag{4.9}$$

Where $i = 1, 2, \ldots, m$.

Step 7: Rank order. Rank alternatives in increasing order according to the ratio value of R_i. The best alternative is the one that having the M-TOPSIS coefficient R_i nearest to 0.

4.4.2 *Example of application of M-TOPSIS method*

The M-TOPSIS procedure described above is applied here on 15 points from a Pareto front obtained after a bi-objective optimization, each point representing a potential solution. The criteria involve the maximization Q_{out} (kWh) and the minimization of EPBT (year). The different stages of the M-TOPSIS algorithm for this example are applied as follows:

From original data, the decision matrix is built (see Table 4-5). Because the *EPBT* criterion represents a cost criterion (minimization), it is transformed into benefit criterion (maximization) by Equation (4.2). The transformed values are displayed in Table 4-6.

Table 4-5 Decision data matrix

		Criteria	
		Q_{out} *max*	EPBT min
Alternatives	1	2,286,757.98	1.753
	2	1,072,808.71	1.699
	3	2,005,066.69	1.730
	4	1,710,340.98	1.711
	5	1,933,294.35	1.727
	6	2,183,467.41	1.747
	7	2,253,731.29	1.749
	8	716,068.22	1.692
Alternatives	9	1,424,028.60	1.701
	10	2,088,618.68	1.735
	11	716,057.32	1.692
	12	2,040,111.49	1.731
	13	358,578.79	1.691
	14	2,076,489.16	1.732
	15	1,760,111.18	1.718

Table 4-6 Transformed values matrix

		Criteria	
		Q_{out} *max*	EPBT max
Alternatives	1	2,286,757.98	0.5705
	2	1,072,808.71	0.5886
	3	2,005,066.69	0.5780
	4	1,710,340.98	0.5845
	5	1,933,294.35	0.5790
	6	2,183,467.41	0.5724
	7	2,253,731.29	0.5718
	8	716,068.22	0.5910
	9	1,710,340.98	0.5879
	10	2,088,618.68	0.5764
	11	716,057.32	0.5910
	12	2,040,111.49	0.5777
	13	358,578.79	0.5914
	14	2,076,489.16	0.5774
	15	1,760,111.18	0.5821

Table 4-7 Normalized decision matrix

		Criteria	
		Q_{out} *max*	EPBT max
Alternatives	1	0.3338	0.2534
	2	0.1566	0.2614
	3	0.2927	0.2567
	4	0.2497	0.2596
	5	0.2822	0.2572
	6	0.3188	0.2542
	7	0.3290	0.2539
	8	0.1045	0.2625
	9	0.2497	0.2611
	10	0.3049	0.2560
	11	0.1045	0.2625
	12	0.2978	0.2566
	13	0.0523	0.2627
	14	0.3031	0.2564
	15	0.2569	0.2585

Table 4-8 Weighted normalized matrix

		Criteria	
		Q_{out} *max*	EPBT max
Alternatives	1	0.3338	0.2534
	2	0.1566	0.2614
	3	0.2927	0.2567
	4	0.2497	0.2596
	5	0.2822	0.2572
	6	0.3188	0.2542
	7	0.3290	0.2539
	8	0.1045	0.2625
	9	0.2497	0.2611
	10	0.3049	0.2560
	11	0.1045	0.2625
	12	0.2978	0.2566
	13	0.0523	0.2627
	14	0.3031	0.2564
	15	0.2569	0.2585

The normalized decision matrix *A* is obtained using Equation (4.3) (see Table 4-7). None of the criteria is preferred over the other, so the coefficient vector of importance W is equal to [1, 1]. The normalized weighted matrix is then represented in Table 4-8. The positive ideal (respectively negative ideal, i.e. non-ideal) solution is determined from the matrix *A* as well as the Euclidean distance matrix (Equations (4.5) to (4.8)). The obtained results are shown in Table 4-9 and Table 4-10. Considering

the point A [min (D_i^+), max (D_i^-)] as the *optimized ideal reference point*, the Figure 4-12 displays the position of all the alternatives in D^+ D^-–plane.

M-TOPSIS coefficient R_i is calculated for each alternative by Equation (4.9) and the ranking is presented in Table 4-11. The Pareto front *EPBT*-Q_{out} in Figure 4-13 indicates the position of the three best alternatives after applying the M-TOPSIS method. The best alternative selected by M-TOPSIS method is alternative 1.

Table 4-9 A^+ and A^- values

	Criteria	
	Q_{out}	EPBT
A^+	0.3338	0.2627
A^-	0.0523	0.2534

Table 4-10 Euclidean distance matrix (D_i^+ and D_i^-)

Alternatives	D_i^+	D_i^-
1	0.0093	0.2815
2	0.1772	0.1046
3	0.0415	0.2404
4	0.0842	0.1974
5	0.0519	0.2299
6	0.0173	0.2664
7	0.0100	0.2767
8	0.2293	0.0530

Alternatives	D_i^+	D_i^-
9	0.0842	0.1975
10	0.0297	0.2526
11	0.2293	0.0530
12	0.0365	0.2455
13	0.2815	0.0093
14	0.0313	0.2508
15	0.0770	0.2047

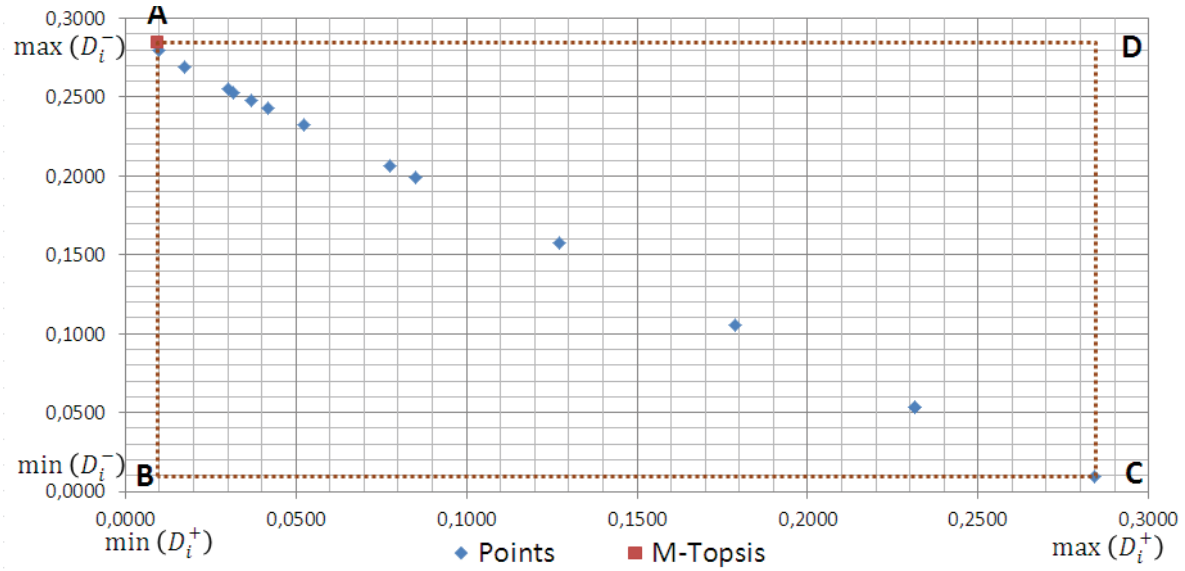

Figure 4-12 D^+ D^-plane for M-TOPSIS example

Table 4-11 Rank alternatives by M-TOPSIS coefficient R_i

Alternatives	R_i	Rank
1	***0.0000***	***1***
2	0.2439	12
3	0.0522	7
4	0.1126	11
5	0.0669	8
6	*0.0171*	*3*
7	*0.0049*	*2*
8	0.3172	13
9	0.1125	10
10	0.0354	4
11	0.3172	14
12	0.0451	6
13	0.3849	15
14	0.0378	5
15	0.1024	9

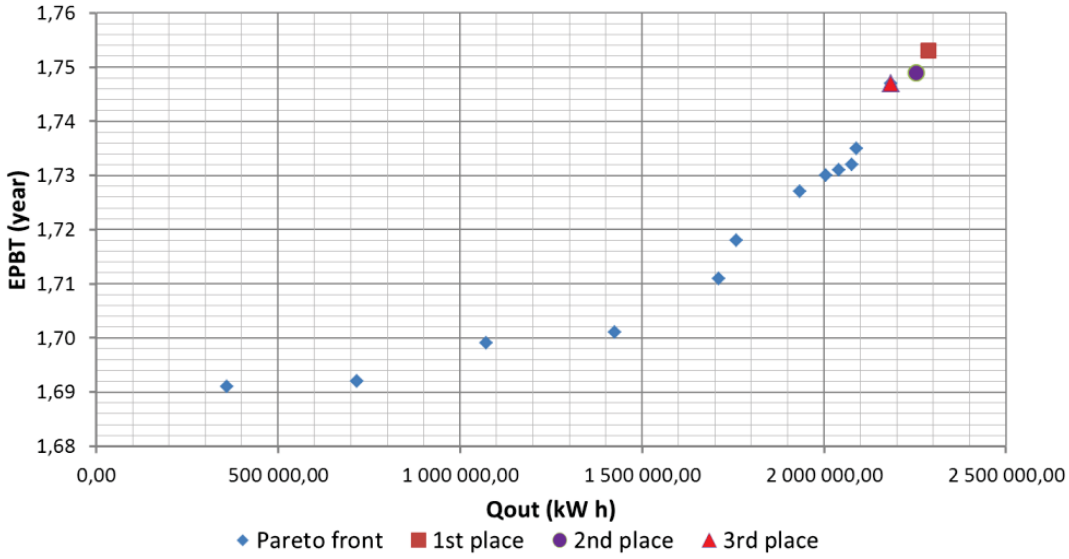

Figure 4-13 Pareto front EPBT-Q_{out} with top 3 ranked alternatives

As it can be seen in Figure 4-13, the best alternatives are located at the upper corner of the curve representing the Pareto front. If these three alternatives are compared with some of the alternatives that are in the knee of the curve, e.g. alternative 4 as shown in Figure 4-14, although EPBT is reduced, the energy produced is also strongly reduced. EPBT reduction is approximately 0.05 year while annual energy produced suffers a reduction of about 30%. The result provided by M-TOPSIS indicates that the best compromise that can be found at equal weight to both objectives in this example is to produce the maximum amount of energy because the difference between the growth in EPBT value is minimal as compared to the gain of Q_{out}.

4.5 Conclusion

In this chapter, three methods to be applied for sizing PVGCS were presented. The number of objectives and the characteristics of the model developed in Chapter 3 make attractive the use of a GA to obtain the best alternatives embodied through a Pareto front. A variant of NSGA-II, embedded in MULTIGEN library, is selected. It must be emphasized that most of the works reported for PVGCS sizing through AG only consider economic or technical aspects. The main contribution of this work will be to integrate the environmental aspect from earlier design stage and not at end-of-pipe stage as

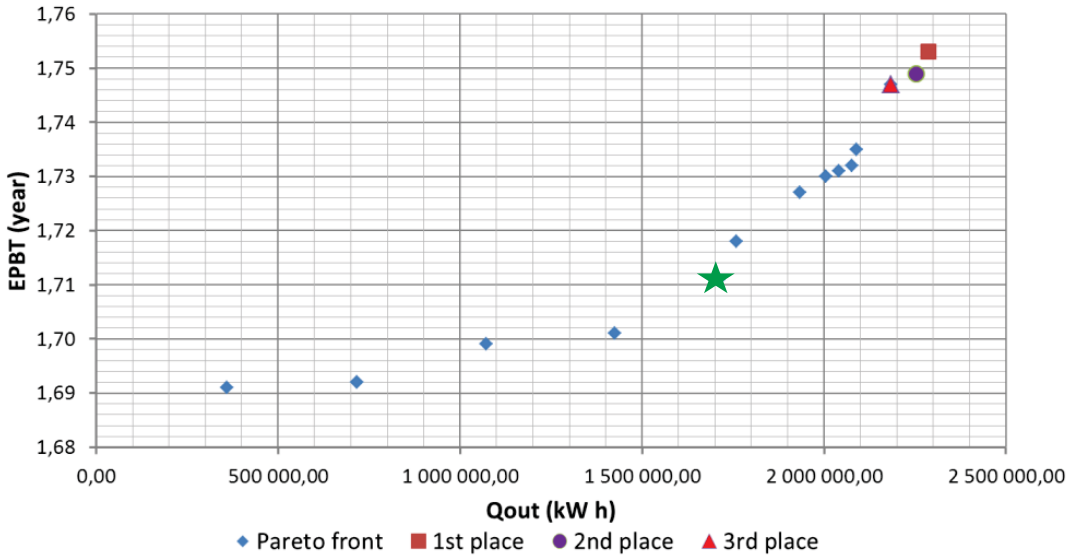

Figure 4-14 Pareto front EPBT-Q_{out} with top 3 ranked alternatives and alternative 4

currently carried out.

The use of PCA is particularly attractive to reduce the number of environmental categories that are generally involved in LCA impact methods as described in Chapter 2. The reduction of intermediate impact categories to be evaluated will save AG computational time and provide a better interpretation of the results. Finally, a post-optimization analysis by use of a MCDM method based on m-TOPSIS is implemented to search for the best configuration among the alternatives represented in the Pareto front.

Figure 4-15 summarizes how the three methods will be integrated and applied for PVGCS, which constitutes the core of the following chapter.

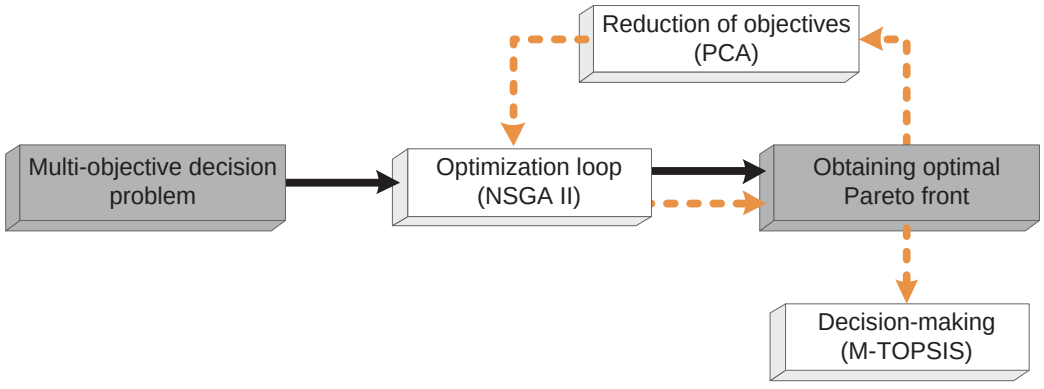

Figure 4-15 Integration of NSGA-II, PCA method and M-TOPSIS method

Chapter 5

ECODESIGN OF LARGE-SCALE PHOTOVOLTAIC POWER PLANTS

Ce chapitre concerne la mise en œuvre du cadre d'écoconception d'un système photovoltaïque connecté au réseau basé sur le couplage du modèle de dimensionnement avec l'algorithme d'optimisation multiobjectif, suivi de l'utilisation d'un outil d'aide à la décision multicritère. Lorsque le nombre d'objectifs devient prohibitif, une méthode systématique d'identification des critères redondants est mise en jeu par analyse en composantes principales. L'ensemble des outils et méthodes utilisé dans le cadre de l'étude a fait l'objet du chapitre précédent. Des cas spécifiques d'optimisation technico-économique qui correspondent à différentes situations auxquelles le praticien est confronté sont traités : par exemple, la maximisation de la production d'énergie à surface de champ donnée, ou la minimisation de l'aire du champ garantissant une fourniture d'énergie annuelle fixée. Les temps de retour sur énergie et sur investissement font partie du jeu de critères considéré.

Des cas d'optimisation multiobjectif faisant intervenir l'ensemble des éléments de la méthodologie, ce qui constitue l'objectif de l'étude, sont également présentés.

Les résultats obtenus dans ce chapitre mettent clairement en évidence le gain environnemental de l'utilisation de modules photovoltaïques de deuxième génération (couche mince) sur les modules photovoltaïques à base de c-Si. L'approche développée est suffisamment générique pour s'adapter à l'étude de différents scénarios.

Nomenclature

Abbreviations

AA	Aquatic Acidification midpoint category
AE	Aquatic Ecotoxicity midpoint category
AEU	Aquatic Eutrophication midpoint category
C	Carcinogen midpoint category
CdTe	Cadmium Telluride
CIS	Copper Indium Diselenide
EPBT	Energy PayBack Time
GA	Genetic Algorithm
GW	Global Warming midpoint category
IO	Ionizing Radiation midpoint category
LCA	Life Cycle Assessment
LO	Land Occupation midpoint category
M-TOPSIS	Technique for Order Preference by Similarity to Ideal Solution
ME	Mineral Extraction midpoint category
NC	Non-Carcinogen midpoint category
NR	Non-Renewable energy midpoint category
NSGA-II	Fast Non-dominated Sorting Genetic Algorithm
OLD	Ozone Layer Depletion midpoint category
PBT	PayBack Time
PCA	Principal Component Analysis
PV	Photovoltaic
PVGCS	Photovoltaic Grid-Connected System
RI	Respiratory Inorganic midpoint category
RO	Respiratory Organic midpoint category
a-Si	Amorphous silicon
m-Si	Monocrystalline silicon
p-Si	Polycrystalline silicon
TAN	Terrestrial Acidification/Nitrification midpoint category
TE	Terrestrial Ecotoxicity midpoint category
WAP	Weinstock and Appelbaum approach

Symbols

β	PV collector inclination angle, degree
η	PV module efficiency, %
A	Surface of PVGCS, m²
a_1	Lower limit of the ratio W/L
a_2	Upper limit of the ratio W/L
D	Distance between PV sheds, m
D_{min}	Minimum distance between PV sheds, m
E_{max}	Maximum PV collector height above ground, m
H	PV collector height, m
H_m	PV module height, m
H_{max}	Maximum PV collector height, m
K	Number of PV sheds
L	Solar field length, m

Symbols

L_m	PV module length, m
L_{max}	Maximum solar field length, m
N_c	Number of PV modules columns in the collector
N_r	Number of PV modules rows in the collector
PC_i	i_{th} Principal component
Q_{min}	Minimum yearly output energy of the field, kWh
Q_{out}	Yearly output energy of the field, kWh
W	Solar field width, m
W_{max}	Maximum solar field width, m

5.1 Introduction

Chapter 1 discusses the importance that represents the use of alternative energy sources for electricity supply as part of the new global policies undertaken favoring the preservation of the environment. Installing PVGCS is one of the most used alternatives globally. A contribution to the development of design procedure was proposed in Chapter 3. The objective of this chapter is to embed this design model into an optimization process. As it was indicated in Chapter 4, when dealing with optimization problems, particularly as far as engineering is concerned, it is very common to consider other objectives besides the traditional economic approach, e.g. risk or environmental assessment. In many real-life problems, objectives under consideration conflict with each other. Hence, optimizing one of them with respect to a single objective often leads to unacceptable results with respect to the other objectives. A perfect multi-objective solution that simultaneously optimizes each objective function is yet impossible. A reasonable solution to a multi-objective problem is to investigate a set of solutions, each of which satisfies the objectives at an acceptable level without being dominated by any other solution. Because of this situation, sizing a PVGCS can become a multi-objective optimization problem.

This chapter is dedicated to the coupling of the PVGCS design model with the three methods described in Chapter 3 at it was indicated in Figure 4-15. Specific cases that correspond to different situations that the practitioner has to cope with are treated: a set of solutions that meets the economic, technical and environmental criteria for designing a PV solar field is thus generated for each case.

The technical options that have been developed for solving the optimization problems of PVGCS design were justified in the previous chapter.

In this chapter, the proposed methodology is evaluated and validated by the treatment of some examples of optimization problems. First, two mono-objective problems taken from the literature (Weinstock & Appelbaum, 2004b, 2009) are investigated. The former example maximizes the output energy of the plant in a specific place. The second example determines the minimum area required to

install a solar field in order to supply a fixed amount of energy per year. PBT, EPBT and environmental impacts assessment are performed for each of the generated solutions.

Then, multi-objective problems that allow the correct integration of all the components of the methodology proposed in this work are solved. Due to the high number of environmental objectives, an analysis in order to eliminate the correlated objectives so that the optimization process performed becomes most efficient. For this purpose, Principal Component Analysis (PCA) is applied to achieve a considerable reduction in terms of the number of environmental impact categories to be considered in the analysis.

In all the optimization problems, M-TOPSIS is then used to select the alternative with the best trade-off among the objectives considered.

5.2 Optimal design of photovoltaic solar fields

Figure 5-1 shows how the three methods described in Chapter 4 are integrated into the general approach proposed in Chapter 3. At first, the model proposed for sizing a PVGCS is coupled with the GA (NSGA-II). The results of a preliminary optimization process will provide the best alternatives in the Pareto front. Then, environmental categories will be reduced by applying the PCA method to the set of alternatives of the Pareto front. A new optimization scheme will be implemented from the categories highlighted by PCA that will be more systematically used in further optimization runs. Finally, the best option is chosen by using the M-TOPSIS method among the solutions of the new Pareto front.

The common parameters of the GA that will be used in each problem resulting from a preliminary study are determined following the guidelines suggested by the MULTIGEN developer (Gomez, 2008) . They are shown in Figure 5-1.

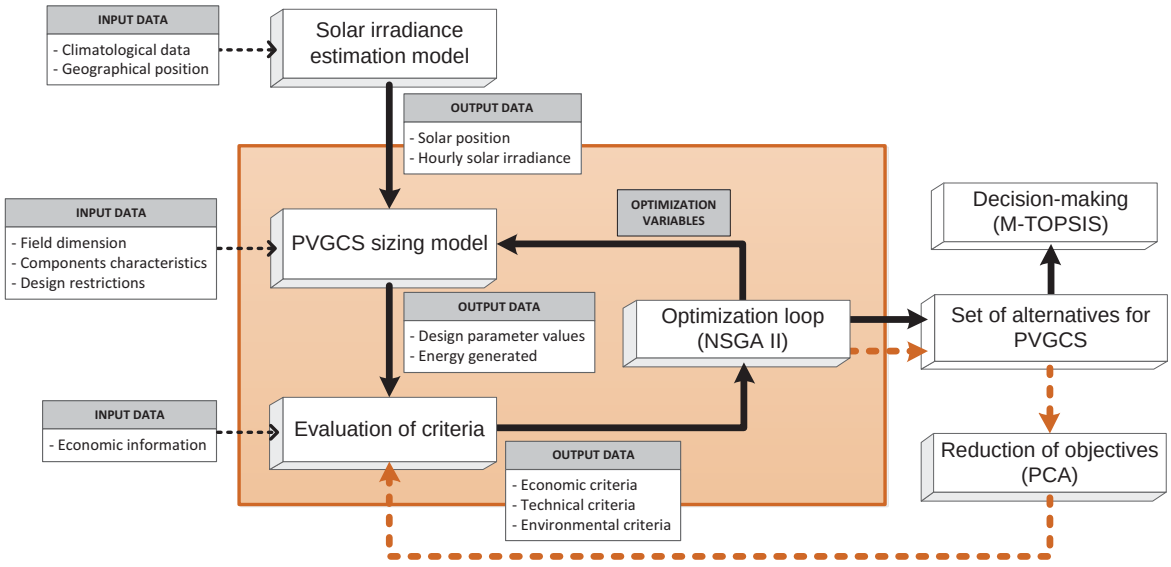

Figure 5-1 Functional flow diagram of the proposed methodology

Table 5-1 Parameter values of NSGA-II for different examples

	1 objective	2 objectives	3 or more objectives
Population size	100	100	200
No. generation	200	200	400
Crossover rate (%)	90	90	90
Mutation rate (%)	50	50	50

5.3 Mono-objective optimization cases

The proposed methodology is first implemented for single objective optimization. Weinstock and Appelbaum (Weinstock & Appelbaum, 2004b, 2009) treat two mono-objective cases to design a PV power plant. The cases are referred as WAP conditions as previously adopted in Chapter 3. The former case is to find the best design that maximizes annual energy output of the facility. This case was used in Section 3.7 for the validation of the simulation tool. The latter one is related to the minimization of the area required to supply a minimum amount of energy in a year. In both cases, the methodology described in Figure 5-1 is modified. PCA and M-TOPSIS method will not be used.

Another set of optimization runs for both cases is carried out considering the five different PV modules technologies presented in Table 3-8. A mix of PV technologies is not allowed to facilitate maintenance. The other objectives (PBT, EPBT and environmental categories) will be only evaluated considering the solution found after the optimization process. Of course, the PCA method will not be applied for mono-objective optimization. A weighted evaluation is proposed to select the best configuration among the five resulting power plant configurations.

5.3.1 *Maximum annual output energy*

As explained in Section 3.7, the example reproduces the WAP conditions for the configuration that maximizes PV power plant annual energy. The same conditions, PV module characteristics and location (Tel Aviv, Israel) used in Section 3.7 are considered as well as the three scenarios mentioned.

Equation (3.30) in Section 3.5.3.2, represents the objective function to maximize for each of the three scenarios. The mathematical model and the constraints of the design problem were described by Equations (3.20) to (3.25) in Section 3.5.3.

The limit values for the involved constraints are the same as those used for WAP: minimum space between collector rows (D_{min}) equal to 0.80 m, maximum collector height (H_{max}) equal to 1.98 m and height of collector above the ground (E_{max}) equal to 1.80 m.

The decision variables that are used are the same as indicated in WAP mathematical model (β, D, K, N_r, N_c).

5.3.1.1 Results

Table 5-2 shows the comparison between the results obtained by the approach proposed and WAP. A good agreement is obtained between both models. Not surprisingly, the difference in the amount of output power for the three cases is mainly due to the improvement in the computation of irradiance

Table 5-2 Comparison between WAP and the proposed approach

Objective function		*K*	*D*(m)	*β* (°)	Q_{out} (kWh)
Maximum incident energy onto total surface of PV modules	WAP	58	0.80	24.62	2,641,034
	PA	58	0.80	24.62	3,201,915
Maximum output energy w shading losses	WAP	58	0.80	24.62	328,048
	PA	58	0.80	24.62	397,793
Maximum output energy of PV array (shading, temperature and interconnections losses)	WAP	57	0.80	21.23	268,000
	PA	57	0.80	21.26	327,338

WAP = Results of Weinstock and Appelbaum PA = Results of proposed approach

received at the facility as presented in Section 3.5.3.

It is worth mentioning that WAP used MATLAB optimization toolbox to solve the optimization problems. This toolbox uses a sequential quadratic programming method (Weinstock & Appelbaum, 2004b).

A modification was done to the previous example. The PV modules considered by WAP do not consider explicitly a PV technology. Only an average efficiency, i.e., 12.4% is mentioned. In this study, the five different PV technologies presented in Table 3-8 are considered. Only the third scenario of previous case is considered, based on the maximization of the output energy with all possible energy losses. Equation (3.30) is kept as the objective function. The conditions and constraint boundaries are the same. The values of the decision variables and annual output energy for each of the resulting configurations are shown in Table 5-3 and Table 5-4. Table 5-4 also presents the results of the simulation made for each configuration in PVsyst for comparison purpose.

The output energy estimated by the model is on average 6.50% higher than that obtained after the simulation of each power plant configuration in PVsyst. The results suggest that the configuration using PV modules based on m-Si generates the highest amount of annual energy under the conditions given in the case study.

The result of the evaluation of PBT and EPBT for each configuration (see Table 5-5) shows that the lowest EPBT is achieved by using PV modules based on CdTe but this technology does not lead to the lowest PBT value. Even though the m-Si PV module generates the maximum output energy, its EPBT is high due to the amount of energy required during the manufacturing phase.

Table 5-3 Values of decision variables for the best configuration of each PV technology.
Maximum output energy

PV module	*β* (°)	*K*	*D* (m)	N_r	N_c
m-Si	18.42	55	0.84	1	12
p-Si	21.22	60	0.80	1	13
a-Si	17.01	54	0.81	1	11
CdTe	25.30	80	0.80	1	21
CIS	22.68	77	0.80	1	13

Table 5-4 Output energy for the best configuration of each PV technology. Maximum output energy.

PV module	Q_{out} (kWh)	Q_{out} *PVsyst* (kWh)	*Gap*
m-Si	430 397	400 336	-7.50%
p-Si	328 453	299 421	-8.84%
a-Si	131 021	119 700	-8.64%
CdTe	275 449	262 042	-4.87%
CIS	293 904	283 558	-3.52%

Table 5-5 PBT and EPBT for each configuration. Maximum output energy

PV module	PBT (yr)	EPBT (yr)
m-Si	5,90	2,36
p-Si	7,59	2,67
a-Si	7,59	2,04
CdTe	9,23	1,77
CIS	6,29	2,14

The results of the environmental impact assessment (15 midpoint categories) for each configuration are shown in Figure 5-2 by the use of radar charts (Comparison 1). To facilitate the comparison, normalisation was performed by assigning the value 1 to the maximum value of each category. The computed relative impacts represent the ratio between the environmental impact and this maximum value.

The analysis of the result shows that in 9 of the 15 categories the highest impacts occur with m-Si technology: in *Global Warming* category, where CO_2 is the reference component, the installation with PV modules based on m-Si, generates a higher CO_2 amount after the characterization of all inventory flows. Likewise, for the *Non-renewable Energy* category, the highest amount of non-renewable primary energy consumed by all the processes evaluated within the boundaries set for the LCA study was found for m-Si based PV modules installation. In spite of its low EPBT, the solar plant with CdTe modules has a significant impact within the category of *Non-carcinogens*, i.e., the characterization of the different flows in the inventory for CdTe module installation results in a large amount of chloroethylene C_2H_3Cl into air, a substance that affects human health.

To select the best PV power plant among the five proposed alternatives, a weighted evaluation is performed for the 18 objectives (maximizing final energy generation output, minimizing PBT, minimizing EPBT and minimizing 15 environmental impacts). First, a ranking for each alternative of solar plant configuration was made giving a value of 1 to the alternative that best meets the objective and 5 to the worst one. The value assigned to each alternative in a given goal is then multiplied by a weighting factor. This factor may be of course subjective. An equal factor for the 18 objectives was assigned, thus giving importance to environmental impact. Then, the scores obtained by each

alternative are added to give a cumulative score. As it can be seen in Table 5-6, the alternative with the lowest total score is the a-Si technology.

As in Section 3.7, another analysis is then performed taking into account the energy generated by each configuration. The results are presented through radar charts normalized to unity (Figure 5-2, Comparison 2). It can be highlighted that the type of PV technology with the higher ratio is the one based on p-Si modules (8 of 15 categories). Although the environmental impacts of m-Si based technology are higher, these are offset by the large amount of energy generated annually.

The same weighted evaluation is made for this analysis and the results are reported in Table 5-7. The alternative of CIS PV module technology best meets the objectives.

Reviewing the results obtained from the weighted evaluation in Table 5-6 and Table 5-7, if all criteria have the same weights, the conversion efficiency of PV module takes an important role depending on the form of evaluation of environmental categories. It may serve as a mitigating circumstance to the values reported for the different environmental categories, e.g. the alternative based on a-Si PV module proved to be the best trade-off for all the objectives considered when only the results obtained from the LCA study are taken into account but it falls to fourth position if these values are divided by the amount of energy produced.

For example, Comparison 2 in Figure 5-2 shows that the configuration with m-Si has a better performance in almost all environmental categories than the results of Comparison 1. This alternative goes from the fifth place to the second one. It is important to keep in mind that the impact assessment does not consider the recycling of PV plant components. Chapter 5 will study the impact of recycling on the final result.

Table 5-6 Final ranking of alternatives. Maximum output energy

PV module	Final weighted evaluation	Ranking
m-Si	72	5
p-Si	71	4
a-Si	32	***1***
CdTe	49	3
CIS	46	2

Table 5-7 Final ranking of alternatives (environmental impact per kWh produced). Maximum output energy

PV module	Final weighted evaluation	Ranking
m-Si	48	2
p-Si	74	5
a-Si	59	4
CdTe	52	3
CIS	37	***1***

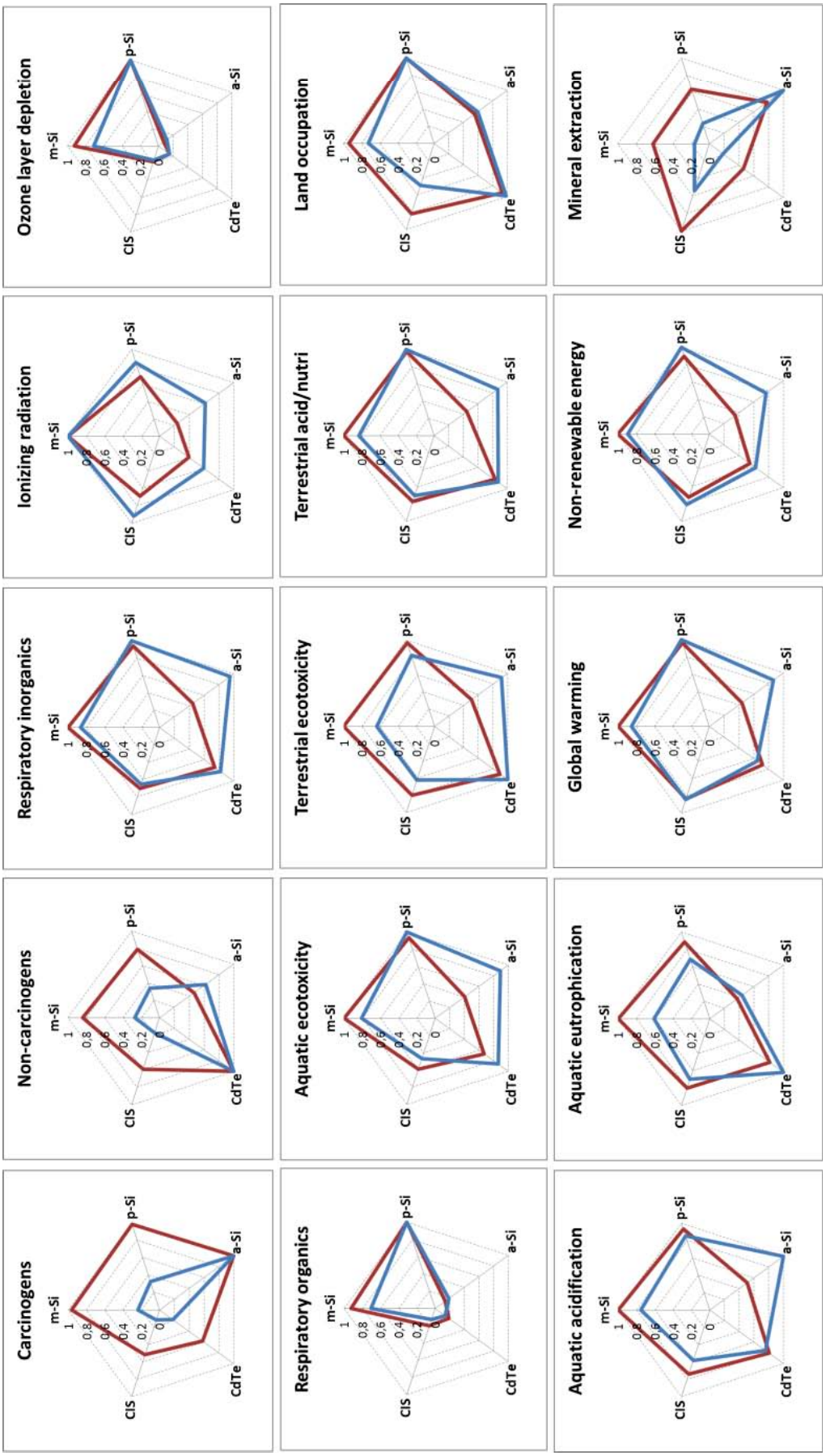

Figure 5-2 Results of the environmental impacts normalized to unity. Maximum output energy

5.3.2 *Minimum Field Area*

Another possible objective function is to find the smallest area, W x L, of a solar field to generate a required yearly output energy Q_{min}. Such a problem occurs where the ground is expensive or on rooftops where the available area for solar collector installation is limited.

Some modifications were made to the mathematical model used until now to fit this case. The new constrains were taken from WAP model. Equation (2.6) represents the new objective function to minimize:

$$W \times L \tag{5.1}$$

Equations (3.20) to (3.25) of Section 3.5.3 are still considered as model constraints. Equation (5.2) to (5.4) are added as constraints in order to delineate the possible area of the solar field.

$$W \leq W_{max} \tag{5.2}$$

$$L \leq L_{max} \tag{5.3}$$

$$a_1 \leq \frac{W}{L} \leq a_2 \tag{5.4}$$

Equation (5.4) represents a relationship between the length and width of the solar field.

The field should generate at least a required amount of yearly energy. Equation (5.5) represents this condition:

$$Q_{out} \geq Q_{min} \tag{5.5}$$

For this second mono-objective case, the following example is proposed in order to test the new model. The main goal is to place a PV power plant capable to produce at least 1 GWh/year in the smallest area possible. The considered constrains are the following ones: D_{min} = 0.80 m, H_{max} = 4.00 m, E_{max} = 3.00 m, W_{max} = 150.00 m, L_{max} = 100.00 m, a_1 = 0.5 and a_2 = 2.

In this second case, in addition to the variables corresponding to the first scenario (β, D, K, N_r, N_c), the length and width of the solar field (W, L) are added. The parameters of NSGA-II were mentioned in Table 5-1.

5.3.2.1 Results

Five different PV module technologies are evaluated. As previously, no mix in the technologies is allowed. The resulting five configurations are shown in Table 5-8. For the sake of illustration, Figure 5-3 shows the 3D-perspective for each configuration that can be obtained from PVsyst. Each square represented 100 m² of land.

Table 5-8 Best configuration that minimizes the surface of PV system

PV module	β (°)	K	D (m)	W(m)	L(m)	A(m²)
m-Si	21.36	21	0.80	46.49	69.04	3,209.55
p-Si	21.06	34	0.80	78.44	52.86	4,146.44
a-Si	9.73	23	0.80	106.55	72.02	7,674.08
CdTe	10.35	18	0.80	77.35	62.40	4,826.39
CIS	9.88	17	0.80	75.86	59.58	4,520.79

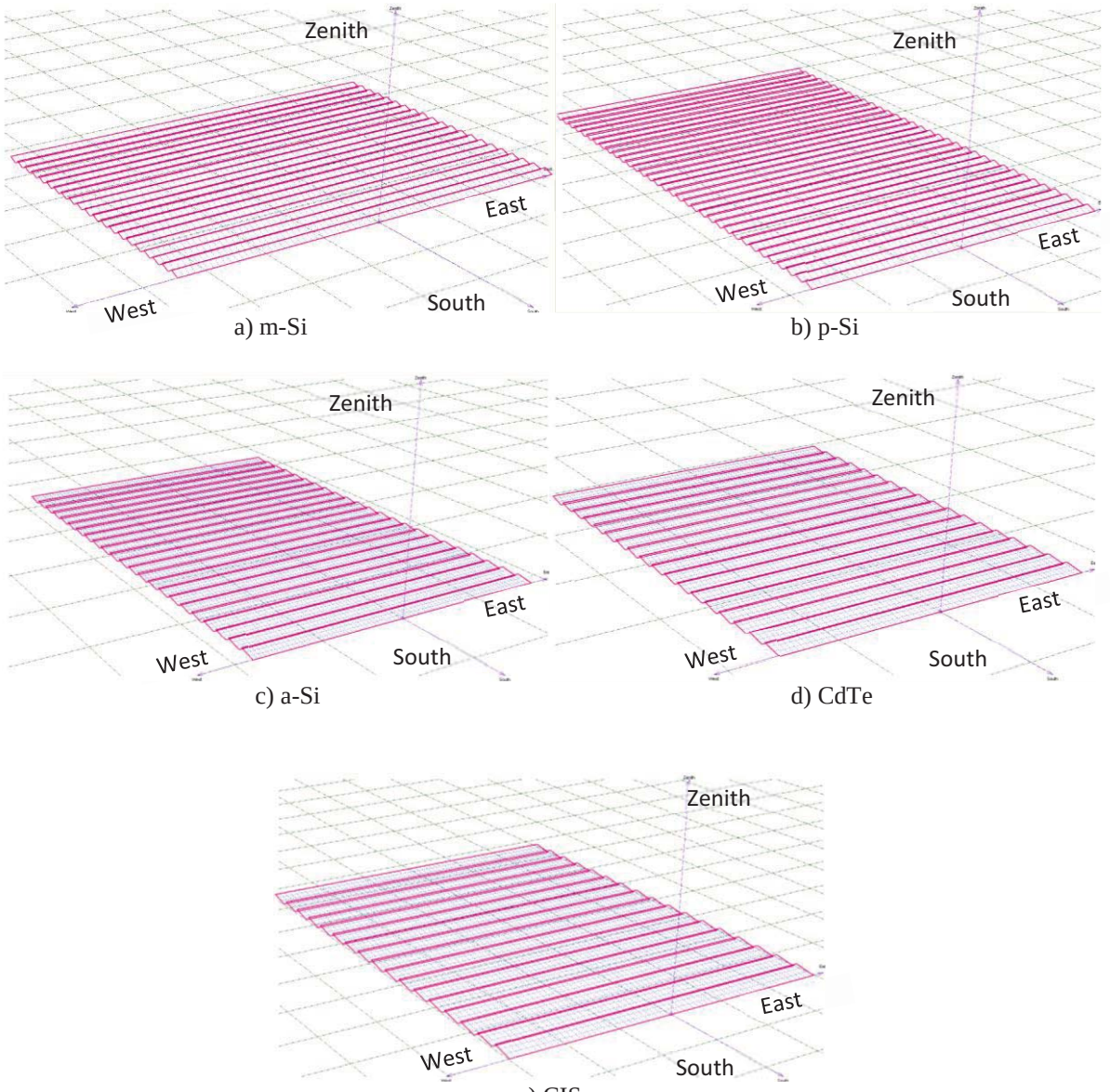

a) m-Si b) p-Si

c) a-Si d) CdTe

e) CIS

Figure 5-3 3-D perpectives of 5 configurations

Not surprisingly, on the one hand, the configuration using PV modules based on m-Si has the smallest surface under the given conditions in the case studied because this technology has the highest conversion rate among all the studied technologies. On the other hand, the configuration with a-Si PV modules which has the lowest efficiency needs the highest surface. As already carried out, the assessment of PBT, EPBT (Table 5-9) and environmental impacts (Figure 5-4) was performed for each of the resulting combinations.

As in the examples discussed in Section 5.3.1.1, the technology based on m-Si has the lowest PBT while the lowest EPBT is found in PV module technology based on CdTe. Table 5-9 reveals that the values of PBT (respectively EPBT) exhibit the same order of magnitude for the five configurations, unlike the case of maximum output energy presented in Table 5-5. It must yet be emphasized that the cost of land is not included in the economic evaluation so there is no penalty for the plant size.

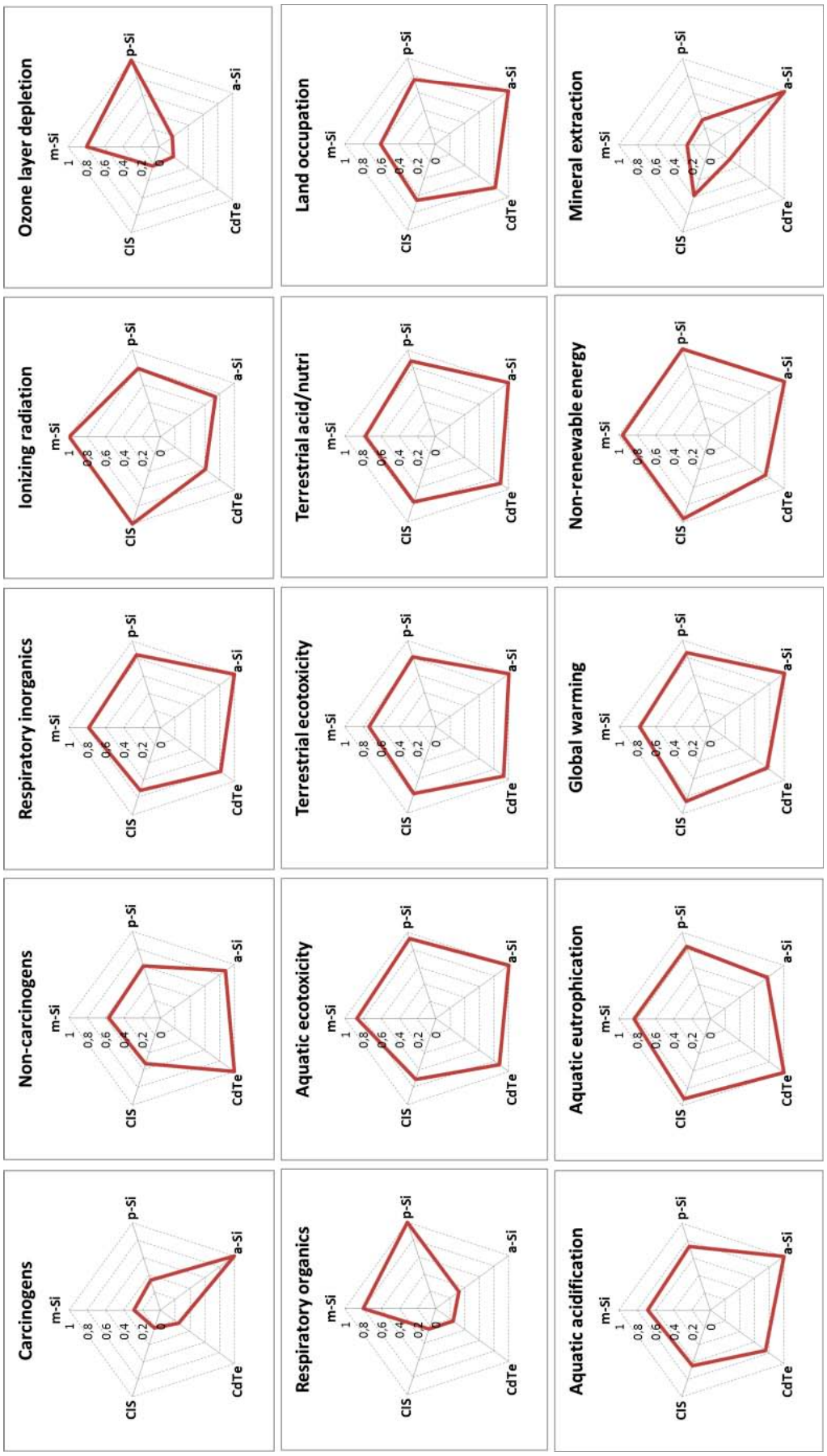

Figure 5-4 Results of the environmental impacts normalized to unity. Minimum field area

Table 5-9 PBT and EPBT for each configuration. Minimum field area.

PV module	PBT (yr)	EPBT (yr)
m-Si	6.34	1.18
p-Si	7.68	1.32
a-Si	7.34	1.18
CdTe	7.43	0.88
CIS	6.48	1.16

Table 5-10 Final ranking of alternatives. Minimum field area

PV module	Final weighted evaluation	Ranking
m-Si	40	***1***
p-Si	65	4
a-Si	72	5
CdTe	51	3
CIS	41	2

Concerning EPBT values, the energy produced by each plant is practically the same, exceeding a minimal annual amount of 1 GWh. Even if the surface of the base configuration of CdTe modules is larger than the one with m-Si technology, the total primary energy for the production of CdTe panels is less than that required for the PV modules based m-Si.

Figure 5-4 shows the standardized radar charts of 15 midpoint categories. The analysis of the chart shows that in 10 of the 15 categories, the a-Si PV module has the highest impact even if it has an average value for EPBT and PBT.

As in previous examples, the weighted evaluation is performed for the 18 targets (minimizing the surface, minimizing PBT, minimizing EPBT and minimizing the 15 environmental impacts). Table 5-10 displays the score and ranking of the 5 configurations. The final classification reveals that PV power plant from m-Si technology corresponds to the best compromise while the a-Si PV modules exhibit the highest score.

As a conclusion of these mono-optimization cases corresponding to different scenarios, it can be said that optimization can be particularly useful as a decision-making aid tool for ecodesign purpose.

Due to the multi-objective nature of the problem, the problem is now treated with more appropriate multi-objective genetic algorithms.

5.4 Bi-objective optimization cases

Different cases of bi-objective optimization for sizing a large-scale photovoltaic power plant are discussed below.

The example which is treated here was part and parcel of a student group project at ENSIACET in the framework of the EcoEnergy programme.

In all cases, PV power plant is placed near the city of Toulouse, France (43.4° N, 1.2° E, elevation 152 m, +1 GMT). The following considerations are taken into account:

- The dimensions of the field is W_{max} = 150.00 m and L_{max} = 100.00 m.
- The minimum separation between each shed is D_{min} = 1.00 m.
- The dimensions of the PV collectors must respect: H_{max} = 3.00 m y E_{max} = 4.00 m.
- Minimum number of shed (K) should be 2.
- The percentage of the loss caused by the array module wiring and mismatch is 5%.
- AC / DC invertor has a nominal power of 300 kW DC with an efficiency of 97.5% and a lifetime of 10 years.

The dimension and characteristics of PV modules used are the same as those indicated in Table 3-8 and no mix in technologies is allowed. The decision variables are the following ones: β, D, K, N_r, N_c.

NSGA-II with continuous-integer variables embedded in MULTIGEN library was used to perform the optimization runs. Each optimization case was run three times to guarantee the stochastic nature of the algorithm.

Five cases of multi-objective optimization are explored. A first set of five bi-objective optimization runs are first studied in order to verify that the objectives are antagonist. Besides, these preliminary examples allow assessing the correct coupling between the proposed model to size a PVGCS and the AG selected. Taking as references the mono-objective cases studied above, these bi-objective cases use the already studied objective (maximize annual Q_{out} and minimize the area, respectively) and a second objective is added. The economic approach through PBT and an energetic criterion through EPBT are selected to take part in these first bi-objective problems. Due to the reduced number of objectives in these studies, PCA is not implemented here. A final bi-objective case will try to optimize EPBT and PBT. In all the multi-optimization runs, although not optimized, the environmental categories will be computed for information. The best alternative will be selected by application of the m-TOPSIS approach.

5.4.1 $Q_{out} - PBT$

The first case of bi-objective optimization is based on the minimization of PBT while maximizing simultaneously the annual amount of energy produced. Figures 5-5 (a to e) show the resulting Pareto fronts for each of the PV technologies discussed. The average computation time for each optimization run is about 2.5 hours CPU on the same PC (Intel Core 2 Duo @ 3.00 GHz).

As already presented in Chapter 4, a choice must be made to select a PV technology among the options in the Pareto front. For this purpose, the decision support tool M-TOPSIS method is used through a prioritization of the objectives only at the end of the optimization process. The 18 objectives are considered even if only two objectives are used in the optimization process.

The purpose of using a decision support tool is to suggest to the decision-maker which configuration found by the GA for all the technologies that are evaluated is the one with the best compromise for the objectives under study. The selection of the best option will involve a two-step application of the M-

TOPSIS method: first, the best alternative in each of the five technologies is chosen (M-TOPSIS application 1); then, from these results, the best compromise is selected (M-TOPSIS application 2).

To study the influence of the weight allocated to each objective under study for selecting the best alternative of PV power plant, four different sets of weights are proposed (see Table 5-11).

These weights will be applied only in the selection of the best option for each of the PV technologies considered. For the second phase, the weight is the same for all objectives. This consideration is taken into account because the alternatives were already evaluated and weighted in the first selection phase.

Table 5-11 Weight proposals

Proposal set of weights	Q_{out}	*PBT*	*EPBT*	15 environmental categories
1	1	1	1	1 each
2	1	1	1	1/15 each
3	1	5	1	1/15 each
4	5	1	1	1/15 each

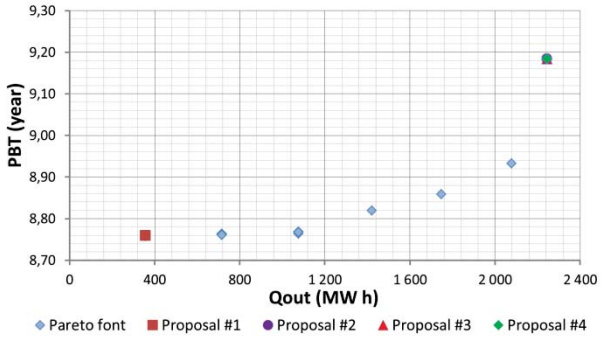

a) m-Si

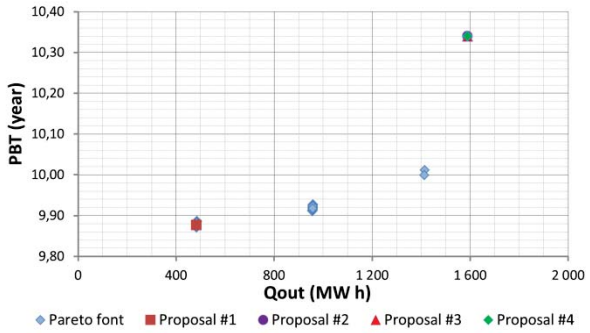

b) p-Si

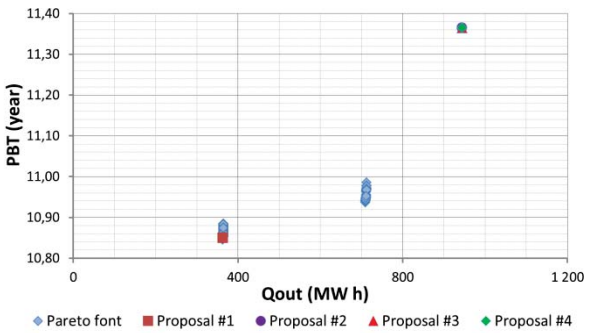

c) a-Si

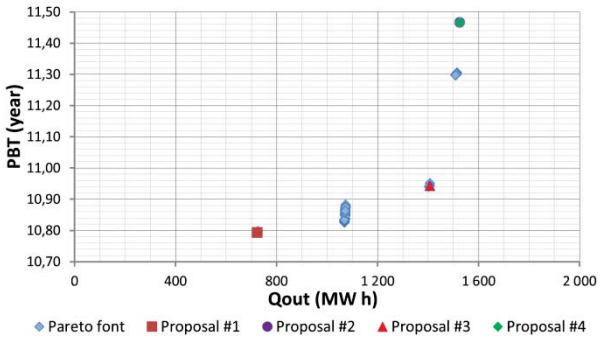

d) CdTe

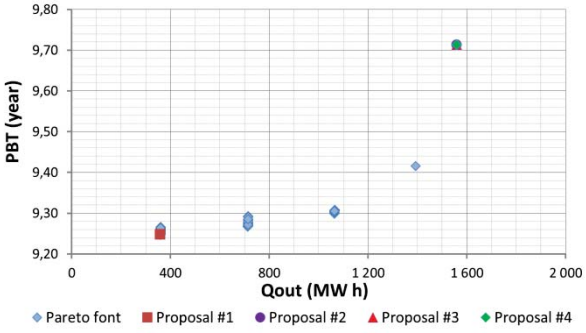

e) CIS

Figures 5-5 (a-e) Pareto fronts with M-TOPSIS selected PV power plant configuration. Max Q_{out} – Min PBT

Table 5-12 Configuration selected by applying M-TOPSIS. Max Q_{out} – Min PBT

PV Techno	Proposal	*β (°)*	*K*	*D (m)*	*Nr*	*Nc*	Q_{out} *(MW h)*	*PBT (year)*	*EPBT (year)*
m-Si	1	27.71	9	16.15	1	94	358.05	8.76	1.69
	2	16.79	58	1.03	1	95	2 245.36	9.18	1.76
	3	16.79	58	1.03	1	95	2 245.36	9.18	1.76
	4	16.79	58	1.03	1	95	2 245.36	9.18	1.76
p-Si	1	27.63	18	7.16	1	93	484.19	9.88	1.84
	2	15.00	54	1.21	1	105	1 590.26	10.34	1.90
	3	15.00	54	1.21	1	105	1 590.26	10.34	1.90
	4	15.00	54	1.21	1	105	1 590.26	10.34	1.90
a-Si	1	24.69	15	8.07	2	88	364.01	10.85	1.73
	2	11.01	40	1.12	2	90	944.78	11.36	1.81
	3	11.01	40	1.12	2	90	944.78	11.36	1.81
	4	11.01	40	1.12	2	90	944.78	11.36	1.81
CdTe	1	22.14	26	3.58	2	129	724.44	10.79	1.30
	2	12.65	45	1.01	2	166	1 526.37	11.47	1.36
	3	13.00	41	1.34	2	164	1 407.29	10.94	1.32
	4	12.65	45	1.01	2	166	1 526.37	11.47	1.36
CIS	1	25.28	11	11.37	2	84	359.95	9.25	1.67
	2	11.08	41	1.23	2	102	1 558.88	9.71	1.74
	3	11.08	41	1.23	2	102	1 558.88	9.71	1.74
	4	11.08	41	1.23	2	102	1 558.88	9.71	1.74

Table 5-12 displays M-TOPSIS selected configurations for the four sets of weights. Figures 5-5 (a to e) shows the location of the resulting configurations in the graphs of the respective Pareto fronts.

From all the evaluated technologies, Figures 5-5 (a to e) show that the M-TOPSIS selected alternatives for the proposal sets (2 to 4) of weights are located at the upper end of the Pareto front. This can be attributed to the scale difference in the coordinates: the range of PBT values is very narrow, only a few months difference while the energy range is quite large. It must be concluded that a higher PBT (a few months) is acceptable here to increase considerably the amount of generated energy. Almost no difference can be observed for TOPSIS- ranked top 1 solution for these three cases as it can be observed in Table 5-12 when varying the weight.

Top ranked solution for proposal 1 is located in the other extreme of Pareto front for all PV technologies. The reason for this trend is that, considering equal weights for all objectives, the compromise to do is higher given the number of objectives to be minimized. This corresponds to the lower amount of Q_{out} for this scenario over the other scenarios.

The environmental impacts corresponding to the studied scenarios (see Figure 5-6) exhibit the same differences. PV power plant with CdTe PV modules is the best in almost all categories, for equal weights (proposal 1) are used whereas m-Si based configurations are the best for the other three scenarios.

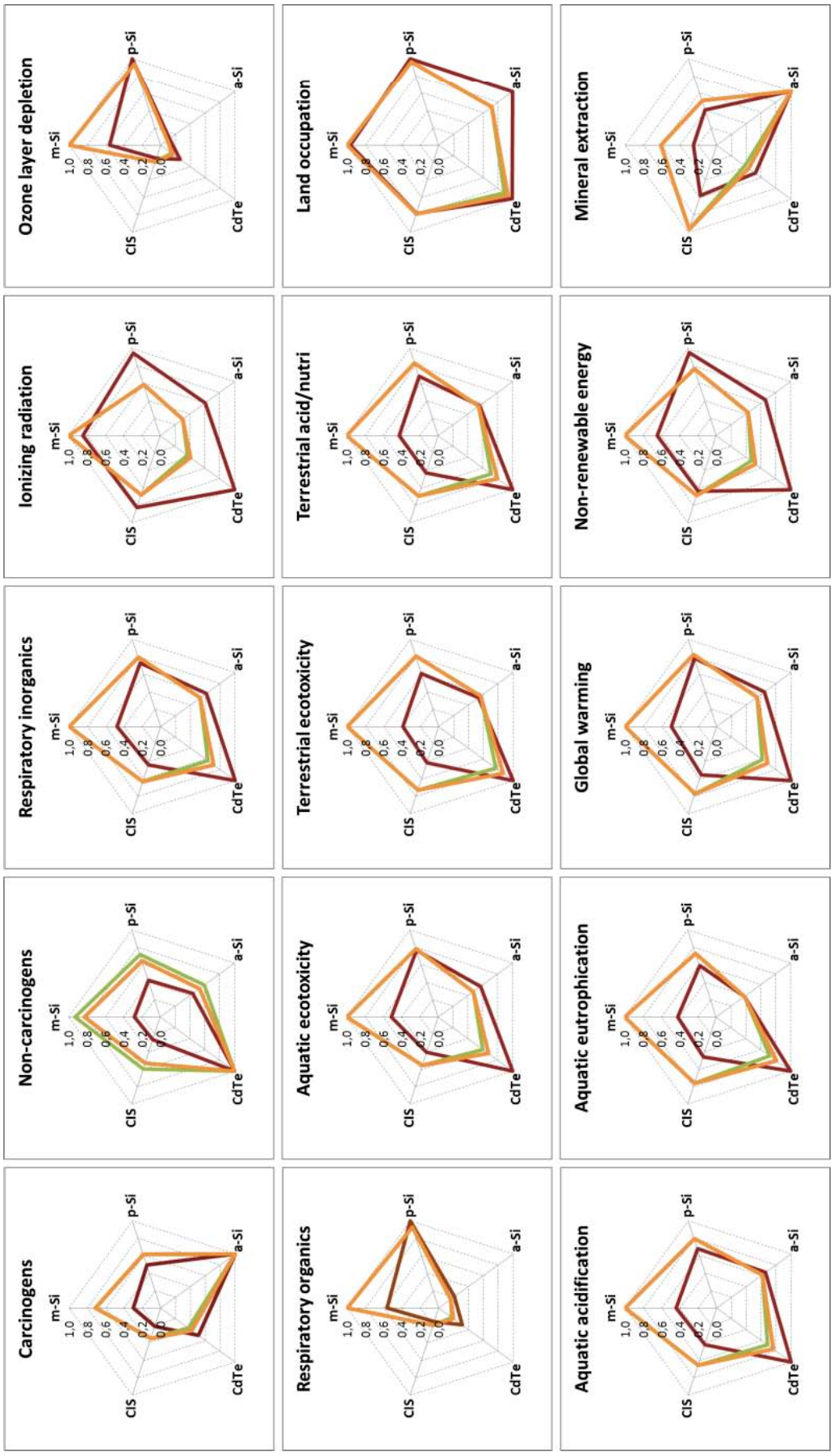

Figure 5-6 Results of the environmental impacts normalized to unity. Max Q_{out} – Min PBT

Table 5-13 Ranking of the resulting configurations after applying M-TOPSIS. Max Q_{out} – Min PBT

PV Techno	Proposal 1	Proposal 2	Proposal 3	Proposal 4
m-Si	2	5	5	5
p-Si	5	4	4	4
a-Si	3	**1**	**1**	**1**
CdTe	4	2	2	2
CIS	**1**	3	3	3

From the results of Table 5-12, if only the two objectives that were optimized are considered to select the best alternative among the five possible configurations, m-Si based PV power plant is the most suitable in all the scenarios.

As already mentioned, M-TOPSIS is once more applied among the set of the best compromises obtained for each technology. The final ranking for the five alternatives of PV power plant for each scenario highlights (see Table 5-13) that a-Si based configurations better fits all the objectives, i.e. the maximization of energy production and minimization of PBT, EBPT and environmental categories.

Table 5-12 and Table 5-13 exhibit the importance of the weight given to each objective. For the following cases where the maximization of the annual energy generation is one objective, only the weights of proposal 2 will be used. The proposal 1 is eliminated since the drastic reduction in annual energy produced (more than 50% in all technologies) while the results of proposals 3 and 4 do not differ from those of the proposal 2.

5.4.2 Q_{out} – *EPBT*

This second optimization case deals with the simultaneous minimization of EPBT and maximization of the energy fed into the grid. The same process as in previous case was followed. The resulting Pareto fronts for each of the technologies are presented in Figures 5-7 (a to e). The average computation time for complete each optimization problem was 2.51 hours CPU on the same PC. The M-TOPIS approach is implemented to select a configuration from the Pareto front. As it was indicated in previous case, only the set of weight of proposal 2 (Table 5-11) is used here. Table 5-14 shows the best alternative for each PV technology.

As in the previous case, it is observed that the range of EPBT values is very narrow and M-TOPSIS selected alternatives are also located in the upper end of the Pareto front. A slight increase in EPBT leads once more to a high gain in the energy injected into the grid.

Table 5-14 Configurations selected by applying M-TOPSIS. Max Q_{out} – Min EPBT

PV Techno	*β (°)*	*K*	*D (m)*	*Nr*	*Nc*	Q_{out} *(MW h)*	*PBT (year)*	*EPBT (year)*
m-Si	14.32	59	1.04	1	95	2 286.76	9.12	1.75
p-Si	15.71	58	1.02	1	105	1 694.19	11.16	1.94
a-Si	10.84	41	1.06	2	90	965.20	11.34	1.81
CdTe	11.64	44	1.08	2	166	1 512.99	11.34	1.35
CIS	9.79	43	1.02	2	102	1 625.08	9.65	1.74

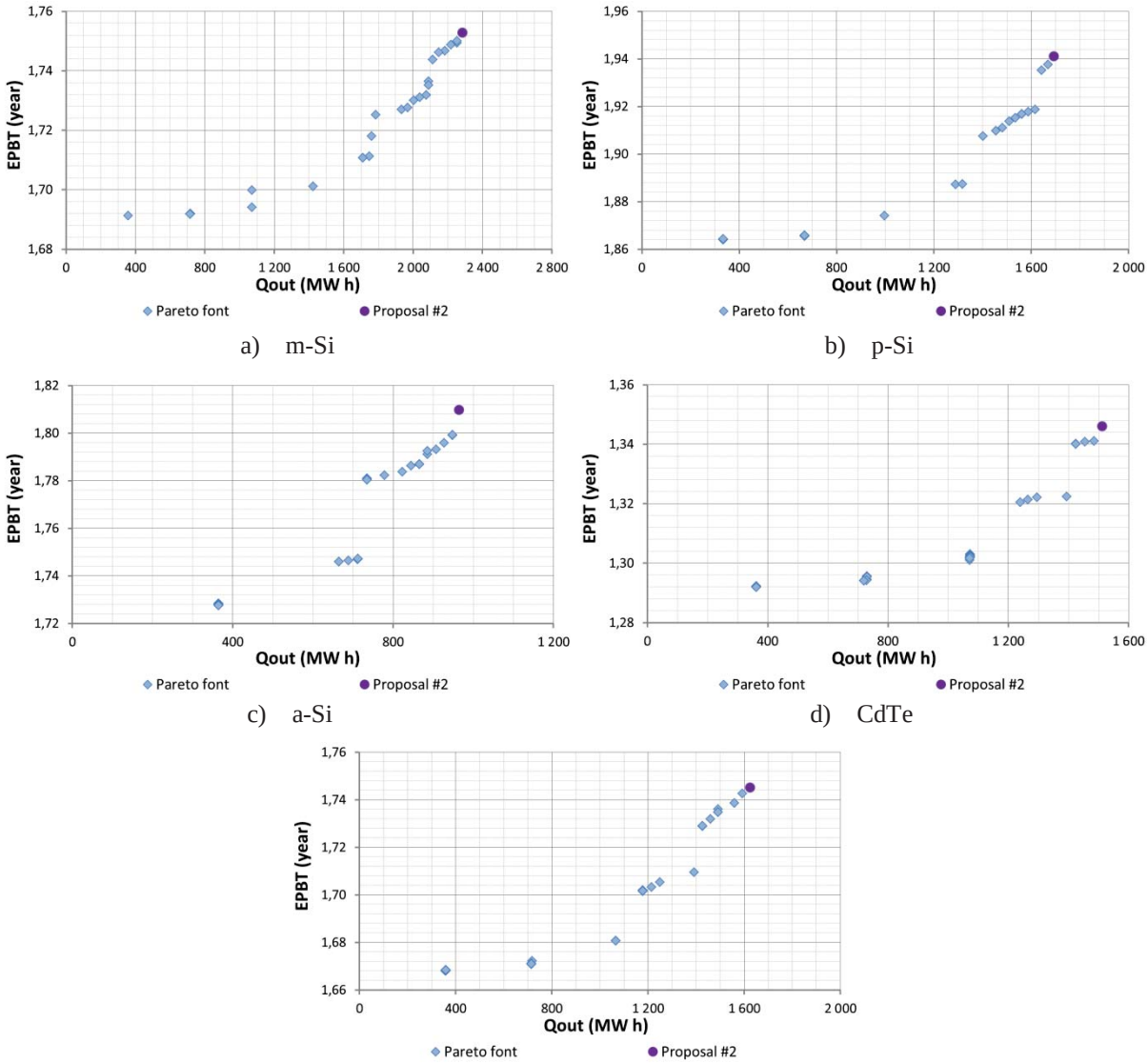

a) m-Si b) p-Si

c) a-Si d) CdTe

e) CIS

Figures 5-7 (a-e) Pareto fronts with M-TOPSIS selected PV power plant configuration. Max Q_{out} – Min EPBT

Table 5-15 Ranking of resulting configuration after applying M-TOPSIS.

Max Q_{out} – Min EPBT

PV Techno	Ranking
m-Si	5
p-Si	4
a-Si	**1**
CdTe	2
CIS	3

From the results of Table 5-14, it is worth mentioning that the configuration based on m-Si generates a larger amount of energy but does have the best EPBT. The CdTe based configuration is the best for the EPBT criterion. Figure 5-8 represents the radar charts of environmental impacts and shows that the m-Si based configuration leads in almost all of the categories.

M-TOPSIS application gives the ranking proposed in Table 5-15 for the 5 PV technologies: a-Si based configuration is best positioned.

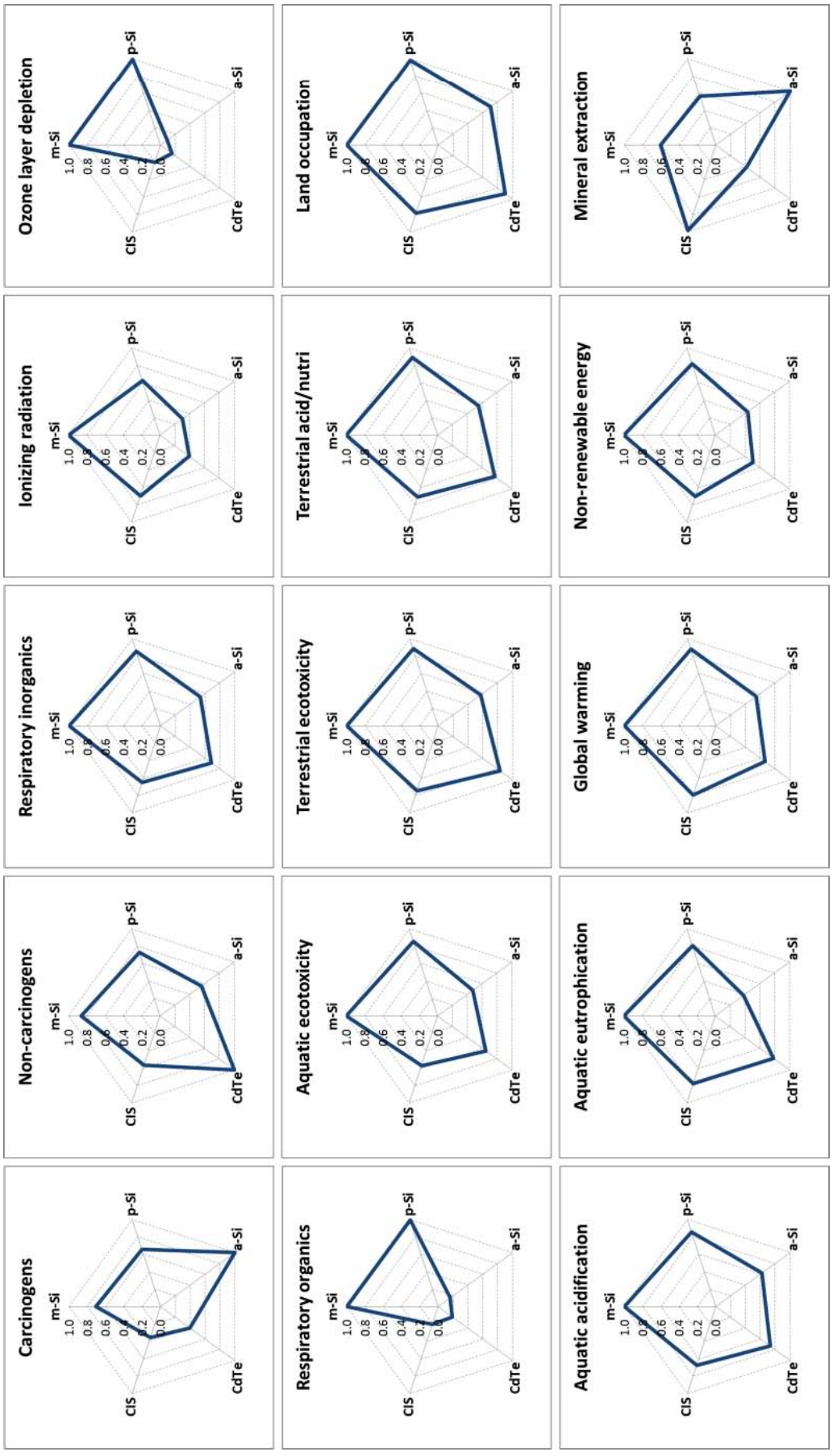

Figure 5-8 Results of the environmental impacts normalized to unity. Max Q_{out} – Min EPBT

The ranking of the five PV technologies in Table 5-13 and Table 5-15 with the proposal 2 of set of weights shows that the PV power plant with a-Si-based PV modules has the best trade-off.

5.4.3 *PBT – EPBT*

The final bi-objective optimization run concerns the simultaneous minimization of PBT and EPBT. The Pareto fronts of the 5 PV module technologies are presented in Figure 5-9 (a to e). The average time for each optimization problem is lower 2.96 hours CPU.

As previously, only the weights indicated in proposal 2 are taken into consideration for M-TOPSIS application. The solutions are also plotted in Figure 5-9 (a to e). Table 5-16 presents the alternatives that will be again evaluated by M-TOPSIS. Not surprisingly, the results confirm that the variation range is not significant in both axes. As compared to the previous cases, the selection of the best alternative is found in the central part of the Pareto front.

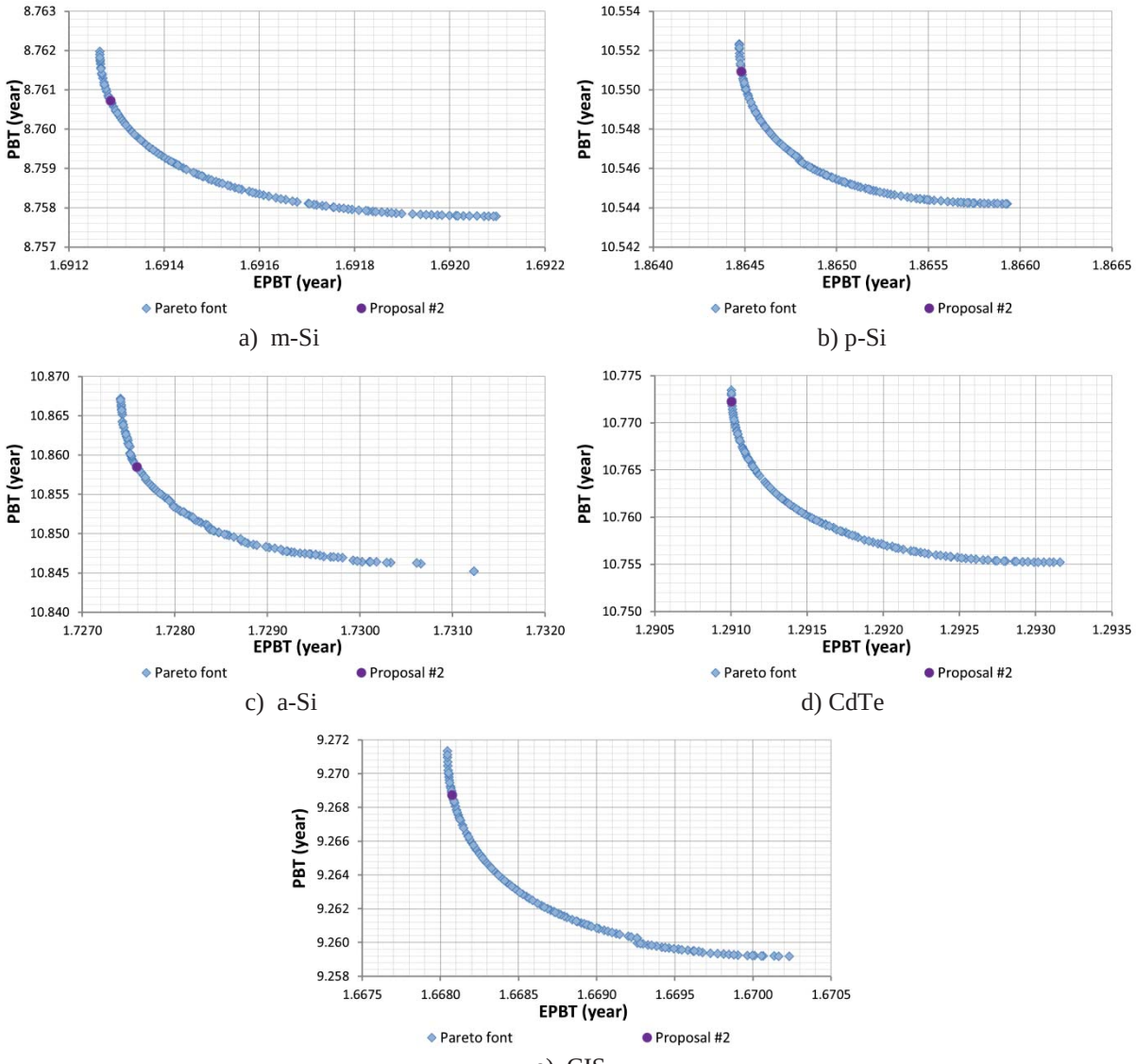

Figure 5-9 (a-e) Pareto fronts with M-TOPSIS selected PV power plant configuration. Min PBT– Min EPBT

Table 5-16 Configuration selected by applying M-TOPSIS. Min PBT– Min EPBT

PV Techno	*β (°)*	*K*	*D (m)*	*Nr*	*Nc*	Q_{out} *(MW h)*	*PBT (year)*	*EPBT (year)*
m-Si	28.60	9	17.01	1	94	408.19	8.76	1.69
p-Si	28.16	21	5.97	1	55	386.75	10.55	1.86
a-Si	26.52	15	8.17	2	88	404.81	10.86	1.73
CdTe	26.00	11	12.61	2	153	409.56	10.77	1.29
CIS	27.91	9	16.19	2	102	404.16	9.27	1.67

Table 5-17 Ranking of the resulting configurations after applying M-TOPSIS. Min PBT – Min EPBT

PV Techno	Ranking
m-Si	3
p-Si	5
a-Si	4
CdTe	**1**
CIS	2

The choice of the best configuration is obtained from M-TOPSIS. Table 5-17 shows the ranking of the alternatives selected: the CdTe-based configuration is the best candidate.

An examination of the radar graphs of environmental impacts (see Figure 5-10) shows that the a-Si based configuration for PV modules exhibits the highest values in most of the categories under evaluation.

One aspect that should be emphasized is the behavior of annual energy produced by any of the five configurations shown in Table 5-16. Not being considered into the objectives to optimize, when the annual energy produced from each of the combinations held after applying M-TOPSIS is compared with the results of the first two bi-objective optimization (Table 5-12 and Table 5-14), the reduction of the amount of energy generated is about 60% on average. This situation demonstrates the importance of considering the annual energy generated as an objective to optimize.

5.4.4 *Area – PBT*

The following case refers to the minimization of the area required for the installation of a PV power plant with a given amount of energy to provide together with the minimization of PBT. Following the model discussed in Section 5.3.2, the minimum Q_{out} is set at 500MWh/year and the geometrical relationship between the length and width of the solar field constraints (a_1 and a_2) are not taken into account.

The Pareto fronts of the 5 PV module technologies are presented in Figure 5-11 (a to e). The same order of magnitude of CPU time is required in this case (about 2.61 hours CPU). Because this purpose is different from the previous ones, the four sets of weights (2 to 4) given in Table 5-11 for the selection of the best alternative in each of the five categories through M-TOPSIS are applied again in order to check the variations that may occur. Q_{out} is replaced by the *Area*.

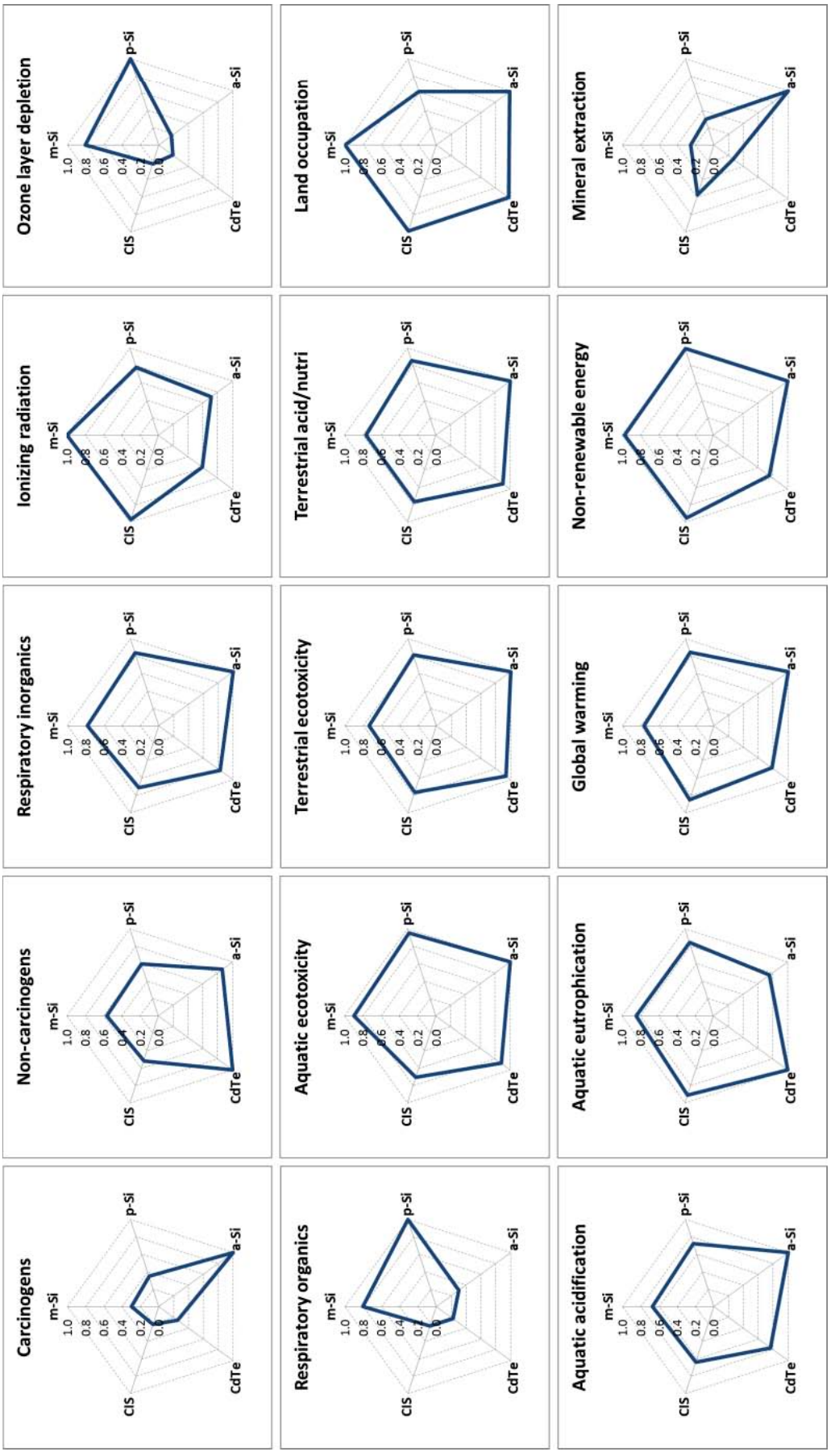

Figure 5-10 Results of the environmental impacts normalized to unity. Min *PBT* – Min *EPBT*

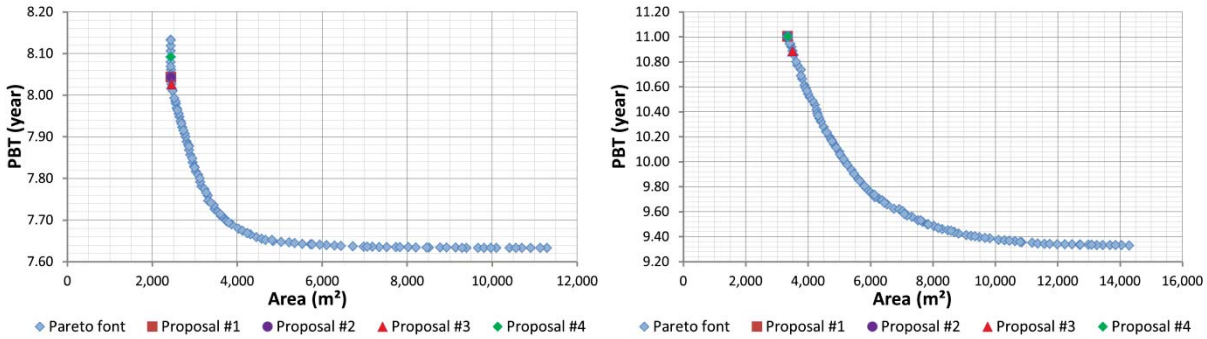

a) m-Si

b) p-Si

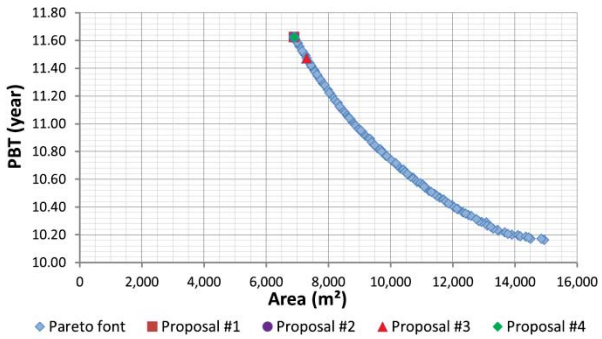

c) a-Si

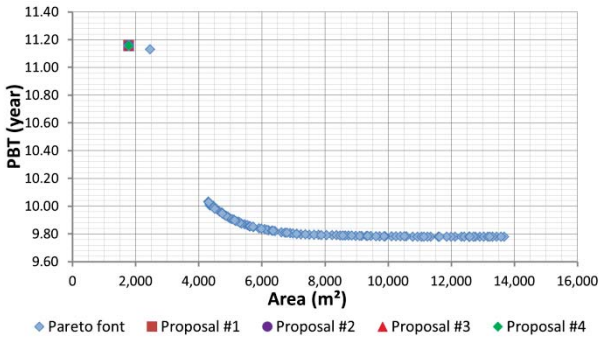

d) CdTe

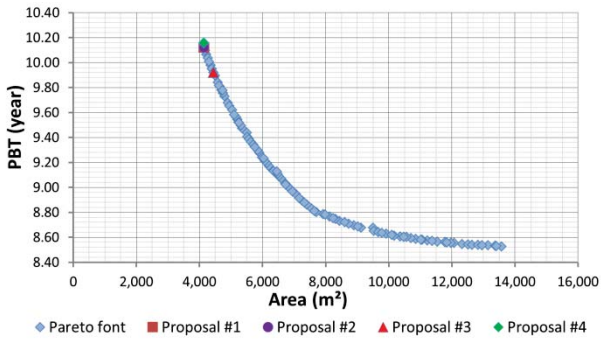

e) CIS

Figure 5-11 (a-e) Pareto fronts with M-TOPSIS selected PV power plant configuration. Min Area – Min PBT

Table 5-18 displays the M-TOPSIS selected configurations for the four different scenarios by varying the preference of each objective. Figure 5-11 (a to e) shows the location of the resulting configurations in the graph of the respective Pareto fronts. While the range of PBT values for the various alternatives represented in each of the Pareto fronts is wider as compared with the previous cases, the selected alternatives after applying M-TOPSIS are at the top of the curve. This indicates that an increase in PBT is acceptable since the reduction in area is important.

If the configuration based on m-Si has the lower PBT in all the cases, the configuration based on CdTe PV modules requires the smallest area. The results show that there is almost no difference in the parameter values even if the set of weights is changed.

The configurations based on a-Si PV modules have the highest values in most of the environmental categories under evaluation (see Figure 5-12).

M-TOPSIS established the proposed ranking in Table 5-19 for the 5 PV technologies. In all scenarios, the CdTe-based configuration is the best positioned.

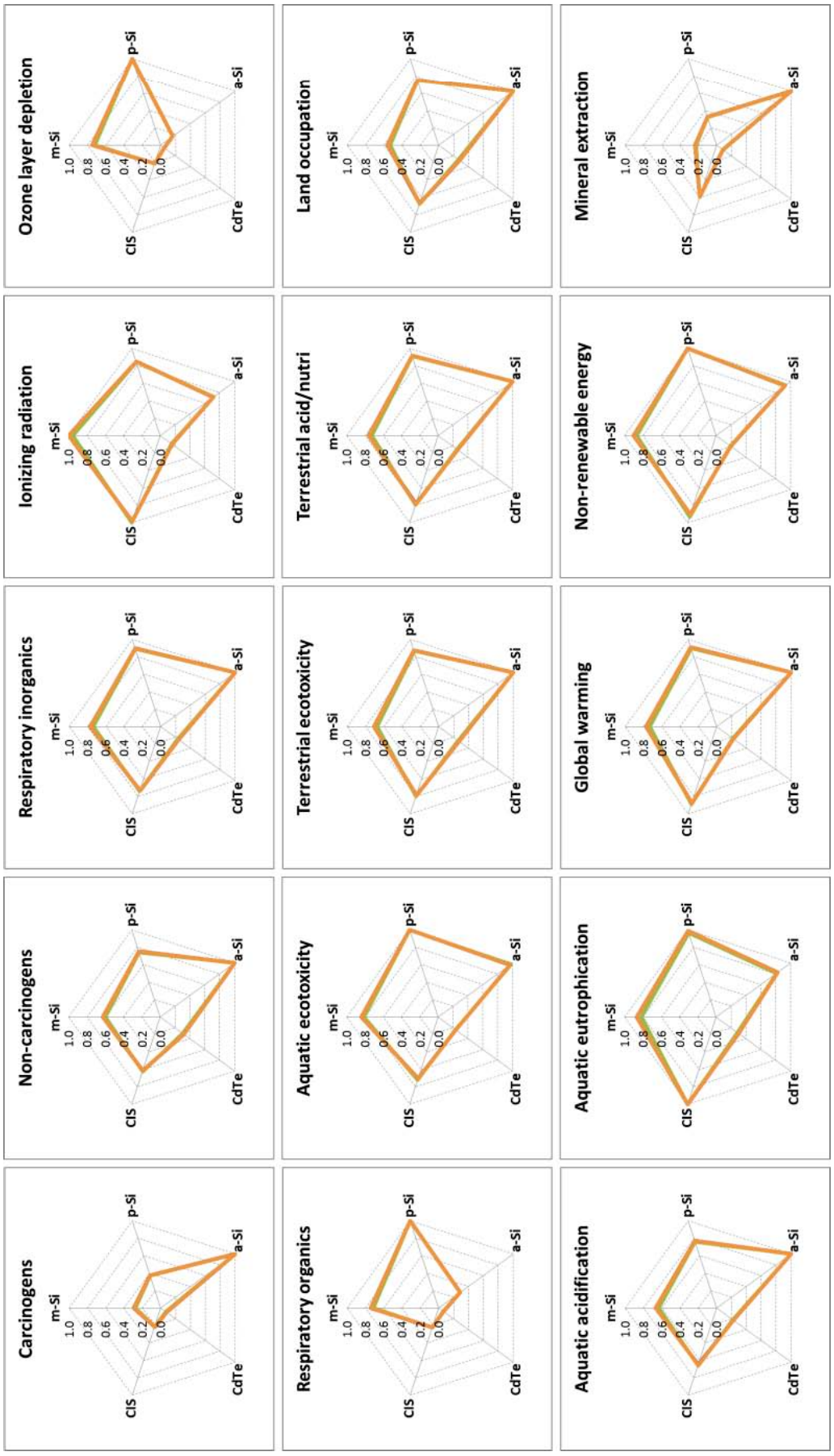

Figure 5-12 Results of the environmental impacts normalized to unity. Min *Area* – Min *PBT*

Table 5-18 Configuration selected by applying M-TOPSIS. Min Area – Min PBT

PV Techno	Proposal	*β (°)*	*K*	*D (m)*	*Nr*	*Nc*	*Area (m²)*	*PBT (year)*	*EPBT (year)*
m-Si	1	5.99	6	1.00	3	71	2,444.14	8.04	1.74
	2	5.99	6	1.00	3	71	2,444.14	8.04	1.74
	3	5.38	6	1.02	3	71	2,453.02	8.03	1.73
	4	6.64	6	1.00	3	71	2,441.39	8.09	1.75
p-Si	1	4.96	6	1.00	3	103	3,346.27	11.00	1.94
	2	4.96	6	1.00	3	103	3,346.27	11.00	1.94
	3	4.97	7	1.00	3	92	3,501.12	10.89	1.94
	4	4.96	6	1.00	3	103	3,346.27	11.00	1.94
a-Si	1	6.08	15	1.00	3	86	6,911.30	11.62	1.81
	2	6.08	15	1.00	3	86	6,911.30	11.62	1.81
	3	6.07	16	1.01	3	85	7,300.96	11.47	1.80
	4	6.08	15	1.00	3	86	6,911.30	11.62	1.81
CdTe	1	18.83	10	1.46	1	122	1,792.35	11.16	1.48
	2	18.83	10	1.46	1	122	1,792.35	11.16	1.48
	3	18.83	10	1.46	1	122	1,792.35	11.16	1.48
	4	18.83	10	1.46	1	122	1,792.35	11.16	1.48
CIS	1	6.25	11	1.00	3	83	4,149.98	10.12	1.76
	2	6.25	11	1.00	3	83	4,149.98	10.12	1.76
	3	6.30	10	1.00	3	98	4,444.85	9.92	1.76
	4	7.41	11	1.00	3	83	4,141.65	10.16	1.77

Table 5-19 Ranking of resulting configuration after applying M-TOPSIS. Min Area – Min PBT

PV Techno	Proposal 1	Proposal 2	Proposal 3	Proposal 4
m-Si	2	2	2	2
p-Si	4	4	4	4
a-Si	5	5	5	5
CdTe	**1**	**1**	**1**	**1**
CIS	3	3	3	3

The final ranking of the five PV technologies in each of the scenarios (Table 5-19) follows the same behavior regardless of the weight given to each of the objectives. Similarly, radar graphs that analyze environmental impacts have an identical behavior. As in the case for Q_{out} maximization, the proposal 2 of weights for the objectives under study is adopted in further optimization runs.

5.4.5 *Area – EPBT*

A second bi-objective optimization run is performed by taking into account the minimization of both the area needed for a PV power plant to supply a certain amount of energy and EPBT. The same conditions as in the previous case are considered.

The alternatives represented in a Pareto front for the five PV module technologies are shown in Figure 5-13 (a to e). The same order of magnitude of CPU time is observed (2.54 h) for each optimization

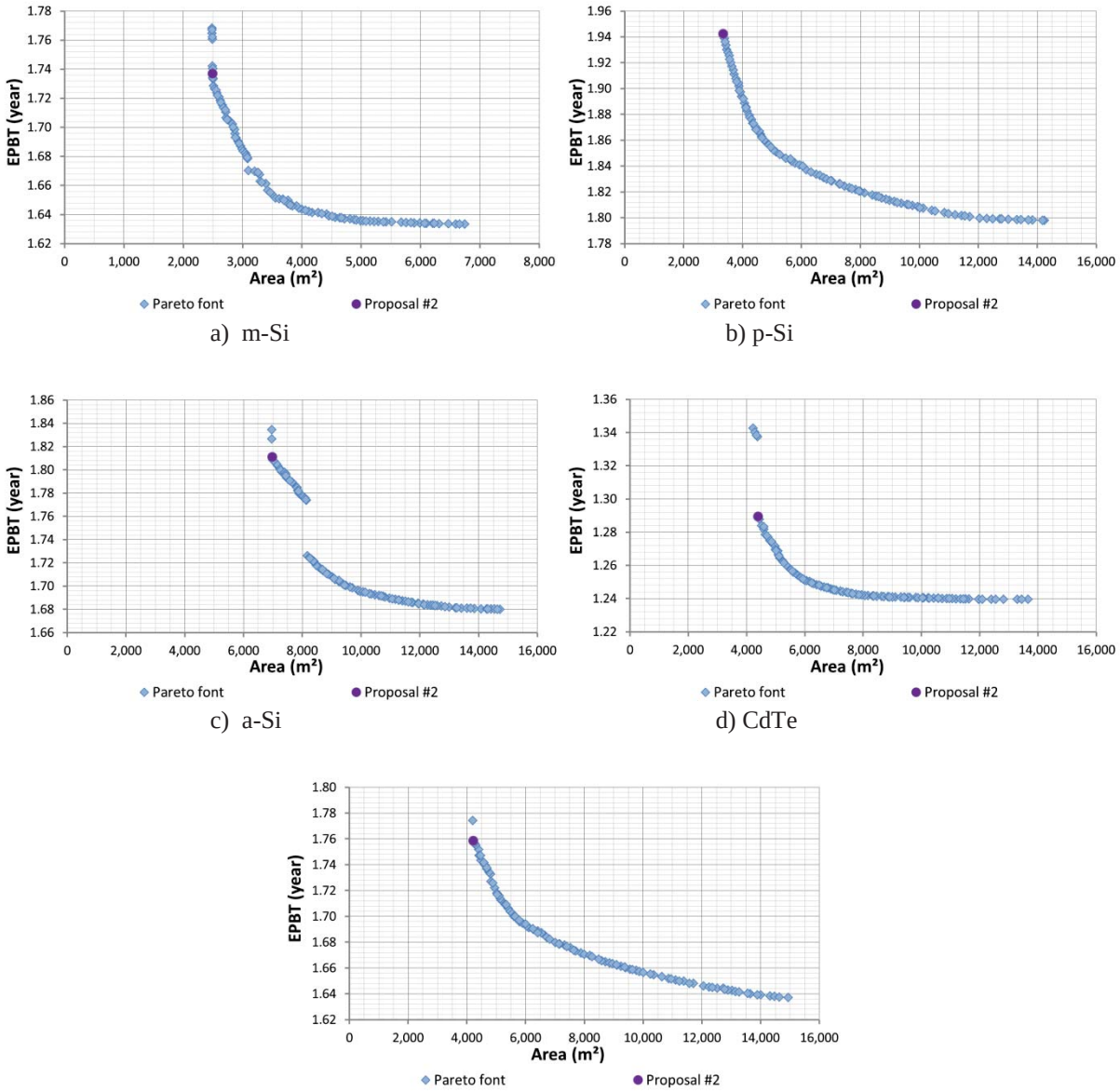

a) m-Si b) p-Si

c) a-Si d) CdTe

e) CIS

Figure 5-13 (a-e) Pareto fronts with M-TOPSIS selected PV power plant configuration. Min Area– Min EPBT

problem. The weights for the 18 objectives under analysis for M-TOPSIS are those indicated in the proposal 2 in Table 5-11.

The M-TOPSIS selected configurations are presented in Table 5-20. The location of the alternatives in the respective graph of Pareto fronts is shown in Figure 5-13 (a to e). The same tendency is observed with identical comments: an increase in EPBT (narrow range of variation) is acceptable since the reduction in area is important.

From the results of Table 5-20, it can be seen that the m-Si-based configurations need the smallest surface while the lowest EPBT is found for CdTe PV modules. M-TOPSIS established the ranking shown in Table 5-21 for the 5 PV technologies. Environmental impact categories are represented in Figure 5-14. As in the latter case, the CdTe based configuration is best positioned.

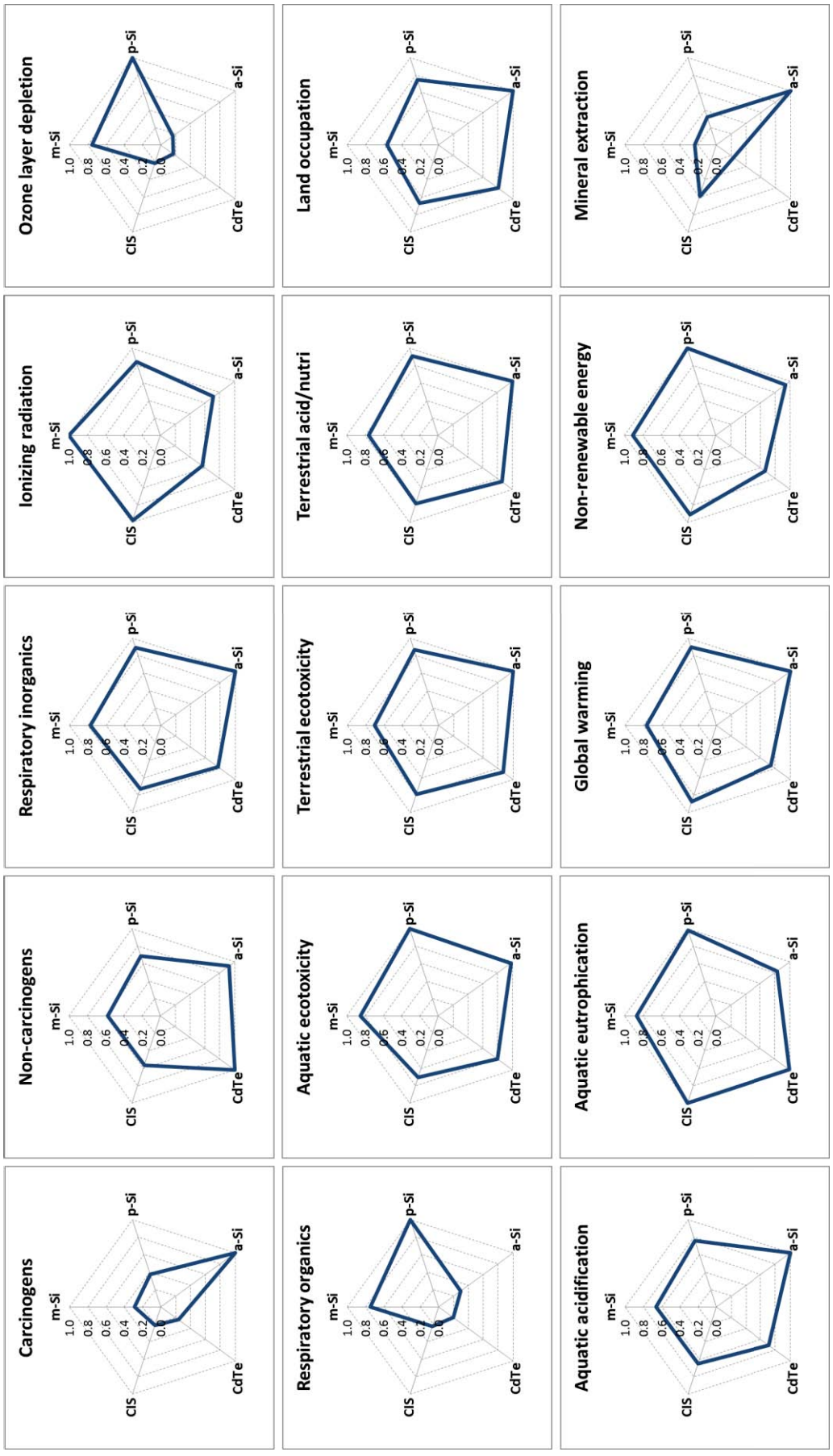

Figure 5-14 Results of the environmental impacts normalized to unity. Min *Area* – Min *EPBT*

Table 5-20 Configuration selected by applying M-TOPSIS. Min Area – Min EPBT

PV Techno	*β (°)*	*K*	*D (m)*	*Nr*	*Nc*	*Area (m²)*	*PBT (year)*	*EPBT (year)*
m-Si	5.81	10	1.00	3	43	2,497.77	8.03	1.74
p-Si	4.56	6	1.00	3	103	3,349.21	11.01	1.94
a-Si	6.53	15	1.00	3	87	6,986.62	11.61	1.81
CdTe	8.20	8	1.43	4	153	4,410.29	10.04	1.29
CIS	7.13	9	1.10	3	102	4,227.91	10.09	1.76

Table 5-21 Ranking of resulting configuration after applying M-TOPSIS. Min Area – Min EPBT

PV Techno	Ranking
m-Si	3
p-Si	5
a-Si	4
CdTe	**1**
CIS	2

5.5 Multi-objective optimization for the optimal design of PV power plant

The previous analysis confirms that the environmental impacts must be taken into account in the ecodesign process since they must drastically influence the final choice. Our experience in multi-objective optimization demonstrates that handling a large number of objectives may lead to a stagnation of the search process, an increased dimensionality of Pareto-optimal front, a large computational cost, and finally a difficulty in visualization of the objective space.

The analysis of the radar charts obtained with IMPACT 2002+ midpoint categories for environmental assessment in both mono- and bi-objectives optimization reveals that some of them exhibit a similar behavior which suggests that these categories may be correlated. For this purpose, a reduction in the number of objectives to be simultaneously optimized is required. Using the guidelines proposed in Chapter 4, the technique of Principal Component Analysis (PCA) was selected.

Let us recall that PCA is one of the extraction methods of factor analysis used to reduce the number of variables, relying on the linear algebra. Different methods based on PCA have been proposed so far for identifying a subset of uncorrelated variables from a wider set of correlated variables for identifying redundant environmental objectives in the multi-objective formulation (Gutiérrez et al., 2010; Sabio et al., 2012).

5.5.1 *Application of PCA method*

The first step for reducing the environmental categories is to perform a preliminary multi-objective optimization that includes the 18 objectives that have been used so far (Q_{out}, PBT, EPBT and 15 environmental categories) to calibrate the optimization and identify the consistent set of objective functions. The model developed for maximizing annual energy produced by the PV solar field is

selected for the multi-objective case. The conditions and considerations in this case are the same as those described in Section 5.4 for the five PV technologies considered.

Not surprisingly, the average time for each optimization run increases significantly, around 15.6 hours CPU.

The correlation matrix as indicated in steps 2 and 3 of the PCA guidelines was generated from the obtained results. Table 5-22 indicates the correlation values for the 15 environmental categories that were obtained using the correlation analysis available in Excel software.

A high percentage of correlation between many of the categories is observed by the information provided by the correlation matrix which would indicate the possibility of eliminating some them for future optimization cases. The next step is to obtain the eigenvalues and eigenvectors matrix. The "pca" function integrated in the Statics toolbox of MATLAB was used to generate them. Table 5-23 presents the eigenvalues, the matrix of eigenvectors as well as the variation represented by each principal component.

Table 5-22 Correlation matrix for the 15 environmental categories

Variables	C	NC	RI	IO	OLD	RO	AE	TE	TAN	AA	AEU	LO	GW	NR	ME
C	**1.000**														
NC	0.673	**1.000**													
RI	0.745	0.926	**1.000**												
IO	0.490	0.705	0.890	**1.000**											
OLD	0.139	0.307	0.521	0.670	**1.000**										
RO	0.302	0.389	0.592	0.700	0.943	**1.000**									
AE	0.727	0.918	0.977	0.873	0.533	0.659	**1.000**								
TE	0.713	0.958	0.991	0.861	0.441	0.512	0.968	**1.000**							
TAN	0.710	0.941	0.997	0.886	0.493	0.559	0.973	0.998	**1.000**						
AA	0.588	0.830	0.889	0.837	0.430	0.528	0.896	0.894	0.897	**1.000**					
AEU	0.796	0.932	0.996	0.856	0.457	0.540	0.970	0.989	0.991	0.878	**1.000**				
LO	0.496	0.894	0.921	0.895	0.475	0.562	0.940	0.941	0.940	0.903	0.898	**1.000**			
GW	0.715	0.885	0.989	0.925	0.505	0.568	0.958	0.981	0.989	0.895	0.983	0.927	**1.000**		
NR	0.667	0.812	0.952	0.954	0.569	0.679	0.963	0.932	0.947	0.898	0.937	0.935	0.969	**1.000**	
ME	0.914	0.649	0.765	0.610	0.580	0.179	0.708	0.751	0.747	0.652	0.811	0.574	0.791	0.733	**1.000**

Table 5-23 PCA results. Eigenvalues and eigenvectors for the 15 environmental categories

	PC_1	PC_2	PC_3	PC_4	PC_5	PC_6	PC_7	PC_8	PC_9	PC_{10}	PC_{11}	PC_{12}
Eigenvalue (λ_e)	11.978	1.746	0.678	0.320	0.169	0.097	0.013	0.000	0.000	0.000	0.000	0.000
Variability (%)	79.852	11.637	4.520	2.130	1.124	0.647	0.088	0.001	0.000	0.000	0.000	0.000
Cumulative % (G_j)	79.852	91.490	96.010	98.140	99.265	99.911	99.999	100.00	100.00	100.00	100.00	100.00
C	0.211	-0.339	0.592	0.246	0.190	-0.065	0.341	0.008	0.039	0.250	0.389	-0.085
NC	0.261	-0.148	-0.285	0.526	-0.078	0.026	0.183	-0.362	0.149	0.217	-0.242	0.000
RI	**0.287**	-0.030	-0.004	0.094	-0.163	0.119	0.057	0.176	0.013	-0.086	0.040	0.529
IO	0.264	0.187	-0.053	-0.520	-0.240	-0.045	0.697	-0.132	0.041	-0.139	-0.025	-0.004
OLD	0.156	**0.603**	0.254	0.115	-0.231	0.409	-0.083	-0.272	-0.204	0.323	0.075	-0.038
RO	0.182	0.533	0.335	0.158	0.289	-0.282	-0.155	0.060	0.127	-0.368	-0.039	0.041
AE	0.285	0.016	-0.017	0.175	0.171	-0.340	0.094	-0.200	0.066	-0.247	-0.373	-0.076
TE	0.284	-0.078	-0.136	0.127	-0.167	0.093	-0.156	0.022	-0.423	-0.086	-0.196	-0.295
TAN	0.286	-0.040	-0.093	0.087	-0.180	0.118	-0.164	0.224	0.260	-0.057	0.086	0.513
AA	0.264	-0.009	-0.224	-0.189	0.751	0.529	0.035	-0.010	0.001	0.000	0.000	0.000
AEU	0.285	-0.093	0.036	0.119	-0.137	0.113	0.083	0.537	-0.341	-0.272	0.060	-0.286
LO	0.270	0.053	-0.387	-0.067	0.058	-0.395	-0.189	-0.255	-0.245	0.023	0.664	0.016
GW	0.286	-0.034	-0.021	-0.150	-0.212	0.114	-0.275	0.042	0.675	0.000	0.139	-0.497
NR	0.282	0.063	0.021	-0.282	0.101	-0.359	-0.134	0.338	-0.066	0.670	-0.322	0.039
ME	0.219	**-0.393**	0.400	-0.367	-0.084	0.059	-0.364	-0.427	-0.170	-0.173	-0.169	0.150

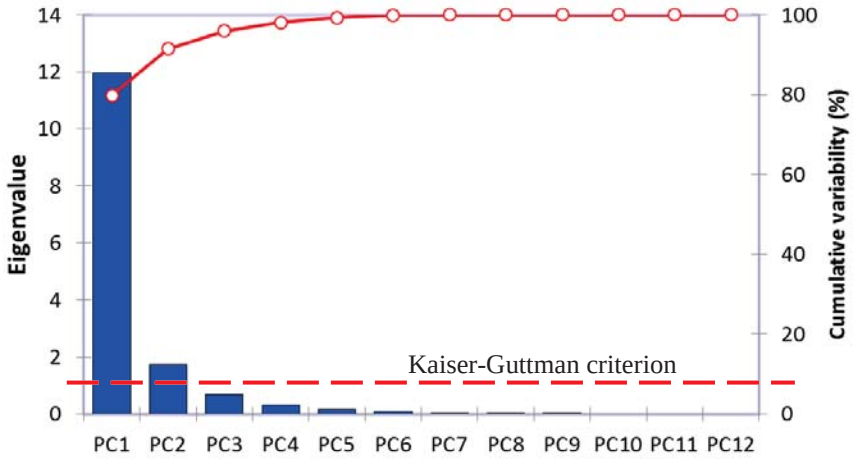

Figure 5-15 Scree plot for the 15 environmental categories

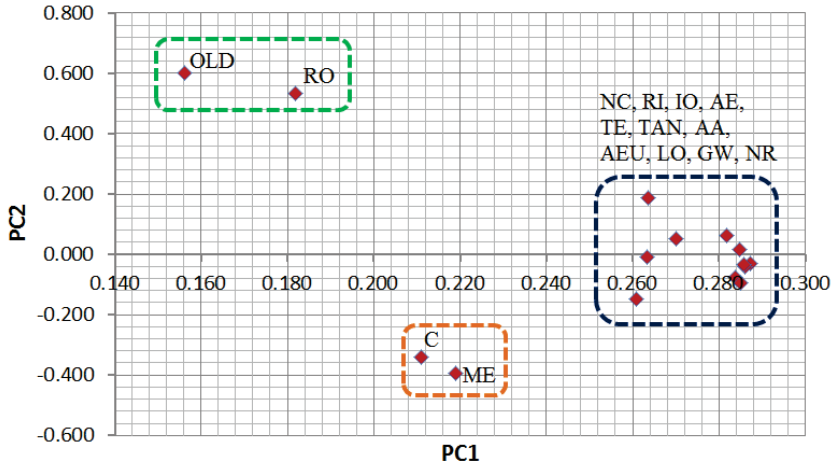

Figure 5-16 PCA results in the bi-dimensional spaces

After applying Kaiser-Guttman rule, only the first two principal components (PC_1, PC_2) are kept for further analysis as shown in the screen plot (Figure 5-15). The cumulative variance of the remaining principal components (0.9144) is fewer than the defined CUT (0.95).

Following the heuristic rule (Figure 4-7), only three environmental indicators (*RI*, *OLD*, *ME*) must be kept for further analysis. Figure 5-16 shows the two-dimensional plots representing the loads of the environmental objectives projected onto the sub-spaces of the first two principal components. The environmental categories are also grouped and located in three zones from the results of the correlation matrix.

5.5.2 *Multi-objective optimization case: Qout – PBT – EPBT – RI – OLD – ME*

A new set of optimizations is then carried out with this reduced set of objective functions and the obtained results are then compared with those of the previous case.

Each optimization run takes on average 10.2 hours CPU, which is reduced from one third as compared to the run with the total number of environmental categories.

The selection of the best alternative is performed again with M-TOPSIS. The weights used in the multi-objective problem with 18 objectives refers to proposal 2 in Table 5-11 while for the multi-objective problem with 6 objectives a weight of 1 is allocated to Q_{out}, PBT and EPBT , and respectively 1/3 to RI, ME and OLD.

Table 5-24 Comparison of results of two multi-objective optimization

Case	PV Techno	Q_{out} (MW h)	PBT (year)	EPBT (year)	C (kg C_2H_3Cl eq)	NC (kg C_2H_3Cl eq)	RI (kg PM2.5 eq)
18 objectives	m-Si	2,322.14	8.49	1.73	32,271.73	78,479.79	1,761.35
	p-Si	1,608.63	10.35	1.91	28,042.93	62,114.83	1,399.16
	a-Si	921.26	10.68	1.78	43,477.17	47,949.20	888.50
	CdTe	1,514.30	10.35	1.31	17,499.69	90,409.98	1,178.14
	CIS	1,539.23	9.62	1.79	15,643.13	50,288.20	1,117.40
6 objectives	m-Si	2,250.96	8.50	1.73			1,704.13
	p-Si	1,615.37	10.34	1.90			1,401.71
	a-Si	947.38	10.59	1.78			909.19
	CdTe	1,384.24	10.49	1.31			1,079.72
	CIS	1,524.48	9.29	1.72			1,063.37

Table 5-24 Continuation

Case	PV Techno	IO (Bq C-14 eq)	OLD (kg CFC-11 eq)	RO (kg C_2H_4 eq)	AE (kg TEG wáter)	TE (kg TEG soil)	TAN (kg SO_2 eq)
18 objectives	m-Si	75,779,566.24	0.44	1,498.64	276,741,480.99	65,302,346.37	35,811.44
	p-Si	43,904,843.16	0.41	1,389.89	219,906,378.08	53,734,861.05	29,660.84
	a-Si	21,341,069.90	0.04	221.73	122,542,189.87	35,147,744.31	18,410.86
	CdTe	28,860,588.78	0.07	266.35	174,783,918.77	53,251,137.41	26,868.77
	CIS	51,030,788.15	0.08	289.24	152,631,961.03	47,778,106.21	24,811.18
6 objectives	m-Si		0.43				
	p-Si		0.41				
	a-Si		0.04				
	CdTe		0.06				
	CIS		0.08				

Table 5-24 Continuation

Case	PV Techno	LO (m^2org.arable)	AA (kg SO_2 eq)	AEU (kg PO_4 P-lim)	GW (kg CO_2 eq)	NR (MJ primary)	ME (MJ surplus)
18 objectives	m-Si	30,228.04	10,941.96	1,369.57	2,423,794.25	37,329,219.80	79,624.96
	p-Si	28,204.34	8,662.39	1,023.96	1,979,693.26	28,473,388.21	69,630.03
	a-Si	20,785.77	6,376.01	484.76	1,243,123.69	15,142,258.88	129,037.18
	CdTe	27,035.49	7,803.03	1,048.94	1,561,837.48	18,383,990.24	52,248.61
	CIS	23,029.54	7,178.96	1,040.82	1,871,273.71	25,500,442.10	130,287.72
6 objectives	m-Si						77,316.43
	p-Si						69,675.70
	a-Si						132,210.36
	CdTe						48,175.48
	CIS						124,433.07

Table 5-25 Ranking of the configurations

PV Techno	18 objectives	6 objectives
m-Si	5	4
p-Si	4	5
a-Si	**1**	2
CdTe	2	**1**
CIS	3	3

Table 5-26 Selected configurations by applying M-TOPSIS. Four objectives

PV Techno	*β (°)*	*K*	*D (m)*	*Nr*	*Nc*	Q_{out} *(MW h)*	*PBT (year)*	RI (kg PM2.5 eq)	OLD (kg CFC-11 eq)
m-Si	14.14	60	1.00	1	95	2,323.27	8.46	1,759.37	0.44
p-Si	13.15	57	1.04	1	105	1,668.83	10.28	1,448.41	0.42
a-Si	11.09	40	1.14	2	90	945.45	10.59	908.41	0.04
CdTe	12.39	43	1.17	2	166	1,483.10	10.40	1,156.00	0.06
CIS	9.79	43	1.03	2	102	1,625.54	9.20	1,134.83	0.09

Table 5-27 Ranking of the resulting configuration after applying M-TOPSIS. Four objectives

PV Techno	Ranking
m-Si	4
p-Si	5
a-Si	**1**
CdTe	2
CIS	3

Table 5-24 shows the obtained configurations. Only the 6 criteria are presented in both cases. No configuration dominates the others for both cases. It is necessary to use M-TOPSIS for selecting the best compromise (see Table 5-25). The a-Si-based configuration is the top-ranked one for 18 objectives and second for 6 objectives while the CdTe-based configuration the top-ranked one for 6 objectives and second for 18 objectives.

5.5.3 *Multi-objective optimization case: Qout – PBT – RI – OLD*

In order to continue reducing the number of objectives to be optimized, PCA was applied again to the results of 6 targets. This new analysis leads to suppress 2 criteria (EPBT and ME). The multi-objective analysis is then conducted with only PBT, RI, OLD and Q_{out} with an average computation time of 8.76 hours CPU, thus reducing it of a 20% factor from the previous case. Table 5-26 shows the five configurations chosen by M-TOPSIS. The weighting for Q_{out} and PBT is $w_1 = w_2 = 1$ and, for RI and OLD $w_3 = w_4 = 1/2$. Under these conditions, the best option among the five proposed configurations is a-Si based (see Table 5-27).

If the ranking of the five technologies of PV modules is now compared among the three multi-objective cases treated in this study, it can be said on the one hand that both a-Si and CdTe PV modules achieve a better compromise regardless of the objective under study. On the other hand, c-Si PV technologies have the lowest rank in all the three cases. Even if they are the ones that produce more energy, they are the less environment-friendly. It must be yet remembered that this analysis does not include the recycling process which can change this trend.

This study emphasizes the interest of PCA multi-objective problem with a second reduction of objectives is capable to find the same results as in the two previous cases in less time and with less information to process.

5.6 Conclusion

In this chapter, a multi-objective optimization procedure based on a variant of NSGA-II has been embedded in the mathematical model within the ecodesign framework that considers simultaneously several technical, economic and life cycle environmental criteria. The environmental performance of the PVGCS has been measured *via* 15 life cycle assessment metrics of IMPACT 2002+ that inform about the damage caused in different midpoint impact categories. The proposed methodology comprises three main steps: first, a multi-objective genetic algorithm is implemented and a set of Pareto solutions are generated that represent the optimal trade-off between the objectives considered in the analysis. A multi-variable statistical method (*i.e.*, PCA) is then applied to detect and omit redundant environmental indicators that can be left out of the analysis without disturbing the main features of the solution space. The capabilities of this technique have been demonstrated through a PVGCS case study. Finally, A decision-making tool made based on M-TOPSIS is used to select the alternative that provides a better compromise among all the objective functions that have been investigated.

The proposed methodology has been incrementally developed. Different optimization cases have been investigated to establish the approach developed for sizing PV systems. The examples discussed in this chapter correspond to two possible issues that arise when designing PV solar plants: what is the ideal configuration to produce the largest amount of energy? what is the minimum area needed to generate a given amount of energy?

First, two examples of mono-objective optimization taken from the literature were used to calibrate the coupling between the model described in Chapter 3 and the optimization loop. Second, bi-objective cases were treated and M-TOPSIS was implemented for selecting the best option that satisfied the set of all criteria (18, *i.e*. 3 technico-economic and 15 environmental ones) taken into account in this work. The influence of the weights assigned to each goal in the final result must be highlighted.

This analysis shows that a similar behavior of some environmental categories plotted in radar charts for each of the bi-objective cases studied and emphasizes that the number of objectives can be reduced from an optimization viewpoint. The proposed approach enabled us to identify redundant environmental metrics making it easier to interpret and analyse the efficient solutions to the problem.

This was carried out through PCA on a post analysis of the multi-objective cases that were treated. Only four objectives (Q_{out}, PBT, RI, and OLD) have been identified as significant to perform the multi-objective optimization for ecodesign of a PV power plant.

The results presented in this chapter highlight the advantage that the use of second-generation PV modules (thin film) over the c-Si based PV modules. While the latter ones have a better performance in energy generation, the environmental aspect is what makes them fall to the last positions. It is necessary to emphasize that recycling the elements of a PV system has not been considered so far. The next chapter addresses a special attention to the recycling phase of the PV modules.

Chapter 6

RECYCLING OF PV MODULES

Dans les chapitres précédents, l'évaluation du cycle de vie a été utilisée comme un outil majeur pour l'évaluation des impacts environnementaux qui se produisent le long de la chaîne logistique de modules photovoltaïques. Pourtant, le démantèlement et le recyclage des modules PV n'ont pas été pris en compte car les données sur les impacts environnementaux associés à ces étapes de fin de vie sont relativement rares et ne figurent pas encore dans les bases de données d'inventaire des logiciels d'ACV classique (EcoInvent par exemple). Ce court chapitre vise à étendre la méthodologie proposée pour l'éco-conception du système PV reliée au réseau, élargissant ainsi les frontières en tenant compte du recyclage du module PV. L'idée est de démontrer que le cadre est suffisamment générique pour intégrer le cycle de vie des modules photovoltaïques. La première partie de ce chapitre traite de la mise en œuvre d'un processus de recyclage dans une étude ACV. Ensuite, une brève description des procédés de recyclage existants correspondant aux différentes technologies de fabrication de modules photovoltaïques est proposée. Deux cas d'ACV extraites de la littérature pour le recyclage des modules PV à base de c-Si and CdTe renforcent l'intérêt de considérer le processus de recyclage au sein d'une ACV. A partir des analyses du chapitre 3, une optimisation de technologies PV représentatives est effectuée. Les résultats confirment les avantages du recyclage, notamment par une réduction des impacts environnementaux globaux lorsqu' un recyclage matière est envisagé.

Nomenclature

Acronyms

CdTe	Cadmium Telluride
CIS	Copper Indium Diselenide
EVA	Ethylene Vinyl Acetate
EPBT	Energy PayBack TIme
GWP	Global Warming Potential
LCA	Life Cycle Assessment
LCI	Life Cycle Inventory
LCIA	Life Cycle Inventory Assessment
PV	Photovoltaic
PVGCS	Photovoltaic Grid-Connected System
a-Si	Amorphous silicon
m-Si	Monocrystalline silicon
p-Si	Polycrystalline silicon
PE	Primary energy demand
WEEE	Waste Electrical and Electronic Equipment

Symbols

Q_{out}	Yearly output energy of the field, kWh

6.1 Introduction

In the previous chapters, Life Cycle Assessment was used as a major tool for the evaluation of the environmental impacts occurring along the supply chain of PV modules. Yet, the decommissioning and recycling of PV modules were not taken into account since data on the environmental impacts associated with these end-of-life steps were relatively scarce and not yet included in classical LCA database. This short chapter aims at extending the proposed methodology to the PVGCS ecodesign, thus broadening the boundaries by taking into account PV module recycling. The product life-cycle will encompass material production, manufacturing, use and service and end-of-life management. The underlying idea is to demonstrate that the framework is generic enough to embed the whole life cycle of PV modules.

Indeed, due to the increase in photovoltaic as a source for generating electricity, it is important not to lose sight of what happens to PV modules and electric components once they reach the end of their lifetime. PV recycling is still a young industry and only taking off (Neidlein, 2010). Many innovations have been made in the past years and the industry continues to heavily invest in this field.

From an environmental perspective, not only does the recycling of a product lead to waste reduction but also the use of recycled materials could contribute to energy saving and emission reductions in manufacturing processes.

The most significant aspect is that recycled materials substitute primary materials, which allows conserving materials (especially for rare materials), energy and land resources. This possible replacement significantly reduces materials and energy needs in the extraction processes of raw materials.

The WEEE (Waste Electrical and Electronic Equipment) Directive came into force on August 13, 2012: by Q1 2014 at the latest, all EU member countries must implement a national WEEE law, regulating for the first time PV modules. Responsible for the free take back and recycling of the photovoltaic modules are the producers (manufacturers or importers) (Neidlein, 2010). As any other waste, the disposal of end-of-life PV modules needs to comply with European, national and local waste legislation.

Nowadays, there are organizations such as PV Cycle and CERES, and companies like First Solar and PV Recycling that are engaged in the recycling of PV modules. These institutions offer different types of services for the collection, transportation, recycling and sale of material once treated for the main PV module technologies.

Due to the long life expectancy, take-back and recycling used PV modules are relatively low at present, but it is expected that there will be a significant increase from 2020 (Larsen, 2009). Since the waste streams are very low, recycling is hardly visible today but in the future, with larger waste streams, it will be a must. According to some studies, PV recycling is not yet economically viable today, in the absence of a carbon pricing scheme (Larsen, 2009).

Unlike other industries, PV waste is unique because it has a long lag time from the time it is produced up to the time it is decommissioned. McDonald and Pearce (McDonald & Pearce, 2010) estimated the expected waste until 2038 assuming the historical percentages and efficiencies of thin film and silicon-based technologies and an end-of-life matching the warranty lag (see Figure 6-1): the amount of PV modules created for any one of these years will correlate to the amount of PV waste that will exist assuming that modules are withdrawn after their warranty has expired.

According to PV Cycle annual report (European Association for the Recovery of Photovoltaic Modules, 2012), in 2012, 3,759 tons of end-of-life PV modules were collected by all the members of the organization. This situation represents an increase of over 160% as compared to the previous year. Table 6-1 shows the percentage of recycled modules according to manufacturing technology. PV modules based on CdTe were not processed by the collective in 2012. These PV modules were collected and treated by the producers themselves as First Solar.

This situation shows that an assessment of the environmental benefits of material recycling must be taken into account for quantifying the environmental performance of PVCGS.

As it was mentioned before, LCA method is a suitable tool to estimate the impacts due to recycling processes of materials as well as to quantify the avoided impacts by returning materials to the value chain.

Table 6-1 End-of-life PV modules collected and treated in 2012 (European Association for the Recovery of Photovoltaic Modules, 2012)

Silicon based		Non-silicon based	
m-Si	51 %	CIS	16 %
p-Si	26 %	CdTe	0 %
a-Si	6 %	Flexible	1 %

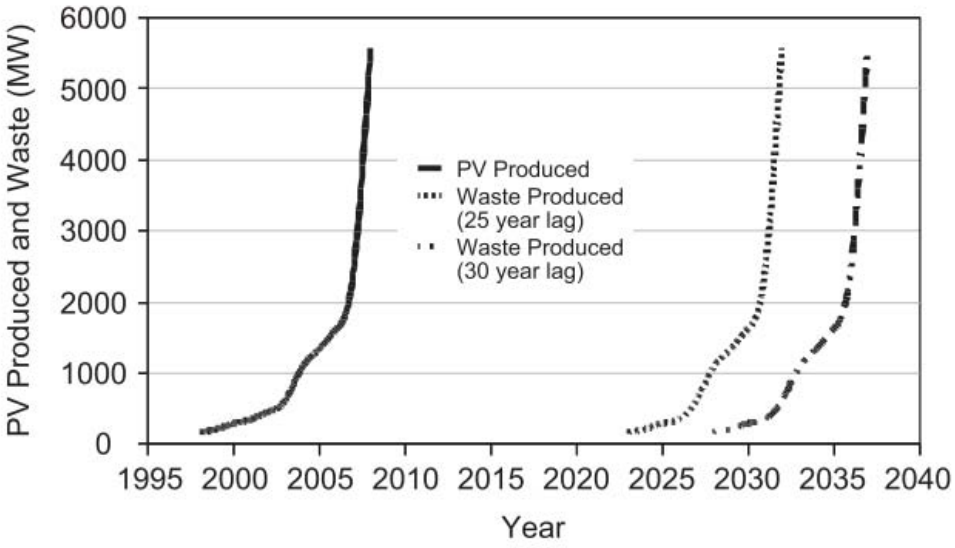

Figure 6-1 Global PV production and projected waste from 1998 to 2038 from (McDonald & Pearce, 2010)

The first part of this chapter addresses how to implement a recycling process in an LCA study. Then a brief description of the different existing recycling processes corresponding to the different manufacturing technologies of PV modules is provided. Two LCA cases from the literature for recycling c-Si and CdTe PV modules serve to explain the importance of considering the recycling process within the LCA. From the published results of these cases and following the guidelines of the procedure described in Chapter 3, an optimization run for both PV technologies is performed.

6.2 Recycling in LCA methodology

The manufacture of a product typically requires a mixture of primary resources and resources from the recycling phase of the same product or from another one. At end-of-life stage, several ways of treatments exist. The main difficulties for recycling process are related to the choice of the boundaries for the different flows that can end in different product systems and to the allocation of the resulting impacts.

To consider recycling process modeling within an LCA study, three schemes are generally reported (Ligthart & Ansems, 2002): closed loop, open loop and semi-closed loop recycling. Figure 6-2 illustrates these schemes differing from where and how the recycled material is used again.

Closed loop recycling. Materials associated with a product are recycled and used again in the same product system. The material properties are not changed in comparison to the original primary material. The so-called bottle-to-bottle recycling is an example of closed loop recycling (Komly, Azzaro-Pantel, Hubert, Pibouleau, & Archambault, 2012; La Mantia, 2010; McNeil, Sunderland, & Zaitseva, 2007; Palmer, Ghita, Savage, & Evans, 2009).

Open loop recycling. A recycled material goes to another product system and the initial material properties are changed. This material cannot be used in its original system. The recycled material does not yet replace all primary raw materials. Plastic recycling is a well-known open loop recycling example (Ha, 2012; Williams, Heidrich, & Sallis, 2010).

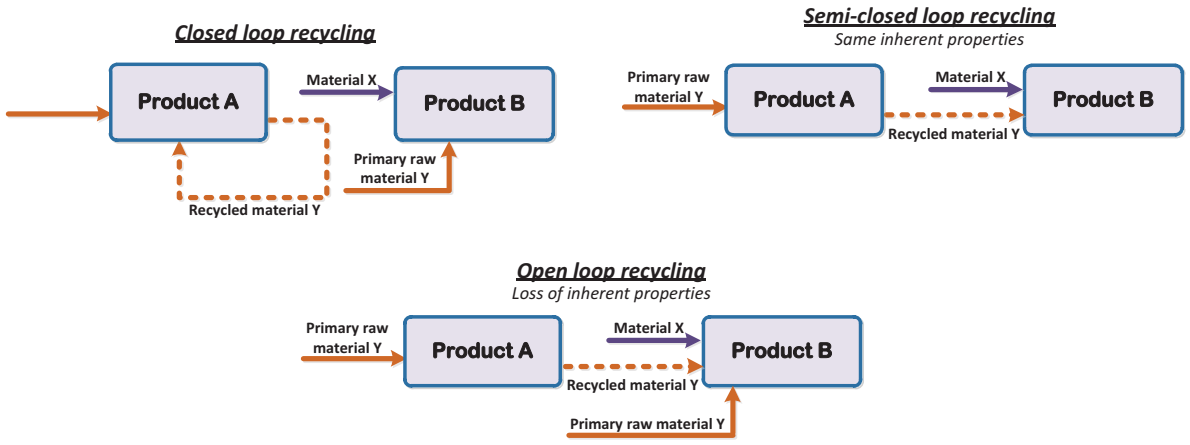

Figure 6-2 Three recycling schemes (inspired from (Ligthart & Ansems, 2002))

Semi-closed loop recycling. Recycled material is used in another product system without changing any material properties. This concerns the case of construction steel (CHEN, YANG, & OUYANG, 2011; Chong & Hermreck, 2010; Ligthart & Ansems, 2002).

A product system does not fully recycle all materials that come available after use. To quantify the efficiency of an end-of-life system, the following indicators can be used:

Recycling efficiency (RE):

$$RE = \frac{amount\ of\ scrap\ reprocessed}{amount\ of\ scrap\ recovered} \times 100 \qquad (6.1)$$

Recycling rate (RR):

$$RR = \frac{amount\ of\ scrap\ reprocessed}{amount\ of\ scrap\ available} \times 100 \qquad (6.2)$$

6.2.1 *Allocation methods*

The allocation or partitioning of environmental burdens between various co-products or processes with multiple inflows is a discussed subject in LCA methodology. The allocation of the benefits obtained in the recycling stage within a LCA study is extremely important for the final result of the impacts caused by a particular product with open loop recycling (Nicholson, Olivetti, Gregory, Field, & Kirchain, 2009; Vogtländer, Brezet, & Hendriks, 2001). Currently, a diverse set of methods exists to address this challenge (Ligthart & Ansems, 2002; Nicholson et al., 2009; Vogtländer et al., 2001). The most common approaches are:

Cut-off method. All environmental impacts directly caused by the production of a product are assigned to that product. An eventual waste treatment, other than recycling, is allocated to the product as shown in Figure 6-3.

Closed-loop method. Each product is equally responsible for the environmental impacts associated with primary material production, recycling, and final waste treatment. The burden is therefore an average impact, equally distributed among products and depending on the number of life cycles studied. Figure 6-4 represents the product material flows and processes for two life cycles. The environmental impacts of each one, applying the closed loop approach, will be a half of the sum of the primary material 1, recycling 1 and final waste treatment.

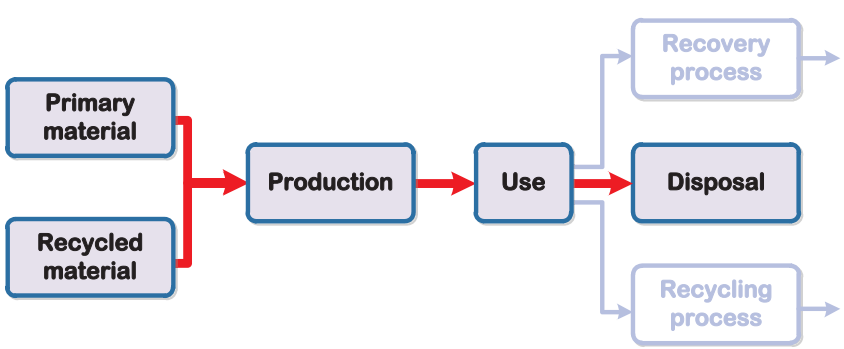

Figure 6-3 Product system for the cut-off approach (Ligthart & Ansems, 2002)

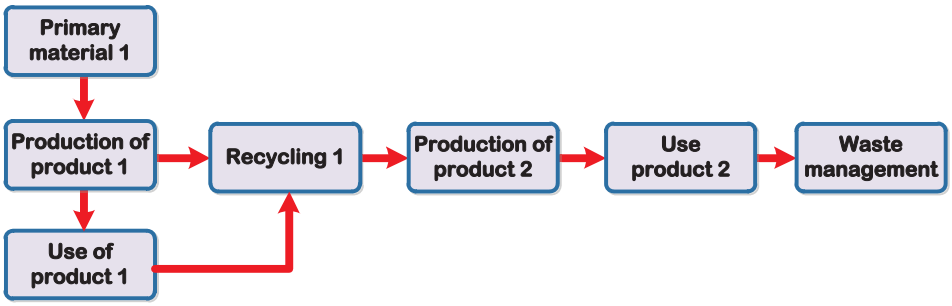

Figure 6-4 Product material flows and processes for 2 life cycles. Closed loop approach (Nicholson et al., 2009)

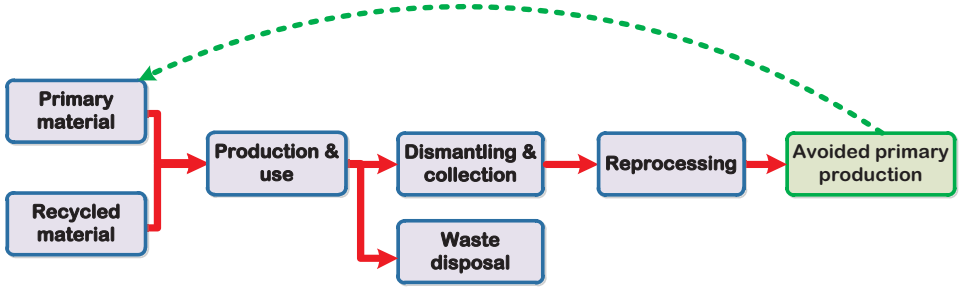

Figure 6-5 Substitution allocation approach (Ligthart & Ansems, 2002)

Substitution method. This allocation method is based upon the substitution of primary raw material by the reprocessed (secondary) material at the end-of-life stage: it occurs when a primary raw material is replaced by a recycled material (Figure 6-5). It is also called the avoided burden or avoided impact method. This method is applied to materials which maintain their inherent properties when they are recycled.

The easiest method to apply is the cut-off method, but the substitution approach is widely used in LCA studies where recycling at the end-of-life is involved (Frischknecht, 2010; Ligthart & Ansems, 2002).

Other allocation methods such as system expansion, economic allocation, input oriented, value-corrected substitution, multiple recycling method could be used (see (Ligthart & Ansems, 2002) for more detail).

The substitution method of allocation of environmental impacts is widely used in LCAs where recycling at the end-of-life is involved (Frischknecht, 2010). This last method will be used in the two cases of PV modules recycling. First, a brief description of the recycling processes of different PV module technologies will be provided. Some of these processes are still under development.

6.3 Recycling process of spent PV modules

Among the components of a PVGCS, PV modules contribute most largely to the environmental impacts as highlighted by the results obtained in Chapter 2. A brief description of the recycling process for the five PV module technologies addressed in this work is given in what follows.

6.3.1 *Crystalline silicon modules*

The recycling process of spent silicon PV modules (m-Si and p-Si) is based on the processes of a flat glass recycling line (Fraunhofer IBP, 2012; Klugmann-radziemska & Ostrowski, 2010; Klugmann-Radziemska, 2012; Sander et al., 2007). Figure 6-6 shows a flowsheet of the recycling process for the

components of crystalline silicon modules and the possible integration of recovered silicon in the production of new PV cells.

The first step consists to remove the aluminium frames and junction boxes in a manual process. A thermal process enabling the quick, simple and efficient disassembly of the module is the next stage in PV module recycling. The ethylene vinyl acetate (EVA) lamination layer is vaporized by the inert atmosphere pyrolysis at about 500ºC by using nitric acid.

The process continues with a chemical etching to remove metal coatings, antireflective coatings and diffusion layers. Common acidic chemical etching mixtures are based on HF-HNO_3-H_2O solutions. The etching recipes have to be adapted to the different PV cell technologies (monocrystalline or polycrystalline). The chemical etching of semiconductors with this mixture is divided into two steps, oxidation and reduction, followed by dissolution of the oxidation products to form a soluble ion complex.

The recovered silicon could be utilised as a raw material in the photovoltaic industry, as an additive to alloy steel to alter its mechanical properties or as a material for ceramics, based on the manufacture of non-metal powders.

The main researches aim at: (1) - improving the pyrolysis process for separation of EVA (Frisson et al., 2000); (2) - choosing a suitable composition and concentration of the etching solution and the optimal temperature range for the chemical reaction (Kang, Yoo, Lee, Boo, & Ryu, 2012; Klugmann-radziemska & Ostrowski, 2010); (3) - reducing the amount of energy required and the total cost of the recycling process.

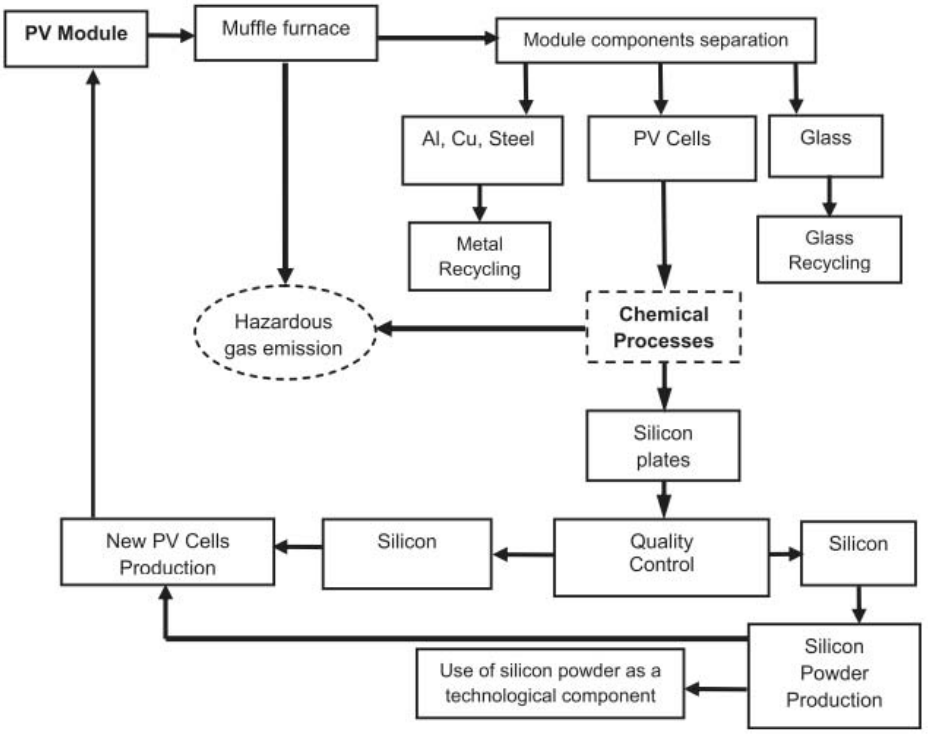

Figure 6-6 Recycling process for PV crystalline module from (Klugmann-Radziemska, 2012)

6.3.2 *CdTe and CIS*

Materials such as In, Ga and Te are regarded as critical because several studies show that the availability of them can, under certain conditions, limit the market growth of this kind of PV technologies (Marwede, Berger, Schlummer, Mäurer, & Reller, 2013; McDonald & Pearce, 2010). Additionally, these PV module technologies contain hazardous materials such as cadmium, tellurium, lead and selenium. For example, cadmium compounds are currently regulated in many countries because of their toxicity to fish and wildlife. Cadmium has also been associated with numerous human illnesses (Bernard, 2008; V. M. Fthenakis, 2004).

Several recycling technologies for CdTe and CIS PV modules have already been developed by PV manufacturers, research institutions and enterprises (Held, 2009; Huot, 2012; Marwede et al., 2013; Sander et al., 2007; Sustainability EvaluatioN of Solar Energy Systems, 2007). It is possible to distinguish three main stages in all processes: delamination of the modules, decoating of the substrate and, extraction and refining of the metals and semiconductors. For each step, mechanical or chemical processes can be used (see Figure 6-7).

Delamination process consists to break laminated modules. One way of delamination is the physical disintegration of the modules by shredding and milling. During those processes, the modules are crushed and milled into small particles. However, it is not possible to fully liberate the semiconductor layer from the glass substrate. This explains why other separation processes are required after this step. For example, the use of micro-emulsion that contains tensides permits to detach all joined compounds (adhesion, encapsulation, sealing, and coatings).

Another type of delamination process tested in laboratory consists to dissolve the encapsulant in a solvent. The European project *Sustainability Evaluation of Solar Energy Systems* (SENSE) proved water jet cutting as one feasible option to delaminate the modules. *5N Plus* also tested irradiation to decompose EVA through the glass.

De-coating and separation of non-metallic fractions from metal compound is the next step. In wet-mechanical processes, broken PV modules are treated in an intensive batch mixer for the complete attrition of the semiconductor materials from the carrier glass. During the mixing process, the material is further crushed due to the strong forces. After the attrition process, the mixture of semiconductors, glass and EVA is rinsed and sieved into different fractions. The fraction <150 mm, containing a pre-concentrate of semiconductor materials and glass dust, can be used for the subsequent flotation process. Leaching of the flotation products is carried out by adding acids (H_2SO_4 or HCl) and hydrogen peroxide, thus leaving an inert material with Cd and Te.

A dry-mechanical method to remove the CIGS absorber layer can be also used (Marwede et al., 2013). The CIGS dust is sucked off and collected by a vacuum dust remover. The very hard Mo electrode remains on the substrate and works as a solid lubricant for the metal blade. A diluted nitric acid is used to remove the Mo back contact from the soda-lime glass. The solution is neutralized and filtered which resulted in a Mo rich sludge.

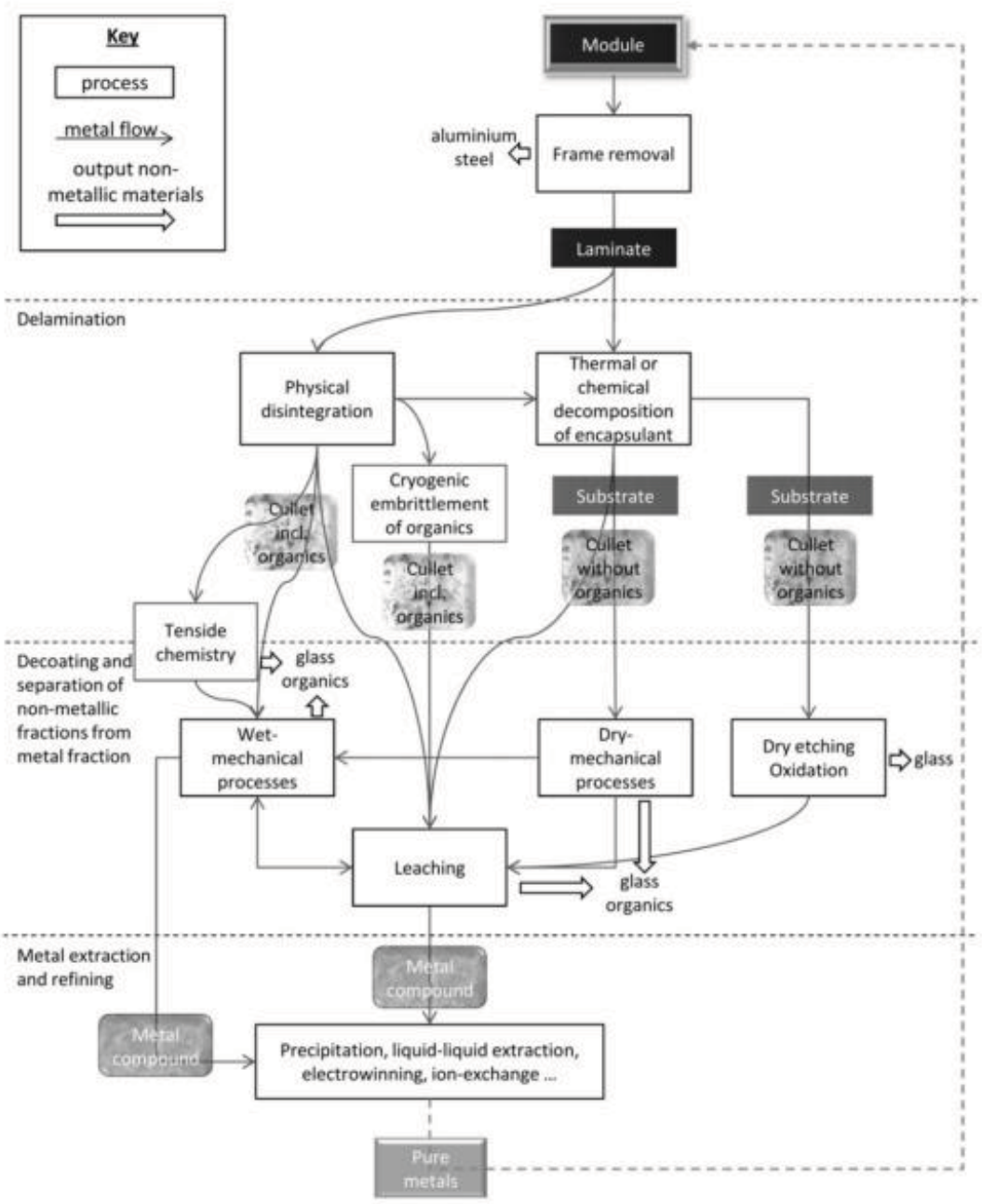

Figure 6-7 Recycling process for CdTe and CIS PV modules from (Marwede & Reller, 2012)

A dry etching process for recycling PV scrap is also used. The PV module fragments are exposed to a chlorine-containing and nitrogenous gas atmosphere at a temperature of more than 400°C, causing an etching process. Gaseous $CdCl_2$ and $TeCl_4$ that are generated in the etching process are made to condense (separately) and precipitate on cold surfaces (cooling traps). Resulting $CdCl_2$ and $TeCl_4$ are sent to a metal refinery where semiconductor grade Tellurium is extracted.

The final phase is the metal extraction and refining. For the production of thin-film PV modules, a high purity of the metals and semiconductors is required. Therefore the pre-processed metals have to be enriched, separated and purified.

Several chemical methods can be used to get the metals from acidic or other solutions: precipitation, liquid-liquid extraction, electro-winning, ion-exchange and oxidation/reduction. Important parameters

to consider are the concentration of the target metals in the feed, their chemical form and other components.

6.3.3 *a-Si*

As the amount of a-Si material in a given module is minimal there is currently no literature explaining the recycling process of amorphous silicon solar cells (McDonald & Pearce, 2010): a-Si based solar cell recycling is likely to be primarily driven to reclaim the substrates using any of the techniques utilized by recycling CdTe or CIS based PV modules.

6.4 LCA of PV modules recycling process

At the beginning of this work, there is a lack of information related to LCA data in the dedicated database for the recycling processes of PV modules. This can be attributed to the fact that PV industry is relatively young and that a large number of PV modules has not yet reached their end-of-life. To our knowledge, in the dedicated literature, the two most reported PV recycling processes concern crystalline silicon and CdTe based modules. The description of these processes, their integration in the Life Cycle Assessment developed in Chapter 2 and the application of the ecodesign approach are presented below. The analysis of the literature survey showed that the results are generally given in terms of Global Warming Potential and Primary Energy Demand. A systematic assessment of all midpoint categories as previously carried out for PV panel production is not yet available.

6.4.1 *Crystalline silicon*

An analysis of the environmental impact of a recycling process for crystalline silicon PV modules is presented by Müller et al. (Bombach et al., 2006; Müller, Wambach, & Alsema, 2006). The data are based on a PV module recycling process of Deutsche Solar AG.

Figure 6-8 displays the recycling process of Deutsche Solar AG. The process consists of two main steps. First, the laminate is burned off in a furnace at a temperature of 600°C to separate the module compound structure. This process makes easier the manual separation of solar cells, glass and metals. The metals and the glass are given to recycling partners for integration in the adequate material loops. During the thermal treatment, a significant amount of energy is consumed by the furnace and after-burner. The recovered cells are treated in the next step.

The metallization, antireflection coating and pn-junction of the cell are removed subsequently by etching. During the chemical process, different chemicals are required. The etching sequence involves removal metallization, removal antireflection layer, isotropic removal of pn-junction, surface finish, rinsing and drying.

Water and energy are consumed in the line and the gas washer. The chemicals used for etching are treated chemically and physically. The resulting sludge is disposed of. The resulting water is delivered to a treatment plant. Broken cells are also collected for reuse as raw materials for ingot growing after etching with a different technology.

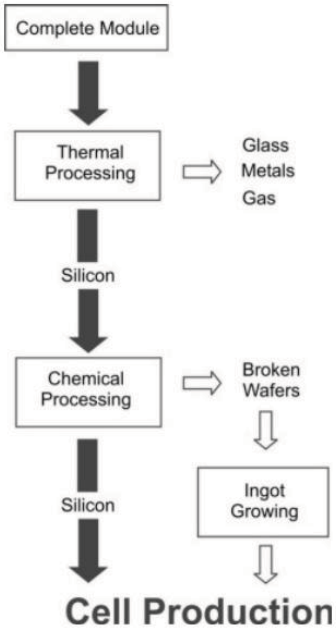

Figure 6-8 Recycling Process of Deutsche Solar AG (Bombach et al., 2006)

(Müller et al., 2006) give an assessment of the total energy demand during the recycling process. They compare the energy consumption during production of a module with new wafers and a module with recycled wafers. They concluded that, due to the recycling process, almost 75% of the necessary primary energy for wafer production can be saved.

The LCA of recycling process of a standard crystalline PV module with 72 cells (12.5 x 12.5 cm), Tedlar as backside foil and an aluminium frame was also performed in (Müller et al., 2006). For the evaluation of the environmental impacts, the CML 2001 method of the institute of Environmental Science in Leiden (CML) was used (Centre of Enviromental Science, 2001). Calculations were based on Deutsche Solar data as well as data from the Ecoinvent database. Inflows and outflows including the treatment of wastewater and used chemicals were considered. Concerning the geographical scope, the recycling plant is considered to be in Germany. Therefore all datasets of used auxiliaries, energies and end-of-life processes like material recycling or disposal on landfill are country representative datasets. The environmental impact of recycling processes of glass and metals as well as the amount of recovered wafers are credited to the impacts of the recycling process, following the substitution method of allocation for environmental impacts.

The highest contribution to disburden of the environment is related to the substitution of new wafers by recycled ones. The burden of the environment is mainly related to the energy consumption during the thermal treatment and the use of chemicals in the etching line. In GWP category, they found a benefit of 59.2 kg CO_2 eq per module recycled used.

From these reported works, the recycling process is now embedded into the environmental model developed for m-Si in order to compute the environmental impact. A new LCA with recycling process is conducted. It must be yet kept in mind that the impact assessment method adopted in this work is not the same as the one mentioned in the reported work. This explains why only GWP and PE

categories are used. We are aware that end-of-life assessment assumptions are not exactly the same as those used for PV processing.

The reference flow used in PV module processing was 1 m^2 of PV module but Müller's results are reported per module. An adjustment is done to have the same reference flow, i.e. 1 m^2 of PV module.

The m-Si based PV module taken as reference in Table 3-8 is kept. The GWP value found by Müller et al. is divided by the PV module surface referenced in their work. The new value results in a benefice of 52.62 kg CO_2 eq per m^2 of PV module. It is assumed that the PE demanded for a recycled module is 75% less than a PV module with new wafers as in Müller et al.'s work.The same efficiency as the value for the new panels has been considered for the recycled panels, i.e., 20%.

A new bi-objective optimization run is performed. The maximum energy produced and the minimum EPBT are searched. The bi-objective optimization is chosen because the analysis performed in Chapter 5 has identified these objectives as antagonist. A cost criterion, for instance, PBT is not considered because of the current lack of reliable information about the costs of recycling process of PV modules as well as the price of PV modules from recycled materials. EBPT is of course useful in order to detect changes due to reduction of primary energy for recycled PV modules. The same conditions and restrictions as those followed in Chapter 5 for bi-objectives case are taken into account.

Four scenarios are considered: (1) - PVGCS with 100% of PV modules with new wafers; (2) - PVGCS with 80% of PV modules with recycled wafers; (3) - PVGCS with 90% of PV modules with recycled wafers; and (4) - PVGCS with 100% of PV modules with recycled wafers. These recycling rates were considered from the information given by Solar World (Wambach, Schlenker, Konrad, & Müller, 2006) and PV CYCLE (PV CYCLE, n.d.). Figure 6-9 represents the system boundary under analysis for the scenarios. Table 6-2 shows the results of bi-objective optimization runs. The value of GWP is also presented in Table 6-2. The impact scores are divided by the energy produced during all the period of evaluation (20 years).

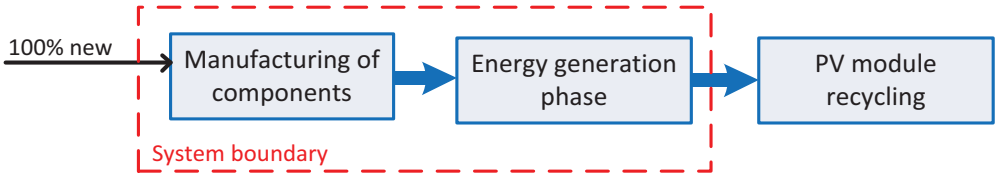

a) 100% new wafer scenario

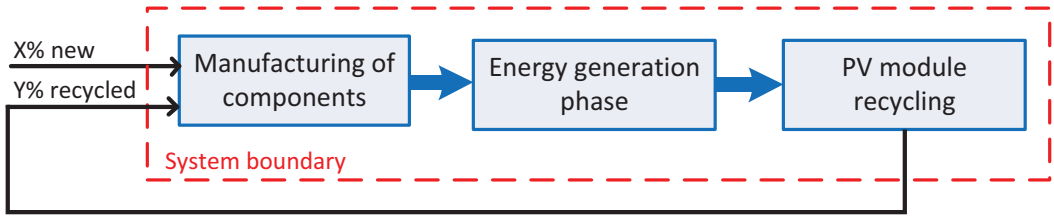

b) New and recycled wafer mix scenario

Figure 6-9 Process flow and system boundary for PVGCS with m-Si PV module

Table 6-2 Results of four scenarios for m-Si based PVGCS configuration

Scenario	Yearly Q_{out} (MW h)	EPBT (year)	GWP (g CO_2 eq/kWh)
100% new	**2,286.76**	**1.753**	**52.621**
80% recycled - 20% new	2,218.50	1.112	43.591
90% recycled - 10% new	2,253.12	1.036	42.604
100% recycled	2,286.67	0.961	41.635

As can be seen in Table 6-2, the use of recycled modules reduces significantly the EPBT (a factor of 1,8 is observed from the 100% new to the 100% recycled case). The yearly produced energy is approximately the same in all the optimization runs since the same efficiency has been considered for the recycled and new panels. Even if the GWP is not optimized, a significant reduction of its impact (per kWh of energy produced) is observed when recycling of PV modules is considered (a 20% reduction is observed in the more extreme case). These results justify and quantify the interest of m-Si PV panels recycling in the ecodesign strategy. Although PV recycling is energy intensive, its implementation compensates for the use of new produced panels.

6.4.2 *CdTe*

A LCA for the end-of-life phase of CdTe PV module was conducted by Held (Held, 2009) following the recycling process established by First Solar. Figure 6-10 illustrates the simplified process flow chart of First Solar CdTe PV module recycling process.

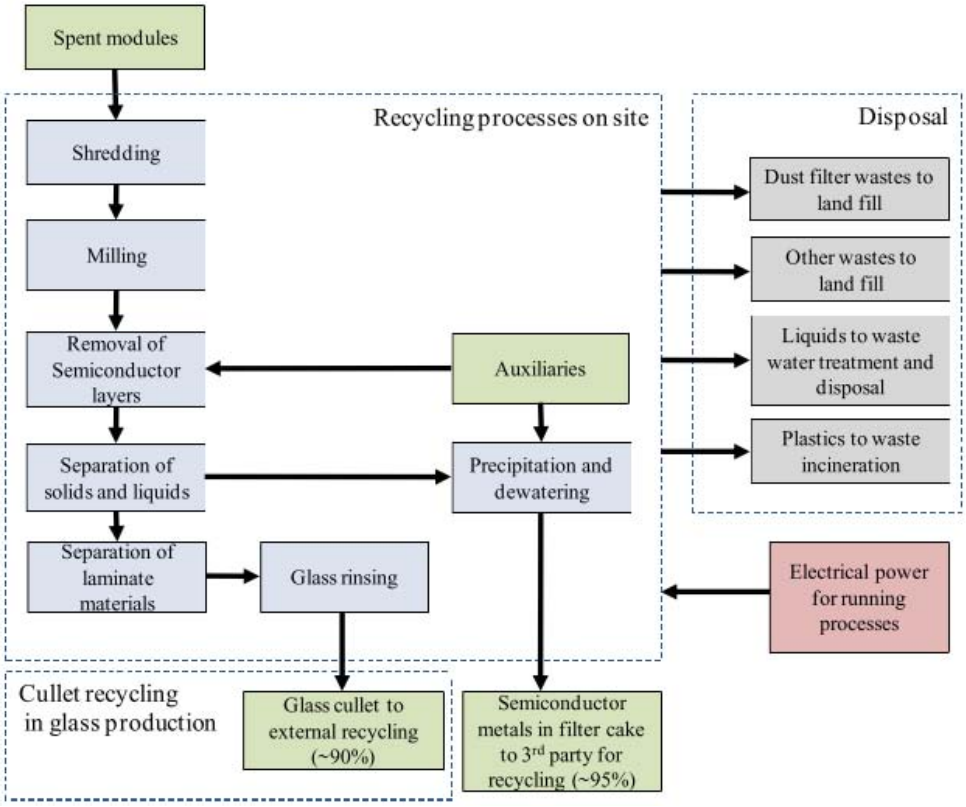

Figure 6-10 Flow chart of First Solar's CdTe PV module recycling process from (Held, 2009).

First Solar recycles spent CdTe PV modules by mechanical and hydrometallurgical process. The process is divided into five main steps:

1. Delamination by shredding and milling. The collected PV modules are reduced in a shredder and crushed in a hammer mill into small pieces from 4-5 mm.
2. Extraction. The semiconductors films are removed physically in a rotating leach drum. Sulphuric acid (H_2SO_4) and hydrogen peroxide (H_2O_2) are added throughout the leach cycle to form tellurous acid (H_2TeO_3).
3. Solid-Liquid separation. After extracting the semiconductor materials, the liquids are separated from solid materials. A spiral classifier with an Archimedean screw allows the separation of the glass pieces from the liquid. The glass pieces are further treated to separate the laminate foil from the glass whereas the extracted liquor leaves to next step.
4. Precipitation and filtration. The extracted liquor is treated by a three-stage precipitation process with an increasing pH using sodium hydroxide for pH control. The precipitated solution is thickened, so the solids settle and increase in a solids loading. The thickened slurry is filtered and ends up in a semiconductor material enriched filter cake and a liquid solution. The filter cake is stored and sent to third party companies to recover the metals. The liquid solution is transferred to waste water treatment.
5. Laminate foil/glass separation and rinsing. In the milling and crushing process, most of the laminate foil is already separated in large pieces from glass. In a vibrating screen, the remaining laminate foil parts are separated from the glass cullet. The separated glass is then discharged and washed and sends to recycling.

Held (Held, 2009) also follows a substitution approach and considers in his work the recycling and further treatment of clean glass cullet, lamination waste and liquid waste. The recycling process for filter cake is not considered in this study. However, it can be expected that the recovery of the metals provides a positive benefit.

The environmental benefits due to the glass cullet recycling are reflected by substituting primary material, which avoids environmental impacts and primary energy demand, and by a reduction of CO_2 emissions in the melting process.

The recycling process for junction box and lead wires is represented by material specific end-of-life treatments. Held (Held, 2009) assumed that all plastic material is burned in a waste incineration plat. The recovery energy by the incineration is reflected as a credit for the substitution of electrical power and thermal energy from fossil fuels. Metal parts, mainly copper, are represented by a copper specific recycling process. Environmental benefits of secondary copper are accounted as a credit.

In Held's work (Held, 2009), all primary data are based on industry data. Additional data are based on available GaBi 4 datasets. Life Cycle Inventory (LCI) is created in GaBi 4. The methodology for quantifying the environmental impact is CML2001 (Centre of Enviromental Science, 2001). Once

more, the recycling plant is considered to be at Germany. The functional unit used is 1m² of spent CdTe modules.

The evaluation of LCIA results of the end-of-life phase CdTe modules is done for two cases: including and excluding environmental credits from material recycling (glass cullet and copper recycling).

In both cases, the same efficiency as the value for the new panels has been considered for the recycled panels, i.e., 11.5%. First Solar recycling process achieves a recycling rate of 95%

The results when environmental benefits from material recycling are included show that the benefits due to material recycling and energetic recovery outweigh the impacts of the recycling process and therefore would lead to a reduction of the environmental profile of the overall CdTe PV module life cycle. Table 6-3 displays the results of both cases. Negative values indicate that the environmental benefits constitute a credit within the life cycle assessment. As in m-Si recycling case, the impact assessment method adopted in this work is not the same as the one mentioned in Held's work. As previously, only GWP and PE categories are reported for further analysis.

From the data reported by Held, it is not possible to perform the same analysis carried out for the case of m-Si. Compared with m-Si case, Held just focus on performing the LCA for the recycling process of PV module based on CdTe and he does not perform the same analysis for the primary energy saved by the use of recycled material in the manufacture of new modules. However, Held performs two scenarios: allocate or not the benefits of recycling the material (glass cullet and copper) into recycling process. These data can complement the LCA already made to the PVGCS using CdTe PV modules described in Chapter 2.

The maximum energy produced and the minimum EPBT are optimized for the same raison as already explained in the previous example. The conditions and restrictions followed in Chapter 5 for bi-objective case are kept. The two scenarios proposed by Held are investigated: including and excluding material recycling credits. Figure 6-11 shows the integration of recycling process within the system boundary for LCA. The results of both cases are presented in Table 6-4.

Table 6-3 LCIA of CdTe PV module recycling per m² (Held, 2009)

	Primary Energy (MJ)	**GWP (kg CO_2 eq)**
Without material recycling credits	81.03	6.03
Including material recycling credits	-12.49	-2.50

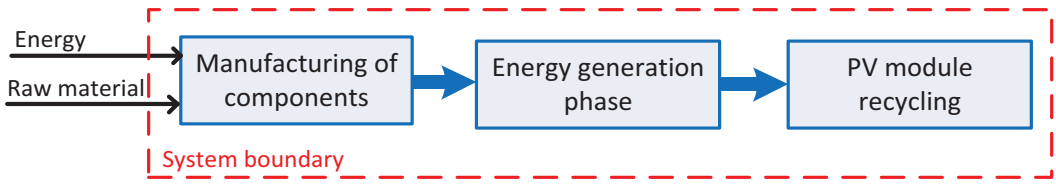

Figure 6-11 Process flow and system boundary for PVGCS with CdTe PV module

Table 6-4 Results of scenarios for CdTe based PVGCS configuration

Scenario	Yearly Q_{out} (MW h)	EPBT (year)	GWP (g CO_2 eq/kWh)
Without material recycling credits	1,494.18	1.444	56.597
Including material recycling credits	1,515.40	1.297	50.686
Without recycling process	**1,512.99**	**1.346**	**52.548**

The results confirm the benefit related to the overall environmental impacts when recycling of material (glass cullet and copper) is considered. The gain concerning EPBT and GWP is not so significant as in the m-Si case. It must be yet highlighted that these results do not consider recycling of cadmium and tellurium included in the filter cake due to a lack of information.

When comparing the two technologies m-Si and CdTe for PVGCS configuration, it must be said that recycling can significantly influence the choice of a technology: recycling will undoubtedly favour m-Si not only from the yearly produced energy (and consequently the economic criterion) but also from the EPBT and related GWP criteria points of view.

6.5 Conclusion

Even if the average lifetime of PV modules can be expected to be more than 25 years, the disposal of PV systems will become a problem in view of the continually increasing production of PV modules. In that context, a sustainable recycling of photovoltaic modules gains in importance due to the considerable growing of the PV market and the increasing scarcity of the resources for semiconductor materials.

In this chapter, an evaluation of photovoltaic recycling strategies showed that currently only two processes in the market are operated in an industrial scale. On the one hand, the company Deutsche Solar applies a treatment to recycle crystalline silicon modules (Bombach et al., 2006; Müller et al., 2006). On the second hand, CdTe thin film modules are recycled using a combination of mechanical and chemical process steps. This technology is established by the company First Solar (Held, 2009). Processes for other technologies are under development, mainly still in laboratory scale.

The data relative to these recycling processes are introduced in the optimization procedure for ecodesign. A bi-objective optimization is carried out in both cases, considering energy production and EPBT as optimization criteria. The results are largely influenced by the recycling strategy.

Concerning crystalline modules, the use of a recycling strategy reduces significantly the EPBT (a factor of 1,8 is observed from the 100% new to the 100% recycled case). It must be yet kept in mind that simplifying assumptions are considered in this preliminary study: the same efficiency has been considered for the recycled and new panels. This explains why the yearly produced energy is approximately the same in all the optimization runs. Even if the GWP is not optimized, a significant reduction of its impact (per kWh of energy produced) is observed when recycling of PV modules is considered (a 20% reduction is observed in the more extreme case). Although PV recycling is energy intensive, its implementation compensates for the use of new produced panels.

For CdTe thin film modules, the results confirm recycling benefit related to the overall environmental impacts when recycling of material (glass cullet and copper) is considered. Yet, the gain concerning EPBT and GWP is not so significant as in the m-Si case.

This study confirms that PV modules end-of-life management must be thoroughly studied not only from the viewpoint of the feasibility of the process but also from a more systemic way in order to assess the energy and global warming potential benefit of the recovery pathway.

Of course, we are aware that an economic study of the recycling strategy must be investigated in order to have a more comprehensive view for decision making. This was not done due to the lack of reliable economic data, but this could be easily taken into account if they are available in the ecodesign procedure. These first results demonstrate the need to encourage producer responsibility not only in the PV manufacturing sector but also in the entire energy industry.

Chapter 7

GENERAL CONCLUSION AND PERSPECTIVES

7.1 General conclusions

Because of the increasing demand for the provision of energy worldwide and the numerous damages caused by a major use of fossil sources, the use of the so-called renewable energies has been increasing significantly with the aim at moving towards a more sustainable development. But, as any artificial installation implies an ecological impact, to be “renewable” is an obvious “necessary” condition but not a “sufficient” one! This explains the use of renewable energy must be efficiently integrated with the natural environment during its whole lifecycle following ecological design (ecodesign). Ecodesign methods are thus a necessary milestone to check whether renewable energy systems are truly sustainable. Now, even if the major renewable sources today are still biomass and electricity generation from hydraulics and wind, a very rapid growth of photovoltaic electricity has been observed in the last decade, logically because the main source that is truly external to the earth system is our Sun. In that context, despite its small use today, solar photovoltaic (PV) power has a particularly promising future.

This work aimed at the development of a general methodology for designing PV systems based on ecodesign principles and taking into account simultaneously both techno-economic and environmental considerations. Most of the works reported in the literature involve PVGCS optimization considering only one criterion or only address the issue of the environmental impact assessment of the components of a PV system with emphasis on PV module technology.

Generally, the environmental assessment is performed as a post-design stage of the PV systems.

In general terms, three main aspects can be highlighted in this work:

1. Environmental modelling

In order to evaluate the environmental performance of PV systems, an environmental assessment technique was used. The well-known Life Cycle Assessment (LCA) method was chosen because it is the most reliable alternative for the type of evaluation proposed in this work: the rigorous framework based on ISO 14000 guidelines and the database that is implemented (i.e., Ecoinvent) for energy solutions guided this choice. From the reported literature and our own experience acquired through this work, the classical LCA tools (SimaPro and other LCA software) turned out to be not flexible and suffer from a lack of interoperability. From a practical viewpoint, a specific environmental module was designed from extraction of the dedicated EcoInvent database and can be used for the studied technologies for PV systems. The environmental model was for successfully embedded in the design stage of a PVGCS.

As part of the LCA guidelines, a description of the manufacturing process of the five PV module technologies that are the most commercialized ones was performed. Data collection highlighted the significant amount of the embodied primary energy required, especially for c-Si based PV module technologies. This situation was observed for three different LCA case studies. IMPACT 2002 + was selected to perform the environmental assessment of the flows and emissions generated during the development of the module. It is also important to highlight the influence of the composition of the

energy mix used in the manufacture of the module in the characterization of environmental impacts. By itself, the development of renewable electricity will mechanically improve this point following a vertuous circle.

2. Techno-economic modelling

The analysis of the reported contributions led to the development of a specific framework for PV modelling and simulation purpose. The main problem that can be encountered when using one commercialized tools is the lack of an approach that allows the optimization of the sizing of a PVGCS considering economic and environmental criteria. Sizing is made taking into account technical objectives. In addition, the coupling of all the components via an external program to optimize the PV plant taking into consideration the three main criteria is difficult due to the closed structure used in each tool. To overcome the problem of interoperability, the design of a simulator for received solar radiation coupled with a sizing module constituted the chosen option. The simulator must be designed in an open manner so that it can be interfaced easily with an outer optimization loop. The estimation of solar radiation and the output energy of the system are the two most critical aspects of any PV system design and sizing tools.

This developed model consists of three stages: (1) the estimation of solar radiation received in a specific geographic location; (2) the design of the PV power plant; the calculation of the annual energy generated from the solar radiation received, the characteristics of the different components that constitute the PV system (PV modules and BOS) and the constraints for the design of the plant; (3) the evaluation of the techno-economic criteria through EPBT and PBT as well as the environmental assessment through 15 midpoint categories. A good agreement between the “hand-made” model and the commercial codes was observed.

3. Ecodesign methodology

An ecodesign framework that considers simultaneously the technical, economic and life cycle environmental criteria was then established. The proposed methodology comprises three main steps: first, a multi-objective optimization procedure based on a variant of NSGA-II was embedded in the mathematical model and a set of Pareto solutions was generated representing the optimal trade-off between the objectives considered in the analysis. A multi-variable statistical method (*i.e.*, PCA) is then applied to detect and omit redundant objectives that can be left out of the analysis without disturbing the main features of the solution space. Finally, a decision-making tool based on M-TOPSIS is used to select the alternative that provides a better compromise among all the objective functions that have been investigated. The capabilities of this technique have been demonstrated through several PVGCS case studies which aim at obtaining either the ideal configuration to produce the largest amount of energy or the minimum area needed to generate a given amount of energy. From the 18 objectives that were considered initially (i.e. 3 techno-economic and 15 environmental), only four objectives (Q_{out}, PBT, RI, and OLD) have been identified as significant to perform the multi-

objective optimization for ecodesign of a PV power plant. The results of the analyzed cases show that while the PV modules based on c-Si have a better performance in energy generation, the environmental aspect is what makes them fall to the last positions. TF PV modules present the best trade-off in all cases under consideration.

A special attention was paid to recycling process of PV module even if there is not yet enough information currently available for all the technologies evaluated. The main cause of this lack of information is the lifetime of PV modules. The data relative to the recycling processes for m-Si and CdTe PV technologies are introduced in the optimization procedure for ecodesign. By considering energy production and EPBT as optimization criteria into a bi-objective optimization cases for m-Si and CdTe PV modules, the importance of the benefits of PV modules end-of-life management was confirmed. An economic study of the recycling strategy must be investigated in order to have a more comprehensive view for decision making.

7.2 Perspectives

After this work, many questions are still outstanding and could motivate other works in the future, from pratctical theoretical viewpoints.

An extension of this work would be in the optimization of PVGCS that are mounted in a single or two-axis tracking system. The particularity of this type of structure is that the PV module is oriented following the movement of the sun in either a single axis or two axes. This type of system generates a greater amount of annual energy compared to traditional photovoltaic installations, even if a higher investment is required. The works that have been reported in the literature are limited to the optimum design of this type of PV systems from a techno-economic viewpoint.

More practically, it would be interesting to evaluate the performance of the methodology within the process of design and construction of PVGCS for a real new project with an industrial partner.

Considering the results obtained by the integration of technical, economic and environmental criteria in designing PVGCS and especially in the use and integration of the Principal Component Analysis (PCA) method to reduce the number of objectives followed by the decision-making tool (M-TOPSIS) for the selection of alternatives generated after multi-objective optimization, the proposed methodology could be applied to the study of other ecodesign problems involving an important number of criteria that can be generated by the application of LCA: the ecodesign of chemical and dairy processes that is currently under investigation, the design of the hydrogen green supply chain are a consistent application of the proposed methodology.

Due to the significant changes in legislation relating to the treatment of electronic waste, including the elements of the PV systems, and considering the discussion in Chapter 6 related to the volume of PV modules that will arrive to their end-of-life in the coming years, the analysis of recycling processes will offer an overview of the implications that we can wait for the future development of these technologies.

The main interest is to know if, by integrating recycling processes within the environmental evaluation model proposed in this work for all technologies under study, the results will follow the same trend.

One of the interesting aspects to evaluate when an alternative source of energy generation is introduced is the social impact that can be generated within a specific area, i.e. changing habits of the people living in a certain region. In the case of large-scale photovoltaic systems, the use of large areas of land for the facilities' installation can lead that economic activities of the site where it is installed change affecting the population that lives near. Similarly it would be interesting to study how power generation from photovoltaic or other renewable energy sources can coexist with other economic activities. For example, it can be imagined that other economic activities, as agriculture or breeding, could be developed in the same area where the PV power plant is installed: the optimization process could help to determine the optimum solution for both activities together. Such a study would lead to introduce agricultural models.

All these questions emphasize that our current energy path is really changing: mixed energy vectors and sources will cohabit on the one hand; mixed approaches will be involved with different economic targets on the same area on the other hand. This issue opens up new fields for multi-optimization challenges.

Bibliography

ADEME, A. de l'Environnement et de la M. de l'Energie. (n.d.). Glossaire. Retrieved January 31, 2013, from http://www2.ademe.fr/servlet/KBaseShow?sort=-1&cid=96&m=3&catid=12843&p1=5&p2=12564

Akella, A. K., Saini, R. P., & Sharma, M. P. (2009). Social, economical and environmental impacts of renewable energy systems. *Renewable Energy*, *34*(2), 390–396. doi:10.1016/j.renene.2008.05.002

Alsema, E. A., & Wild-scholten, M. J. De. (2006). Environmental Impacts of Crystalline Silicon Photovoltaic Module Production System boundary LCA study New LCI data set. In *CIRP International Conference on Life Cycle Engineering* (pp. 1–6). Leuven, Belgium.

Appelbaum, J., & Bany, J. (1979). Shadow Effect of Adjacent Solar Collectors in Large Scale System. *Solar Energy*, *23*(4), 497–507.

Ayompe, L. M., Duffy, A., McCormack, S. J., & Conlon, M. (2010). Projected costs of a grid-connected domestic PV system under different scenarios in Ireland, using measured data from a trial installation. *Energy Policy*, *38*(7), 3731–3743. doi:10.1016/j.enpol.2010.02.051

Ayres, R. U., & Ayres, L. W. (2002). *A Handbook of Industrial Ecology*. (R. U. Ayres & L. W. Ayres, Eds.)*A Handbook of Industrial Ecology* (1st ed., p. 680). United Kingdom: Edward Elgar Publishing.

Bernard, A. (2008). Cadmium and its adverse effects on human health. *Indian Journal of Medical Research*, *128*(4), 557–564.

Beylot, A., Payet, J., Puech, C., Adra, N., Jacquin, P., Blanc, I., & Beloin-Saint-Pierre, D. (2012). Environmental impacts of large-scale grid-connected ground-mounted PV installations. *Renewable Energy*, 1–5. doi:10.1016/j.renene.2012.04.051

Bhat, I. K., & Prakash, R. (2009). LCA of renewable energy for electricity generation systems—A review. *Renewable and Sustainable Energy Reviews*, *13*(5), 1067–1073. doi:10.1016/j.rser.2008.08.004

Boix, M. (2011). *Optimisation multicritère de réseaux d'eau*. Université de Toulouse - Institut National Polytechnique de Toulouse.

Bombach, E., Röver, I., Müller, A., Wambach, K., Kopecek, R., & Wefringhaus, E. (2006). Technical experience during thermal and chemical recycling of a 23 year old PV generator formely installed on Pelllworm island. In *21st European Photovoltaic Solar Energy Conference* (pp. 2048–2053). Dresden, Germany.

Boulanger, P. (2003). *Guide de rédaction du cahier des charges techniques des générateurs photovoltaïques connectés au réseau* (p. 72). France.

Brigand, S. (2011). *Installations solaires photovoltaïques: Dimensionnement, Installation et mise en oeuvre, maintenance*. (L. Moniteur, Ed.) (1st ed., p. 280). Paris, France.

Brunner, P. H., & Rechberger, H. (2011). *Practical Handbook of Material Flow Analysis* (p. 318). USA: Lewis Publishers. doi:10.1016/B978-1-85617-809-9.10003-9

Burgess, A. A., & Brennan, D. J. (2001). Application of life cycle assessment to chemical processes. *Chemical Engineering Science*, *56*(8), 2589–2604. doi:10.1016/S0009-2509(00)00511-X

Calow, P. (1998). *Handbook of Environmental Risk Assessment and Management*. (P. Calow, Ed.) (1st ed., p. 600). United Kingdom: Blackwell Science Ltd.

Centre of Enviromental Science. (2001). CML: Caracterization and normalization factors. Leiden, The Netherlands: Leiden University.

Chen, B., Yang, J., & Ouyang, Z. (2011). Life Cycle Assessment of Internal Recycling Options of Steel Slag in Chinese Iron and Steel Industry. *Journal of Iron and Steel Research, International*, *18*(7), 33–40. doi:http://dx.doi.org/10.1016/S1006-706X(11)60087-3

Chong, W. K., & Hermreck, C. (2010). Understanding transportation energy and technical metabolism of construction waste recycling. *Resources, Conservation and Recycling*, *54*(9), 579–590. doi:http://dx.doi.org/10.1016/j.resconrec.2009.10.015

Coello Coello, C. A. (2005). Recent Trends in Evolutionary Multiobjective Optimization. In A. Abraham, L. Jain, & R. Goldberg (Eds.), *Evolutionary Multiobjective Optimization: Theoretical Advances And Applications* (1st ed., pp. 7–32). London, U.K.: Springer-Verlag.

Coello Coello, C. A. (2010). List of References on Evolutionary Multiobjective Optimization. Retrieved May 30, 2013, from http://www.lania.mx/~ccoello/EMOO/EMOObib.html

Coello Coello, C. A., & Becerra, R. L. (2009). Evolutionary Multi-Objective Optimization in Materials Science and Engineering. *Materials and Manufacturing Processes*, *24*(2), 119–129.

Dale, M. (2012). The Energy Balance of the Photovoltaic (PV) Industry: Is the PV industry a net electricity producer? Stanford, USA: Stanford University.

De Wild-Scholten, M. J., & Alsema, E. A. (2005). Environmental life cycle inventory of crystalline silicon photovoltaic module production. In *Material research Society1* (pp. 1–14). Boston, USA.

Deb, K., Pratap, A., Agarwal, S., & Meyarivan, T. (2002). A fast and elitist multiobjective genetic algorithm: NSGA-II. *Evolutionary Computation, IEEE Transactions on*, *6*(2), 182–197.

Deb, Kalyanmoy, & Saxena, D. K. (2005). *On Finding Pareto-Optimal Solutions Through Dimensionality Reduction for Certain Large-Dimensional Multi-Objective Optimization Problems EMO for Many Objectives* (pp. 1–19).

Demain, C., Journée, M., & Bertrand, C. (2013). Evaluation of different models to estimate the global solar radiation on inclined surfaces. *Renewable Energy*, *50*, 710–721. doi:10.1016/j.renene.2012.07.031

Desideri, U., Proietti, S., Zepparelli, F., Sdringola, P., & Bini, S. (2012). Life Cycle Assessment of a ground-mounted 1778kWp photovoltaic plant and comparison with traditional energy production systems. *Applied Energy*, *97*, 930–943. doi:10.1016/j.apenergy.2012.01.055

Di Dio, V., Miceli, R., Rando, C., & Zizzo, G. (2010). Dynamics photovoltaic generators: Technical aspects and economical valuation. In *SPEEDAM 2010* (pp. 635–640). IEEE. doi:10.1109/SPEEDAM.2010.5542261

Diez-Mediavilla, M., de Miguel, A., & Bilbao, J. (2005). Measurement and comparison of diffuse solar irradiance models on inclined surfaces in Valladolid (Spain). *Energy Conversion and Management*, *46*(13-14), 2075–2092. doi:10.1016/j.enconman.2004.10.023

Dones, R., & Frischknecht, R. (1998). Life-cycle Assessment of Photovoltaic Systems: Results of Swiss Studies on Energy Chains. *Progress in Photovoltaics: research and applications*, *125*(December 1997), 117–125.

Duffie, J. A., & Beckman, W. A. (2006). *Solar Engenierring of Thermal Process* (3rd ed., p. 893). USA: John Wiley & Son.

Dufo-López, R., Bernal-Agustín, J. L., & Contreras, J. (2007). Optimization of control strategies for stand-alone renewable energy systems with hydrogen storage. *Renewable Energy*, *32*(7), 1102–1126. doi:http://dx.doi.org/10.1016/j.renene.2006.04.013

Ecoinvent Center. (2010). The life cycle inventory data v2.2. Ecoinvent Center.

El-Hefnawi, S. H. (1998). Photovoltaic diesel-generator hybrid power system sizing. *Renewable Energy*, *13*(1), 33–40. doi:http://dx.doi.org/10.1016/S0960-1481(97)00074-8

EPIA. (2011). *Solar generation 6. Solar photovoltaic electricity* (p. 100). Netherlands.

EPIA. (2012). *Solar Photovoltaic on the Road to Large Scale Grid Integration* (p. 22). Belgium.

EPIA. (2013). *Global Market Outlook For Photovoltaics 2012-2017* (p. 60). Belgium: European Photovoltaic Industry Association (EPIA).

European Association for the Recovery of Photovoltaic Modules. (2012). *Anual Report 2012* (p. 19).

European Commission, Joint Research Centre, & Institute for Environment and Sustainability. (2010). *International Reference Life Cycle Data System (ILCD) Handbook - Analysis of existing methodologies for use in Life Cycle Assessment* (1st ed., p. 115). Luxembourg: Publication Office of the European Union.

Fernández-Infantes, A., Contreras, J., & Bernal-Agustín, J. L. (2006). Design of grid connected PV systems considering electrical, economical and environmental aspects: A practical case. *Renewable Energy*, *31*(13), 2042–2062. doi:10.1016/j.renene.2005.09.028

Finnveden, G., Hauschild, M. Z., Ekvall, T., Guinée, J., Heijungs, R., Hellweg, S., … Suh, S. (2009). Recent developments in Life Cycle Assessment. *Journal of environmental management*, *91*(1), 1–21. doi:10.1016/j.jenvman.2009.06.018

Fonseca, C. M., & Fleming, P. J. (1993). Genetic Algorithms for Multiobjective Optimization: Formulation, Discussion and Generalization. In S. Forrest (Ed.), *Fifth International Conference on Genetic Algorithms* (pp. 416–423). San Mateo, California: Morgan Kauffman Publishers.

Fouquet, D. (2009). *Prices for Renewable Energies in Europe* (p. 141).

Fouquet, D. (2012). *Prices for Renewable Energies in Europe* (p. 70).

Fraunhofer IBP. (2012). Life Cycle Assessment (LCA) screening of the Maltha recycling process for Si-PV modules. Germany.

Frischknecht, R. (2010). LCI modelling approaches applied on recycling of materials in view of environmental sustainability, risk perception and eco-efficiency. *The International Journal of Life Cycle Assessment*, *15*(7), 666–671. doi:10.1007/s11367-010-0201-6

Frischknecht, R., Jungbluth, N., Althaus, H., Bauer, C., Doka, G., Dones, R., … Nemecek, T. (2007). *Implementation of Life Cycle Impact Assessment Methods* (p. 151).

Frisson, L., Lieten, K., Declercq, K., Szlufcik, J., de Moor, H., Goris, M., … Aceves, O. (2000). Recent improvements in industrial PV module recycling. In *16th European Photovoltaic Solar Energy Conference* (pp. 1–4). Glasgow, UK.

Fthenakis, V., Frischknecht, R., Raugei, M., Kim, H. C., Alsema, E., Held, M., & de Wild-Scholten, M. (2011). *Methodology Guidelines on Life Cycle Assessment of Photovoltaic Electricity* (p. 20).

Fthenakis, V. M., & Kim, H. C. (2011). Photovoltaics: Life-cycle analyses. *Solar Energy*, *85*(8), 1609–1628. doi:10.1016/j.solener.2009.10.002

Fthenakis, V., Wang, W., & Kim, H. C. (2009). Life cycle inventory analysis of the production of metals used in photovoltaics. *Renewable and Sustainable Energy Reviews*, *13*(3), 493–517. doi:10.1016/j.rser.2007.11.012

Fthenakis, Vasilis M. (2004). Life cycle impact analysis of cadmium in CdTe PV production. *Renewable and Sustainable Energy Reviews*, *8*(4), 303–334. doi:10.1016/j.rser.2003.12.001

Garcia, J. S. D., Avila, S. L., Carpes, W. P. W. P., & Avila, L. (2005). Introduction to Optimization Methods : a Brief Survey of Methods. *IEEE multidisciplinary engineering education magazine*, *2*(2), 1–5.

García-Cascales, M. S., & Lamata, M. T. (2012). On rank reversal and TOPSIS method. *Mathematical and Computer Modelling*, *56*(5-6), 123–132. doi:10.1016/j.mcm.2011.12.022

García-Valverde, R., Miguel, C., Martínez-Béjar, R., & Urbina, a. (2009). Life cycle assessment study of a 4.2kWp stand-alone photovoltaic system. *Solar Energy*, *83*(9), 1434–1445. doi:10.1016/j.solener.2009.03.012

Gautam, N. K., & Kaushika, N. D. (2002). An efficient algorithm to simulate the electrical performance of solar photovoltaic arrays. *Energy*, *27*(4), 347–361. doi:10.1016/S0360-5442(01)00089-5

Goedkoop, M., & Spriensma, R. (2001). *The Eco-indicator 99: A Damage Oriented Method for Life Cycle Assessmen, Mehodology report* (3rd ed.). Amersfoort (NL): Pré Consultants.

Goedkoop, Mark, Heijungs, R., Huijbregts, M., Schryver, A. De, Struijs, J., & Zelm, R. Van. (2009). *ReCiPe 2008* (p. 126). Netherlands.

Gomez, A. (2008). *Optimisation technico-économique multiobjectif de systèmes de conversion d'énergie: cogénération électricité-hydrogène à partir d'un réacteur nucléaire de IVème génération*. Université de Toulouse - Institut National Polytechnique de Toulouse.

Gomez, A., Pibouleau, L., Azzaro-Pantel, C., Domenech, S., Latgé, C., & Haubensack, D. (2010). Multiobjective genetic algorithm strategies for electricity production from generation IV nuclear technology. *Energy Conversion and Management*, *51*(4), 859–871. doi:10.1016/j.enconman.2009.11.022

Gómez-Lorente, D., Triguero, I., Gil, C., Estrella, A. E., & Espín Estrella, a. (2012). Evolutionary algorithms for the design of grid-connected PV-systems. *Expert Systems with Applications*, *39*(9), 8086–8094. doi:10.1016/j.eswa.2012.01.159

Gong, X., & Kulkarni, M. (2005). Design optimization of a large scale rooftop photovoltaic system. *Solar Energy*, *78*(3), 362–374. doi:10.1016/j.solener.2004.08.008

Guillén-Gosálbez, G. (2011). A novel MILP-based objective reduction method for multi-objective optimization: Application to environmental problems. *Computers & Chemical Engineering*, *35*(8), 1469–1477. doi:10.1016/j.compchemeng.2011.02.001

Guinée, J. B., Gorrée, M., Heijungs, R., Huppes, G., Kleijn, R., van Oers, L., … Huijbregts, M. A. J. (2002). *Life Cycle Assessment: An Operational Guide to the ISO Standards*. Dordrecht (NL): Kluwer Academic Publishers.

Gutiérrez, E., Lozano, S., Moreira, M. T., & Feijoo, G. (2010). Assessing relationships among life-cycle environmental impacts with dimension reduction techniques. *Journal of environmental management*, *91*(4), 1002–1011. doi:10.1016/j.jenvman.2009.12.009

Ha, K. H. (2012). Open-loop recycling to apply refrigerator plastics from post-consumer waste polypropylene. *Materials & Design*, *35*(0), 310–317. doi:http://dx.doi.org/10.1016/j.matdes.2011.09.062

Hanley, N., & Spash, C. L. (1993). *Cost-Benefit Analysis and the Environment*. *Cost-Benefit Analysis and the Environment* (1st ed., p. 275). United Kingdom: Edward Elgar Publishing.

Hayoun, L.-P., & Arrigoni, A. (2012). *Les installations photovoltaïques: Conception et dimensionnement des installations raccordées au réseau* (1st ed., pp. 1–232). Paris, France: Eyrolles.

Heijungs, R., Huppes, G., Zamagni, A., & Masoni, P. (2011). Life Cycle Assessment: Past, Present, and Future. *Environmental Science & Technology*, *45*(1), 90–96.

Held, M. (2009). Life cycle assessment of CdTe module recycling. In *European Photovoltaic Solar Energy Conference* (pp. 21–25). Hamburg, Germany.

Hondo, H. (2005). Life cycle GHG emission analysis of power generation systems: Japanese case. *Energy*, *30*(11-12), 2042–2056. doi:10.1016/j.energy.2004.07.020

Horn, J., Nafpliotis, N., & Goldberg, D. E. (1994). A niched Pareto genetic algorithm for multiobjective optimization. In *Proceedings of the First IEEE Conference on Evolutionary Computation. IEEE World Congress on Computational Intelligence* (pp. 82–87). Orlando, Fl: IEEE. doi:10.1109/ICEC.1994.350037

Huang, Y. P., Poh, K. L., & B.W., A. (1995). Decision analysis in energy and environmental modeling. *Energy*, *20*(9), 843–855.

Huot, J.-Y. (2012). Recycling of solar Thin Film PV modules and scraps , and closed-loop use of metals. Freiberg, Germany: 5N PLUS.

Hwang, C. L., & Yoon, K. (1981). *Multiple Attribute Decision Making: Methods and Applications*. Berlin: Springer.

Institut National de l'Energie Solaire. (n.d.). CALSOL. Retrieved March 13, 2013, from http://ines.solaire.free.fr/

Institute for Energy and Transport, & European Commission. (n.d.). Photovoltaic Geographical Information System (PVGIS). Retrieved March 18, 2013, from http://re.jrc.ec.europa.eu/pvgis/

International Standard Organization. (1997). ISO 14040. Environmental management-life cycle assessment—principles and framework. Geneva, Switzerland.

International Standard Organization. (2000). ISO 14044. Environmental management-life cycle assessment-requirements and guidelines. Geneva, Switzerland.

Ito, M., Kato, K., Komoto, K., Kichimi, T., & Kurokawa, K. (2008). A Comparative Study on Cost and Life - cycle Analysis for 100 MW Very Large-scale PV (VLS-PV) System in Deserts Usinf m-Si, a-Si, CdTe, and CIS Module. *Progress in Photovoltaics: research and applications*, *16*(May 2007), 17–30. doi:10.1002/pip

Ito, M., Komoto, K., & Kurokawa, K. (2010). Life-cycle analyses of very-large scale PV systems using six types of PV modules. *Current Applied Physics*, *10*(2), S271–S273. doi:10.1016/j.cap.2009.11.028

Jolliet, O., Margni, M., Charles, R., Humbert, S., Payet, J., & Rebitzer, G. (2003). Presenting a New Method IMPACT 2002 + : A New Life Cycle Impact Assessment Methodology, *8*(6), 324–330.

Jolliet, O., Saadé, M., & Crettaz, P. (2010). *Analyse du Cycle de Vie: Comprendre et réaliser un écobilan*. (Presses polytechniques et universitaires romandes, Ed.) (2nd ed., p. 302). Lausanne: Presses polytechniques et universitaires romandes.

Kang, S., Yoo, S., Lee, J., Boo, B., & Ryu, H. (2012). Experimental investigations for recycling of silicon and glass from waste photovoltaic modules. *Renewable Energy*, *47*, 152–159. doi:10.1016/j.renene.2012.04.030

Kannan, R., Leong, K. C., Osman, R., Ho, H. K., & Tso, C. P. (2006). Life cycle assessment study of solar PV systems: An example of a 2.7kWp distributed solar PV system in Singapore. *Solar Energy*, *80*(5), 555–563. doi:10.1016/j.solener.2005.04.008

Kaushika, N. D., & Rai, A. K. (2006). Solar PV design aid expert system. *Solar Energy Materials and Solar Cells*, *90*(17), 2829–2845. doi:10.1016/j.solmat.2006.04.010

Kessler, J. J. (200AD). *Booklet with theoretical background to Strategic Environmental Analysis (SEAN)* (p. 100). Rotterdam, the Netherlands.

Klugmann-Radziemska, E. (2012). Current Trends in Recycling of Photovoltaic Solar Cells and Modules Waste. *Chemistry Didactics Ecology Metrology*, *17*(1-2), 89–95. doi:10.2478/cdem-2013-0008

Klugmann-Radziemska, E., & Ostrowski, P. (2010). Chemical treatment of crystalline silicon solar cells as a method of recovering pure silicon from photovoltaic modules. *Renewable Energy*, *35*(8), 1751–1759. doi:10.1016/j.renene.2009.11.031

Knapp, K. E., & Jester, T. L. (2000). An Empirical Perspective on the Energy Payback Time for Photovoltaic Modules. In *Solar 2000 Conference* (pp. 1–6). Madison, Wisconsin, USA.

Komly, C.-E., Azzaro-Pantel, C., Hubert, A., Pibouleau, L., & Archambault, V. (2012). Multiobjective waste management optimization strategy coupling life cycle assessment and genetic algorithms: Application to PET bottles. *Resources, Conservation and Recycling*, *69*(0), 66–81. doi:http://dx.doi.org/10.1016/j.resconrec.2012.08.008

Konak, A., Coit, D. W., & Smith, A. E. (2006). Multi-objective optimization using genetic algorithms: A tutorial. *Reliability Engineering & System Safety*, *91*(9), 992–1007. doi:10.1016/j.ress.2005.11.018

Kornelakis, A., & Koutroulis, E. (2009). Methodology for the design optimisation and the economic analysis of grid-connected photovoltaic systems. *IET Renewable Power Generation*, *3*(4), 476. doi:10.1049/iet-rpg.2008.0069

Kornelakis, Aris, & Marinakis, Y. (2010). Contribution for optimal sizing of grid-connected PV-systems using PSO. *Renewable Energy*, *35*(6), 1333–1341. doi:10.1016/j.renene.2009.10.014

Koutroulis, E., Kolokotsa, D., Potirakis, A., & Kalaitzakis, K. (2006). Methodology for optimal sizing of stand-alone photovoltaic/wind-generator systems using genetic algorithms. *Solar Energy*, *80*(9), 1072–1088. doi:http://dx.doi.org/10.1016/j.solener.2005.11.002

Kumar Sharma, V., Colangeki, A., & Spagna, G. (1995). Photovoltaic Technology: Basic Concepts, Sizing of a Stand Alone Photovoltaic System for Domestic Applicationds and Preliminary Economic Analysis. *Energy Conversion*, *36*(3), 161–174.

La Mantia, F. P. (2010). Closed-loop recycling. A case study of films for greenhouses. *Polymer Degradation and Stability*, *95*(3), 285–288. doi:http://dx.doi.org/10.1016/j.polymdegradstab.2009.11.030

Lai, Y. J., Lui, T. Y., & Hwang, C. L. (1994). TOPSIS for MODM. *European Journal of Operational Research*, *76*, 486–500.

Laplace System Co. (n.d.). Solar Pro. Retrieved March 18, 2013, from http://www.lapsys.co.jp/english/products/pro.html

Larsen, K. (2009). End-of-life PV: then what? *Renewable Energy Focus*, *10*(4), 48–53. doi:10.1016/S1755-0084(09)70154-1

Li, F., Li, W., Xue, F., Fang, Y., Shi, T., & Zhu, L. (2010). Modeling and simulation of large-scale grid-connected photovoltaic system. In *2010 International Conference on Power System Technology* (pp. 1–6). Hangzhou, China: IEEE. doi:10.1109/POWERCON.2010.5666736

Ligthart, T. N., & Ansems, T. A. M. M. (2002). Modelling of Recycling in LCA. In *Post-Consumer Waste Recycling and Optimal Production* (p. 294). InTech.

Lloyd, B., & Forest, A. S. (2010). The transition to renewables: Can PV provide an answer to the peak oil and climate change challenges? *Energy Policy*, *38*(11), 7378–7394. doi:10.1016/j.enpol.2010.08.014

Lorenzo, E. (2003). Energy Collected and Delivered by PV Modules. In A Luque & S. Hegedus (Eds.), *Handbook of Photovoltaic Science and Engineering* (1st ed., pp. 905–970). John Wiley & Son.

Lund, H., Nilsen, R., Salomatova, O., Skåre, D., & Riisem, E. (2008). Solar Cells. Retrieved June 10, 2013, from http://org.ntnu.no/solarcells/index.php

Luque, Antonio, & Hegedus, S. (2003). *Handbook of Photovoltaic Science and Engineering* (1st ed., p. 1115). John Wiley & Sons.

Manuilova, A., Suebsiri, J., & Wilson, M. (2009). Should Life Cycle Assessment be part of the Environmental Impact Assessment? Case study: EIA of CO2 Capture and Storage in Canada. *Energy Procedia*, *1*(1), 4511–4518. doi:10.1016/j.egypro.2009.02.269

Margni, M., Jolliet, O., & Humbert, S. (2005). *IMPACT 2002 + : User Guide* (p. 36).

Markovic, Z. (2010). Modification of TOPSIS method for solving of multicriteria tasks. *Yugoslav Journal of operations Research*, *20*(1), 117–143.

Markvart, T., & Castañer, L. (2003). *Practical Handbook of Photovoltaics: fundamentals and applications* (p. 984). Elsevier B.V.

Marwede, M., Berger, W., Schlummer, M., Mäurer, A., & Reller, A. (2013). Recycling paths for thin-film chalcogenide photovoltaic waste – Current feasible processes. *Renewable Energy*, *55*, 220–229. doi:10.1016/j.renene.2012.12.038

Marwede, M., & Reller, A. (2012). Future recycling flows of tellurium from cadmium telluride photovoltaic waste. *Resources, Conservation and Recycling*, *69*, 35–49. doi:10.1016/j.resconrec.2012.09.003

McDonald, N. C., & Pearce, J. M. (2010). Producer responsibility and recycling solar photovoltaic modules. *Energy Policy*, *38*(11), 7041–7047. doi:10.1016/j.enpol.2010.07.023

McNeil, S. J., Sunderland, M. R., & Zaitseva, L. I. (2007). Closed-loop wool carpet recycling. *Resources, Conservation and Recycling*, *51*(1), 220–224. doi:http://dx.doi.org/10.1016/j.resconrec.2006.09.006

Mellit, A., Kalogirou, S. A., Hontoria, L., & Shaari, S. (2009). Artificial intelligence techniques for sizing photovoltaic systems: A review. *Renewable and Sustainable Energy Reviews*, *13*(2), 406–419. doi:10.1016/j.rser.2008.01.006

Mellit, Adel, & Benghanem, M. (2007). Sizing of stand-alone photovoltaic systems using neural network adaptive model. *Desalination*, *209*(1-3), 64–72. doi:10.1016/j.desal.2007.04.010

Ménard, L., Gschwind, B., Blanc, I., Beloin-saint-pierre, D., Blanc, P., Ranchin, T., … Grassin, C. (2011). Environmental impact assessment of electricity production by photovoltaic system using GEOSS recommendations on interoperability. In *25th EnviroInfo Conference Environmental Inforlmatics* (pp. 5–7). Italy: Shaker Verlag.

Mermoud, A. (2011). *Note sur le comparatif de programmes de simulation PV de PHOTON* (p. 3). Geneva, Switzerland.

Mirhosseini, M., Agelidis, V. G., & Ravishankar, J. (2012). Modelling of large-scale grid-connected photovoltaic systems: Static grid support by reactive power control. In *IEEE Power and Energy Society Conference and Exposition in Africa: Intelligent Grid Integration of Renewable Energy Resources (PowerAfrica)* (pp. 1–8). Johannesburg, South Africa: IEEE. doi:10.1109/PowerAfrica.2012.6498626

Mondol, J. D., Yohanis, Y. G., & Norton, B. (2006). Optimal sizing of array and inverter for grid-connected photovoltaic systems. *Solar Energy*, *80*(12), 1517–1539. doi:10.1016/j.solener.2006.01.006

Mondol, J. D., Yohanis, Y. G., & Norton, B. (2009). Optimising the economic viability of grid-connected photovoltaic systems. *Applied Energy*, *86*(7-8), 985–999. doi:10.1016/j.apenergy.2008.10.001

Montenon, A. (2013). *Analyse, mutualisation et optimisation par la commande de la consommation énergétique des héliostats autonomes des centrales à concentration solaire*. Université de Toulouse - Institut National Polytechnique de Toulouse.

Müller, A., Wambach, K., & Alsema, E. (2006). Life Cycle Analysis of Solar Module Recycling Process. *Materials Research Society symposia proceedings*, *895*, 2–4.

National Renewable Energy Laboratory. (n.d.). MIDC Solar and Lunar Position Calculators. Retrieved July 05, 2013, from http://www.nrel.gov/midc/solpos/

National Renewable Energy Laboratory. (2000). SOLPOS. National Renewable Energy Laboratory.

Nawaz, I., & Tiwari, G. N. (2006). Embodied energy analysis of photovoltaic (PV) system based on macro- and micro-level. *Energy Policy*, *34*(17), 3144–3152. doi:10.1016/j.enpol.2005.06.018

Neidlein, H.-C. (2010). PV module recycling mandatory for all EU members by Q1 2014. *PV Magazine*. Retrieved May 30, 2013, from http://www.pv-magazine.com/news/details/beitrag/pv-module-recycling-mandatory-for-all-eu-members-by-q1-2014_100008396/#ixzz2UlCmgGYE

Nicholson, A. L., Olivetti, E. A., Gregory, J. R., Field, F. R., & Kirchain, R. E. (2009). End-of-life LCA allocation methods : open loop recycling impacts on robustness of material selection decisions. In *Sustainable Systems and Technology* (pp. 1–7). IEEE.

Nishimura, A., Hayashi, Y., Tanaka, K., Hirota, M., Kato, S., Ito, M., … Hu, E. J. (2010). Life cycle assessment and evaluation of energy payback time on high-concentration photovoltaic power generation system. *Applied Energy*, *87*(9), 2797–2807. doi:10.1016/j.apenergy.2009.08.011

Noorian, A. M., Moradi, I., & Kamali, G. A. (2008). Evaluation of 12 models to estimate hourly diffuse irradiation on inclined surfaces. *Renewable Energy*, *33*(6), 1406–1412. doi:10.1016/j.renene.2007.06.027

Notton, G., Lazarov, V., & Stoyanov, L. (2010). Optimal sizing of a grid-connected PV system for various PV module technologies and inclinations, inverter efficiency characteristics and locations. *Renewable Energy*, *35*(2), 541–554. doi:10.1016/j.renene.2009.07.013

Observ'ER. (2012). *Worldwide electricity production from renewable energy sources. Electricity production in the world: general forecasts* (p. 6). France.

Opricovic, S., & Tzeng, G.-H. (2004). Compromise solution by MCDM methods: A comparative analysis of VIKOR and TOPSIS. *European Journal of Operational Research*, *156*(2), 445–455. doi:10.1016/S0377-2217(03)00020-1

Orion Energy Corporation. (n.d.). NSol. Retrieved March 13, 2013, from http://www.nsolpv.com/

Ouattara, A. (2011). *Méthodologie d'éco-conception de procédés par optimisation multiobjectif et aide à la décision multicritère*. Université de Toulouse - Institut National Polytechnique de Toulouse.

Pacca, S., Sivaraman, D., & Keoleian, G. A. (2006). *Life Cycle Assessment of the 33 kW Photovoltaic System on the Dana Building at the University of Michigan :* (pp. 1–87). Michigan, USA.

Palmer, J., Ghita, O. R., Savage, L., & Evans, K. E. (2009). Successful closed-loop recycling of thermoset composites. *Composites Part A: Applied Science and Manufacturing*, *40*(4), 490–498. doi:http://dx.doi.org/10.1016/j.compositesa.2009.02.002

Pearce, D., Giles, A., & Mourato, S. (2006). Executive Summary. In *Cost-Benefit Analysis and the Environment: Recent Developments* (pp. 15–27). France: OECD Publishing.

Pehnt, M. (2006). Dynamic life cycle assessment (LCA) of renewable energy technologies. *Renewable Energy*, *31*(1), 55–71. doi:10.1016/j.renene.2005.03.002

Pennington, D. W., Potting, J., Finnveden, G., Lindeijer, E., Jolliet, O., Rydberg, T., & Rebitzer, G. (2004). Life cycle assessment part 2: current impact assessment practice. *Environment international*, *30*(5), 721–39. doi:10.1016/j.envint.2003.12.009

Perpiñan Lamigueiro, O. (2012). *Energía Solar Fotovoltaica* (1st ed., p. 194). Spain: Creative Commons.

Petter Jelle, B., Breivik, C., & Drolsum Røkenes, H. (2012). Building integrated photovoltaic products: A state-of-the-art review and future research opportunities. *Solar Energy Materials and Solar Cells*, *100*(7465), 69–96. doi:10.1016/j.solmat.2011.12.016

Pinter, U., & Pšunder, I. (2013). Evaluating construction project success with use of the M-TOPSIS method. *Journal of Civil Engineering and Management*, *19*(1), 16–23. doi:10.3846/13923730.2012.734849

Posadillo, R., & López Luque, R. (2008). Approaches for developing a sizing method for stand-alone PV systems with variable demand. *Renewable Energy*, *33*(5), 1037–1048. doi:10.1016/j.renene.2007.06.004

Prakash, R., & Bhat, I. K. (2009). Energy, economics and environmental impacts of renewable energy systems. *Renewable and Sustainable Energy Reviews*, *13*(9), 2716–2721. doi:10.1016/j.rser.2009.05.007

PV CYCLE. (n.d.). Recycling of photovoltaic modules. Retrieved May 27, 2013, from http://www.pvcycle.org/about/recycling/

Raugei, M., Bargigli, S., & Ulgiati, S. (2007). Life cycle assessment and energy pay-back time of advanced photovoltaic modules: CdTe and CIS compared to poly-Si. *Energy*, *32*(8), 1310–1318. doi:10.1016/j.energy.2006.10.003

Raugei, M., & Frankl, P. (2009). Life cycle impacts and costs of photovoltaic systems: Current state of the art and future outlooks. *Energy*, *34*(3), 392–399. doi:10.1016/j.energy.2009.01.001

Rebitzer, G., Ekvall, T., Frischknecht, R., Hunkeler, D., Norris, G., Rydberg, T., … Pennington, D. W. (2004). Life cycle assessment: Part 1: Framework, goal and scope definition, inventory analysis, and applications. *Environment International*, *30*(5), 701–720. doi:10.1016/j.envint.2003.11.005

Reda, I., & Andreas, A. (2008). *Solar Position Algorithm for Solar Radiation Applications* (p. 56).

Ren, L., Zhang, Y., Wang, Y., & Sun, Z. (2007). Comparative Analysis of a NovelM-TOPSISMethod and TOPSIS. *Applied Mathematics Research eXpress*, *Vol. 2007*(Article ID abm005), 10 pages. doi:doi:10.1093/amrx/abm005

Ren, Lifeng, Zhang, Y., Wang, Y., & Sun, Z. (2007). Comparative Analysis of a Novel M-TOPSIS Method and TOPSIS. *Applied Mathematics Research eXpress*, *2007*, 1–10. doi:10.1093/amrx/abm005

Ritthof, M., Liedtke, C., & Merten, T. (2002). *Calculating MILP: Resource productivity of products and services* (p. 56). Wuppertal, Germany.

Sabio, N., Kostin, A., Guillén-Gosálbez, G., & Jiménez, L. (2012). Holistic minimization of the life cycle environmental impact of hydrogen infrastructures using multi-objective optimization and principal component analysis. *International Journal of Hydrogen Energy*, *37*(6), 5385–5405. doi:10.1016/j.ijhydene.2011.09.039

Sadler, B., & Verheem, R. (1996). *Strategic Environmental Assessment. Status, challenges and future directions*. The Hague.

Sander, K., Schilling, S., Reinschmidt, J., Wambach, K., Schlenker, S., Müller, A., … Chrometzka, T. (2007). Study on the development of a take back and recovery system for photovoltaic products.

Sandia National Laboratories. (n.d.). Photovoltaics. Retrieved March 18, 2013, from http://energy.sandia.gov/?page_id=2727

Schachinger, M. (2012). Module price index. *PV-magazine*. Retrieved April 16, 2012, from http://www.pv-magazine.com/investors/module-price-index/#axzz2c79c34GK

Schaffer, J. D. (1985). Multiple Objective Optimization with Vector Evaluated Genetic Algorithms. In *1st International Conference on Genetic Algorithms* (pp. 93–100). NJ, USA: Erlbaum Associates Inc.

Schmidt-Bleek, F. (1993). MIPS : A New Ecological Measure. In *The Fossil Makers* (pp. 66–99). Factor 10 and more.

Seeling-hochmuth, G. (1998). *Optimisation of Hybrid Energy Systems Sizing and Operation Control*. University of Kassel.

Senjyu, T., Hayashi, D., Yona, A., Urasaki, N., & Funabashi, T. (2007). Optimal configuration of power generating systems in isolated island with renewable energy. *Renewable Energy*, *32*(11), 1917–1933. doi:10.1016/j.renene.2006.09.003

Sherwani, A. F., & Usmani, J. A. (2010). Life cycle assessment of solar PV based electricity generation systems: A review. *Renewable and Sustainable Energy Reviews*, *14*(1), 540–544. doi:10.1016/j.rser.2009.08.003

Singh Solanki, C. (2011). *Solar Photovoltaics: Fundamentals, Technologies and Applications* (2nd ed., p. 478). India: PHI Learning.

Smiley, E. W., Jones, J. D., & Stamenic, L. (2000). *Optimizing photovoltaic array size in a hybrid power system* (pp. 1640–1643).

Solar Thermal. (2008). *Solar Thermal Energy* (p. 7).

Solarbuzz. (2012a). Inverter Prices. Retrieved April 24, 2012, from http://www.solarbuzz.com/facts-and-figures/retail-price-environment/inverter-prices

Solarbuzz. (2012b). Module Pricing. Retrieved April 12, 2012, from http://www.solarbuzz.com/facts-and-figures/retail-price-environment/module-prices

Srinivas, N., & Deb, K. (1994). Muiltiobjective Optimization Using Nondominated Sorting in Genetic Algorithms. *Evolutionary Computation*, *2*(3), 221–248.

Sumper, A., Robledo-García, M., Villafáfila-Robles, R., Bergas-Jané, J., & Andrés-Peiró, J. (2011). Life-cycle assessment of a photovoltaic system in Catalonia (Spain). *Renewable and Sustainable Energy Reviews*, *15*(8), 3888–3896. doi:10.1016/j.rser.2011.07.023

Sustainability EvaluatioN of Solar Energy Systems. (2007). *Recycling of Production Waste* (pp. 1–14). Germany.

Szargut, J. (2005). *Exergy Method: Technical and Ecological Applications* (p. 164). United Kingdom: WIT Press.

The Solar Design Company. (n.d.). PV*SOL. Retrieved March 18, 2013, from http://www.solardesign.co.uk/index.php

United Nations. (2013). Kyoto Protocol. *Framework Convention on Climate Change*. Retrieved July 09, 2013, from http://unfccc.int/kyoto_protocol/items/2830.php

University of Geneva. (n.d.). PVSyst. Retrieved March 18, 2013, from http://www.pvsyst.com/fr/

Vogtländer, J. G., Brezet, H. C., & Hendriks, C. F. (2001). Allocation in Recycling Systems An Integrated Model for the Analyses of Environmental Impact and Market Value. *International Journal of Life Cycle Assessment*, *6*, 1–12.

Wambach, K., Schlenker, S., Konrad, B., & Müller, A. (2006). Sources of secondary Silicon. Germany: Solar World.

Weinstock, D., & Appelbaum, J. (2004a). Shadow variation on photovaltaic collectors in a solar field. *IEEE*, (1), 4–7.

Weinstock, D., & Appelbaum, J. (2004b). Optimal Solar Field Design of Stationary Collectors. *Journal of Solar Energy Engineering*, *126*(3), 898. doi:10.1115/1.1756137

Weinstock, D., & Appelbaum, J. (2007). Optimization of Economic Solar Field Design of Stationary Thermal Collectors. *Journal of Solar Energy Engineering*, *129*(4), 363. doi:10.1115/1.2769690

Weinstock, D., & Appelbaum, J. (2009). Optimization of Solar Photovoltaic Fields. *Journal of Solar Energy Engineering*, *131*(3), 031003. doi:10.1115/1.3142705

Williams, T. G. J. L., Heidrich, O., & Sallis, P. J. (2010). A case study of the open-loop recycling of mixed plastic waste for use in a sports-field drainage system. *Resources, Conservation and Recycling*, *55*(2), 118–128. doi:http://dx.doi.org/10.1016/j.resconrec.2010.08.002

Wissem, Z., Gueorgui, K., & Hédi, K. (2012). Modeling and technical–economic optimization of an autonomous photovoltaic system. *Energy*, *37*(1), 263–272. doi:10.1016/j.energy.2011.11.036

World Energy Council. (2004). *Comparison of energy systems using life cycle assessment* (p. 61). London, U.K.

Xu, D., Kang, L., & Cao, B. (2006). Graph-Based Ant System for Optimal Sizing of Standalone Hybrid Wind/PV Power Systems. In D.-S. Huang, K. Li, & G. Irwin (Eds.), *Computational Intelligence SE - 141* (Vol. 4114, pp. 1136–1146). Springer Berlin Heidelberg. doi:10.1007/978-3-540-37275-2_141

Xu, D., Kang, L., Chang, L., & Cao, B. (2005). Optimal sizing of standalone hybrid wind/pv power systems using genetic algorithms. *Canadian Conference on Electrical and Computer Engineering, 2005.*, (May), 1722–1725. doi:10.1109/CCECE.2005.1557315

Yokoyama, R., Yuasa, Y., & Ito, K. (1994). Multiobjective Optimal Unit Sizing of Hybrid Power Generation Systems Utilizing Photovoltaic and Wind Energy. *Journal of Solar Energy Engineering*, *116*(4), 167–173. Retrieved from http://dx.doi.org/10.1115/1.2930078

Zhou, P., Ang, B., & Poh, K. (2006). Decision analysis in energy and environmental modeling: An update. *Energy*, *31*(14), 2604–2622. doi:10.1016/j.energy.2005.10.023

Ziar, H., Mansourpour, S., Salimi, A., & Afjei, E. (2011). Analysis of shadow effect in photovoltaic array using binary coding method. In *2nd International Conference on Electric Power and Energy Conversion Systems (EPECS)* (pp. 1–6). IEEE.

Zitzler, E., & Thiele, L. (1999). Multiobjective evolutionary algorithms: a comparative case study and the strength Pareto approach. *IEEE Transactions on Evolutionary Computation*, *3*(4), 257–271. doi:10.1109/4235.797969

LISTE OF FIGURES

Figure 1-1 Structure of electricity production in 2011 (Observ'ER, 2012) 8
Figure 1-2 Solar irradiation versus global energy resources (EPIA, 2011) 10
Figure 1-3 Photovoltaic effect (EPIA, 2011) 12
Figure 1-4 Different configurations of PV solar systems from (EPIA, 2011) 12
Figure 1-5 PV module technology market share, based on (EPIA, 2013) 14
Figure 1-6 Evolution of global cumulative installed capacity 2000-2012 (MW) (EPIA, 2013) 15
Figure 1-7 Evolution of global PV cumulative installed capacity per region until 2017 in MW (EPIA, 2013) 16
Figure 1-8 Power generation capacities added in the EU 27 in 2012 (MW) (EPIA, 2013) 17
Figure 1-9 European new grid-connected PV capacities in 2012 (EPIA, 2013) 17
Figure 1-10 Global PV production in 2012 by region (EPIA, 2013) 18
Figure 1-11 Global utility-scale PV development scenarios until 2017 (MW) (EPIA, 2013) 18
Figure 1-12 General scheme for the configuration of a PVGCS 19
Figure 1-13 Organization of manuscript 22
Figure 2-1 Production flow of crystalline silicon PV modules based on (de Wild-Scholten & Alsema, 2005) 26
Figure 2-2 Main manufacturing processes of SoG-Si 27
Figure 2-3 Manufacturing processes of silicon wafer 28
Figure 2-4 Production flow of a-Si PV modules 30
Figure 2-5 Principle of a RF-PECVD deposition tool (Luque & Hegedus, 2003) 31
Figure 2-6 Structure of a-Si:H-based solar cell (Singh Solanki, 2011) 32
Figure 2-7 Production flow of CdTe PV modules (V. Fthenakis et al., 2009) 32
Figure 2-8 Flows in Zn refining (V. Fthenakis et al., 2009) 33
Figure 2-9 Extractive metallurgy of Cu (V. Fthenakis et al., 2009) 33
Figure 2-10 Schematic CSS deposition tool (Singh Solanki, 2011) 34
Figure 2-11 Structure of CdTe-based solar cell (Singh Solanki, 2011) 35
Figure 2-12 Production flow of CIS PV module 36
Figure 2-13 Process flows for In production (V. Fthenakis et al., 2009) 36
Figure 2-14 Process flows for Ga production (V. Fthenakis et al., 2009) 37
Figure 2-15 Process flows for Se production (V. Fthenakis et al., 2009) 38
Figure 2-16 Deposition of CIGS layer using co-evaporation (Singh Solanki, 2011) 38
Figure 2-17 Structure of CIS-based solar cell (Singh Solanki, 2011) 39
Figure 2-18 Schematic representation of the life cycle of a generic product (based on (Rebitzer et al., 2004)) 43
Figure 2-19 LCA framework (ISO 14040:1997) 45

Figure 2-20 LCI schema 46
Figure 2-21 Elements of LCIA (ISO 14042:2000) 47
Figure 2-22 General approach of LCIA of emissions on the major categories of environmental damage 50
Figure 2-23 System boundaries for m-Si PV module LCA 54
Figure 2-24 Normalised scores for both mid-point and damages categories. IMPACT 2002+ 61
Figure 2-25 Energy mix composition of Germany, USA, China, Spain and France 61
Figure 2-26 Normalized scores both mid-point and damages categories of five scenarios. IMPACT 2002+ 62
Figure 2-27 Scheme of system boundaries 63
Figure 2-28 Normalised results for the three PV module technologies. IMPACT 2002+ 64
Figure 2-29 Normalised results for the three PV module technologies. FU: 1 kWh demanded. IMPACT 2002+ 64
Figure 2-30 Result of main processes in Global Warming category for 3 PV module technologies 65
Figure 2-31 Score of the five main resources that contribute to GW characterization for m-Si PV module at wafer elaboration process. 65
Figure 2-32 Boundaries of the system examined to compare different PV technologies 66
Figure 2-33 Normalized results for the five PV installation considering 1200 kWh/m^2 yr of irradiation on an inclined plane (30°). IMPACT 2002+ 68
Figure 3-1 Functional flow diagram of the proposed methodology 77
Figure 3-2 Different components of solar radiation in a tilted surface 78
Figure 3-3 Data flow diagram of solar irradiance estimation model 79
Figure 3-4 Sun-Earth relationship 80
Figure 3-5 Sequence for determination of hourly global tilted irradiance 81
Figure 3-6 Data flow diagram of PVGCS model 86
Figure 3-7 Solar collector field reproduced from (Weinstock & Appelbaum, 2009) 87
Figure 3-8 Shading by collectors in a stationary solar field reproduced from (Weinstock & Appelbaum, 2009) 89
Figure 3-9 Evaluation of criteria model 90
Figure 3-10 Field layout of PV power plant made in PVsyst 95
Figure 3-11 Results of the environmental impacts normalized to unity 97
Figure 3-12 Results of the environmental impacts per annual energy generated ratio normalized to unity 98
Figure 4-1 Classification of optimization methods (Garcia, Avila, Carpes, & Avila, 2005) 104
Figure 4-2 Genetic Algorithm operators 106
Figure 4-3 Genetic Algorithm flow chart 106
Figure 4-4 Operating principle of NSGA II (Part 1) (Gomez, 2008) 110
Figure 4-5 Operating principle of NSGA II (Part 2) (Gomez, 2008) 111
Figure 4-6 Operating principle of NSGA II (Part 3) (Gomez, 2008) 111
Figure 4-7 Scheme of the PCA procedure for selecting environmental impact categories (Sabio et al., 2012) 113
Figure 4-8 Screen plot for Sabio et al. case 115
Figure 4-9 PCA results in the bi- and tri-dimensional spaces for Sabio et al. case 116
Figure 4-10 Decision matrix 117

Figure 4-11 Example D^+ D^- – plane of M-TOPSIS method (Lifeng Ren et al., 2007) 119
Figure 4-12 D^+ D^-plane for M-TOPSIS example 121
Figure 4-13 Pareto front EPBT-Q_{out} with top 3 ranked alternatives 122
Figure 4-14 Pareto front EPBT-Q_{out} with top 3 ranked alternatives and alternative 4..... 123
Figure 4-15 Integration of NSGA II, PCA method and M-TOPSIS method 123
Figure 5-1 Functional flow diagram of the proposed methodology 128
Figure 5-2 Results of the environmental impacts normalized to unity. Maximum output energy 133
Figure 5-3 3-D perpectives of 5 configurations 135
Figure 5-4 Results of the environmental impacts normalized to unity. Minimum field area 136
Figures 5-5 (a-e) Pareto fronts with M-TOPSIS selected PV power plant configuration. Max Q_{out} – Min PBT 139
Figure 5-6 Results of the environmental impacts normalized to unity. Max Q_{out} – Min PBT 141
Figures 5-7 (a-e) Pareto fronts with M-TOPSIS selected PV power plant configuration. Max Q_{out} – Min EPBT..... 143
Figure 5-8 Results of the environmental impacts normalized to unity. Max Q_{out} – Min EPBT 144
Figure 5-9 (a-e) Pareto fronts with M-TOPSIS selected PV power plant configuration. Min PBT– Min EPBT..... 145
Figure 5-10 Results of the environmental impacts normalized to unity. Min *PBT* – Min *EPBT*..... 147
Figure 5-11 (a-e) Pareto fronts with M-TOPSIS selected PV power plant configuration. Min Area – Min PBT 148
Figure 5-12 Results of the environmental impacts normalized to unity. Min *Area* – Min *PBT*..... 149
Figure 5-13 (a-e) Pareto fronts with M-TOPSIS selected PV power plant configuration. Min Area– Min EPBT..... 151
Figure 5-14 Results of the environmental impacts normalized to unity. Min *Area* – Min *EPBT* 152
Figure 5-15 Scree plot for the 15 environmental categories 155
Figure 5-16 PCA results in the bi-dimensional spaces..... 155
Figure 6-1 Global PV production and projected waste from 1998 to 2038 from (McDonald & Pearce, 2010) 164
Figure 6-2 Three recycling schemes (inspired from (Ligthart & Ansems, 2002)) 165
Figure 6-3 Product system for the cut-off approach (Ligthart & Ansems, 2002)..... 166
Figure 6-4 Product material flows and processes for 2 life cycles. Closed loop approach (Nicholson et al., 2009) 167
Figure 6-5 Substitution allocation approach (Ligthart & Ansems, 2002) 167
Figure 6-6 Recycling process for PV crystalline module from (Klugmann-Radziemska, 2012) 168
Figure 6-7 Recycling process for CdTe and CIS PV modules from (Marwede & Reller, 2012) 170
Figure 6-8 Recycling Process of Deutsche Solar AG (Bombach et al., 2006) 172
Figure 6-9 Process flow and system boundary for PVGCS with m-Si PV module..... 173
Figure 6-10 Flow chart of First Solar's CdTe PV module recycling process from (Held, 2009)..... 174
Figure 6-11 Process flow and system boundary for PVGCS with CdTe PV module..... 176

LISTE OF TABLES

Table 1-1 World electricity production by source in TWh (2001-2011) (Observ'ER, 2012) 9
Table 1-2 Top 10 countries with the highest PV cumulative installed capacity in 2012 (EPIA, 2013) 15
Table 1-3 Summary of literature works for sizing PV systems 20
Table 1-4 Summary of literature works for environmental assessment of PV systems 21
Table 2-1 Environmental assessment techniques 41
Table 2-2 Methods for LCIA (European Commission et al., 2010) 47
Table 2-3 Characterisation reference substances and reference flow used in IMPACT 2002+ (Based on (Margni, Jolliet, & Humbert, 2005)) 49
Table 2-4 Main LCA software tools 53
Table 2-5 LCI data for manufacturing process of m-Si PV module from (de Wild-Scholten & Alsema, 2005) 55
Table 2-6 LCI of total flows for production of 1 piece of m-Si PV module 56
Table 2-7 LCI of total emission for manufacturing a m-Si based PV module (extracted from SimaPro) 57
Table 2-8 Characterization of LCI emission into GW impact category 58
Table 2-9 Characterization of LCI emission into RI impact category 58
Table 2-10 Characterization score of impact categories 59
Table 2-11 Characterization score of damage categories 59
Table 2-12 IMPACT 2002+ reference values for normalisation (Margni et al., 2005) 60
Table 2-13 Normalised scores for both impact and damage categories 60
Table 2-14 Efficiencies and number of PV modules required 64
Table 2-15 Key features for LCA study 67
Table 3-1 System sizing and simulation programs 75
Table 3-2 Root mean square (RMSE) and mean bias errors (MBE) of proposed simulator 84
Table 3-3 Comparison of G_{β} estimated 84
Table 3-4 Summary of the main energy losses (Brigand, 2011; Hayoun & Arrigoni, 2012) 90
Table 3-5 Main elements of economic evaluation 91
Table 3-6 Parameter values for each scenario of WAP example 93
Table 3-7 Comparison of output energy from the example of WAP and the proposed tool 93
Table 3-8 Typical features of various commercial PV modules technologies 94
Table 3-9 Values of Nc and Nr for simulation 94
Table 3-10 Comparison of output energy from PVsyst and the proposed tool 95
Table 3-11 PBT and EPBT for each configuration 96
Table 4-1 List of well-known MGA (based on (Konak et al., 2006)) 108
Table 4-2 Summary of applications of GAs for sizing PV systems 108
Table 4-3 Correlation matrix for Sabio et al. case 114

Table 4-4 PCA results for Sabio et al. case. Eigenvalues and eigenvectors 115
Table 4-5 Decision data matrix 119
Table 4-6 Transformed values matrix 120
Table 4-7 Normalized decision matrix 120
Table 4-8 Weighted normalized matrix 120
Table 4-9 A^+ and A^- values 121
Table 4-10 Euclidean distance matrix (D_i^+ and D_i^-) 121
Table 4-11 Rank alternatives by M-TOPSIS coefficient R_i 122
Table 5-1 Parameter values of NSGA II for different examples 129
Table 5-2 Comparison between WAP and the proposed approach 130
Table 5-3 Values of decision variables for the best configuration of each PV technology. Maximum output energy 130
Table 5-4 Output energy for the best configuration of each PV technology. Maximum output energy. 131
Table 5-5 PBT and EPBT for each configuration. Maximum output energy 131
Table 5-6 Final ranking of alternatives. Maximum output energy 132
Table 5-7 Final ranking of alternatives (environmental impact per kWh produced). Maximum output energy 132
Table 5-8 Best configuration that minimizes the surface of PV system 134
Table 5-9 PBT and EPBT for each configuration. Minimum field area. 137
Table 5-10 Final ranking of alternatives. Minimum field area 137
Table 5-11 Weight proposals 139
Table 5-12 Configuration selected by applying M-TOPSIS. Max Q_{out} – Min PBT 140
Table 5-13 Ranking of the resulting configurations after applying M-TOPSIS. Max Q_{out} – Min PBT 142
Table 5-14 Configurations selected by applying M-TOPSIS. Max Q_{out} – Min EPBT 142
Table 5-15 Ranking of resulting configuration after applying M-TOPSIS. Max Q_{out} – Min EPBT 143
Table 5-16 Configuration selected by applying M-TOPSIS. Min PBT– Min EPBT 146
Table 5-17 Ranking of the resulting configurations after applying M-TOPSIS. Min PBT – Min EPBT 146
Table 5-18 Configuration selected by applying M-TOPSIS. Min Area – Min PBT 150
Table 5-19 Ranking of resulting configuration after applying M-TOPSIS. Min Area – Min PBT 150
Table 5-20 Configuration selected by applying M-TOPSIS. Min Area – Min EPBT 153
Table 5-21 Ranking of resulting configuration after applying M-TOPSIS. Min Area – Min EPBT 153
Table 5-22 Correlation matrix for the 15 environmental categories 154
Table 5-23 PCA results. Eigenvalues and eigenvectors for the 15 environmental categories 154
Table 5-24 Comparison of results of two multi-objective optimization 156
Table 5-25 Ranking of the configurations 157
Table 5-26 Selected configurations by applying M-TOPSIS. Four objectives 157
Table 5-27 Ranking of the resulting configuration after applying M-TOPSIS. Four objectives 157
Table 6-1 End-of-life PV modules collected and treated in 2012 (European Association for the Recovery of Photovoltaic Modules, 2012) 164
Table 6-2 Results of four scenarios for m-Si based PVGCS configuration 174
Table 6-3 LCIA of CdTe PV module recycling per m² (Held, 2009) 176
Table 6-4 Results of scenarios for CdTe based PVGCS configuration 177

Appendix A

COMPARATIVE LIFE CYCLE ASSESSMENT OF AUTONOMOUS AND CLASSICAL HELIOSTATS FOR HELIOTHERMODYNAMIC POWER PLANTS FOR CONCENTRATED SOLAR POWER

2012 First International Conference on Renewable Energies and Vehicular Technology

Comparative Life Cycle Assessment of Autonomous and Classical Heliostats for Heliothermodynamic Power Plants for Concentrated Solar Power

Perez Gallardo Jorge Raul[1a], Montenon Alaric[2b], Maussion Pascal[3b], Azzaro-Pantel Catherine[4a] and Stephan Astier[5b]

[a]Université de Toulouse ; INPT, UPS ; Laboratoire de Génie Chimique ; 4, Allée Emile Monso, F-31030 Toulouse, France. CNRS ; Laboratoire de Génie Chimique ; F-31030 Toulouse, France

[b]Université de Toulouse ; INPT, UPS ; LAPLACE (Laboratoire PLAsma et Conversion d'Energie) ; ENSEEIHT, 2 rue Charles Camichel, BP 7122, F-31071 Toulouse cedex 7, France. CNRS ; LAPLACE ; F-31071 Toulouse, France

[1]jorgeraul.perezgallardo@ensiacet.fr [2]alaric.montenon@laplace.enseeiht.fr
[3]pascal.maussion@laplace.enseeiht.fr[4]catherine.azzaropantel@ensiacet.fr
[5]stephan.astier@laplace.enseeiht.fr

ABSTRACT

For concentrated solar plants with a tower receiver, in almost all cases, heliostats are fed by an electrical network, which crosses a large field by long cables. This situation leads to the need to dig trenches all across the field yet it is possible to use autonomous fields provided by photovoltaic panels and storage system, to avoid those long cables and trenches. The approach developed here is to analyze and compare the effective environmental impact of the autonomous heliostat field and a classical field by use of a Life Cycle Assessment (LCA) approach. In this paper, the components of each kind of fields are described and LCA is applied to both types of heliostat structures. Based on the obtained results, the energy supplied in the electrical grid heliostat is responsible for the higher environmental impact over its life-time even if the photovoltaic panel itself generates a huge amount of environmental impacts during production phase.

Index Terms— Life cycle assessment, heliostat, autonomous, renewable energy, environmental impact

1. INTRODUCTION

Heliothermodynamic power is an emerging resource that is going to gain importance in the future to cope with the scarcity of fossil fuels. Plants using this kind of power with a tower run by the use several heliostats. These ones reflect the sun beams on the top of the tower where the heat receiver stands. After heat transfer to a fluid in the receiver and due to thermodynamic transfer, electricity is generated by a turbine. Yet, the advantages of this technology have to be proved to enter in a non-carbonic energy strategy market to reduce greenhouse gas effect. Indeed the starting investments of heliostat field are huge and can delay the payback investment time. Heliostats track the sun on two axes by the use of motors which are powered in most of the configurations by long electric cables across the field inside trenches that must be dug. Another powering method has been studied [1] which consists in using an autonomous heliostat field, meaning that each heliostat is powered by a photovoltaic generator and batteries via a MPPT chopper. So it is interesting to compare the environmental impacts generated by an autonomous heliostat field with those induced by a classical field that is thrown by hundreds of cable meters to power each heliostat. In this paper, the results of a life cycle assessment corresponding to both solutions are analyzed: the former deals with an autonomous heliostat, the latter is relative to a heliostat connected to the local power grid. In the first part of the paper, the components of the two configurations are described. In the second part, LCA is developed for both configurations and the results are then compared.

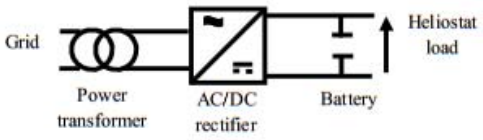

Figure 1. Classical heliostat components

978-1-4673-1170-0/12/$31.00 ©2012 IEEE

2. COMPARISON OF THE CONFIGURATIONS FOR HELIOSTAT FIELD

2.1. Common components of the two architectures

There are some common components on both configurations. A heliostat has to track the sun to reflect the beam on a receiver by use of a mirror. Its structure is composed of two motors; one per axis whatever the method to track the sun all day long to reflect the beams is (spinning-elevation [2] or azimuth-elevation [3]).The structure moves by use of a control card board and power is given by a 24VDC battery via a chopper. So both motors that control the rotations of the heliostat structures, i.e., the control board and the chopper, are the same for either an autonomous or a non autonomous heliostat. Batteries are required for an autonomous heliostat to overcome the lack of solar irradiance in the night or in cloudy days to go on running with the stored energy. To maintain these conditions, a lead/acid battery of 720 Wh is used as in PSA project [4].

Batteries are also needed on heliostats when they are powered by the electrical grid, in order to prevent from power high current demand at the beginning or the end of the day. Indeed, during the night, the heliostat stands in stow position. It means that it is pointing to the celestial vault. But at the beginning of the day, heliostats must reach the tracking position in some minutes. So the needed current to go from stow position to tracking position of the crepuscule is high. This current is provided by a battery. The current demand is also high at the end of the day for the heliostat to go from tracking position to the stow one. For this purpose, to support 10A current under 12Vdc during 10 minutes (which corresponds to an initialization time gap) a 26 Wh battery is necessary, considering a maximum discharge of 70%. These elements are necessary for both architectures but the battery for the autonomous heliostat has a higher storage. Data of each element that compose the lead/acid batteries are described by Rantik, 1999 [5].

It must be emphasized that this study does not embed the global life cycle assessment (LCA) of an autonomous heliostat field and a classical one. It focuses only on the components that are different for both architectures.

2.2. Grid-connected heliostat

In the classical heliostat field, all heliostats must be powered by a 20kV/380VAC power transformer (Figure 1).The power is distributed by long cables at the bottom of the heliostat. The set reference is the THEMIS plant in the French Eastern Pyrenees.

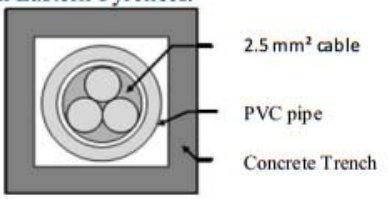

Figure 2. Profile view of the trenches

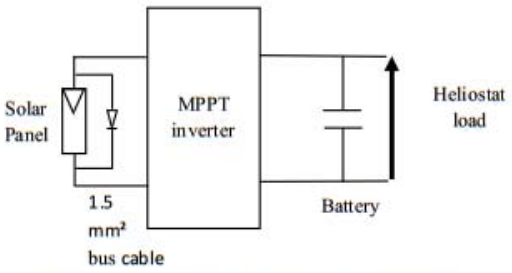

Figure 3. Autonomous heliostat components

The length of cables which allow connecting every heliostat is 1866 m (the profile is described in Figure 2).This is also the necessary length of the trenches to protect the cables. The size of the concrete formwork is 30 cm x 30 cm and 5 cm thin. The cables are three conductor cables with a cable sheath having a same length.

The number of heliostats in the THEMIS power plant is 201 [6]. LCA of power transformer, cables, sheath and trenches will be divided by the number of heliostat to get results for one heliostat. In this way, the contribution of each heliostat can be evaluated. But the electrical energy amount of the non autonomous heliostat has to be calculated because the local production of energy has also its own environmental impact as described in what follows.

2.3. Autonomous heliostat

Autonomous heliostat is composed of three elements: a multi-crystalline (multi-Si) solar panel of 55 Wp as implanted in the PSA project, one MPPT converter, three cables bus of 1.5 m long and a thickness of 1.5 mm² as shown in Figure 3.

3. LIFE CYCLE ASSESSMENT

3.1. LCA basic guidelines

Life Cycle Assessment characterizes and assesses the total environmental burdens associated with a product and a system, from raw materials acquisition to end-of-life management. It identifies the points on which a product can be improved and also contributes to the development of new products. This method is used to compare the environmental costs of different products, processes or systems together, and analyzes the different stages of the life cycle of a product. LCA provides support elements for industrial policies such as the choice of design and improvement of products or the selection of a production method, and is also interesting for public actions. According to the norms ISO-14040-44 [7], LCA is divided into 4parts.

- *Defining objectives and scope of the study* where the problem, the objectives and scope of the study are described and *establishing the functional unit* to which emissions and extractions are reported;

- *Analysis of inventory* of emissions to air, water and soil as well as extraction of renewable and non-renewable raw materials;
- *Analysis of the environmental impact* of emissions and extractions inventoried in the previous phase;
- *Interpretation of results* for making recommendations, based on the results of the previous phase [8,9].

LCA is now developed for the two previously mentioned configurations of heliostats.

3.2. LCA for heliostats field

Following the methodology of LCA, the objective of this work is to compare a heliostat which is connected to the grid and an autonomous one. As a first step, it is necessary to define the scope of study and the functional unit. This work is limited to the key elements that characterize each of the two configurations. The common elements are excluded from the analysis. First of all, the LCA of autonomous heliostat and of the grid-connected heliostat is performed only with consideration of the materials that compose their own design architecture. A more realistic comparison for evaluating both configurations is to consider their performance during a specific time period. So, as a secondcase of analysis, the use of a heliostat for 20 years will be considered as anew functional unit.

The second step of LCA concerns Life Cycle Inventory (LCI), which consists in the list of materials, energy and pollutant flows that cross the boundaries of the system under study. Ecoinvent database [10], the most widespread and acknowledged LCI database worldwide, allowed us to establish the inventory of materials and flows for both configurations. The computation of the generated impacts by each of the described elements in the inventory constitutes the next step. The method of analysis of the environmental impact IMPACT 2002+ [11] is used. It proposes a feasible implementation of a combined midpoint/damage approach. The impacts are grouped into 14 midpoint categories and four damage categories listed in the method.The amount of each of the described elements in the inventory is multiplied by a factor of characterization, as presented in equations (1) and (2).

$$SI_i = \sum_s FI_{s,i} \cdot M_s \qquad (1)$$

$$SD_d = \sum_i FD_{i,d} \cdot SI_i \qquad (2)$$

where SI_i is the midpoint characterization score of the midpoint category i, $FI_{s,i}$ represents the midpoint characterization factor of the substance s in the midpoint category i, M_s is the mass emitted or extracted from the substance s, SD_d is the endpoint characterization score of the endpoint category d and $FD_{i,d}$ represents the endpoint characterization factor of the midpoint category i in the endpoint category d.

The LCA software tool SimaPro is adopted in order to calculate and classify the impacts.

3.3. Results and interpretation

We focused on two of the four principal damage categories in which environmental impacts are classified according to the method IMPACT 2002+: *Climate Change*, based on the total emissions of greenhouse gases and expressed in kg equivalent CO_2 ($kg_{eq}CO_2$), and *Resources*, base on the consumption of non-renewable primary energy in $MJ/unit_{consumed}$. Tables 1 and 2 present the endpoint characterization factors for the elements under analysis for both configurations.

To compare them, a normalization of the impacts results was conducted to highlight their contributions in the global worldwide effect in a given category of environmental impact. The idea of normalization is to analyze the respective share of each impact to the overall damage by applying normalization factors to damage impact classes in order to facilitate interpretation. The normalized damage impact (N_d) is determined by endpoint characterization score of the endpoint category d (SD_d)divided by the normalization factors for damage category d (FN_d) as it showed in equation (3) [8]. An overview of normalization factors for the two damage categories selected is given in table 3.

$$N_d = \frac{SD_d}{FN_d} \qquad (3)$$

Table 1. Endpoint characterization factor for a grid-connected heliostat [5, 8 and 10]

	Climate change		*Resources*	
Cable 2.5mm²	2.30	kg_{eq} CO_2/m	66.68	MJ/m
Concrete trench	0.12	kg_{eq} CO_2/kg	0.76	MJ/kg
Power transformer	5.06	kg_{eq} CO_2/kg	98.73	MJ/kg
Cable 1.5mm²	2.30	kg_{eq} CO_2/m	66.68	MJ/m
Cable sheath	3.59	kg_{eq} CO_2/kg	86.72	MJ/kg
Rectifier	3.66	kg_{eq} CO_2/piece	58.19	MJ/piece
Energy consumed	0.09	kg_{eq} CO_2/kWh	11.61	MJ/kWh
Excavation	0.53	kg_{eq} CO_2/m³	8.06	MJ/m³
Lead-Acid battery	0.17	kg_{eq} CO_2/piece	6.98	MJ/piece

Table 2. Endpoint characterization factors for an autonomous heliostat [5, 8, and 10]

	Climate change		*Resources*	
MPPT chopper	36.25	kg_{eq} CO_2/piece	649.94	MJ/piece
Multi-Si solar panel	155.72	kg_{eq} CO_2/m²	2609.42	MJ/m²
Cable bus	0.33	kg_{eq} CO_2/m	9.62	MJ/m
Lead-Acid battery	0.17	kg_{eq} CO_2/piece	6.98	MJ/piece

Table 3. Normalization factors for the damage Categories [8]

Damage category	*Normalization factor*	*Unit*
Climate Change	9950	kg_{eq} CO_2
Resources	152000	MJ

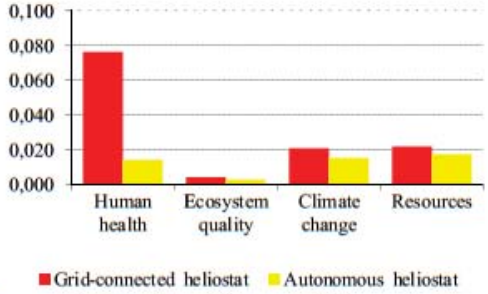

Figure 4. Normalized impacts of the two heliostats at construction time.

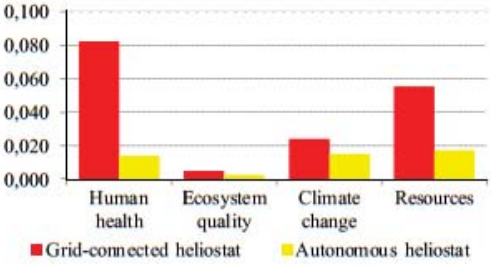

Figure 5. Normalized impacts of the two heliostats after 20 years.

As shown in Figure 4, grid-connected heliostat has the biggest impacts in both categories if we evaluate only the installation of the elements of each configuration (first case studied). After 20 years of operation, the situation is the same; the grid–connected heliostat has the most important impact (Figure 5). The main difference is found in the *Resource* category which presents an increase in over 350%.

A more detailed analysis was performed for the purpose of finding the root causes of this increment. A new analysis was performed for the electrical grid connected heliostat but now with evaluation of the individual contribution of each of the elements that comprises it. The obtained results for both categories under analysis are presented in Figures 6 and 7 where the required energy to operate the heliostat is the main cause of increased impacts to the environment. It is clear that after 20 years of service of heliostat, the consumed energy for its operation generates a significant increase in the total score in *Resources* category because of the source of that energy. Principally, it comes from non-renewable sources such as fossil fuels or nuclear industry and very little from renewable sources according to the French electrical generation [12]. The annual evolution of the recorded impacts within both categories under analysis for the electrical grid heliostat is shown in Figure 8.

As shown in Figure 4, grid-connected heliostat has the biggest impacts in both categories if we evaluate only the installation of the elements of each configuration (first case studied). After 20 years of operation, the situation is the same; the grid–connected heliostat has the most important impact (Figure 5). The main difference is found in the *Resource* category which presents an increase in over 350%.

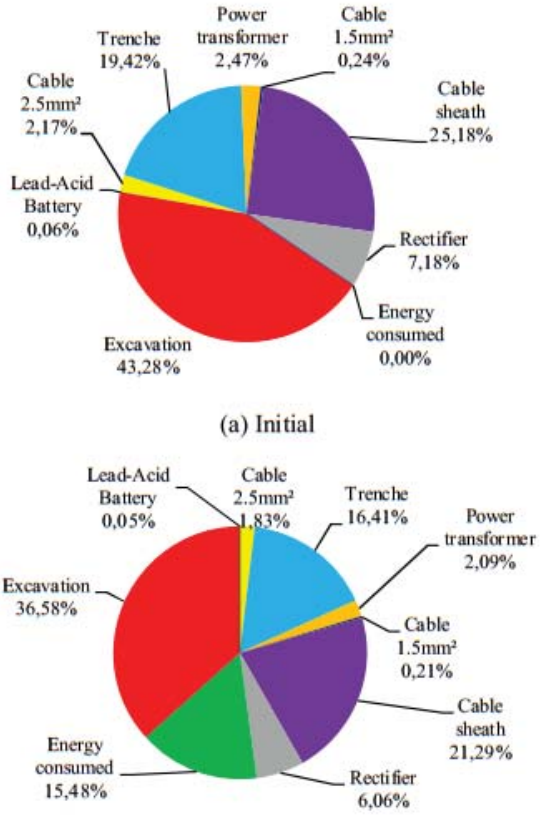

Figure 6. Element contribution to Climate Change category

As shown in Figure 4, grid-connected heliostat has the biggest impacts in both categories if we evaluate only the installation of the elements of each configuration (first case studied). After 20 years of operation, the situation is the same; the grid–connected heliostat has the most important impact (Figure 5). The main difference is found in the *Resource* category which presents an increase in over 350%.

A more detailed analysis was performed for the purpose of finding the root causes of this increment. A new analysis was performed for the electrical grid connected heliostat but now with evaluation of the individual contribution of each of the elements that comprises it. The obtained results for both categories under analysis are presented in Figures 6 and 7 where the required energy to operate the heliostat is the main cause of increased impacts to the environment. It is clear that after 20 years of service of heliostat, the consumed energy for its operation generates a significant increase in the total score in *Resources* category because of the source of that energy. Principally, it comes from non-renewable sources such as fossil fuels or nuclear industry and very little from renewable sources according to the French electrical generation [12].

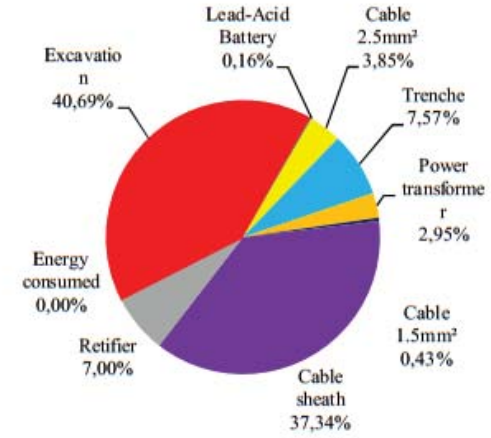

(a) Initial

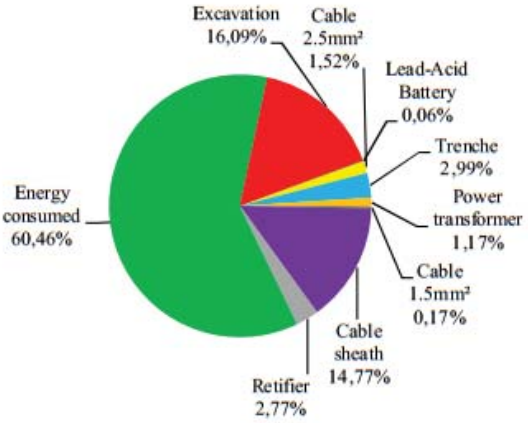

(b) After 20 years

Figure 7. Element contribution to Resources category

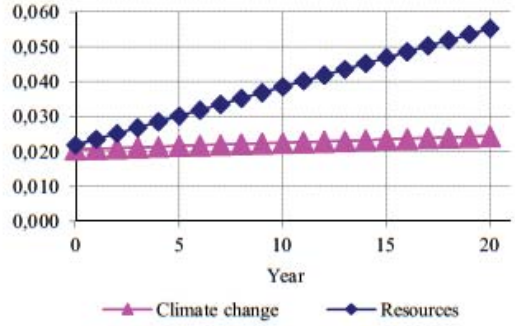

Figure 8. Cumulative impact evolution for a grid-connected heliostat

The annual evolution of the recorded impacts within both categories under analysis for the electrical grid heliostat is shown in Figure 8.

It was shown that the increase in environmental impacts within the non autonomous heliostat is due to the power supply for its operation as it depends on each country's energy mix. Most of this provided energy has its origins in non-renewable sources.

The impact of a non autonomous heliostat has to be regarded within the context the French specificity where the electricity has low gas emissions because 74.1% of the produced energy comes from nuclear power and only 10.8% come from fossil fuels (in 2010, [12]). But the impact of the nuclear wastes is not taken in account in LCA database.

So the real impact into a large period of evaluation could strongly affect the LCA of the non autonomous heliostat, encouraging the use of an autonomous heliostat despite the produced contamination during the elaboration of silicon photovoltaic panels.

Figures 9 and 10 show the results of a third analysis in order to prove if the grid-connected heliostat implanted in other countries such as Spain and the United Stated follows the same path in the two categories under evaluation after 20 years. It is relevant that after 20 years of operation, only 10 % of the climate change category in France is due to the consumed energy. But in Spain, 50% of the contribution of climate change category is due to the consumed energy.

For United States, 60% of the climate change category is due to the consumed energy. It can also be pointed out that (Figure 10), currently in the resources category the consumed energy has more or less the same contribution as in the three mentioned countries (about 60%).

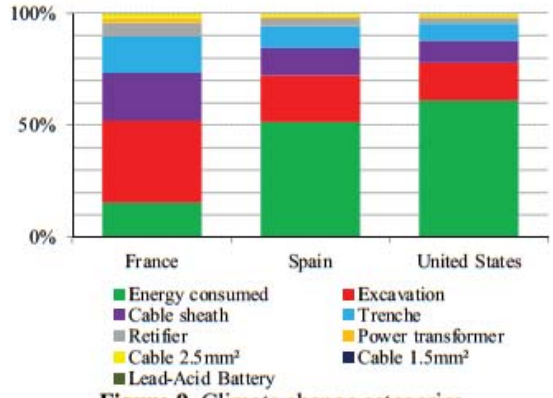

Figure 9. Climate change categories

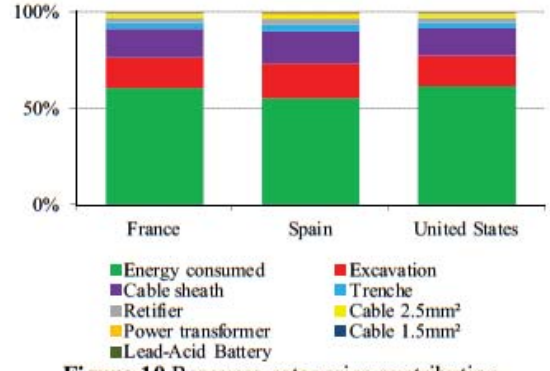

Figure 10. Resource categories contribution

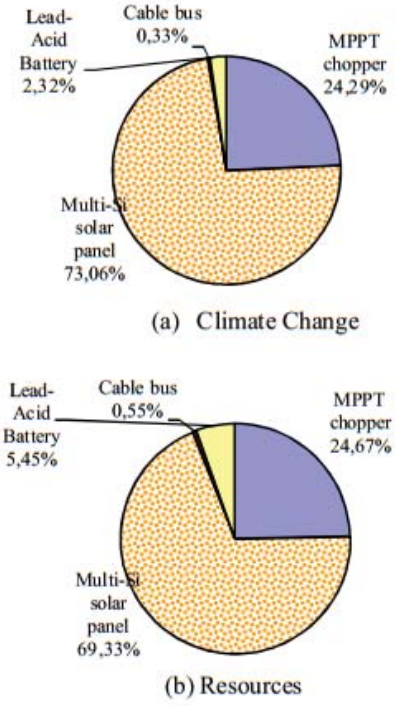

Figure 11. Autonomous heliostat element single

Finally, it could be interesting to study the causes why the installation of an autonomous heliostat has a higher score in the selected categories as observed in this work. Therefore it was decided, as in the case of the electrical grid heliostat, to evaluate the individual contribution of its elements. The results (Figure11) show that the solar panel contributed for over 70% of the computed impact damages within two categories. This is mainly due to the manufacturing process and energy requirement that are involved to manufacture silicon solar panels [13, 14].

4. CONCLUSION

The objective of this work was to make a Life-Cycle Assessment of two heliostat configurations: an autonomous heliostat a grid connected one. Even if the variation between the two configurations is not so high at design stage, the electrical grid heliostat generates the most important impacts to the environment after 20 years of operation.

The energy supplied for operating the grid-connected heliostat is the main element that affects the different categories analyzed in LCA. It depends on the energy mix of the country in which the power station will be built.

REFERENCES

[1] A. Montenon, P. Maussion and A. Ferrière, "An advanced control system for an autonomous héliostat", Perpignan, France, SolarPAces Conference Review, 2010

[2] Y. T. Chen, B. H. Lim and C. S. Lim, "General Sun Tracking Formula for Heliostats with Arbitrarily Oriented Axes", *J. Sol. Energy Eng.*, vol.128, no. 2 pp. 245-250, 2006.

[3] Y. T. Chen, A. Kribus, B. H. Lim, C. S.Lim, K. K. Chong, J. Karni, R.Buck, A. Pfahl, and T. P.Bligh, "Comparison of Two Sun Tracking Methodsin the Application of Heliostat Field," *ASME J. Sol. Energy Eng.*, vol. 126, no. 1, pp.1–7, 2004.

[4] G. García, A. Egea and M. Romero, "Performance evaluation of the first solar tower operating with autonomous heliostats: PCHA project", proceedings of the 12th SolarPACES International Symposium, C. Ramos and J. Huacuz, eds , 2004.

[5] M. Rantik, "Life Cycle Assessment of Five Batteries for Electric Vehicles under Different Charging Regimes", Chalmers University of Technology, KFB-Meddelande, Sweden, p12, 1999

[6] B.Rivoire, 1987, "Experimentation of THEMIS solar power plant. THEMIS results and projections Experimentation de la centrale THEMIS. Resultats et projections", Internal report, CNRS.

[7] ISO (International Organization for Standardization) 14040 standard, "Environmental management – life cycle assessment – principles and framework", 2004.http://www.iso.org/iso/iso_catalogue/management_and_leadership_standards/environmental_management.htm

[8] O. Jolliet, M. Saadé, and P. Crettaz, *Analyse du cycle de vie, comprendre et réaliser un écobilan.* Presses polytechniques et universitaires romandes, Switzerland, 2005.

[9] N. Boeglin, and D. Veuillet, *Introduction à l'Analyse de Cycle de Vie (ACV)*,Département Eco-Conception et Consommation Durable, ADEME, France, 2005.

[10] Ecoinvent Centre, "Database ecoinvent v2.2", Swiss Centre for Life Cycle Inventories, 2009 http://www.ecoinvent.org/database/

[11] O. Jolliet, M. Margni, R. Charles, and S. Humbert, "IMPACT 2002+: a new life cycle impact assessment methodology", *Int. J. LCA*, vol. 6, pp.324-330, 2003.

[12] Réseau de Transport d'Electricité, "Statistiques de l'Energie Electrique en France Juin 2010", p17, 2011, Internal report.

[13]E.A. Alsema, and M.Wild-Scholten, "Environmental impact of crystalline silicon photovoltaic module production", presented at the 13th CIRP International Conference on Life Cycle Engineering, Leuven, Belgium, 31st of May – 2nd of June 2006.

[14] J.R. Perez-Gallardo,S. Astier, C. Azzaro-Pantel, L.Pibouleau, and S. Domenech, "Multiobjective Optimization of Large Scale Photovoltaic (PV) Systems Design: Technico-Economic and Life-Cycle Assessment Considerations", *Chemical Engineering Transactions*, Vol. 25, 483 – 488, 2011.

Appendix B

ANGLE RELATIONSHIP FOR GLOBAL IRRADIANCE ESTIMATION

To estimate the radiation received onto the PVGCS, it is necessary to know the position of the sun during the day throughout the year. As presented in Figure 3-5, to calculate the irradiance received by each PV module that composes the PVGCS, a three-step computation is used. The relationship between these 3 levels can be established through the concepts that are explained below (Duffie & Beckman, 2006; Lorenzo, 2003; Perpiñan Lamigueiro, 2012).

The *extraterrestrial radiation* in the plane normal to the radiation referred as G_{on} on the n th day of the year is the variation of extraterrestrial radiation flux resulting from the distance between the Sun and the Earth due to the orbit that Earth follows. An expression is proposed by Spencer (1971) with an accuracy of ± 0.01%:

$$G_{on} = G_{sc}(1.000110 + 0.034221\cos B + 0.001280\sin B + 0.000719\cos 2B + 0.000077\sin 2B) \quad \text{(B.1)}$$

G_{sc} represents the solar constant (1,367 W/m²) and, B is a value which depends on the day of the year, given by:

$$B = (n-1)\frac{360}{365} \quad \text{(B.1)}$$

To estimate each of the components of the global radiation, it is important to understand the relationship between a plane at any orientation at any given time and the incoming solar radiation due to the position of Sun with respect to the plane. This relationship is established through the following angles (Figure B-1).

The latitude *angle*, ϕ, representing the angle of the surface respect to Equator, north positive; $-90° \leq \phi \leq 90°$.

The declination angle of the Sun, δ, is the angle between the rays of the Sun and the plane of the Earth's equator. It is positive on the north. Spencer (1971) provides the following equation with an error of less than 0.035 ° ($-23.45° \leq \delta \leq 23.45°$). B is given by the Equation (B.2).

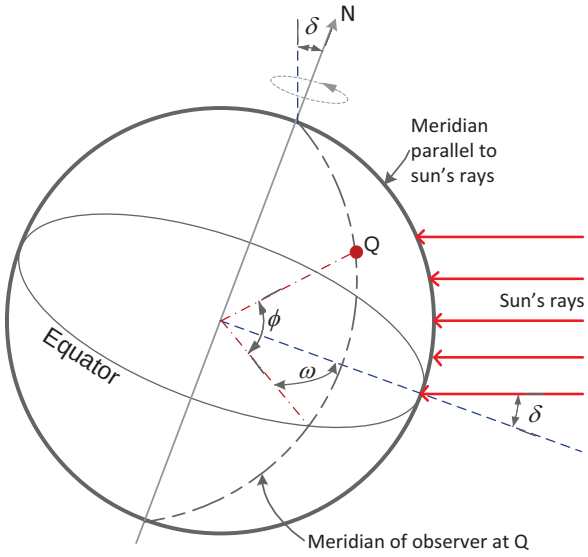

Figure B-1 Angular relationships

$$\delta = (180\ \ \pi)\,(0.006918 - 0.399912\,cos\,B + 0.070257\,sin\,B - 0.006758\,cos\,2B + 0.000907\,sin\,2B - 0.002697\,cos\,3B + 0.00148\,sin\,3B) \quad \text{(B.3)}$$

The *solar hour angle*, ω, converts the *solar time* (*ST*) into the number of degrees which the Sun moves across the sky. By definition, the *hour angle* is 0° at solar noon. Since the Earth rotates 15° per hour, each hour away from solar noon corresponds to an angular motion of the sun in the sky of 15°. In the morning the angle is negative, in the afternoon the angle is positive.

$$\omega = 15(ST - 12) \quad \text{(B.4)}$$

The calculation of this angle needs to determine the *ST*, which does not match with the local time (*LT*). There are two corrections to be made. The former correction corresponds to the difference in length between the observer's meridian (longitude) and the meridian in which the *LT* is based. The sun takes 4 minutes to transverse 1° of longitude. The latter takes into account the disturbance originated by the Earth's rotation that affects the time when the Sun crosses the meridian of the observer. Equation (B.5) determines the solar time taking into account the corrections mentioned above.

$$ST - LT = 4(LSTM - Longitude_{Local}) + E_{ST} \quad \text{(B.5)}$$

LSTM represents the *local standard time meridian*, Equation (B.6). Spencer (1971) sets the parameter E_{ST}, equation of time in minutes, through the expression (B.7):

$$LSTM = 15(LT - Greenwich\ Mean\ Time) \quad \text{(B.6)}$$

$$E_{ST} = 229.2(0.000075 + 0.001868\cos B - 0.032077\sin B - 0.014615\cos 2B - 0.04089\sin 2B) \quad \text{(B.7)}$$

B is calculated through the Equation (B.2); $1 \leq n \leq 365$.

The *zenith angle*, θ_z, the angle between the vertical and the line to the sun corresponds to the angle of incidence of beam radiation on a horizontal surface.

$$\cos\theta_z = \cos\phi\cos\delta\cos\omega + \sin\phi\sin\delta \quad \text{(B.8)}$$

The angle of incidence θ is the angle between the beam radiation on a surface and the normal to that surface. Equation (B.8) calculates this angle taking into account the angles that were calculated before.

$$\cos\theta = \sin\phi\,\sin\delta\cos\beta - \cos\phi\sin\delta\sin\beta\cos\gamma + \cos\phi\,\cos\delta\cos\beta\cos\omega + \sin\phi\cos\delta\sin\beta\cos\gamma\cos\omega + \cos\delta\sin\beta\sin\gamma\,\sin\omega \quad \text{(B.9)}$$

where β symbolizes the tilt angle between the plane of the surface in question and the horizontal ($0 \leq \beta \leq 90$) and γ the azimuth angle of the surface, with zero due north.

The *solar altitude angle*, α_s, the angle between the horizontal and the line to the Sun is given by:

$$\alpha_S = \sin^{-1}\theta_z \quad \text{(B.10)}$$

The solar azimuth angle, γ_s, the angular displacement from north of the projection of beam radiation on horizontal plane:

$$\gamma_S = 180 + sign(\omega)\cos^{-1}\left(\frac{\sin\alpha_S \sin\phi - \sin\delta}{\cos\alpha_S \cos\phi}\right) \tag{B.11}$$

Figure B-2 shows the geometrical relationship between the angles described above.

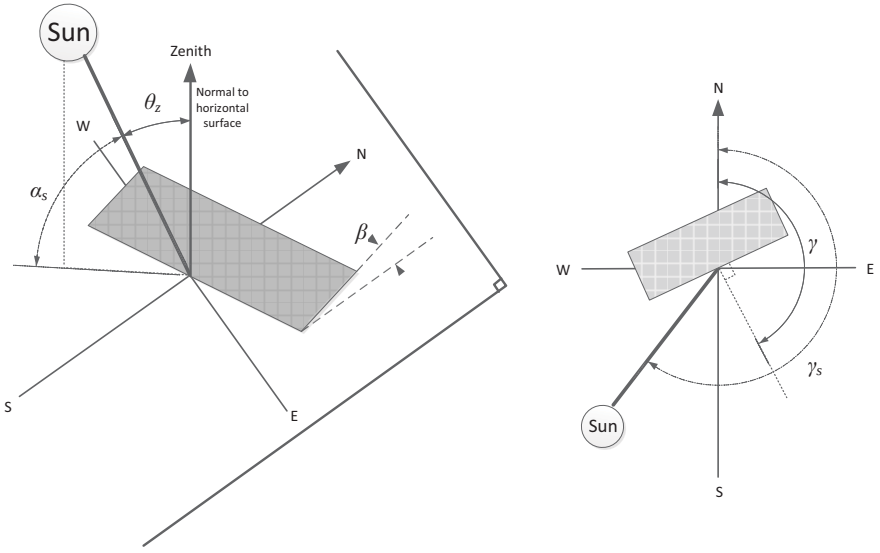

(a). isometric projection (b). top view

Figure B-2 Relationship between zenith angle, solar altitude, solar azimuth angle and tilt angle relative to a fixed point

Appendix C

VALIDATION OF IRRADIANCE SIMULATION TOOL

Table C-1 RMSE and MBE for global irradiance onto PV collector plane for different tilt angle. Lu et al. model

	Titl (°)	0	10	20	30	40	50	60	70	80	90
Mexico City	**RMSE**	39.526	46.219	47.323	47.780	47.502	46.427	44.554	42.135	39.294	36.119
	MBE	-1.530	11.859	11.718	12.099	11.920	10.849	9.295	8.149	6.658	5.161
	% RMSE	18.787	21.784	22.199	22.700	23.264	23.878	24.519	25.272	26.134	27.237
	% MBE	-0.727	3.552	3.437	3.576	3.591	3.330	2.875	2.590	2.122	1.627
Singapore	**RMSE**	35.704	35.343	34.634	33.492	32.092	30.768	29.593	28.416	26.472	23.994
	MBE	-1.557	-1.189	-0.509	0.313	1.499	2.860	4.347	5.631	6.288	6.457
	% RMSE	19.247	0.193	0.195	0.199	0.206	0.219	0.239	0.267	0.289	0.307
	% MBE	-0.839	-0.006	-0.003	0.002	0.010	0.020	0.035	0.053	0.069	0.083
Sydney	**RMSE**	34.633	37.587	41.317	45.067	48.352	50.702	52.011	52.342	51.483	49.697
	MBE	-0.976	-3.135	-5.021	-6.487	-7.330	-7.576	-7.360	-6.560	-5.225	-3.510
	% RMSE	18.870	0.194	0.207	0.223	0.243	0.265	0.289	0.319	0.353	0.398
	% MBE	-0.532	-0.016	-0.025	-0.032	-0.037	-0.040	-0.041	-0.040	-0.036	-0.028
Toulouse	**RMSE**	27.489	30.336	33.444	36.312	38.634	40.113	40.587	39.873	38.349	35.913
	MBE	-1.284	-3.351	-4.948	-6.240	-7.210	-7.530	-7.232	-6.733	-5.761	-4.332
	% RMSE	17.945	0.187	0.200	0.214	0.230	0.247	0.264	0.281	0.301	0.325
	% MBE	-0.838	-0.021	-0.030	-0.037	-0.043	-0.046	-0.047	-0.047	-0.045	-0.039

Table C-2 RMSE and MBE for global irradiance onto PV collector plane for different tilt angle. Hay et al. model

	Titl (°)	0	10	20	30	40	50	60	70	80	90
Mexico City	**RMSE**	39.526	41.034	42.015	42.420	42.173	41.219	39.556	37.409	34.886	32.067
	MBE	-1.530	-1.609	-1.590	-1.642	-1.618	-1.472	-1.261	-1.106	-0.903	-0.700
	% RMSE	18.787	19.057	19.420	19.858	20.352	20.888	21.449	22.108	22.862	23.827
	% MBE	-0.727	-0.749	-0.724	-0.754	-0.757	-0.702	-0.606	-0.546	-0.447	-0.343
Singapore	**RMSE**	35.704	35.236	34.188	32.460	29.989	27.154	23.867	20.543	17.657	15.177
	MBE	-1.557	-1.346	-1.115	-1.024	-0.789	-0.570	-0.323	-0.113	0.058	0.092
	% RMSE	19.247	19.220	19.264	19.294	19.246	19.293	19.293	19.295	19.280	19.423
	% MBE	-0.839	-0.734	-0.628	-0.609	-0.507	-0.405	-0.261	-0.106	0.064	0.118
Sydney	**RMSE**	34.633	36.985	38.565	39.391	39.372	38.320	36.446	33.923	30.480	26.625
	MBE	-0.976	-1.296	-1.518	-1.753	-1.819	-1.764	-1.742	-1.601	-1.347	-1.062
	% RMSE	18.870	19.068	19.278	19.533	19.816	20.036	20.283	20.645	20.916	21.342
	% MBE	-0.532	-0.668	-0.759	-0.869	-0.916	-0.922	-0.970	-0.974	-0.924	-0.851
Toulouse	**RMSE**	27.489	30.128	32.538	34.657	36.406	37.430	37.602	37.007	35.770	33.647
	MBE	-1.284	-1.412	-1.362	-1.373	-1.470	-1.308	-0.944	-0.829	-0.648	-0.357
	% RMSE	17.945	18.583	19.418	20.448	21.693	23.036	24.473	26.086	28.089	30.416
	% MBE	-0.838	-0.871	-0.813	-0.810	-0.876	-0.805	-0.614	-0.585	-0.509	-0.323

Table C-3 RMSE and MBE for global irradiance onto PV collector plane for different tilt angle. Reindl et al. model

	Titl (°)	0	10	20	30	40	50	60	70	80	90
Mexico City	**RMSE**	39.526	42.748	43.769	44.192	43.935	42.940	41.208	38.971	36.343	33.406
	MBE	-1.530	1.441	1.424	1.471	1.449	1.319	1.130	0.990	0.809	0.627
	% RMSE	18.787	20.037	20.419	20.880	21.399	21.963	22.553	23.246	24.038	25.053
	% MBE	-0.727	1.291	1.249	1.300	1.305	1.210	1.045	0.941	0.771	0.591
Singapore	**RMSE**	35.704	35.238	34.204	32.522	30.177	27.610	24.832	22.304	20.432	18.878
	MBE	-1.557	-1.326	-0.966	-0.550	0.246	1.247	2.425	3.599	4.627	5.275
	% RMSE	19.247	0.192	0.193	0.193	0.194	0.196	0.201	0.209	0.223	0.242
	% MBE	-0.839	-0.007	-0.005	-0.003	0.002	0.009	0.020	0.034	0.051	0.068
Sydney	**RMSE**	34.633	37.688	41.400	45.226	48.710	51.435	53.325	54.321	54.089	52.785
	MBE	-0.976	-1.086	-1.201	-1.157	-0.736	0.001	0.835	1.816	2.815	3.627
	% RMSE	18.870	0.194	0.207	0.224	0.245	0.269	0.297	0.331	0.371	0.423
	% MBE	-0.532	-0.006	-0.006	-0.006	-0.004	0.000	0.005	0.011	0.019	0.029
Toulouse	**RMSE**	27.489	30.129	32.541	34.667	36.438	37.531	37.852	37.451	36.477	34.656
	MBE	-1.284	-1.396	-1.240	-0.983	-0.618	0.187	1.317	2.224	3.110	3.905
	% RMSE	17.945	0.186	0.194	0.205	0.217	0.231	0.246	0.264	0.286	0.313
	% MBE	-0.838	-0.009	-0.007	-0.006	-0.004	0.001	0.009	0.016	0.024	0.035

Appendix D

SHADOW ESTIMATION ONTO A TILTED PV SHED

The estimation of linear shading between two PV shed was based on Appelbaum and Bany work (Appelbaum & Bany, 1979). A pole OO' of length A in the *ZY* plane (Figure D.1), inclined at angle *β*, causes a shadow on the tilted shed MM'NN' placed at distance $\overline{OM} = R$. The shed is perpendicular to the *ZY* plane inclined with respect to *XY* plane with the same angle *β*. The shadow length is $OC = P$ and the components of the pole shadow on the *XY* plane are $\overline{IC} = P_x$ (Equation (D.1)) and $\overline{OI} = P_y$ (Equation (D.2)) and its shadow projection on the PV shed is $\overline{EF}$.

$$P_X = A \sin\beta \frac{\sin\gamma}{\tan\alpha} \tag{D.1}$$

$$P_y = A(\cos\beta + \frac{\cos\gamma}{\tan\alpha}\sin\beta) \tag{D.2}$$

The coordinates of the point *E* are:

$$X_E = \frac{RP_x}{P_y} \tag{D.3}$$

$$Y_E = (A\frac{\cos\beta}{P_y})(P_y - R) + R \tag{D.4}$$

$$Z_E = (A\frac{\sin\beta}{P_y})(P_y - R) \tag{D.5}$$

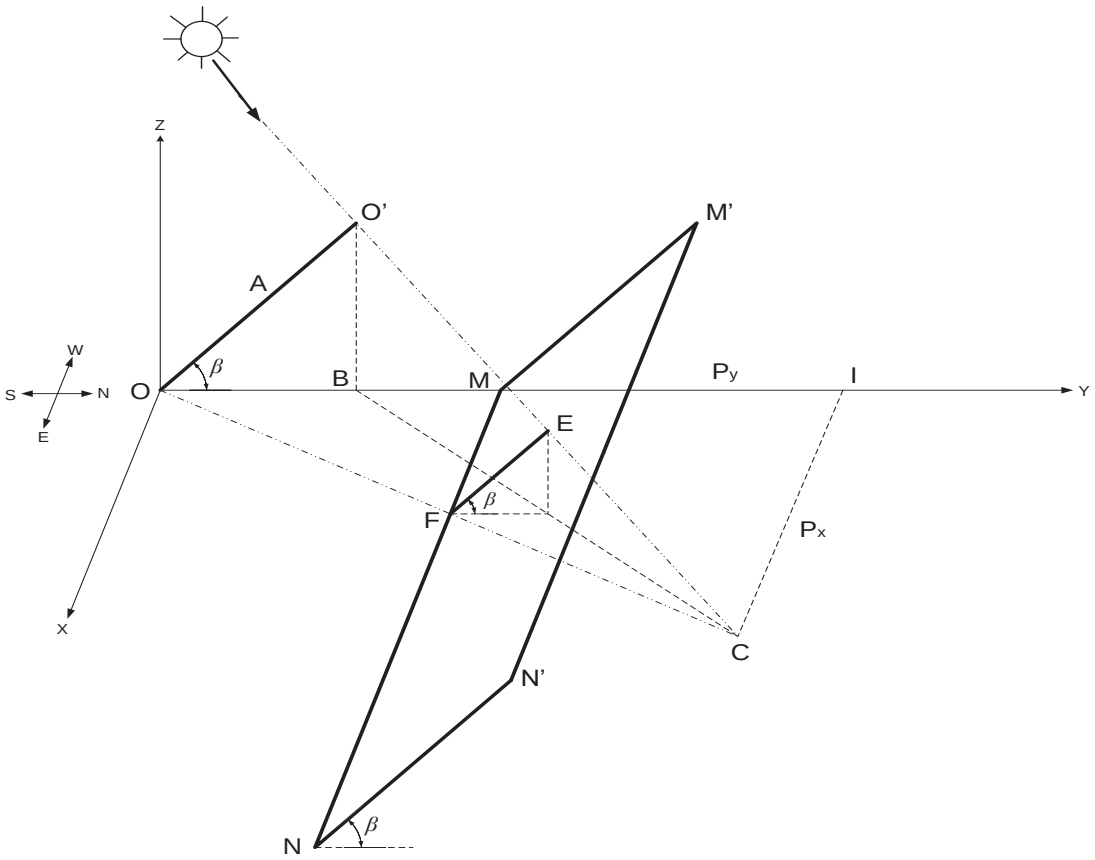

Figure D-1 Shadow of an inclined pole on a tilted PV shed (with same angle β) from Appelbaum and Bany (Appelbaum & Bany, 1979)

The shadow height is therefore:

$$EF = A(1 - \frac{R}{P_y}) \quad \text{(D.6)}$$

As the pole OO' and shed MM'NN' have the same tilted angle β, the distance $\overline{MF}$ is equal to X_E.

The energy produced by the PV shed field depends on the shaded area. A solar field is shown in Figure D-2. The position of two inclined PV shed OLO'L' and MNM'N' and the shadow shape caused by them is presented. A module is defined "shaded" once a shadow is cast on it even on a smallest part of its area. The power output of this module is considered to be zero as long as the shadow prevails on the module. This is the extreme case because some power may be delivered by the module when partially shaded but this case is most simple to program.

The length of the shadow projected from OLO'L' into MNM'N' is $\overline{JN} = L_s$ and the height of the shadow $\overline{JJ'} = H_s$. To predict the number of shaded PV modules, the following steps were established:

Step 1. Set the number of rows shaded. From the EF value, the number of rows shaded in the PV collector can be calculated (Equation (D.7)). The value must be rounded up to the nearest integer.

$$\text{Row shaded} = round.up\left|\frac{EF}{H_m}\right| \quad \text{(D.7)}$$

Where H_m represent the PV module height. Care must be taken for determinate if there is a shadow on the PV collector MNM'N', i.e. $Y_E > R$, $Z_E > 0$ and $|X_E| \leq BM$.

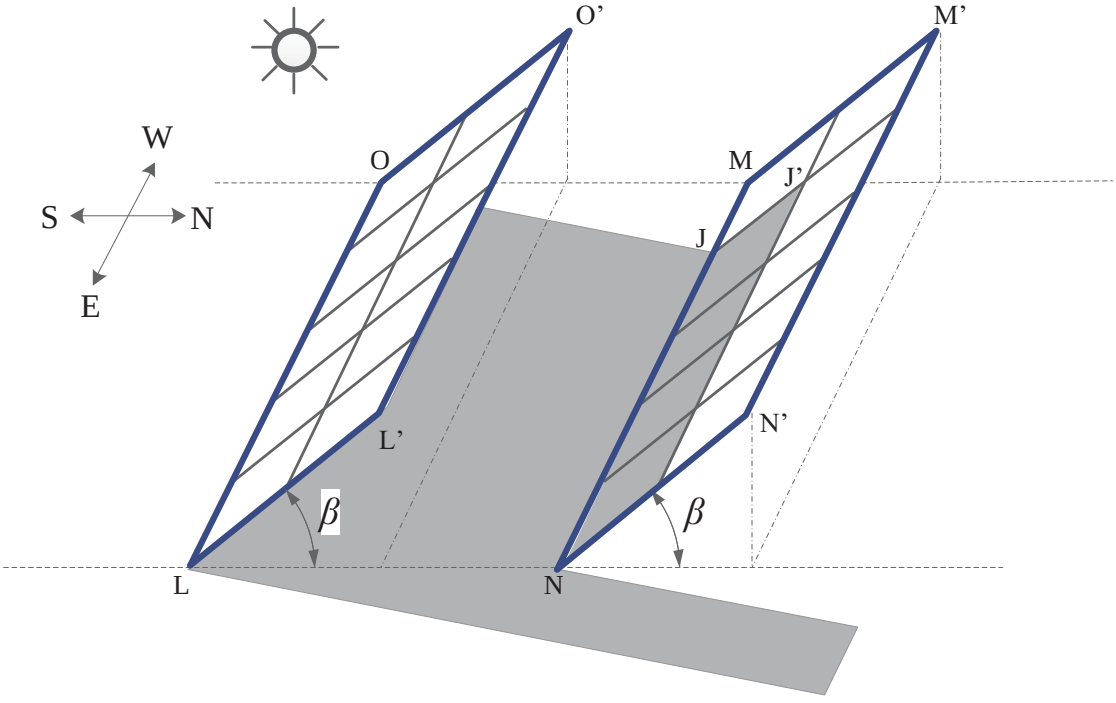

Figure D-2 Shading by PV sheds in a solar field

Step 2. Set the number of columns non-shaded. Equation (D.8) allows for the calculation of non-shaded columns in a PV collector. To apply the Equation (D.8), the following condition must be true: the s*un elevation angle (α)* > 0 and $|X_E| < solar\ field\ length\ \ L$. Otherwise, the value is 0.

$$Column\ non\text{-}shaded = round.down\left|\frac{X_E}{L_m}\right| \quad \text{(D.8)}$$

L_m represents PV module length. If the sign of X_E is positive, it indicates that the point O' is reflected on the collector MNM'N', if the sign is negative, it is the point L' which is reflected.

Step 3. Number of lighted PV modules. From the number of non-shaded columns and shaded rows is possible to determinate the number of lighted PV modules of the PV collector in a specific hour. The calculation is divided into two parts (AZ_1 and AZ_2).

$$AZ_1 = N_c(N_r - Row\ shaded) \quad \text{(D.9)}$$

$$AZ_2 = Row\ shaded \times Column\ non\text{-}shaded \quad \text{(D.10)}$$

$$Lighted\ PV\ modules = AZ_1 + AZ_2 \quad \text{(D.11)}$$

N_c and N_r represent the number of columns and rows of PV modules respectively that make up the PV collector.

Appendix E

BALANCE OF SYSTEM (BOS) SIZING

The Balance of the System (BOS) is the term used to refer to all the other components in the PV installation besides the modules. The BOS includes the structure to support the modules and the electrical installation (inverters and cables).

E.1 Mounting structure

The PV modules are designed to be placed on the outside without protection, so it is fundamental to provide a medium that resists all meteorological conditions occurs. Manufacturers offer a variety of support structures for mounting the PV modules of PVCGS.

There are two types of mounting structures for PV modules. Fixed mounting structures are the most common for PVGCS. They are made principally in aluminium and stainless steel. The second type of structure, called tracking system, allows the PV collector to move either in one or two axes trying to follow the sun during the day. This type of structures permits to generate a greater amount of energy.

Kornelakis and Koutroulis (Aris Kornelakis & Marinakis, 2010) propose a generalised model for the PV module fixed mounting structures in order to incorporate the cost of the PV module mounting structures in economic evaluation. Figure E-1 corresponds to the schema of fixed mounting structure used by Kornelakis and Koutroulis.

The mounting structures are constructed using metallic rods and the estimation of the corresponding cost is based on the calculation of the total length of the metallic rods required for the installation of the PVGCS. Each PVGCS row is comprised of multiple, identical mounting structures. The intermediate vertical rods are installed at each point that the row vertical height has been increased by 2 m. The PV modules metallic mounting frames are installed on concrete foundation bases. The total length in meters of the metallic rods, *B*, required for the installation of the entire PVGCS, is calculated as follows:

$$B = n_b B_1 \tag{E.1}$$

$$B_1 = [(B_{TOT} + H \sin\beta + H) + L_m(2 + B_2)](1 + SF) \tag{E.2}$$

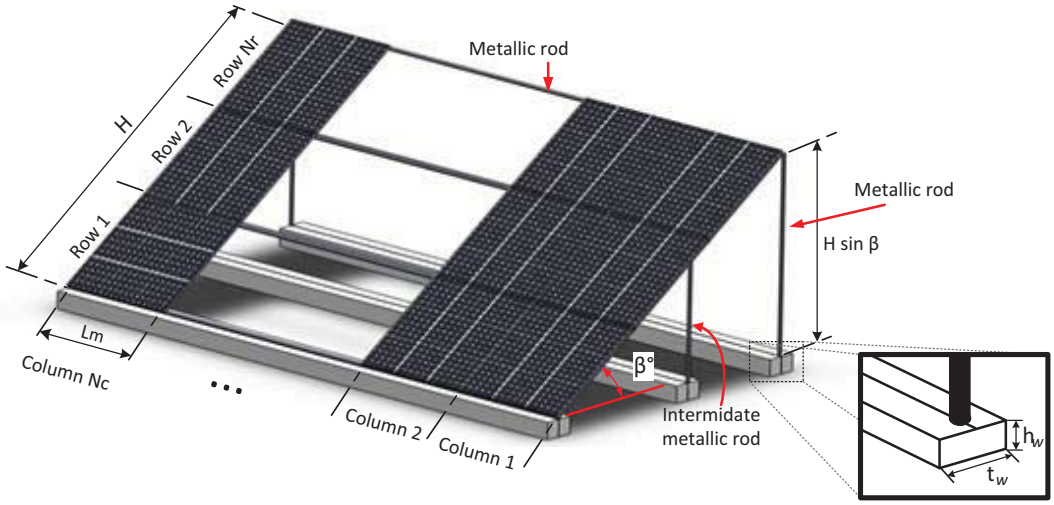

Figure E-1 Schema of the mounting structures

$$n_b = K\ N_c \tag{E.3}$$

$$B_{TOT} = 2\sum_{i=1}^{B_2} i \tag{E.4}$$

$$B_2 = round.down(\frac{H \sin\beta}{2}) \tag{E.5}$$

where B_1 is the total length in meter of the metallic rods required to construct the metallic frames of a vertical line, n_b is the total number of vertical lines comprising the PVGCS installation, B_{TOT} is the total length in meter of the vertical rods of each side of a vertical line, B_2 is the total number of the intermediate vertical rods of each side of a vertical line and SF is an over-sizing factor for security reason during the construction of the frames.

The total volume (m^3) of the concrete foundation bases required to support the PVGCS PV module metallic mounting frames, B_B, is equal to:

$$B_B = (2 + B_2)h_w t_w L_m n_b \tag{E.6}$$

h_w represents the concrete foundation base height and t_w is the corresponding thickness, both specified by the designer at the beginning of the PVGCS optimal sizing procedure. The total cost of the PVGCS mounting structures, C_{MS}, is equal to the sum of the metallic rods and the concrete foundation bases costs.

$$C_{MS} = Bc_S + B_B c_B \tag{E.7}$$

where c_S is the cost per length unit of the metallic rods and c_B is the cost per volume unit of the concrete foundation bases.

E.2 Inverter

PV inverter converts the direct current (DC) output of a PVGCS to deliver alternating current (AC), which can be fed into the electrical grid. Solar inverters have special functions adapted for use with photovoltaic arrays, including maximum power point tracking. Grid frequency and voltage are two important aspects to take into account for select an inverter. The lifetime of the inverter, as a rule, is 10 years. Manufacturers often offer in option an extension of the warranty for 20 years.

The Agence de l'*Environnement* et de la Maîtrise de l'*Energie* (ADEME in french) (Boulanger, 2003) analyses three different types of integration of PV inverters in a PV power plant (see Figure E-2). The Table E-1 lists the characteristics, advantages and disadvantages of each of the three configurations.

A3 is discarded due to size of the large-scale PVGCS and the maintenance cost of the number of inverters. The two remaining alternatives are appropriate for this type of facility and a combination of them can be used depending on the dimension of PVGCS.

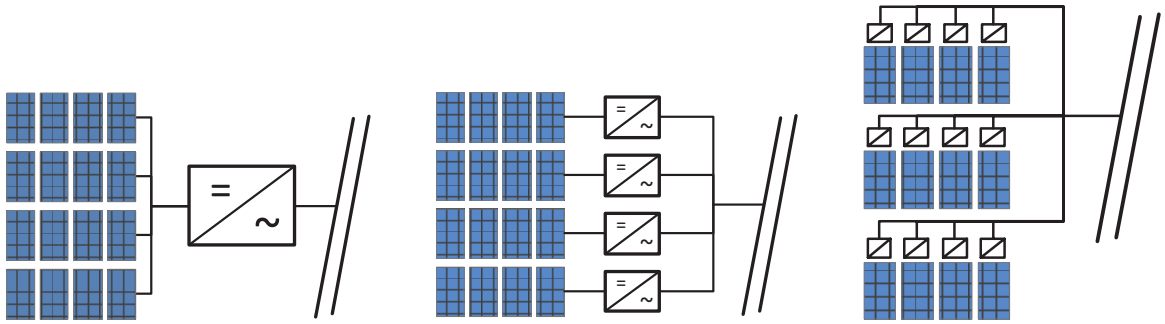

Figure E-2 Types of integration of PV inverters

Table E-1 Characteristics of each of the three configurations for inverters (Boulanger, 2003)

Type	Description	Advantages	Disadvantages
A1	Several lines of PV modules are connected directly or via a connection box, into a centralized inverter.	- Best DC/AC efficiency.	- Maintenance (no redundancy). - Energy loss by matching and shadow. - High voltage wiring.
A2	Each line of PV modules is connected to an inverter (some inverters can connect two or three parallel lines directly). The inverters are connected in parallel to the network.	- Modular block design. - Correct DC/AC conversion	- Incompatibility if different inverters of different manufacturer are used.
A3	Each PV module is connected to a small inverter (some inverters can connect up to five PV modules in series). The inverters are connected in parallel over the network.	- Modularity. - Independence of modules (minimum loss by pairing). - Reliable architecture (high redundancy and parallelism).	- The lowest DC/AC conversion efficiency

The number of DC/AC inverters required is determinate according to the methodologies presented by Hayoun and Arrigoni (Hayoun & Arrigoni, 2012), and Kornelakis and Koutroulis (Aris Kornelakis & Marinakis, 2010). The first step is to set the maximum ($N_{s,max}$) and minimum ($N_{s,min}$) number of PV modules connected in series. Equations (E.8) and (E.9) obtain these values from voltage compatibility between PV modules and the DC/AC inverter.

$$N_{s,min} = round.up(\frac{V_{MPPT,min}}{0.85V_{MPP}}) \quad \text{(E.8)}$$

$$N_{s,max} = round.down(\frac{V_{MPPT,min}}{kV_{MPP}}) \quad \text{(E.9)}$$

Where, $V_{MPPT,min}$ and $V_{MPPT,max}$ corresponds to the minimum and maximum values for voltage respectively which the tracker (MPPT) of the DC/AC inverter operates; V_{MPP} is the voltage at nominal power. 0.85 and k are coefficients imposed for security reason by the guide UTE C15-712-1 (Hayoun & Arrigoni, 2012) corresponding to the change of voltage generated by the PV modules by the temperature variation of the solar cells.

The number of PV modules in series (N_s) must satisfy the condition indicated in Equation (E.10). Generally corresponds to the value $N_{s,max}$.

$$N_{s,min} \leq N_s \leq \frac{P_{max}}{P_{M,max}} \quad \text{(E.10)}$$

P_{max} represent the maximum input DC power of DC/AC inverter and $P_{M,max}$ is the maximum possible PV module output power at the MPP.

The maximum number of parallel branches connected to a DC/AC converter, $N_{p,max}$, is calculated using the following equation:

$$N_{p,max} = round.down\ (\frac{I_{max}}{I_{MPP}}) \quad \text{(E.11)}$$

The maximum possible number of PV modules, N_{block}, that the DC/AC inverter can support is:

$$N_{block} = N_s N_{p,max} \quad \text{(E.12)}$$

Total DC/AC inverters N_{INV} for the PVGCS is:

$$N_{INV} = round.up(\frac{Total\ number\ of\ PV\ modules\ of\ PVGCS}{N_{block}}) \quad \text{(E.13)}$$

The cost of inverters varies strongly (depending on project size, supplier, promotional offers...). Solarbuzz (Solarbuzz, 2012a) periodically analyzes the price of inverters on the market and establish a price per kilowatt-pick, C_{kWp}. The total cost for inverters, C_{INV}, is given by the following expression:

$$C_{INV} = N_{INV} P_{INV,DC} C_{kWp} \quad \text{(E.14)}$$

3. Wiring

Since the system is composed of PV modules and DC/AC inverters, the most important section to wire is that connects the PV collectors and the DC/AC inverters. The length of the cable, $Length_{Total}$, is estimated from the scheme shown in Figure E-3. It is observed that all DC/AC investors are placed in the same space.

$Length_1$ and $Length_3$ are considered as constant values for all the PV collectors. $Length_2$ varies depending on the location of the PV collector with respect to where the DC/AC inverters are installed. The sum of all $Length_2$ can be defined as:

$$Length_{2T} = 2 \sum_{x=1}^{n_K} x(D + H \cos\beta) \quad \text{(E.15)}$$

$$n_K = round.down(\frac{K}{2}) \quad \text{(E.16)}$$

Being K the number of PV collectors. The series above is simplified to obtain the following equation:

$$Length_{2T} = \ D + H \cos\beta \ [n_K \ n_K + 1 \ ] \quad \text{(E.17)}$$

The total length is given by the Equation (E.18).

$$Length_{Total} = K(Length_1 + Length_3) + Length_{2T} \quad \text{(E.18)}$$

Total cost of wiring concept, C_{WC}, is represented by the Equation (E.19). C_W is the cost per m of cable.

$$C_{WC} = C_W \ Length_{Total} \tag{E.19}$$

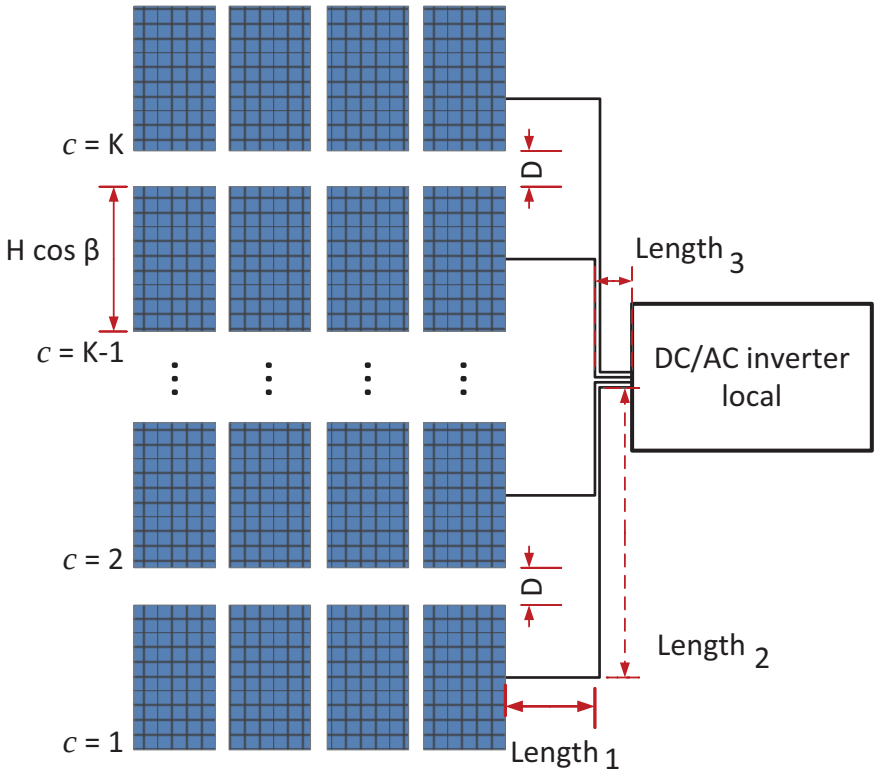

Figure E-3 Wiring schema